Australian Government
Bureau of Meteorology

HYDROLOGY REPORT SERIES

HRS Report No. 12

CLIMATE CHANGE AND PROBABLE MAXIMUM PRECIPITATION

Water Division
Melbourne
March 2009

HYDROLOGY REPORT SERIES

HRS Report No. 12

CLIMATE CHANGE AND PROBABLE MAXIMUM PRECIPITATION

Dörte Jakob, Robert Smalley, Jeanette Meighen, Karin Xuereb, Brian Taylor

Hydrometeorological Advisory Service
www.bom.gov.au/hydro/has/
Water Division
Melbourne
March 2009

Table of Contents

Page No.

List of Figures

Page No.

Introduction

A 2-year project to investigate potential effects of climate change on estimates of Probable Maximum Precipitation (PMP) was funded jointly by the Queensland Department of Natural Resources and Water and the Commonwealth Department of Climate Change, with in-kind contribution by the Bureau of Meteorology.

The number of queries received indicates that results from this work are of interest to a wider audience and this report was prepared to address that need. The current document is a shortened and slightly revised version of the final scientific report delivered as part of the project.

There are two main parts to the report. The first part presents an assessment of how individual factors used in deriving PMP estimates might be changing over time. After assessing changes separately, the resulting effect of these changes on PMP estimates is explored. The factors considered are: local moisture availability, storm types, depth-duration-area curves and relative storm efficiency. A recent noteworthy event is also discussed in this context and an overview of the steps required in deriving PMP estimates is given, which provides an instructional example for those not familiar with the techniques.

The second part of the report is focussed entirely on rainfall. A set of 'extreme rainfall indices' is used to explore changes in observed rainfall, for validation of modelled rainfall, and in assessing projections from global climate models (GCMs).

An executive summary is provided to give a very brief overview of the most important results from this work, including recommendations for further work. This summary does not assume prior knowledge of the subject matter.

Acknowledgements

We are grateful to Neville Nicholls (Bureau of Meteorology Research Centre) and David Jones (Bureau's National Climate Centre) for their involvement in the setting up of this project.

Thanks to Tracey Elliott (CSIRO Marine and Atmospheric Research) for supplying output from the CSIRO Mk 3.0 model. Garry Moore (Hydrometeorology Advisory Service) is thanked for support in analysing data. RJS gratefully acknowledges Hank de Wit from the SA Regional Office for providing the upper-air precipitable water data and both Lisa Alexander and Xuebin Zhang (Expert Team on Climate Change Detection and Indices) for code used in calculating robust linear trends and assessing trend significance.

We acknowledge the modelling groups, the *Program for Climate Model Diagnosis and Intercomparison* and the *World Climate Research Programme's Working Group on Coupled Modelling* for their roles in making available the WCRP CMIP3 multi-model dataset. Support of this dataset is provided by the Office of Science, U.S. Department of Energy.

Executive summary

1. Background

This executive summary was prepared as part of the final scientific report on a study with the aim of assessing whether potential effects of climate change have to be considered when deriving estimates of Probable Maximum Precipitation (PMP).

The 2-year project was jointly funded by the Queensland Department of Natural Resources and Water and the Commonwealth Department of Climate Change, with in-kind contributions by the Bureau of Meteorology.

This summary aims to present findings without expecting prior knowledge about procedures for estimation of Probable Maximum Precipitation (PMP). The intention is to provide the reader with a concise overview of the project without the need to refer to the full report.

Probable Maximum Precipitation (PMP) is *'The greatest depth of precipitation for a given duration meteorologically possible over a given size storm area at a particular location at a particular time of the year, with no allowance made for [future] long term climatic trends.'* (WMO 1986). PMP is a theoretical concept and can only be estimated. Using an appropriate generalised method for the duration and location in question, estimates can be derived for any catchment in Australia.

For certain applications (including the design of dams) engineers need an estimate of what is referred to as the 'PMP Design Flood'. PMP is one of the required inputs when estimating the PMP Design Flood. However, PMP estimation currently does not take into account that estimates might change under a changing climate. Since structures designed using such estimates have long life spans it is vital to consider potential effects of climate change on estimates of Probable Maximum Precipitation.

2. Introduction to basic procedures used in PMP estimation

Different methods of PMP estimation apply, depending on the location and duration for which estimates are required. The three most important methods are the Generalised Tropical Storms Method Revised (GTSMR), the Generalised South East Australia Method (GSAM) and the Generalised Short Duration Method (GSDM). For this study we focus mainly on the GTSMR because this method has been revised most recently and is applicable for most of mainland Australia. The GTSMR approach consists of three components: the GTSMR database, generalising the GTSMR storm database and the PMP estimation technique. The following section will first describe how storms are selected for inclusion in the GTSMR database, then how those storms are generalised and finally how PMP estimates for catchments are derived based on these generalised storms.

GTSMR database

The Bureau of Meteorology's database of daily rainfalls was screened to identify the top ten events at each station for durations from 1 to 7 days. Storms were ranked by the number of locations for which the event was rarer than 1 in a 100 years. To ensure all areas of Australia were represented, subzones were defined and the highest-ranked storms for each of these subzones were selected. Many more storms than ultimately required were inspected using GIS software. The final selection consists of 122 storms, dating back to 1893. These storms were then analysed manually and digitised to allow constructing depth-area curves. For about 70% of all storms additional (pluviograph) data was available. This allowed the construction of temporal distributions for standard areas.

Generalising the GTSMR database

Storms from the GTSMR database were generalised to remove features specific to a location that influence the depth of rain.

- Most locations have a preferential spatial distribution of rainfall. This information is no longer relevant when transferring to another location; it is therefore replaced by more general depth-duration-area curves.
- Zones, in which particular methods for PMP estimation apply, are defined based on storm types that 'operate' in a region, since significant rainfall is produced by different mechanisms.
- Rainfall can be enhanced orographically. The portion of rainfall deemed to be due to orographic enhancement is removed, leaving just the 'synoptic component'.
- Local moisture availability is maximised (with respect to the location and time of year) and standardised (using Broome as a reference station).
- An adjustment factor is derived to account for the decay of storms as they move south and away from the coast.

Deriving PMP estimates for catchments

PMP estimates are required for deriving the PMP Design Flood. Therefore estimates need to be derived on a catchment basis. This requires re-constructing catchment-specific features including orographic enhancement, moisture availability and decay of storms. The result is a set of PMP estimates for a given catchment for a number of durations. These estimates are enveloped to derive the final PMP estimates. For further hydrological analyses one often requires the *spatial and temporal distribution for the PMP storm*. The spatial distribution is derived by distributing the PMP estimate over sub-catchments. Temporal patterns are provided for standard areas.

3. Results

The following factors have been assessed in this study to assess for potential changes due to climate change: moisture availability, depth-area-curves, storm types, storm efficiency and generalised rainfall depths. Since the PMP method is related to very large rainfall events, changes in both observed and projected extreme rainfall are also assessed.

Moisture availability

Moisture availability is estimated for storms (within the generalised methods) and when determining the PMP estimate for a particular catchment. Moisture availability is expressed as the moisture content of a column of air, referred to as *precipitable water* (PW, in mm). Estimates of this moisture content can be derived in two different ways: from upper-air soundings (using weather balloons) and from surface observations.

When generalising events (removing local effects), the ratio of *extreme precipitable water* to *storm precipitable water* is required. When deriving PMP estimates for a catchment, the ratio of *extreme precipitable water for the catchment* to the *extreme precipitable water for a reference station* is required. Changes in both the *storm precipitable water* and *extreme precipitable water* had to be investigated to answer the question how maximised rainfall might change.

Observed changes in moisture availability

Upper-air soundings are only available at a very limited number of stations, typically taken once or twice a day. The instrumentation used has changed over time, which makes it difficult to assess for changes in *precipitable water* derived from upper-air data. The network of surface stations is much denser and observations are taken more frequently. At these stations measurements of dew point temperatures are undertaken. The *dew point temperature* (or, in short: dew point) is the temperature at which the moisture in air will be just sufficient to saturate it (100% relative humidity). The *dew point temperature* too is therefore a measure of moisture availability. Using assumptions about the vertical profile of moisture, surface observations of *dew point temperatures* can be converted to precipitable water.

The moisture availability at a given location varies over time and exhibits a degree of seasonality. To study the average and the extremes of moisture availability, *percentiles* were used. The 50^{th} percentile (also known as the median) is the moisture availability that would be equalled or exceeded in half of the cases. For the PMP however the most extreme cases of moisture availability are important, such as for instance the 90^{th} percentile which would only be exceeded in 10% of all cases. Changes in estimates were studied by comparing moisture availability for two periods: 1960 to 1980 and 1981 to 2003.

While average moisture availability typically has a tendency to decrease (not shown), most stations show an increase in more extreme moisture availability. The significance of changes was assessed on the basis of number of days exceeding the 90th percentile in 24-hour minimum surface dew point temperatures (Figure E-1). Based on events from the Generalised Tropical Storm Method (GTSMR) and the Generalised South East Australia Method (GSAM) databases, changes in moisture availability are typically not statistically significant.

When assessing changes in moisture availability which are relevant for the generalisation procedures, no large-scale significant changes are found. However, moisture availability as used for deriving PMP estimates for catchments shows significant increase along parts of the east coast but also a region with decrease in south-eastern Australia for *summer*.

Moisture transport from sources such as large lakes or the ocean may change the moisture availability at a given location. The sea-surface temperatures (SST) surrounding mainland Australia were compared with monthly extreme surface dew-point temperatures to determine if changes in SST could be correlated with changes in moisture availability. Although an association exists, it is not possible to directly relate a particular sea-body SST, using the moisture inflow wind direction, with the monthly extreme surface dew-point temperatures at a location.

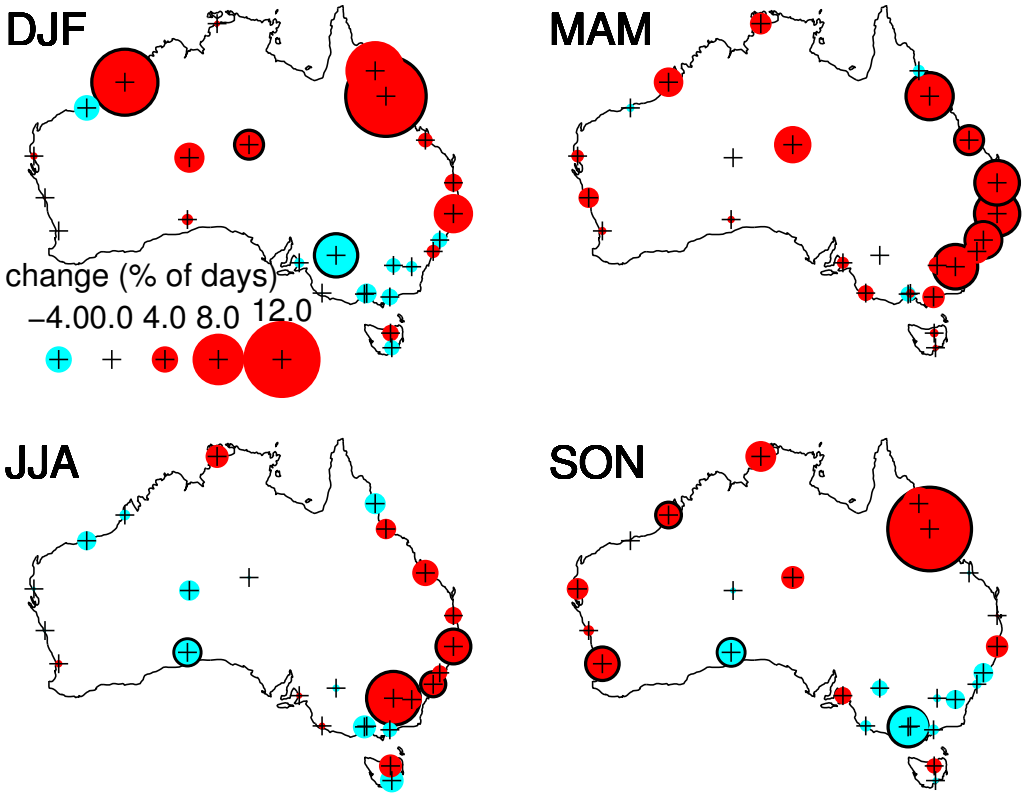

Figure E-1 Percentage change in the seasonal median between two time periods (1960–1980 and 1981–2003) for the index TdN90p (number of days exceeding the 90th percentile of daily minimum surface dew-point). Black circle outline indicates change is statistically significant at the 0.05 level.

Projected changes in moisture availability

Observations from upper-air and surface data spanning the last four decades allow an assessment of how moisture availability has changed in the past. Output from a climate model is used to project possible changes in moisture availability over the coming decades. The validity of output produced by one particular model (CSIRO Mk3.0) was assessed by comparing observed and modelled precipitable water. It was found that the model gives a fairly accurate description of the moisture availability and how it varies over the seasons and with geographical location.

One of the required inputs for climate models is the level of future greenhouse gas emissions. *Scenarios* are commonly used to indicate the range of likely changes in emissions since it is not known exactly how population, technology, society and ultimately greenhouse gas emissions will develop over the next few decades. A number of scenarios have been developed. Three of these have been considered here: A2 (high), A1B (medium) and B1 (low).

Comparing moisture availability modelled for the current climate (1981-2000) and the next few decades, it was found that relative changes in average moisture availability (50th percentile) are smaller than for more extreme cases (90th percentile). On average, the 90th percentile tends to increase from the 2020s to the 2050s and the 2090s. This increase is most pronounced for the A2 (high) scenario, less strong for the A1B (medium) scenario and weakest for the B1 (low) scenario (Figure E-2). However, there is also a possibility that some regions may see lower extreme moisture availability in the future.

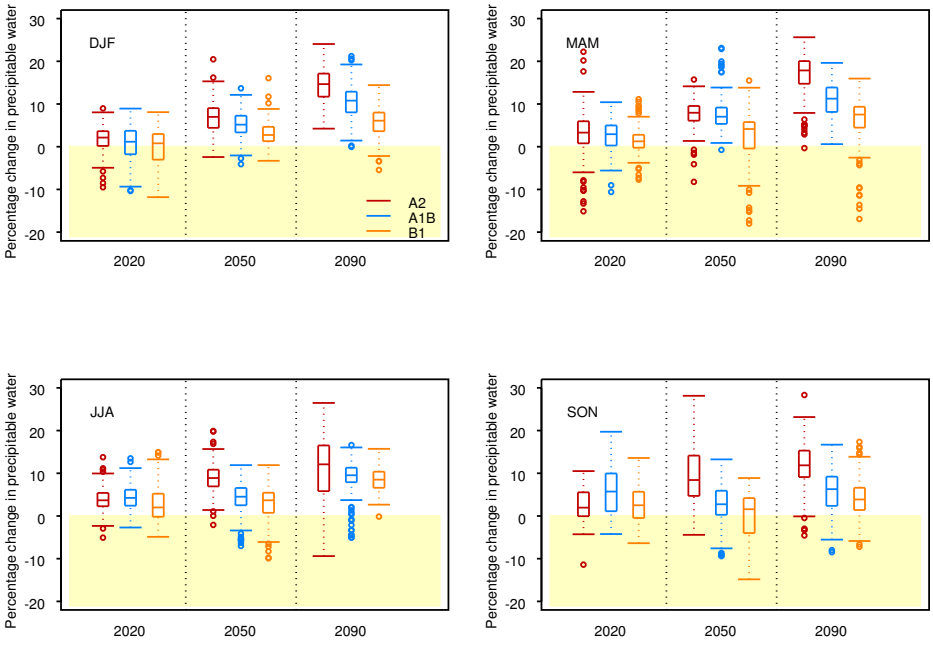

Figure E-2 Percentage change in the 90th percentile of precipitable water by season for scenarios A2, A1B and B1 (compared to current climate). The box-whisker plots indicate the range of projected changes (solid horizontal lines at the ends of the dashed vertical lines). The box indicates the first and third quartile. The distance between these quartiles is also referred to as 'interquartile range' (IQR).The horizontal short lines at the end of the dashed vertical lines are plotted at 1.5 IQR. Values outside this range are considered outliers and are plotted as open circles. The line dividing each of the boxes is the median (indicating the average change), the circles indicate outliers.

These results are based on output from one climate model only. The climate system is highly complex and while today's models are able to capture the main aspects, there are shortcomings which to some extent are model dependent. Ideally one would therefore consider output from a range of models for a higher degree of reliability.

Depth-duration-area curves

The rainfall depth (in mm) associated with significant rainfall events (sometimes referred to as 'rain storm' or just 'storm') can be presented for a set of standard sized areas (from less than 10 km^2 to above 10,000 km^2) and standard durations (from hours out to a number of days) using so-called *depth-area curves*. These curves can be used to derive the maximum rainfall depth for a given area and duration. Possible changes in depth-area curves were studied by constructing these curves for two non-overlapping 25-year periods. It was found that based on the last 50 years, there is no evidence that the rainfall depth from the most significant events has increased.

Alternatively, one can estimate the rainfall depth that (for a given location and duration) is likely to be equalled or exceeded once every 10 years, once every 100 years and so on. Such estimates are referred to as 'design rainfalls'. Changes in *design rainfalls* were investigated for an area spanning parts of southeast Queensland and parts of north eastern NSW. Analyses were carried out for two sets of rainfall stations - once for a 50-year period (1951 - 2000) using 121 stations (to give a good spatial coverage) and then again for a smaller number of stations (26 sites) for a 100-year period (1901 - 2000).

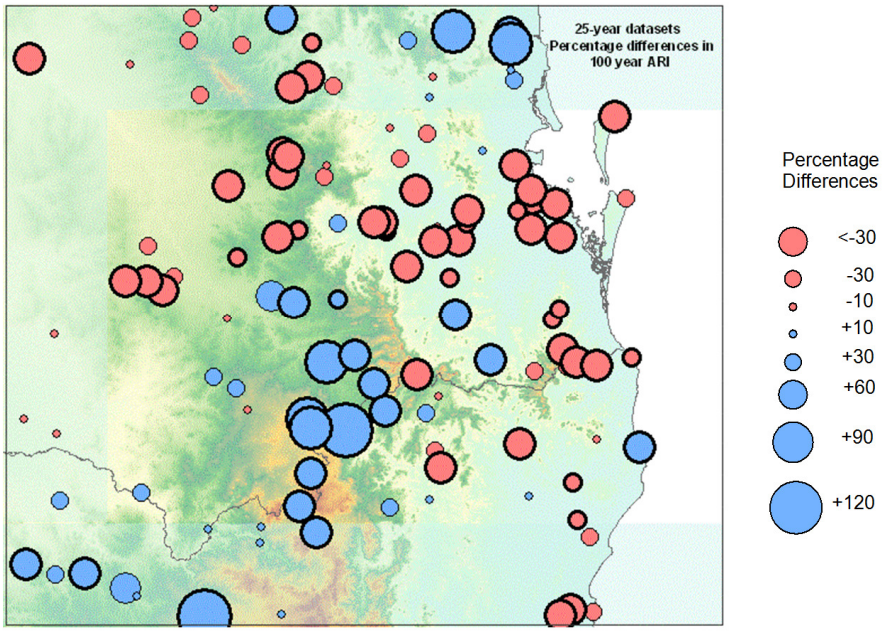

Figure E-3 Percentage differences in design rainfall estimates for two 25-years periods (1951-1975 and 1976-2000) for the 24-hour duration and an average recurrence interval (ARI) of 100 years. Solid black outline indicates differences are statistically significant. Blue indicates design rainfall estimates are higher for the later period.

Design rainfall estimates typically decreased based on the analyses for the last 100 years. For the last 50 years the picture is less homogeneous. On average, design rainfall estimates for this period have decreased but there are geographically contiguous regions (in particular those at higher elevations) where design rainfalls have increased (Figure E-3).

Storm types

Significant rainfall events (storms) had been classified by assigning '*storm types*' such as 'tropical cyclone' or 'monsoon low' based on the use of synoptic (i.e. surface weather) charts and where available upper-air charts. These storm types were used in defining zones in which certain methods for PMP estimation apply.

One type of event capable of producing significant rainfalls are tropical cyclones. There has been some debate in the scientific literature about whether intensity, frequency or tracks of tropical cyclones might have changed due to a changing climate. Because of interdecadal and multi-decadal variations and issues with the existing Australian cyclone database, there is little certainty about changes in frequency and intensity of tropical cyclones in the Australian region. Based on the last 50 years, there is little evidence to support the notion that tropical cyclones (connected to major rainfall events) are penetrating further south or have become more frequent (Figure E-4). The absolute (and relative) frequency of such events is lowest for the most recent period (1976 - 2001). Based on events selected for the GTSMR database, it appears possible that the frequency of events with durations of 7 days and longer has increased. This raises the question whether it is likely that significant rainfall events might show a tendency to become more prolonged in the future.

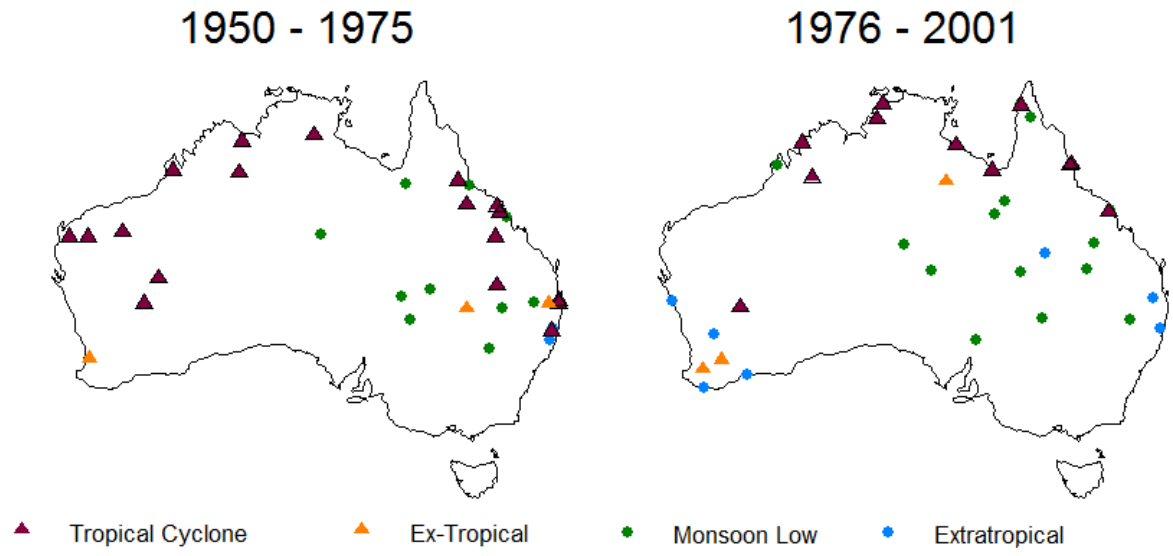

Figure E-4 Location of storm centres for storms from the GTSMR database for two periods (1950-1975 and 1976-2001), symbol and colour of points indicate storm type.

Relative storm efficiency

Relative storm efficiency is a measure for the efficiency with which available moisture is converted into precipitation. Definitions may take into account factors such as orographic enhancement, wind speed and the height dependent changes in both wind speed and direction. Storm efficiency was assessed using events from storm databases and using the largest events at selected stations.

Event-based analyses

Storm efficiency derived for GTSMR events was found to vary with geographical location. Typically, storm efficiency decreases for events with storm centres further inland (Figure E-5).

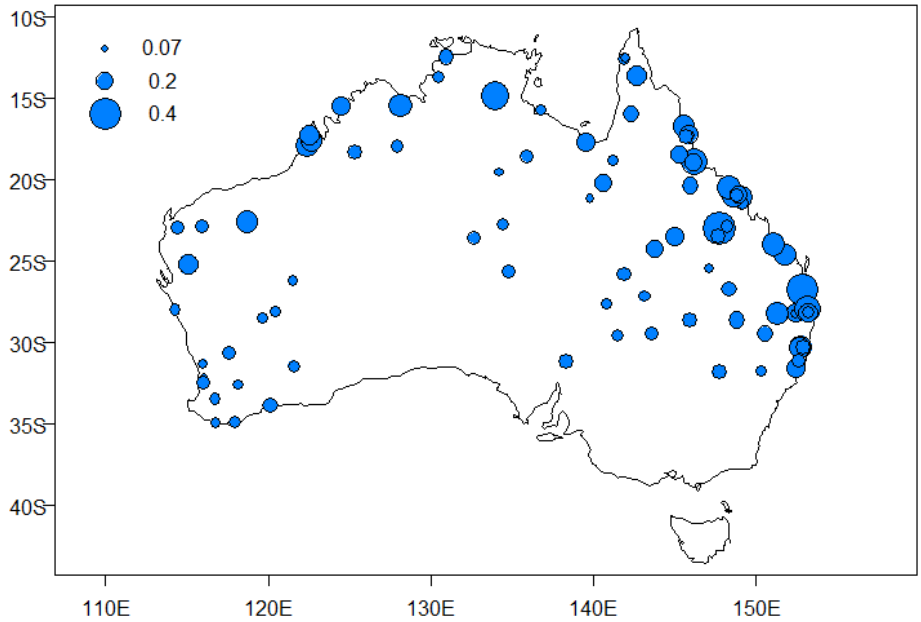

Figure E-5 Storm efficiency for events from the GTSMR database. Relative storm efficiency is calculated as ratio of storm depth (at 24 h, 1000 km^2 converted to rain rate and adjusted for orographic enhancement of rainfall) and storm precipitable water. Symbols are plotted at the location of storm centres. Symbol size denotes storm efficiency (dimensionless).

The average storm efficiency for events during a period will depend on the location of storms sampled. This average could change purely because the preferred location of storms has changed. During the later period (1975-2000) fewer events from regions where storm efficiency tends to be highest were included in the GTSMR database. Based on events from the GTSMR database no increase in observed storm efficiency was found (Figure E-6).

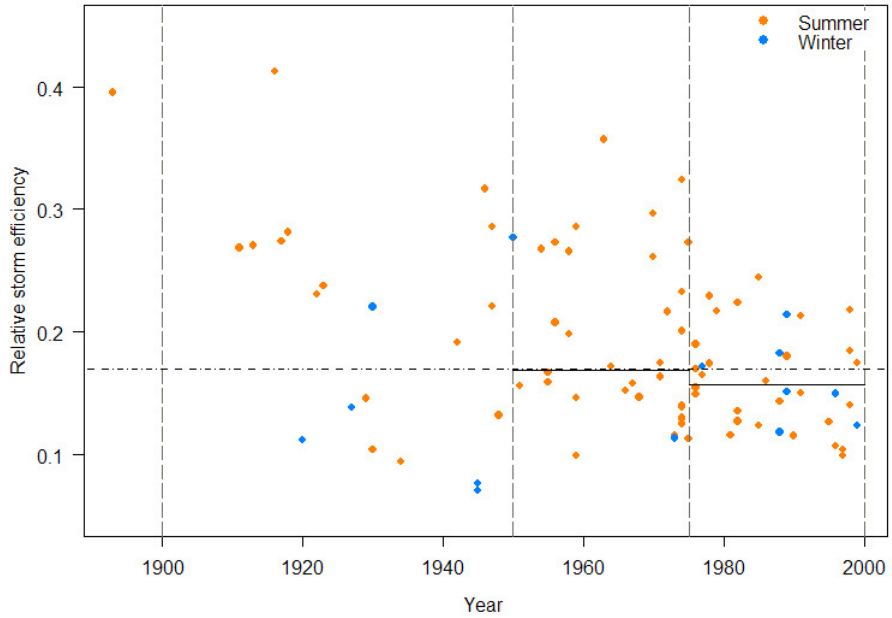

Figure E-6 Storm efficiency calculated as ratio of rainfall rate (adjusted for orographic enhancement) and storm precipitable water for events between 1893 and 2000 (standard area 1000 km^2, duration 24 hours). Horizontal lines indicate median ratio for periods (dashed line for 1900 to 2000, solid lines for 1950–1975 and 1975–2000). Colour of dots indicates seasons as defined in GTSMR database: *summer* from October to April and *winter* from May to September.

Station-based analyses

Alternatively, relative storm efficiency can be assessed at stations. This also has the advantage that an adjustment for orographic enhancement of rainfall is not required. Based on the 30 largest events for each of the periods 1960–1980 and 1981–2003, changes in relative storm efficiency (Figure E-7) and rainfall depths (not shown) were assessed. Only two locations show statistically significant changes (Darwin: an increase in storm efficiency for *summer*, and Coffs Harbour: a decrease for *autumn*). Typically, changes in rainfall depth are a good indicator for changes in storm efficiency. Analyses based on events from the storm databases and from station data are not strictly comparable. Results based on station data are indicative of changes in more frequent events and point rainfall depths.

A recent noteworthy event

A recent noteworthy event was assessed. This event occurred during the *winter* months (June 2005). Record rainfalls led to extensive flooding along parts of the Gold Coast. For a number of durations and areas, the depth-area estimates exceed the design estimates for the Coastal Application Zone - *Winter* (Figure E-8). The relative storm efficiency for this event is similar to the highest efficiency for events in the GTSMR database. Even after taking topographic enhancement of rainfall into account, the efficiency for this event ranks amongst the highest efficiencies derived for GTSMR events.

Based on the assessment of this recent event and the results from the station-based approach, we need to consider the possibility that relative storm efficiency of events could increase for certain locations, event types and seasons.

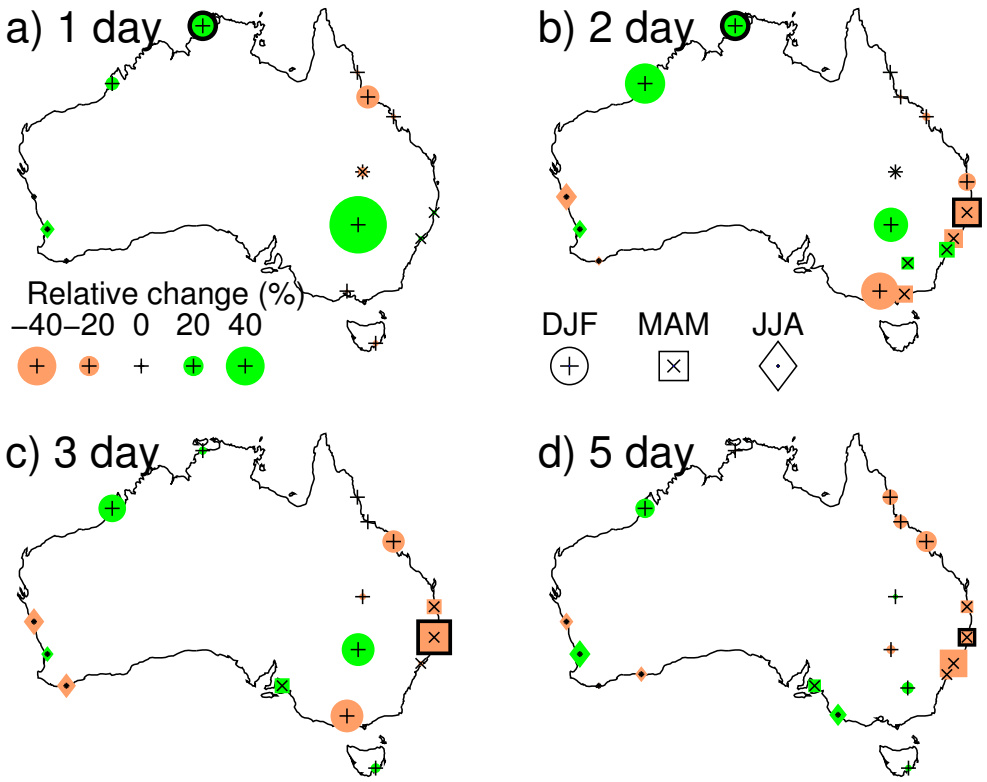

Figure E-7 Seasonal variation of relative change in relative storm efficiency for the 30 largest independent rainfall events for different durations: a) 1 day, b) 2 day, c) 3 day and d) 5 day durations. The black outline indicates change is significant at the 0.05 level. Different symbols correspond to different seasons. Crosses, plus signs and point symbols denote locations that have sufficient data (10 events in each of 1960-1980 and 1981-2003) for *summer*, *autumn* and *winter* events respectively.

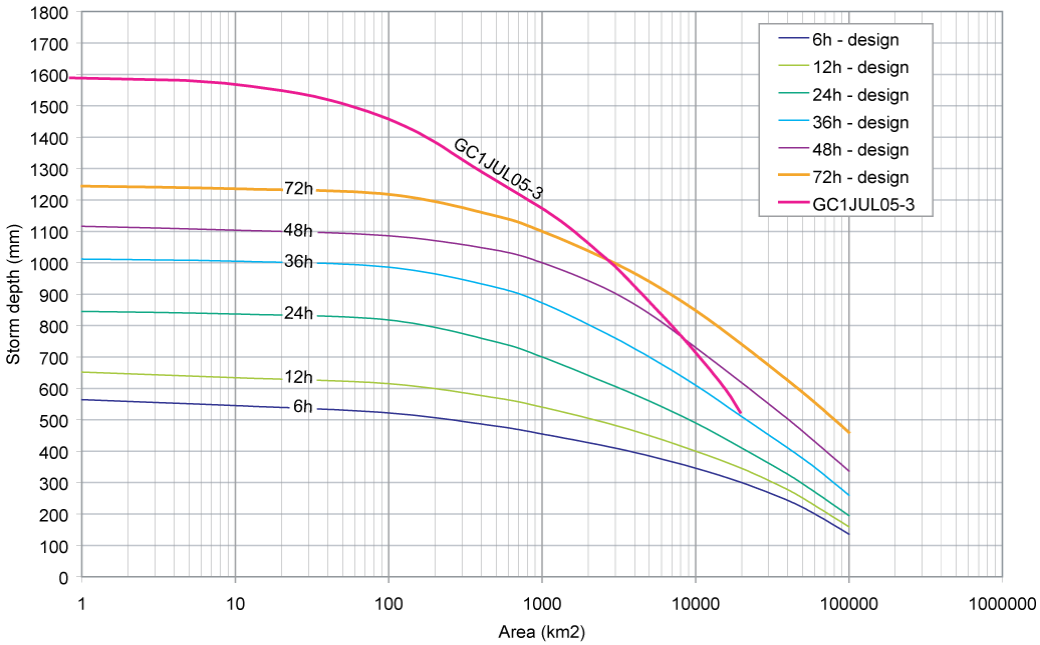

Figure E-8 Depth-duration-area curves for the Coastal Application Zone *Winter* (CAZ-W) and 3-day Gold Coast 2005 event.

Changes in generalised rainfall depths

Changes in generalised depths reflect changes in both relative storm efficiency and moisture maximisation. Changes in the median of generalised rainfall depths (from an earlier to a later period) were assessed for events from the GTSMR and GSAM databases. For events from both databases, changes were assessed for a number of combinations of durations, areas, seasons and zones. After correcting for artefacts in storm selection, significant changes are found for one category only (GSAM, inland, *summer*, 24 h, 100 km^2, decrease from 1950–1975 to 1976–2003).

Typically, the maximum generalised depth derived for the top ranking event (for a given combination of area, durations, zone and season) is not significantly higher than the generalised depth for the events ranked second or third, indicating a degree of robustness in the generalized methods.

Changes in rainfall extremes

Trends in observed rainfall extremes

Based on the methodology for PMP estimation, a large part of the study is concerned with establishing how factors like moisture availability might change under a changing climate. An alternative approach is based on the assumption that changes in PMP are likely to be related to changes in extreme rainfall. Trends in observed and modelled rainfall extremes are therefore assessed.

Observed trends in rainfall extremes were assessed using a range of extreme indices together with trends in the annual rainfall. Trends over the period 1910-2005 are shown in Figure E-9 for three indices: the number of days with more than 10 mm of rain (*R10mm*), the maximum 5-day rainfall totals (*RX5day*) and the proportion of annual rainfall from the upper 5% of rainfall, for days with at least 1mm of rainfall *(R95pT)*; or more simply, proportion from very wet days. Each index allows assessing different aspects of changes in the extremes. *R10mm* may be interpreted as an indication of how the *frequency* of heavy events has changed over the last 86 years whereas *RX5day* indicates how the *magnitude* of significant events has changed over the same period. *R95pT* provides an indication of changes in both the frequency and magnitude of more extreme events. Trends in annual rainfall (from days with at least 1 mm) are shown for comparison.

For coastal south-west Western Australia, all indices indicate a significant decrease over the period 1910-2005. This means significant events in this region may have become *less severe and less frequent* and rainfall totals over this period have decreased. Other regions (such as inland New South Wales and parts of Victoria) show a significant *increase in the frequency of heavy events (R10mm).* A statistically significant *increase in the magnitude of events* (based on *RX5day*) is found for only two locations.

Changes in the proportion of annual rainfall from very wet days *(R95pT)* are spatially less consistent than for the other indicies but there are regions with significant decreases (south-west Western Australia) and significant increases (northern NSW,

southern Queensland) respectively. For most stations, the sign of the trends in the extreme indices agree with the sign of the trends in annual rainfall totals (for days with at least 1 mm rainfall).

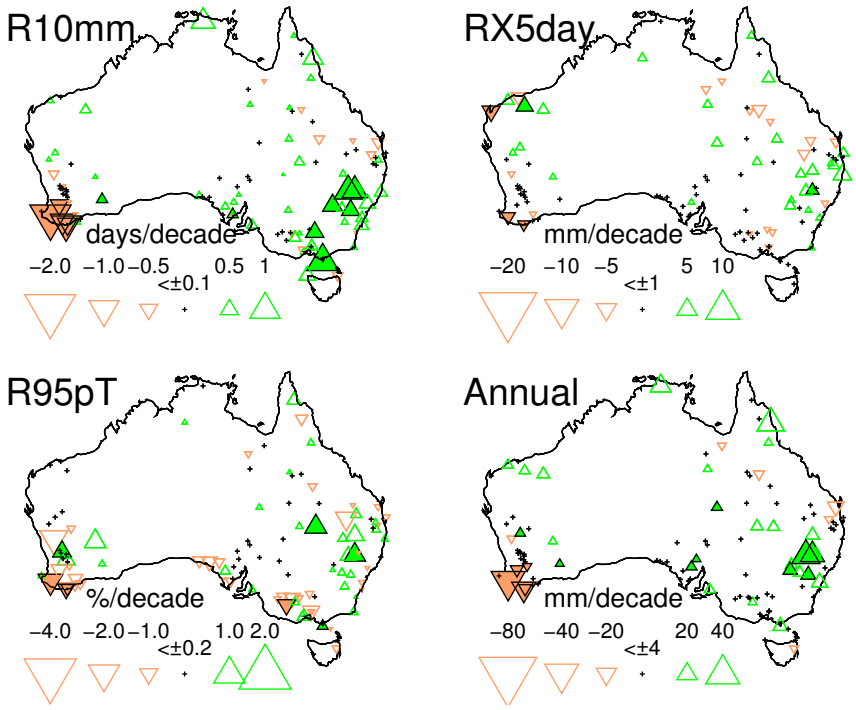

Figure E-9 Trends in extreme rainfall indices and annual rainfall for the period 1910-2005. Trends significant at the 0.05 level are solid with a black outline. Trends with a magnitude of less than 5% of the maximum trend in each figure are shown as a black +.

Model validation

To assess the skill of climate models in modelling rainfall extremes, indices based on observations (Figure E-9) were gridded for comparison with indices derived from climate model data. The three extreme rainfall indices (*R10mm*, *RX5day* and *R95pT*) were calculated from global climate model simulations of 20th century rainfall (using 9 models and a multi-model ensemble). A summary of model performances is shown in Figure E-10 using a combined box-and-whisker plot in which averages are compared using blue symbols. The range of the models' pattern correlation (*R*) and a measure of the spatial variability (E'/σ_{obs}) are represented by vertical and horizontal box-and-whisker plots. A well performing model has high pattern correlation and E'/σ_{obs} near 1.

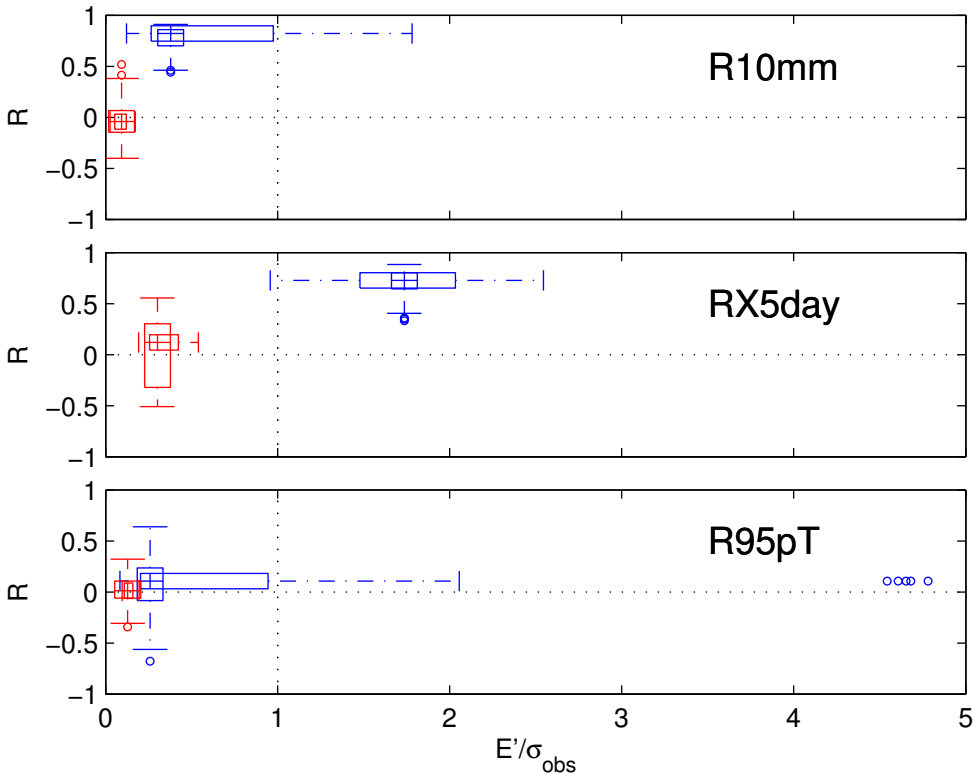

Figure E-10 Pattern correlation (R: vertical box and whiskers) and a measure of spatial variability (E'/σ_{obs}: horizontal box and whiskers) relative to the observations for the mean (blue) and trends (red) for the period 1951-2005. The axis for each box and whisker for (R,E'/σ_{obs}) is centred on the median of its counterpart (E'/σ_{obs},R). The length of the box is equal to the inter-quartile range (IQR). The bars extending from each box are at 1.5 times the IQR, or the limit of data – whichever occurs first. The model run outliers are indicated by circles. A well performing model should sit close to R = 1 and E'/σ_{obs} = 1.

Global climate models have some skill in simulating the spatial pattern for the mean of *R10mm* and *RX5day*. However, the models have very limited ability in simulating the mean for the most extreme rainfall index (*R95pT*). None of the models adequately account for the spatial pattern of trends (red symbols) across all rainfall indices throughout the period 1951-2005. The lack of agreement in model trends could be due to lack of skill in simulating the large-scale mechanisms affecting Australian rainfall such as ENSO.

Projected changes in extreme precipitation

There is a large degree of uncertainty in projected changes in rainfall extremes across the nine models considered. Even if just one model were considered, the range in projected changes across all of Australia, for different time horizons and emission scenarios would be large. However, the three indices may exhibit markedly different changes over time. While the frequency of heavy events *(R10mm)* might decrease from the 2020s to the 2050s and the 2090s, the magnitude of extreme events *(RX5day)* might show a slight increase and the most extreme index *(R95pT)* might increase even more (Figure E-11).

Climate models have limited skill in simulating trends in extreme precipitation. However, both climate model data and theoretical considerations lead to the same conclusion: a warming climate may influence extreme precipitation more than the mean (Randall et al. 2007). Anthropogenic influence may therefore become easier to detect in changes in extreme precipitation (Bates et al. 2008), since extreme precipitation (i.e. that associated with *R95pT*) is more likely to be constrained by the availability of water vapour, which increases globally at approximately 7% per °C increase in global mean temperature (Held and Soden 2006).

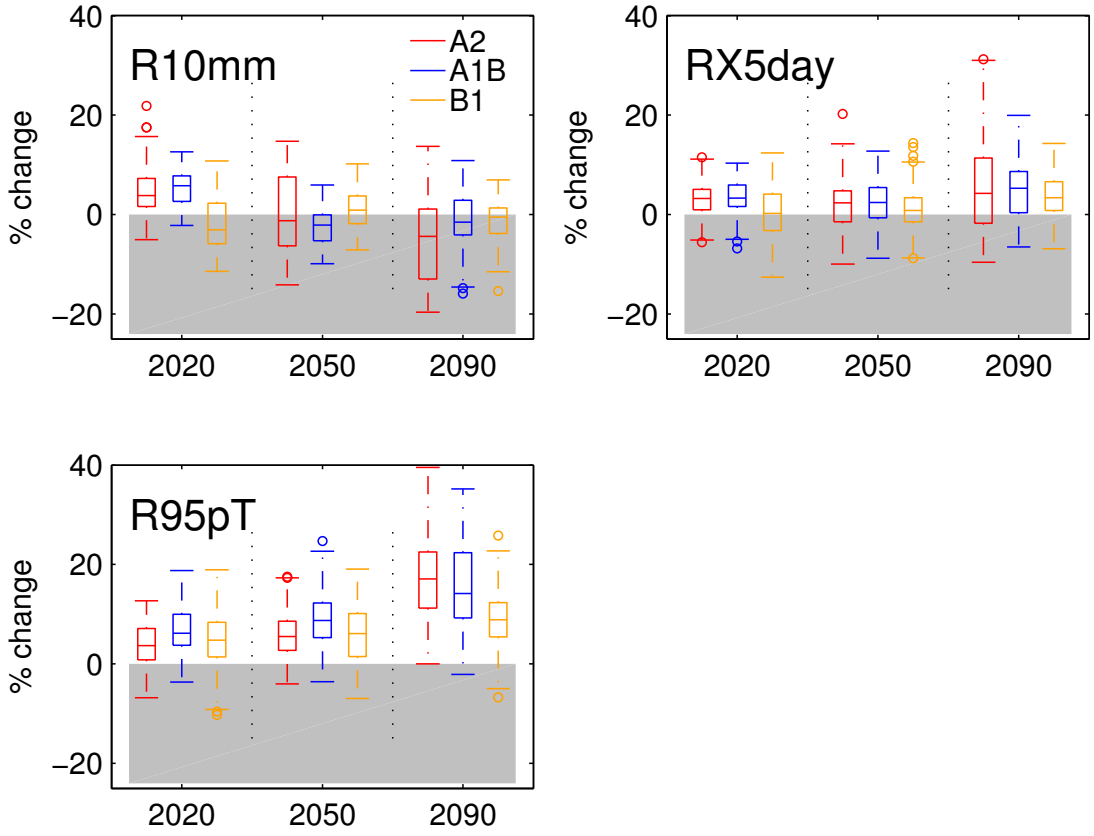

Figure E-11 Box-and-whisker plots summarising the percentage change in the multi-model mean indices for three periods relative to the period 1980-1999 for indices *R10mm*, *RX5day*, *R95pT* and for SRES scenarios A2, A1B and B1. The markers 2020, 2050 and 2090 correspond to periods 2010-2029, 2040-2059, 2080-2099.

4. Discussion

This section will cover some of the more philosophical issues behind the project. Some of these points have been raised in other parts of the report. The purpose of this section is to highlight these issues and following on from that help interpreting results from this study and suggest focus for possible further investigations.

The generalised methods used to derive PMP estimates for locations in Australia are well established and have large databases as their foundation. An assessment (Green and Meighen 2006) showed that Australian PMP estimates are not unrealistically high. Our assessments show that PMP estimates are robust; they are not based on outliers but usually backed up by a number of events.

PMP may be considered a 'worst case scenario' ─ something that could happen if all the factors are 'just right'. One could consider PMP estimates as an asymptote which rainfall events might converge to but should never reach (or exceed). One problem with this approach is that an estimate for this asymptote is constructed using only currently available observations of significant rainfall events. When methods have been revised and databases have been updated in the past, sample sizes have gone up and the picture became more complete. Due to the methods used, such updates have typically led to an increase in PMP estimates. It is possible that in the future, PMP estimates may increase as a result of an increased sample size, even without allowing for climate change.

The basic assumption behind PMP estimation is the occurrence of maximum moisture availability together with maximum storm efficiency. Therefore, to answer the question whether climate change could lead to increased PMP estimates, it is reasonable to start by assessing these two factors based on observations and climate model data. Based on likely changes to maximum moisture and maximum storm efficiency, our investigations did not lead us to conclude that PMP estimates would definitely increase under a warming climate. However:

- For our analysis we have used output from Global Climate Models (GCMs). While these models are physically sound, due to their limited resolution (typically in the order of 3° by 3°) they are not able to resolve some of the processes that lead to extreme rainfall, and parameterisation is used instead. Downscaling approaches (dynamical, stochastic and statistical) can be applied to address this issue. Given the resources and time frame for this project, GCM output had to be used without downscaling the data first. Suitable downscaling approaches are available for some regions in Australia, including south-west WA (Charles et al. 2004, Timbal 2004), eastern South Australia and Western Victoria (Timbal and Jones 2007) and North Queensland (Robertson et al. 2006).

- The basic assumption that a PMP event has maximum moisture availability may not be satisfied in practice (Chen and Bradley 2006). Basing our estimates on this assumption will typically lead us to overestimate PMP. So if PMP estimates were shown to have a tendency to increase based on increases to extreme precipitable water as a result of climate change, there may be some in-built 'buffer' in our current estimates. Current projections using one climate model (Figure E-8) indicate a possibility that the extreme precipitable water may increase in many

areas of Australia by about 5 to 10% and for some cases up to 28%. It is desirable to try and translate changes in maximum moisture availability into changes in PMP estimates. However, it would be overly simplistic to assume that the PMP estimates would increase proportionally to increased maximum moisture availability. This approach would only be defendable if we assumed that increased maximum moisture availability necessarily leads to higher extreme rainfall events. To clarify to which extent this assumption holds, one would have to investigate whether extreme rainfall events do indeed occur under maximum moisture availability.

- There are a number of possible definitions for storm efficiency; only the simplest have been used in this study. More recently, other measures of storm efficiency have been proposed which provide a better quantitative measure of moisture inflow and resulting precipitation efficiency for rainfall events by incorporating upper-air data (available since approximately 1960).

Another way to assess how PMP estimates may change is via physical and meteorological considerations. There have been attempts to develop physical models for PMP estimation (Hardaker 1996) but this is a challenging if not impossible task for all of Australia. One can use climate model output to investigate how extreme precipitation is likely to change under climate change. Our assessments show that individual GCMs do not replicate rainfall totals and spatial and temporal variability well and that there is strong disagreement between projections from different models. These differences are mainly due the limited ability in simulating rainfall producing mechanisms such as El-Nino Southern Oscillation (ENSO) and the Australian monsoon. As a result, it is difficult to have confidence in projections of rainfall extremes.

Despite the lack of agreement between models and observed data, it is likely that rainfall extremes may increase and that these changes are to some degree driven by increasing moisture availability in a warmer climate. A notable conclusion from IPCC Working Group I is that extremes of daily rainfall are very likely to increase, except in regions of large decrease in mean rainfall (Christensen 2007). As a result, both thermodynamical and dynamical factors will play a role in a changing climate (Emori and Brown 2005). According to the Clausius-Clapeyron relation (a thermodynamic relationship) for each 1 °C increase in global mean temperature, the precipitable water increases by about 7%. For the mid-latitudes there is good agreement between estimated changes in extreme precipitation based on this relationship and projections from at least one climate model. According to Pall et al. (2007), increase in extreme precipitation throughout the mid-latitudes may be constrained by the Clausius-Clapeyron relation. However, to fully capture changes in extreme precipitation in other regions, changes in dynamics (and how they affect extreme precipitation) need to be accounted for. These ideas could be used for further investigations: by separately assessing the effects (and their relative magnitudes) of the thermodynamical and dynamical components, it might be possible to reduce the uncertainty in projected changes for extreme precipitation. Results from our study show that while for most of Australia the frequency of heavy rainfall events has increased, such events have become less intense and less frequent in a region with decline in annual rainfall totals. Changes in this region have been attributed to changes in dynamics (storm track shifted polewards).

The model projections considered here were based on emission scenarios developed for the IPCC special report on emission scenarios (Nakićenović and Swart 2000). Of the six emission scenarios available, three have been utilised in this study (B1, A1B, A2), since they are publicly available. Throughout this report, these have been referred to as 'low', 'medium' and 'high' emission scenarios. In 2007, the rate of global greenhouse gas emissions was higher than projected for the 'high' emission scenario (A2), and might have exceeded even the most extreme emission scenario (fossil fuel intensive scenario A1FI; Raupach et al. 2007). Unlike changes in temperature, changes in precipitation do not readily scale with changes in emissions and global temperature changes. Projections based on the high scenario (A2) should be considered the closest approximation while projections based on the medium and low scenarios are less valid.

5. Conclusions

A number of factors relevant to PMP estimation were assessed (using both an event-based and a station-based approach). Some significant increases in moisture availability were found for coastal Australia, and climate models project further general increases, although with some regions of decrease. Very few significant changes in storm efficiency were found, although there is a tendency to a reduction in storm efficiency for coastal parts of eastern Australia.

Typically, no significant changes were found in generalised rainfall depths, but a recent event was record breaking (both in terms of storm efficiency, generalised rainfall depth) if only for the season during which the event occurred (*winter*).

PMP estimates are robust estimates (not typically based on single outliers). Recent significant rainfall events are regularly screened to check whether including these events in the storm databases would increase PMP estimates. There have not been any cases recently where PMP estimates had to be updated.

Long-term trends in rainfall extremes were found for only two regions: a decrease in coastal southwest Western Australia and an increase in parts of northern New South Wales. The fact that trends were found for only two regions implies that for most of Australia current generalised estimates are representative of current climate conditions.

Global climate models do not accurately model the trends of late 20th century Australian rainfall. However, there is an indication that due to the overall increase in moisture availability in a warming climate the most extreme rainfall is likely to increase in the 21st century.

So far we can not confirm that PMP estimates will definitely increase under a changing climate.

Some recommendations for further work

This study did not intend to revise PMP estimates or amend the PMP methodology in order to account for effects of climate change. Below we recommend areas for possible future work which were identified through the course of our study.

- Consider a scoping study to decide whether it would be feasible to attempt modelling PMP using a ***physical model***. Possible starting point could be a model used to investigate likely changes to hailstorms under climate change (Leslie et al. 2008). This would free us from the need to build our methodology on the basis of databases of observed events and would allow including changes of relevant factors in modelling PMP to directly derive PMP estimates under a changing climate.

- Alternatively, ***downscaling*** output from the next generation of climate models could be considered. It is likely that existing approaches could be tailored to ensure they perform well for rainfall extremes. However, this would still not allow us to 'directly' investigate how PMP estimates might change under climate change.

- Investigate by how much we are likely to overestimate PMP when we are assuming that storms satisfy conditions of maximum moisture availability and maximum storm efficiency (conversion of moisture into precipitation) for given locations and seasons. Using a joint probability approach, it might also be feasible to answer the question whether a ***simultaneous occurrence*** of these conditions might be more or less likely under climate change.

- PMP estimates are sensitive to estimates of maximum moisture availability; this is an issue particularly for *winter* events. The problem in deriving the estimates is two-fold: there are potential data and method effects to consider. ***Estimates of maximum moisture availability*** are derived from 24-hour persisting dewpoints, which due to the method and measurement, may introduce an error in the order of 20%. Since dew points are measured at the surface they may not be representative of moisture content throughout the atmosphere. While it is difficult to find a substitute for surface dewpoint observations (especially for events in the 19th and early 20th century), it might be possible to refine the method for estimating extreme precipitable water. This may also involve a re-assessment of whether the assumption of a saturated atmosphere is valid when providing an estimate of maximum moisture availability.

- Extreme rainfall caused severe flooding in parts of Queensland in February 2008 (Bureau of Meteorology 2008), just weeks before this report was finalised. The objective assessments in our study may confirm subjective assessments that rainfall extremes along parts of the central east coast could have become more severe. These changes may have some bearing on PMP estimates. Recently developed measures such as in Rakish et al. (2008) could be used to assess effects of changes in ***moisture transport*** (due to climate variability and/or climate change) on rainfall extremes in this region.

- Mailhot et al. (2007) suggest that rainfall at durations below 24 hours (the shortest duration assessed in this report) could be affected more severely by climate change than rainfall at longer durations. Currently there are no methods in Australia available to derive ***PMP estimates for durations between 6 and 24 hours*** (such estimates are derived by interpolation between the shorter and longer duration methods). For a recent significant event (Mackay, February 2008) the associated return period for rainfall at the 6 hour duration was assessed as particularly high. If there were a requirement to assess how PMP estimates at durations below 24 hours might be affected by climate change, suitable methods for deriving PMP estimates for these durations would have to be developed first.

6. References

Bates, B C et al. (2008). IPCC Technical Paper on Climate Change and Water. Available online http://www.ipcc.ch/meetings/session28/doc13.pdf (accessed 30 April 2008).

Bureau of Meteorology (2008). Report on Queensland Floods February 2008, available online http://www.bom.gov.au/hydro/flood/qld/fld_reports/queensland_floods_february_2008.pdf (accessed 24 April 2008)

Charles, S, Bates, B C, Smith, I and Hughes, J (2004). Statistical downscaling of daily precipitation from observed and modelled atmospheric fields. Hydrological Processes, 18, 1374–1394.

Chen, L-C and Bradley, A A (2006). Adequacy of using surface humidity to estimate atmospheric moisture availability for probable maximum precipitation. Water Resources Research. 42, W09410, DOI:10.1029/2005WR004469.

Christensen, J H et al. (2007). Regional Climate Projections. In: Climate Change 2007: The Physical Science Basis. Contribution of Working Group I to the Fourth Assessment Report of the Intergovernmental Panel on Climate Change [Solomon, S., D. Qin, M. Manning, Z. Chen, M. Marquis, K.B. Averyt, M. Tignor and H.L. Miller (eds.)]. Cambridge University Press, Cambridge, United Kingdom and New York, NY, USA.

Emori, S and Brown, S J (2005). Dynamic and thermodynamic changes in mean and extreme precipitation under changed climate. Geophysical Research Letters. L17706. 10.1029/2005GL023272.

Green, J H and Meighen, J (2006). PMP estimates - are we kidding ourselves. ANCOLD 2006 conference

Hardaker, P J (1996). Estimation of Probable Maximum Precipitation (PMP) for the Evinos catchment in Greece using a storm model, Meteorol. Appl. 3, 137-145.

Held, I M and Soden, B J (2006). Robust responses of the Hydrological Cycle to Global Warming, Journal of Climate, 19 (21), 5686-5699.

Leslie, L M and Leplastrier, M (2008). Estimating future trends in severe hailstorms over the Sydney Basin: A climate modelling study. Atmospheric Research 87, 37-51.

Mailhot, A, Duchesne, S, Caya, D, and Talbot, G (2007). Assessment of future change in intensity–duration–frequency (IDF) curves for Southern Quebec using the Canadian Regional Climate Model (CRCM). Journal of Hydrology 347, 197-210.

Nakićenović, N and Swart, R (eds.) (2000). Special Report on Emissions Scenarios. A Special Report of Working Group III of the Intergovernmental Panel on Climate Change. Cambridge University Press, Cambridge, United Kingdom and New York, NY, USA, 599 pp.

Pall, P, Allen, M R and Stone, D A (2007). Testing the Clausius–Clapeyron constraint on changes in extreme precipitation under CO2 warming. Climate Dynamics 28, 351–363. DOI: 10.1007/s00382–006–0180–2

Rakich, C S, Holbrook, N J H and Timbal, B (2008). A pressure gradient metric capturing planetary-scale influences on eastern Australian rainfall, Geophysical Research Letters, 35, L9813, DOI:10.1029/2007GL032970

Randall, D A et al. (2007). Climate Models and Their Evaluation. In: Climate Change 2007: The Physical Science Basis. Contribution of Working Group I to the Fourth Assessment Report of the Intergovernmental Panel on Climate Change [Solomon, S., D. Qin, M. Manning, Z. Chen, M. Marquis, K.B. Averyt, M.Tignor and H.L. Miller (eds.)]. Cambridge University Press, Cambridge, United Kingdom and New York, NY, USA

Raupach, M R, Marland, G, Ciais, P, Le Quere, C, Canadell, J G, Klepper, G and Field, C B (2007). Global and regional drivers of accelerating CO2 emissions. Proceedings of the National Academy of Sciences, 104, 10288-10293.

Robertson, A W, Kirshner, S, Smyth, P, Charles, S P and Bates, B C (2006). Subseasonal-to-interdecadal variability of the Australian monsoon over North Queensland. Quarterly Journal of the Royal Meteorological Society, 132, 519-542.

Timbal, B (2004). Southwest Australia past and future rainfall trends. Climatic Research, 26, 233–249.

Timbal, B and D A Jones (2007). Future projections of *winter* rainfall in southeast Australia using a statistical downscaling technique. Climatic Change. DOI 10.1007/s10584-007-9279-7

World Meteorological Organisation (1986). Manual for Estimation of Probable Maximum Precipitation. Second Edition. Operational Hydrology Report No. 1, WMO – No. 332, Geneva.

1. Factors used in estimating PMP

1.1 Local moisture availability

In the process of generalising significant rainfall events in order to obtain a PMP estimate, the maximised moisture availability is calculated for all historical extreme rainfall events. Determining the moisture availability for an extreme rainfall event requires knowledge of both the low-level mass convergence, and the moisture content of the air mass. Although it is possible to determine the moisture content of an air mass for a significant rainfall event, there is no satisfactory method to quantify the mass flow convergence. The PMP estimation procedures (WMO 1986) suggest that *'…extreme rainfall events are indicators of maximum rates of convergence and vertical motion in the atmosphere'*. Since this assumption is not of relevance when determining the local moisture availability, it will not be assessed, and will be accepted as valid for the purpose of this study.

1.1.1 Factors used in adjusting for moisture availability

Three factors are used in adjusting for moisture availability. These factors are required at different stages in the generalised PMP methods. The factors may be summarised by using the terms *maximisation*, *standardisation* (both applied to the significant rainfall event data) and *adjustment* (applied to the catchment).

For each significant rainfall event, the moisture content is maximised using the moisture maximisation factor, defined as the ratio of the *extreme* to *storm precipitable water* (MF = EPW/SPW).

- The *extreme precipitable water* (EPW) is an estimate of the maximum amount of atmospheric water vapour available in a vertical column of air, at a particular location and for a particular time of year (usually monthly).
- The *storm precipitable water* (SPW) is the amount of atmospheric water vapour available in a vertical column of air in the surrounding area, and usually prior to the significant rainfall event.
- The moisture maximisation is based on the assumption that a small increase in rainfall is linearly related to a small increase in moisture. Since the EPW varies throughout Australia, comparison of each significant rainfall event's maximised moisture can only be achieved once standardised to a particular location.

Figure 1 shows the standardisation process, with a hypothetical 'standard' location indicated by ✦. The standardisation factor (SF) is defined by $EPW_{standard}/EPW$. The product of the MF and SF, which accounts for the full effects of moisture, is formed from the combined maximisation-standardisation factor (MSF). For a significant rainfall event, *i*, at a particular location and time of year, the MSF is given by

$$MSF^i = \frac{EPW}{SPW^i} \cdot \frac{EPW_{standard}}{EPW} = MF \cdot SF = \frac{EPW_{standard}}{SPW^i} \qquad (1)$$

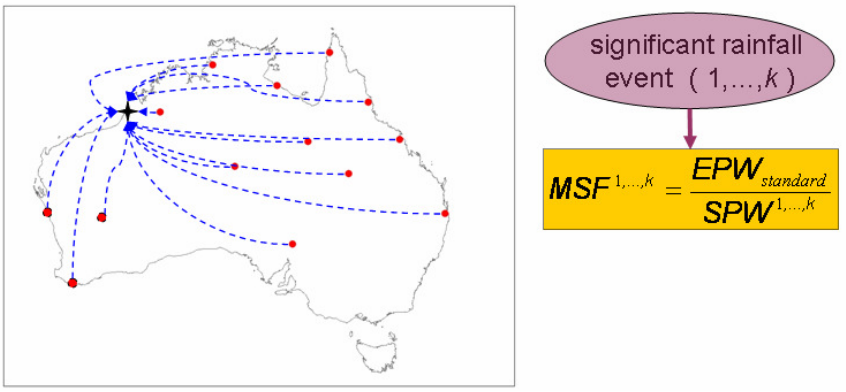

Figure 1 Diagram indicating the standardisation of selected significant rainfall events (event centres indicated by red circles) for selected events (i = *1,..,k*).

In practice, the first factor (MF) in equation (1) is often restricted to a realistic upper limit (here denoted as MF_{lim}). This procedure departs from that indicated in WMO (1986). For the GTSMR[1] this limit is 2.0, which is exceeded for 0.8% of significant rainfall events (corresponding to one event), whereas for GSAM[2] the limit is 1.8, which is exceeded 26% of the time. Minty et al. (1996) noted that GSAM events where MF > 1.8 (particularly during *autumn* and *winter*) may be attributed to occasions when the assumption of a saturated atmosphere is generally invalid, and the usual method of estimating the SPW is not representative of the inflow moisture conditions. When MF_{lim} is exceeded, the rainfall event's MF is reduced to equal the upper limit. Under these situations, the equality for the right-hand side of (1) is invalid, and instead

$$MSF^{i} = MF_{\lim} \cdot \frac{EPW_{\text{standard}}}{EPW} = MF_{\lim} \cdot SF \qquad (2)$$

where $MF_{\lim} = 1.8$ and 2.0 for GSAM and GTSMR events respectively. It should be noted that the value for MF_{lim} is a subjective choice, and does not relate to the frequency distribution of PW at a particular location. Perhaps a better choice would be to define MF_{lim} by the difference in the EPW to the median or mean of the PW distribution for each location. However, application to this analysis is beyond the scope of the current project.

Once the convergence component rainfall[3] for all significant rainfall events has been maximised and standardised[4], catchment PMP estimates can be derived. For moisture, this is achieved by adjusting the standardised moisture availability to a particular catchment (indicated schematically in Figure 2). The moisture adjustment factor (MAF) for a particular catchment, *n* is

$$MAF^{n} = \frac{EPW^{n}_{catch}}{EPW_{\text{standard}}} \qquad (3)$$

Since the MAF is only a function of EPW, assessing for its change is simpler than for the MSF. In (1), (2) and (3) since $EPW_{standard}$ is at a hypothetical location, it can be assumed not to vary in a changing climate.

[1] Generalised Tropical Storm Method-Revised
[2] Generalised Southeast Australia Method
[3] Total observed storm rainfall is considered to be partly due to topographic enhancement. The convergence component is derived by removing topographic precipitation.
[4] For the GTSMR, the convergence component rainfall is also modified by a decay-amplitude factor.

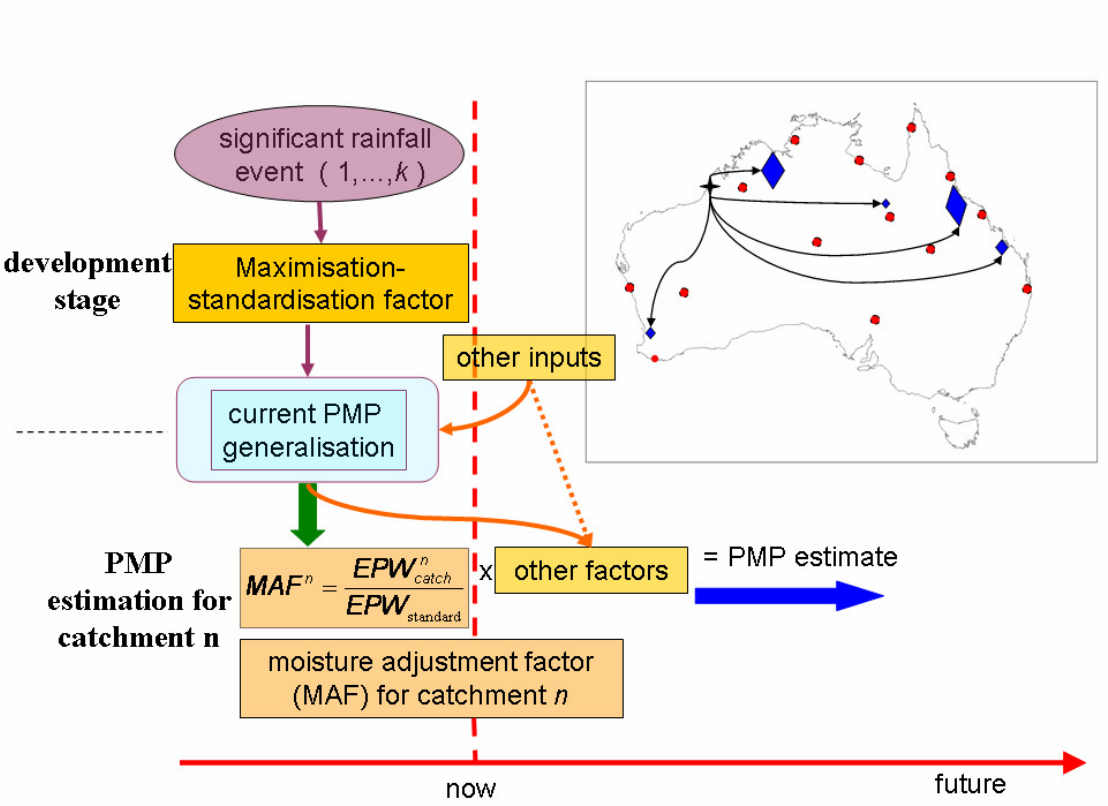

Figure 2 Diagram indicating current PMP estimate obtained by applying the moisture adjustment factor (MAF) for different catchments (blue diamonds in the inset figure).

Estimates of precipitable water

Theoretically, the precipitable water (PW) is derived from the integrated upper-air specific humidity (q):

$$PW = -\frac{1}{g}\int_{p=surface}^{p=200hPa} q(p)dp\,, \qquad (4)$$

where p and g are the pressure and acceleration due to gravity respectively. This is the most accurate measure of the available moisture in the atmosphere, although only if it is within the extent of a significant rainfall event.

Compared with the relatively sparse horizontal spatial distribution of *upper-air* observation locations, the higher density of *surface* dew-point locations often provides a more practical basis when obtaining the SPW and EPW. A surrogate for both the SPW and EPW, derived from dew-point temperatures, has been recommended in the PMP manual (WMO 1986) as the preferred method. However, this method relies on the assumption of a saturated atmosphere with a pseudo-adiabatic lapse rate. Although this assumption may generally be satisfied for tropical rainfall events during *summer* (Walland et al. 2003), it may not generally be applicable for significant rainfall events during *autumn* and *winter* (Minty et al. 1996).

Trends in *surface dew-points* have not been as extensively investigated as trends of suitable indices for *surface air temperature*. One reason for this is that the dew-point temperature is not a directly observable quantity, and it is more susceptible to errors that may arise from instrumentation changes and observation techniques.

Nevertheless, there are a few studies which provide some general conclusions. Results from both the United States and China show an overall increase in surface dew-point and specific humidity in the latter part of the 20th century (e.g. Gaffen and Ross 1999, Wang and Gaffen 2001), although to the authors' knowledge no similar analysis has yet been conducted for surface dew-points across Australia.

To best assess for changes and trends in the moisture availability, changes in EPW and SPW at specific locations will be considered. Although this departs slightly from the generalised aspect of the PMP methodology, this is necessary to make best use of available data in assessing trends in the factors that contribute to PMP estimates.

In coastal regions with limited spatial distribution of reliable surface dew point data, the WMO (1986) recommends using sea-surface temperature (SST). It is suggested that these are representative of the atmospheric moisture, in particular for areas which have little modification of the moist air by passage over land surfaces. The WMO (1986) notes that for Australia, "*extreme coastal dew point temperatures are about 4°C below extreme upwind sea-surface temperature values*", but no suitable reference is given. It was therefore considered worthwhile to assess how reliably the SST can be used as a surrogate for the monthly extreme $24T_d$ at various locations around Australia.

Data and Methodology

Changes in quantities representative of the EPW are calculated over two time periods: 1960-1980 and 1981-2003. There are 19 and 57 locations for the upper-air and surface dew-point data respectively. All upper-air locations are located in the vicinity of a surface dew-point location, although the spatial distribution of upper-air locations is biased towards southern Australia, with only four stations north of 23°S. Surface dew-point stations are predominately located across central and eastern Australia. These stations form part of the high-quality, homogenised dataset of Lucas (2006). Data were homogenised following the homogenisation method of Peterson and Easterling (1994). Although 57 locations are available, due to the limited frequency of observations in the more remote locations, a reduced set of only 38 locations will be used throughout this analysis.

Upper-air data

Precipitable water derived from upper-air data at Australian locations has neither been homogenized nor undergone robust data quality assurance checks. Gaffen (1993) provides the most complete WMO documentation of upper-air radiosonde metadata. The metadata relating to Australia's observations (provided by the Bureau of Meteorology) indicate that between 1960 and 1987 at least five types of radiosondes from three different manufacturers were used. Although the performance characteristics of the pressure and temperature measurement sensor are documented in more detail than those of the relative humidity sensor, there has been no detailed assessment into to the relative accuracy of all quantities, and how these change with height or directly influence PW estimates. Since 1992, the number of observation levels in an upper-air profile has at most locations increased from a median of 12 (mandatory levels) to a median of 47 (significant and mandatory levels). Although

not yet quantified, the increase of data resolution should generally increase both the accuracy PW estimates and the possible spread of the PW distribution. This in turn might influence the estimate of the EPW. Statistics of PW obtained using upper air data will generally be denoted using PW(ua).

Surface dew-point data

Surface dew-point (T_d) observations are used as a surrogate for upper-air precipitable water (PW).The relevant statistics (e.g. median and 90th percentile) are first computed for the representative surface T_d estimate, and these are subsequently converted to PW by assuming a saturated atmosphere with a pseudo-adiabatic lapse rate[5]. The calculation of T_d for a particular significant rainfall event depends on the rainfall event moisture inflow path, the suitability of nearby observation stations and the required duration of persisting moisture prior to a significant rainfall event. Generally, stations that are within the moisture inflow path, and are not adversely affected by nearby anomalous moisture sources (e.g. sea spray or significant wetlands) are considered for analysis. The most representative dew-point for calculating the PW is obtained using a persisting dew-point over a fixed time period. Although the PMP procedures (WMO 1986) recommend using a 'highest'[6] persisting 12h dew-point ($12T_d$), the persisting 24h dew-point, ($24T_d$) may be used as an alternative, especially when observations are infrequent or unevenly spaced. For the generalised methods, the Bureau of Meteorology has always used $24T_d$. Hereafter, PW(T_d) refers to an estimate based on $24T_d$.

In general, the persisting *n*-hour T_d (nT_d) is defined as the minimum from all observations of T_d, across an inclusive period of *n* hours, with the restriction that a set threshold of rainfall accumulation has not been reached. Only discrete observations of T_d are available and nT_d and is a function of the number of observations within the measuring period. $24T_d$ from twice daily observations will be equal to or higher than that determined from observations made at 3 hourly intervals. Daily frequency of observations decreased for only one location in the high-quality dew-point data set. Of the remaining locations, 30% have had an increase from twice daily in 1960 to 5-8 times daily in 2003.

To make the most appropriate comparison between changes in the climatology of PW(T_d) and PW(ua), rainfall-free observations are used ($\leq$ 0.2 mm of accumulated rainfall in the previous 24-h period). Rain-free observations are required to avoid rainfall contamination of dew-point estimates. Uncertainty in estimates for dew-point temperatures are likely to be greater than those for air temperature. Lucas (1996) indicated that inconsistent observer practices, changes to site characteristics and differences in instrumentation or screens can lead to a bias of between -2.0 °C to 1.6 °C at a particular site. An additional positive bias may result when calculating $24T_d$ from twice daily data, rather than using more frequent observed daily data. Overall, it is expected that the uncertainty in estimates of precipitable water derived from $24T_d$ would be in the order of 18%.

[5]This is consistent with the method described by WMO (1986).
[6]The 'highest' persisting 12h dew-point is the maximum value of the persisting 12h dew-point, from a time interval equal to or longer than 12h.

Sea-surface temperature (SST) and upper-air wind data

The monthly gridded SST data (denoted HadSST2) described in Rayner et al. (2006) are used. These are averaged over regions similar to those that are large enough to contain relevant climatology particular to the sea body. Upper-air winds in the lower troposphere were used to characterise the moisture inflow direction. An extensive analysis of the inter-relationship between monthly SST and $24T_d$ was carried out, but no rules could be derived that would allow for changes in SST to be used as a surrogate for changes in the climatology of EPW at a particular location.

Changes in estimates of precipitable water

Maps of seasonal relative changes in median PW, 90th percentile PW and extreme PW (50PW, 90PW and EPW respectively) were generated from both surface $24T_d$ and upper-air data. For each estimate, data were conditioned on the amount of accumulated rainfall, set at different thresholds. Seasonal maps are preferred in this comparison, since they more clearly and easily indicate the relationship in seasonal trends between the different estimates[7]. Changes in PW are reported as relative percentage changes, rather than as an absolute change in PW (mm). The relative change, defined for a generic quantity αPW is given by

$$\frac{\alpha PW_{1981}^{2003} - \alpha PW_{1960}^{1980}}{\alpha PW_{1960}^{1980}} \times 100\% \qquad (5)$$

where α is one of 50 or 90, corresponding to the median or 90th percentile. Also assessed were changes in storm precipitable water (SPW), through the maximisation factor (MF) for selected rainfall events at individual locations and changes in the MF for GTSMR and GSAM events.

Changes in percentiles of PW should be interpreted with caution. Although changes in the median are more reliable when assessing for changes, the median PW does not represent the moisture content required for the extreme precipitable water (EPW). However, since changes in the actual extreme of PW are very difficult to quantify, it is best to assess for trends that occur systematically in each of the percentile groups (50th and 90th percentile). Changes in the EPW are considered first, since they contribute to both the generalisation process (equation 2) and the PMP estimate at a particular catchment (equation 3). It is not necessary to consider changes in $EPW_{standard}$.

Changes in upper-air precipitable water [PW(ua)]

Methods for obtaining upper-air data have undergone significant changes in instrumentation and data quality has generally improved over time. When combined with the relatively sparse spatial distribution (in particular in northern Australia), there is less certainty about these changes compared with changes in surface T_d.

[7] Seasons used are the conventional 3-month climatological seasons, (DJF, MAM, JJA and SON for *summer*, *autumn*, *winter* and *spring* respectively). This contrasts with the different definition of seasons used for both the GSAM and GTSMR.

Climate model output of PW will be used to study projected trends in PW. This is PW integrated over an air column. Therefore changes in PW from upper-air data are reported here. Data were excluded where accumulated rainfall over the 24-h period was greater than 0.2 mm. This approach is consistent with the criterion used with surface dew-point measurements. Hereafter, 'limited' will be used to denote estimates where the 24h accumulated rainfall ≤ 0.2 mm.

An initial test comparing the difference between PW for all rainfall accumulations and PW limited to occurrences of 24h accumulated rainfall ≤ 0.2 mm was carried out for all upper-air locations (Figure 3). For mainland Australia, no location shows negative relative differences of the median (50PW) across all seasons. Only Hobart has a small (< 1% of PW, but insignificant) lower estimate in *summer* and *spring*. For southern and eastern coastal Australia there is a higher estimate in the median during *winter* for some locations, and a higher estimate occurs for *spring* and *autumn* across central, northern and eastern Australia.

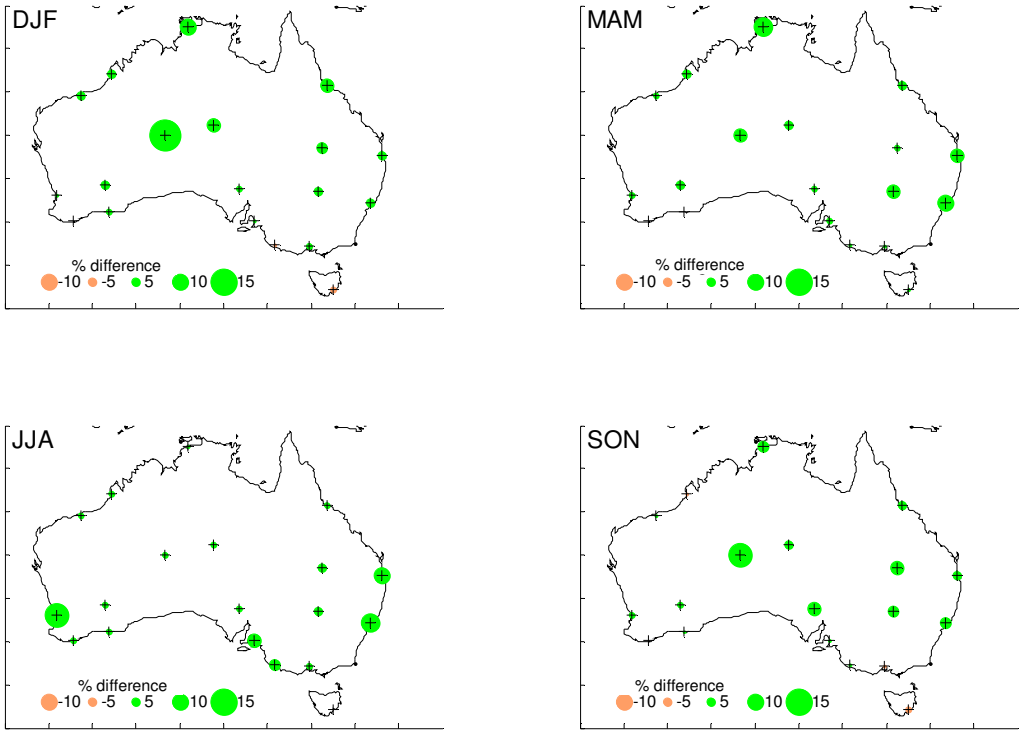

Figure 3 Percentage differences in estimates of the seasonal median [50PW(ua)] excluding rainfall accumulations ≤ 0.2 mm and using all rainfall events for 1981-2003.

The *relative changes* in the limited precipitable water for the seasonal median [50PW(ua)] and 90th percentile [90PW(ua)] are shown in Figure 4 and Figure 5 respectively. The relative changes are across two periods, 1960-1980 and 1981-2003.

For the median, there are increases only across northern Australia, particularly in the north-west, during *summer*. Over the same period, there is a decrease across southern coastal Australia, but with little change for eastern Australia. During the *winter*, northern and inland Australia show the most significant decreases, with almost no change across the southern coastal region. *Autumn* and *spring* have relatively similar

distributions across southern Australia, both indicating a decrease in the median. For South Australia, all locations have a decrease greater than 5% in 50PW(ua) during *summer*, *autumn* and *spring*.

These results contrast with those for the relative change in 90PW(ua) (Figure 5) for which the largest changes are associated with increases in coastal locations. In particular, northern coastal Australia has a greater increase in 90PW(ua) during *summer* and *autumn*, and both southern and south-eastern coastal Australia have an increase during *winter*. The only large decrease (≈-4%) in 90PW(ua) is found for south-west Western Australia during *summer*. The increase in the 90th percentile is reflected in the distribution of the relative change in standard deviation of PW(ua) (Figure 6), where there is no decrease in the standard deviation of PW(ua). These changes may be due to increased in the data resolution from 1992 and improvement in instrumentation.

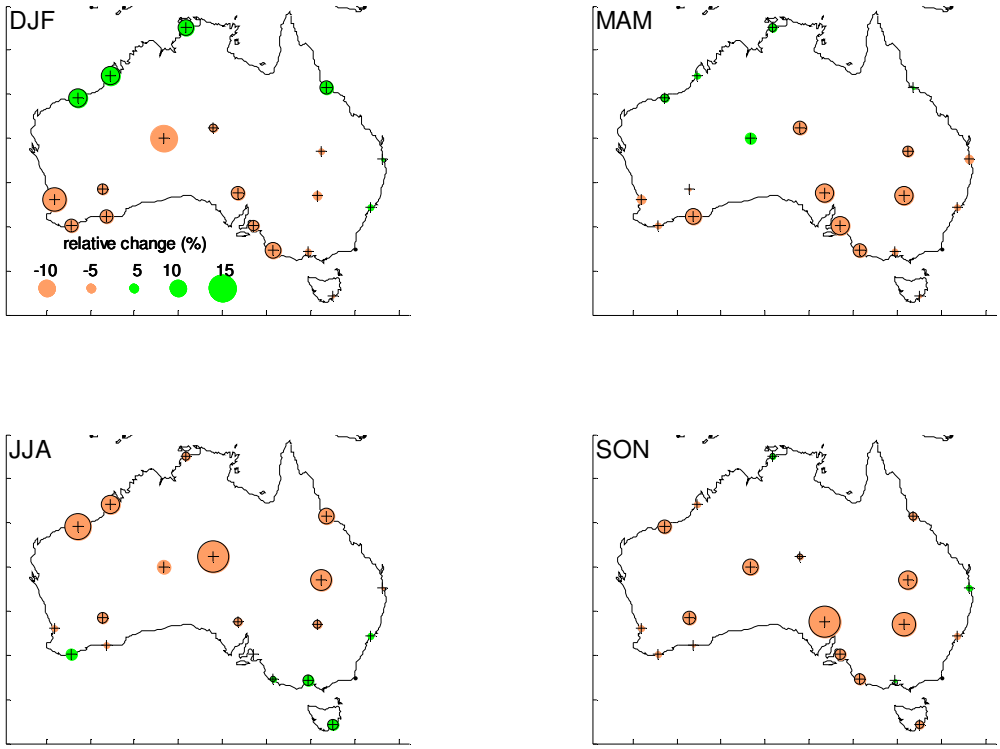

Figure 4 Relative change in the upper-air seasonal median PW [50PW(ua)], limited to occurrences of 24h accumulated rainfall ≤ 0.2 mm for periods 1960-1980 and 1981-2003. The black circle outline indicates change is significant at the 0.05 level.

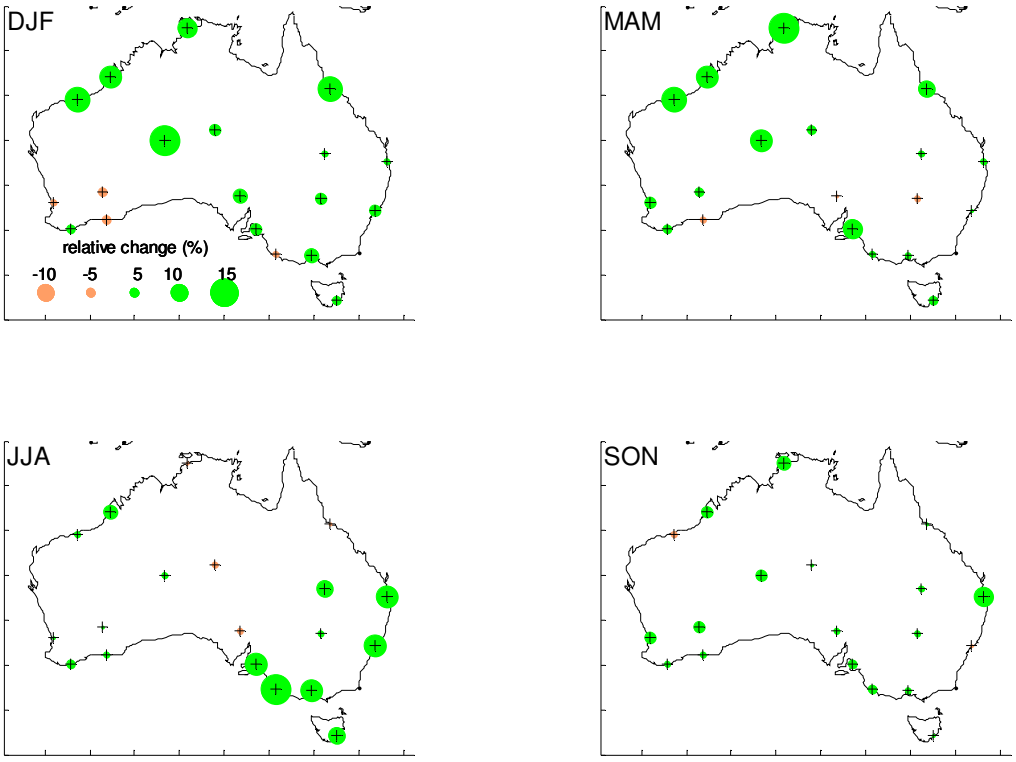

Figure 5 Relative changes in the upper-air seasonal 90th percentile PW [90PW(ua)], limited to occurrences of 24h accumulated rainfall ≤ 0.2 mm for periods 1960-1980 and 1981-2003.

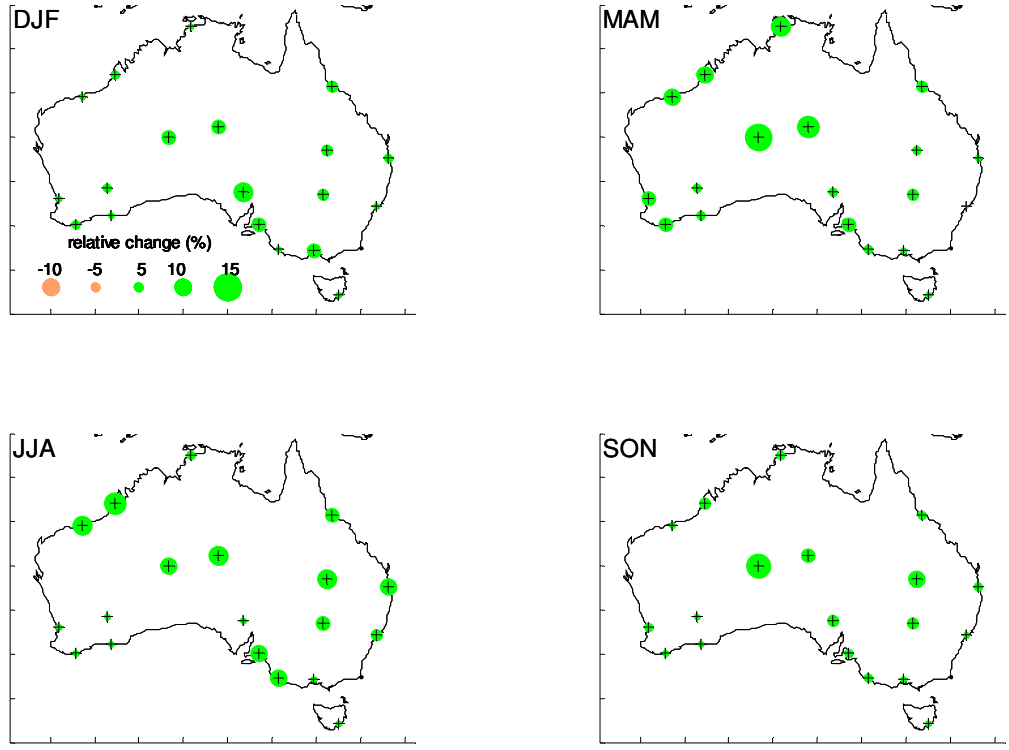

Figure 6 Relative changes in the upper-air seasonal standard deviation for PW(ua), limited to occurrences of 24h accumulated rainfall ≤ 0.2 mm for periods 1960-1980 and 1981-2003.

Precipitable water derived from surface dew points [PW(T_d)]

The PW derived from surface dew point data is a more reliable measure of the change between two time periods. The data used are those which have at least 6 observations a day. The relative changes in the median [50PW(T_d)] are shown in Figure 7. The changes are greatest over inland southern Australia for *summer* (magnitudes are generally greater than 15%). During *autumn* and to a lesser extent during *winter*, a moderate increase occurs for coastal eastern Australia. There are less spatially consistent changes for other regions during each season. Locations tend to exhibit changes of the same sign for the median and the 90th percentile (Figure 8), particularly for *summer* and *winter* and to a lesser degree during *autumn* and *winter*. The similarity on a regional basis is less apparent during *spring* and *autumn*. Assuming that a saturated atmosphere with a pseudo-adiabatic lapse rate assumption is reasonable across all seasons and locations (equivalent to that used when generalising a significant rainfall event for a PMP estimate), these data suggest that an increase in PW has occurred along parts of eastern Australian during *winter* (> 10%). Generally for tropical northern Australia the change in the 90th percentile is smaller than that for the median, and overall there is little change in Tasmania for all seasons, with the possible exception of *summer*.

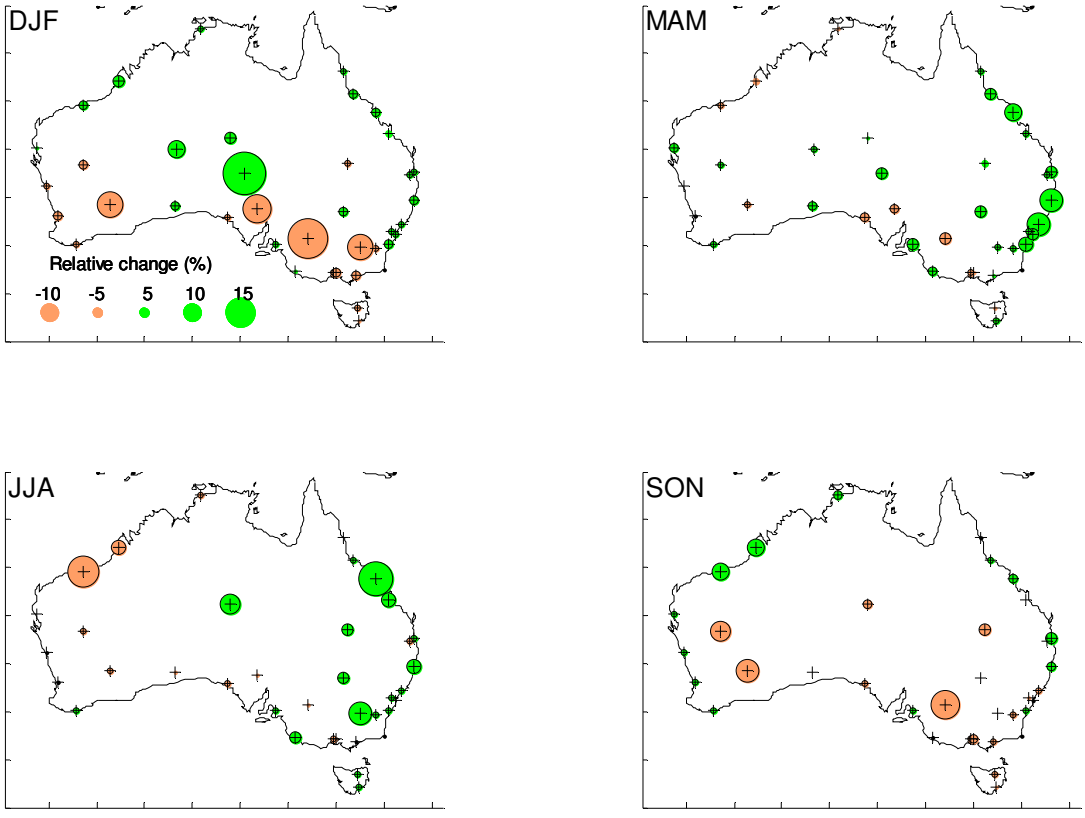

Figure 7 Relative change in median PW(T_d) [50PW(T_d)] with a restriction of at least 6 observations per day. Statistically significant changes at the 0.05 level are outlined.

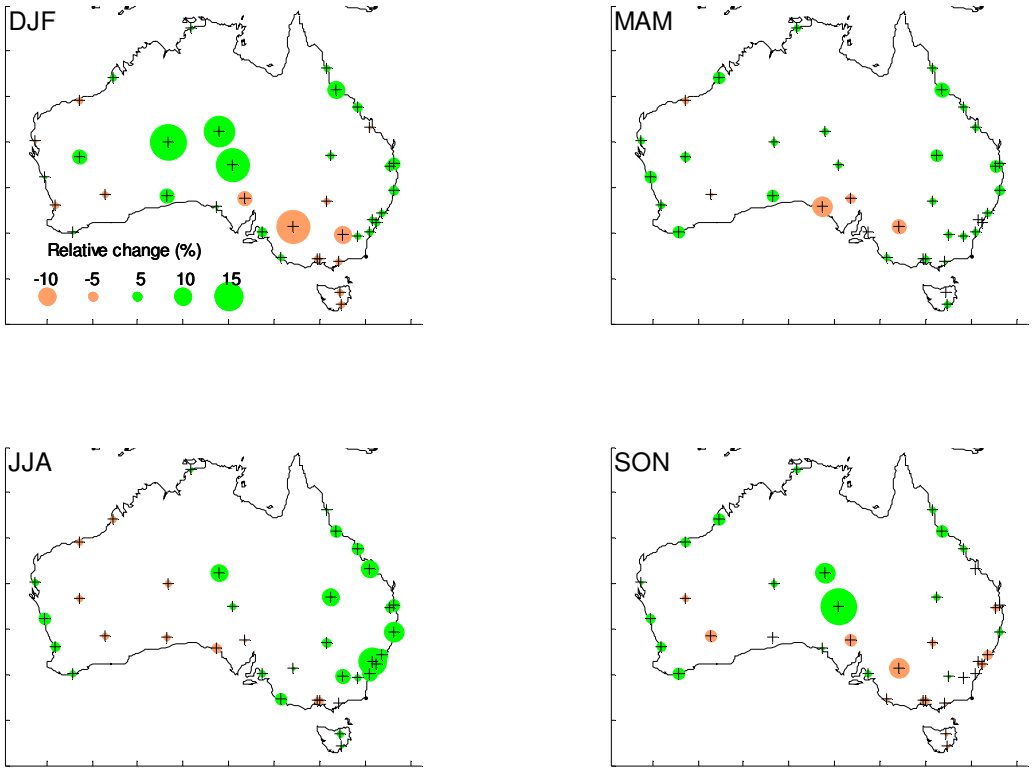

Figure 8 Relative change in 90th percentile PW(T_d) [90PW(T_d)] with a restriction of at least 6 observations per day.

Changes in the extreme index of the daily minimum T_d

The change in PW(T_d) between the two time periods was assessed at the 50th and 90th percentiles. A Mann-Whitney test was performed to judge the significance of changes at the 0.05 level. An underlying assumption is that the shape of distributions for the data for two time periods is similar. This test was used for changes in the 50th percentile, however, it could not be used to assess the significance of change for the 90th percentile. Instead, the *Expert Team on Climate Change Detection, Monitoring and Indices* (ETCCDI) has developed software that provides a standardised method to assess and report change for climate extreme variables (e.g. at the 10th and 90th percentile). Although these methods were tailored to assess changes in daily maximum and minimum temperature and rainfall, one of the indices can be applied to the high-quality 24T_d data.

The most appropriate index (T_dN90p) is that associated with the number of days (represented as a percentage) where the daily minimum T_d is greater than the 90th percentile of an appropriate climatological base period. This index is reported on a monthly basis, and can be averaged over seasons or years. The notation is similar to that used by Alexander et al. (2006)[8], except that 'T_d' is used instead of 'T' (temperature); here 'N' denotes minimum. The climatological base-period used is 1961-1990, with the statistics for daily data averaged over a 5-day running window.

[8] In Alexander et al. (2006) TN90p corresponds to 'warm nights', but since T_d does not exhibit a similar diurnal variation as temperature, this descriptor cannot be used here.

To avoid inhomogeneities resulting from data within the base period, the bootstrap procedure of Zhang et al. (2005) was used to estimate the exceedance rate. It should be noted that although the daily minimum T_d is similar to the 24h persisting T_d, it is not exactly representative as a surrogate for precipitable water, since no segregation according to rainfall accumulation is made. The data cannot be segregated according to rainfall, since the data quality control procedure used by the ETCCDI ensures that there are no more than 3 days are missing each month. Exclusion of rainfall events would significantly reduce the amount of data available for analysis. Therefore care needs to be taken when interpreting these results. Data are restricted to periods (starting from 1960) where at least 6 observations a day are available, to ensure a realistic minimum value.

Figure 9 shows the changes in the median (on a seasonal time-scale) between two time periods for the index T_dN90p. This figure indicates that an increase (decrease) implies that the number of days for which the 90th percentile is exceeded has increased (decreased). The greatest positive and most significant changes are for coastal eastern Australia during *autumn* and SE Australia (but not Victoria) during *winter*. For SE Australia (and in particular for Victoria) there is an overall decrease in T_dN90p, although this is significant at the 0.05 level for only two locations, (Mildura during *summer* and Laverton during *spring*). Nevertheless, these changes are generally consistent with those obtained for 90PW (Figure 8). For all seasons except *winter*, the largest overall (and significant) change is at Townsville.

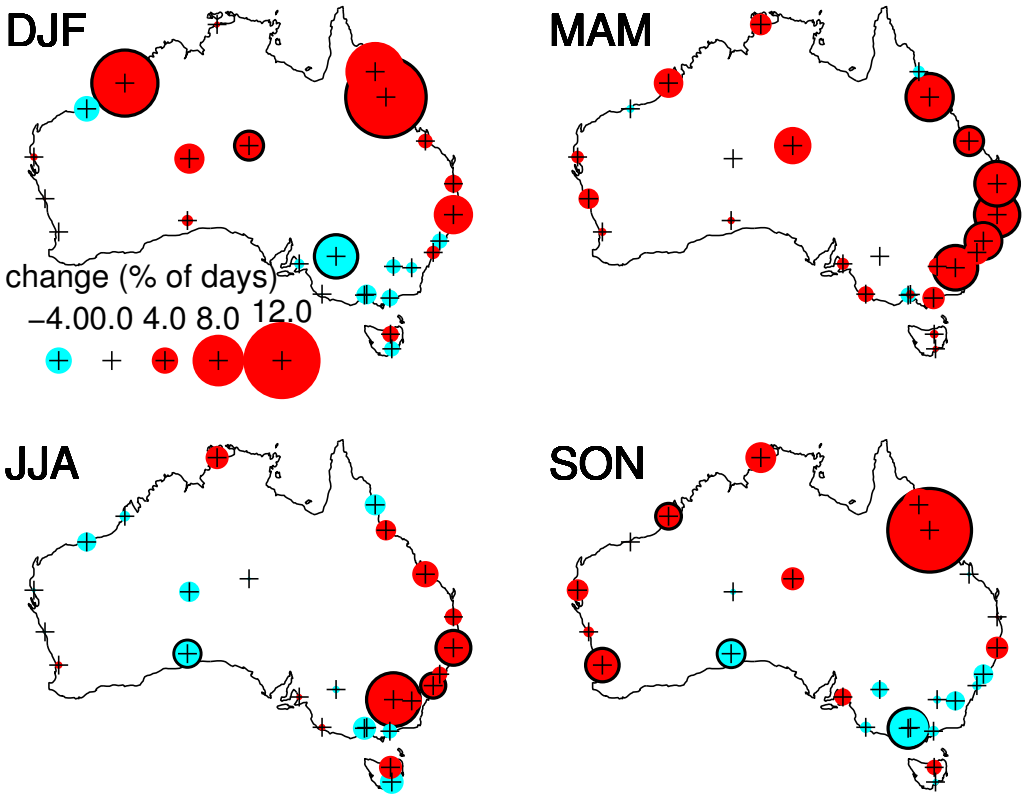

Figure 9 Change in the seasonal median between two time periods (1960-1980 and 1981-2003) for the index TdN90p. Solid symbol indicates change is significant at the 0.05 level.

On a seasonal basis, assessing changes T_dN90 is more informative than assessing changes in 90PW(T_d), since the latter will be influenced by extremes associated with a particular month's local extremes relative to the season.

Changes in the Extreme Precipitable Water (EPW) using the EPW(T_d)

The quantity used in the generalised methods for the EPW is derived from the weekly maximum of rainfall-free 24T_d observations. The EPW is obtained by applying the automated enveloping technique of Jones and Minty (1996) to 24T_d data. The enveloping technique is based on the combination of a two-harmonic Fourier fit and spline fitted to the local maxima of the residuals of the fit. The combined spline and fit provides the weekly extreme 24T_d. The monthly extreme 24T_d is the value of the envelope at the mid-monthly position, and therefore may not actually be the monthly maximum. As a result, this method should not be used for assessing for changes in EPW. It is still reasonable to use the method operationally for PMP estimation, as it follows the procedure in WMO (1986).

Changes in the Storm Precipitable Water (SPW)

The generalised methods require the storm precipitable water (SPW) to be estimated for each significant rainfall event, and these events occur over a period of more than 100 years. Since the SPW may take any value within the PW distribution for that time of year, the method of assessing how the SPW may change differs from that used when estimating change in the EPW. The main difference relates to the large variability in the magnitude of the SPW, which also depends on the location and time of year. An additional difference relates to the fact that SPW had only been derived for storms in existing databases.

Maximisation factor (MF) for events used in the generalised methods

For all significant rainfall events that are used in the generalised databases, the maximisation factor (MF) can be used as a measure of the (inverse) rainfall event moisture availability [see equation (1)]. This quantity equals one for events that have the maximum amount of moisture available (i.e. SPW = EPW) and increases for events with lower moisture availability. To estimate the change in SPW (and hence the MF) between two periods, the EPW has to be assumed constant over the entire time period associated with the generalisation[9]. Consequently, the MF for events provides the most appropriate method to assess for changes in the SPW.

A positive (negative) relative change in the MF corresponds to a decrease (increase) in the relative SPW assuming constant EPW[10]. The MF also allows comparison of events between different locations, and to some extent, between different seasons. The time period used for each generalised database was selected to be as close as possible to that associated with the full period of the high-quality data. Although MF

[9] This is a necessary assumption. To assess for change in the SPW, it needs to be divided by a suitable quantity that is constant, and yet will allow removing dependence on latitude and seasons. Since the current generalised methods do not make allowance for the contributing factors to change with a changing climate, the EPW obtained from the full time period is used. Here, it is reasonable to use the MF of the generalised events. It is implicitly assumed that EPW is constant.

[10] $\Delta MF/MF \approx -\Delta SPW/SPW$

from the generalised events extends as far back as 1883, less emphasis will be placed on the changes between two of the longer periods (1883-1949, compared with 1950-2003), as dew-points estimated from the earlier period have greater uncertainty than those measured during the latter period. There is also reduced coverage of events recorded for inland Australia.

Figure 10 shows the GTSMR maximisation factor for independent[11] storm events for each of the two periods 1950-1975 and 1976-2003, where events of multiple durations (e.g. 2, 3 and 4 days) over the same time period at approximately the same location are only considered once. For the sake of clarity only, the *summer* events (Figure 10a and b) have been separated from those in other months (Figure 10c and d). A Mann-Whitney test did not indicate any significant difference in the MF at the 0.05 level, between the two time periods when the data were segregated by either season[12] or storm type[13]. However, there is an apparent increase in the number of extra-tropical events (from two events for the earlier period to seven events in the later period) that occurred during autumn and specifically during May.

The GSAM maximisation factors for storm events between two periods (1950-1975 and 1976-2003) are shown in Figure 11[14]. The GSAM database used a different event classification compared to the GTSMR. In GSAM, both a moisture source and storm mechanism were identified. Segregating all GSAM events according to both the moisture source and mechanism would have resulted in very small samples for statistical analysis for each type. Instead, the classification was based only on the storm mechanism. Comparison of the MF between two periods for combinations of the storm types and seasons did not indicate any significant change for any combination of storm types or seasons.

[11]Selection of independent events is described in Appendix A1.

[12] Two sets of seasonal groups were used. 'Conventional seasons' were defined according to 3-month seasons (DJF, MAM, etc) and 'GTSMR seasons' were defined following the GTSMR method, with '*summer*': October – April and '*winter*': June – September.

[13]A second test was carried out using all events in the database, although no difference in the tests for significance were found.

[14] The GSAM (Minty et al. 1996) analysed events up to 1995, which was selected as the end year for the present work. However, subsequent analysis indicated no further significant rainfall events have occurred in the period between 1996 and 2003.

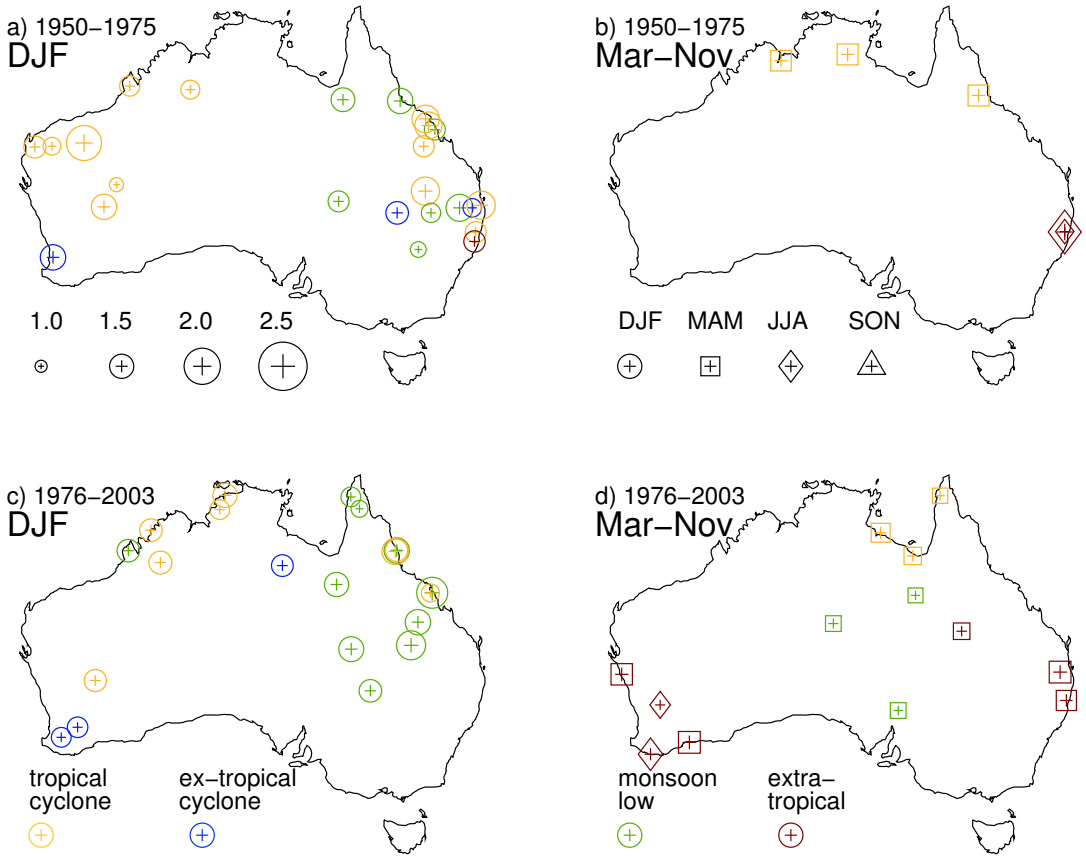

Figure 10 Maximisation factor for each GTSMR event for two periods, 1950-1975 and 1976-2003 (upper (a,b) and lower (c,d) plots respectively), with symbol size corresponding to the magnitude of the MF. Each season is represented by different symbols, with the left (a,c) and right (b,d) plots corresponding to *summer* and all other seasons respectively. Note that there are no *spring* (SON) events. Event type is indicated by colour.

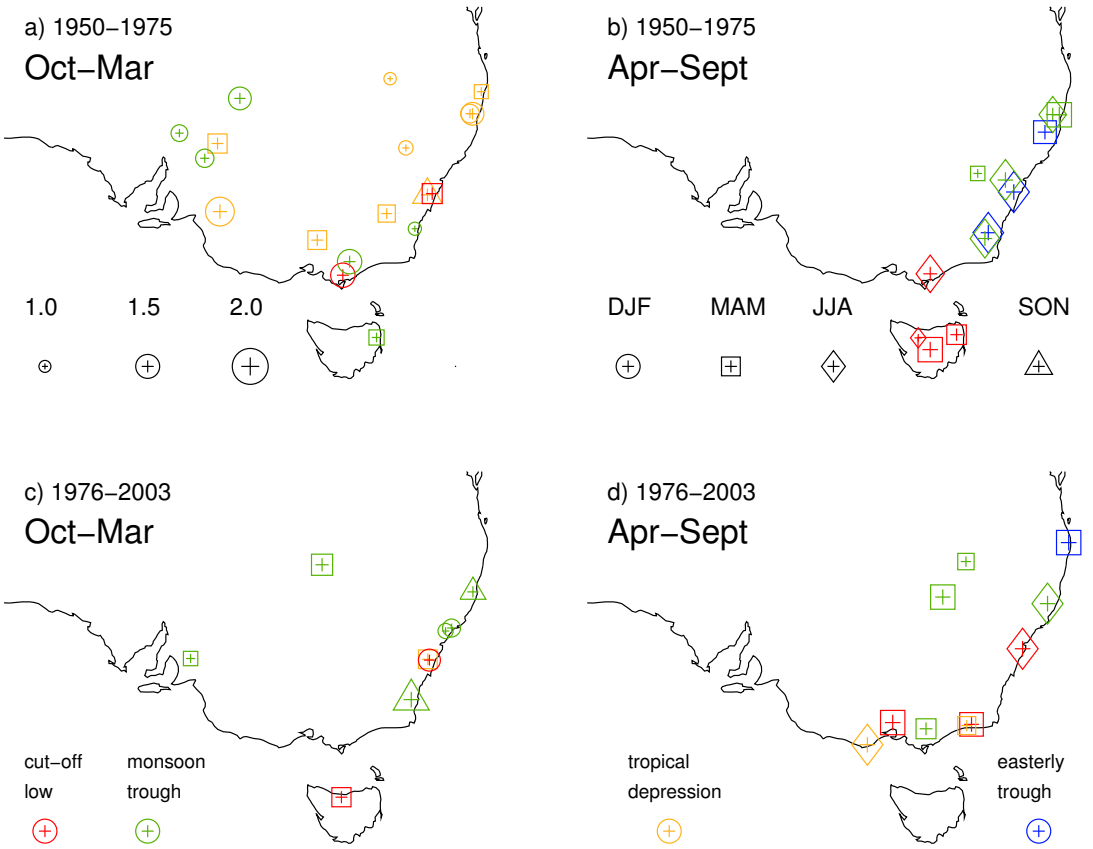

Figure 11 Maximisation factor for each GSAM event during the two periods, 1950-1975 and 1976-2003 (upper (a,b) and lower (c,d) plots respectively), with symbol size corresponding to the magnitude of the MF. The definition of season ranges and storm type classification differ slightly from those used in the GTSMR. The left (a,c) and right (b,d) figure parts correspond to Oct-Mar (GSAM *spring* and *summer*) and Apr – Sept (GSAM *autumn* and *winter*) respectively.

Maximisation factor (MF) for events at high-quality dew-point locations

So that more data can be included in the analysis, the SPW and corresponding MF were computed at 38 locations that correspond to surface T_d locations having at least 6 daily observations. For each location, rainfall events are selected according to ranked rainfall accumulations over 1, 2, 3 and 5 days. A total of 20 independent rainfall accumulation events are selected in each of period (1960-1980; 1981-2003). To be consistent with the generalised methodology, the SPW is calculated from the $24T_d$ in the rain-free period immediately prior to the beginning of the significant rainfall event. The magnitude of the SPW depends on the time of year and the length of time between the start of the event and the heaviest fall within the event. As with the previous analysis, division by the relevant EPW (across the complete time period) is necessary. It is initially assumed that the 20 greatest rainfall events at a specific location can be used as a surrogate for large-area events, similar to those used for the generalised events. The effect of this assumption will be assessed below.

For most tropical coastal locations the resulting MF is generally less than 2.5, although for southern Australian locations, the MF often exceeds 3. The increase in MF with latitude is consistent with the general results of GSAM (which have many more occurrences of MF>2 than for the GTSMR). To ensure that only events that may be reasonably associated with a significant rainfall are considered, we exclude

those with MF > 3.5. The seasonal distribution of the MF between two periods of the events for a selection of locations (with a focus on those in Queensland) is shown in Figure 12. The three locations north of the tropic of Capricorn (Darwin, Townsville and Rockhampton) all have their selected rainfall events in the *summer*. For these events the MF is generally less than 2 and has a relatively small spread, consistent with most GTSMR events in the tropics. Only one inland location (Charleville) had a sufficient number of events such that it could be included in the analysis; even so, the spread in the MF is reasonably large. For the remainder of inland locations, the small number of large rainfall events across the inland of the continent prevented detailed analysis using this method. For the remainder of coastal Australia, the locations Brisbane, Sydney, Mt Gambier and Perth provided the most reliable data where MF did not frequently exceed 3.5. These locations also provided a sample of the estimate of the MF for different seasons.

Therefore, it may be possible to establish some systematic similarities from changes in the inverse of the MF, which is an approximate representation of changes in the SPW.

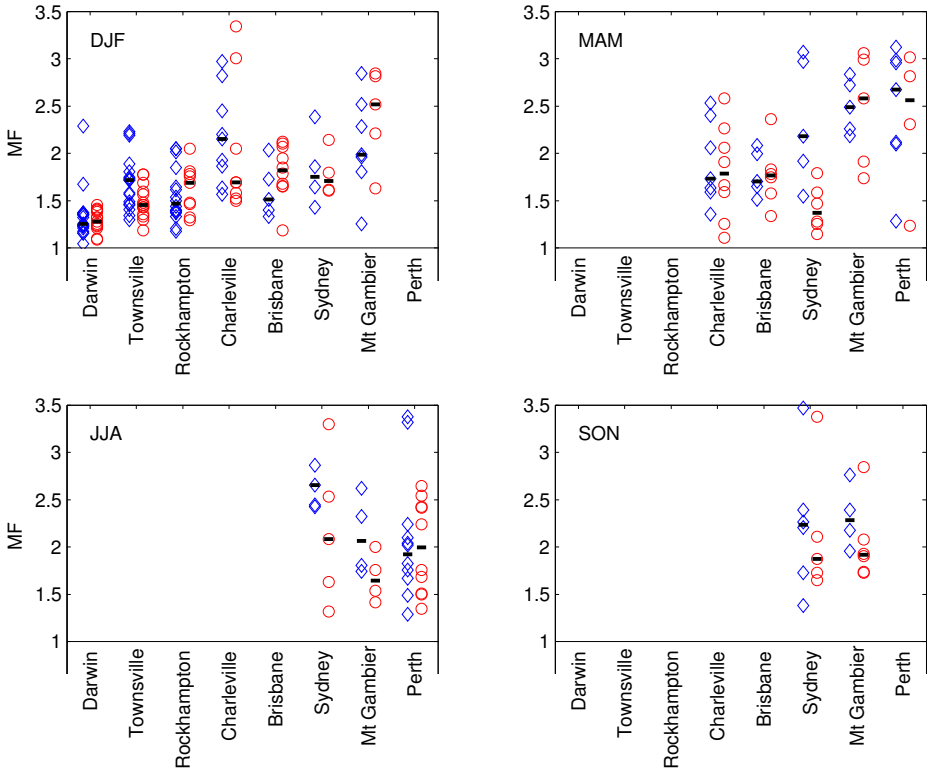

Figure 12 The seasonal distribution of the MF for selected locations within two periods. Blue: 1960-1980; Red: 1981-2003. Symbols are only shown if there are at least 4 events within each period and with MF < 3.5. The median within each period and for each location is indicated by a black horizontal line.

The geographical distribution of changes in the seasonal median MF^{-1} for 38 locations, including those in Figure 12, are shown in Figure 13. Changes in MF^{-1} approximately corresponds to the ratio of median of SPW(1981-2003)/EPW(1960-2003) to the median of SPW(1960-1980)/EPW(1960-2003). Despite the lack of widespread significant change, overall the most spatially consistent results indicate a

decrease in MF^{-1} for the central region of coastal eastern Australia during *summer*. Only two locations (Townsville and Sydney for *summer* and *autumn* respectively) show a statistically significant increase of the SPW relative to EPW. Also of particular note is the lack of any change for Darwin during *summer*, which has only one event where the MF > MF_{lim}. Regions indicating a tendency toward coherent change are SW WA during *winter* (possibly no change, or increase) and SE Australia during *summer* (increase).

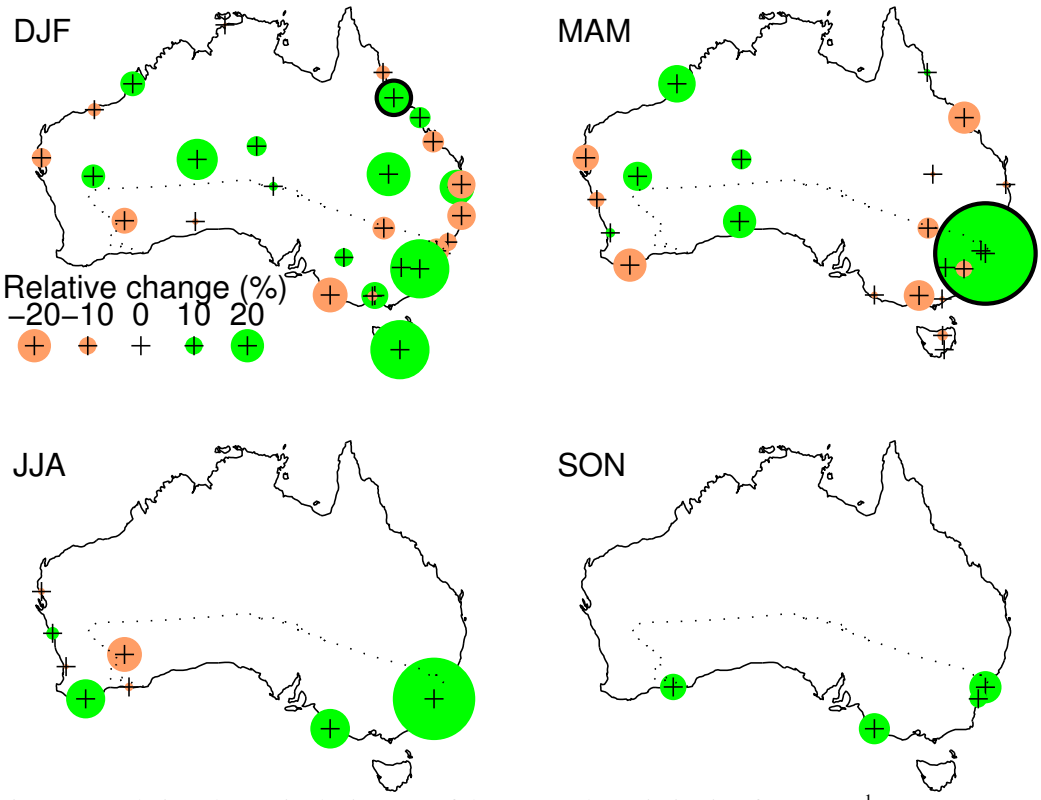

Figure 13 Relative change in the inverse of the seasonal maximisation factor $MF^{-1} \approx SPW/EPW$, between two periods (1960-1980, 1981-2003). A negative (positive) change corresponds to a decrease (increase) in the SPW relative to EPW. The black circle outline indicates change is significant at the 0.05 level. The dotted line indicates the approximate boundary between the GSAM and GTSMR regions.

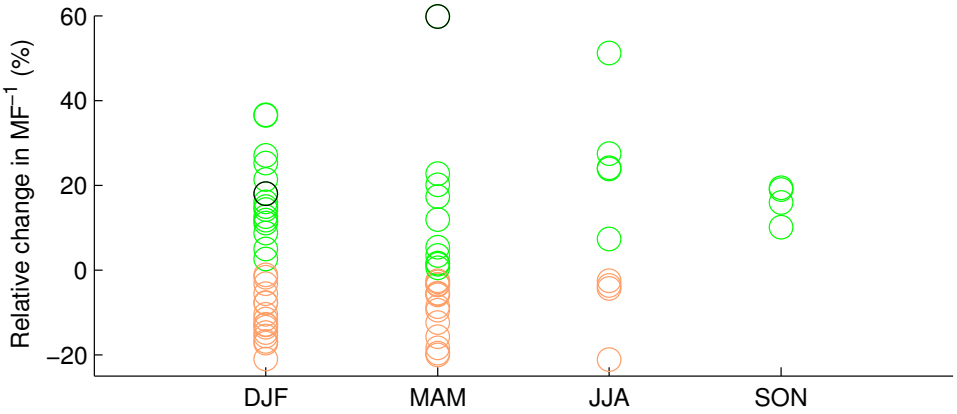

Figure 14 Relative change in the inverse of the seasonal maximisation factor $MF^{-1} \approx SPW/EPW$, between two periods (1960-1980, 1981-2003). The magnitudes from Figure 13 are used. The two black circles correspond to the data significant at the 0.05 level.

Figure 14 provides a summary of these changes, indicating that across Australia, the spread in the magnitude of the change is evenly distributed, particularly for *summer* and *autumn* periods.

Application to changes in the maximisation-standardisation factor (MSF)

Changes in the MSF rely on both the magnitude and changes in the maximisation factor, and subsequently, changes in the standardisation factor. When combined, these are best assessed using the relevant equations (1) and (2). Since the MSF for a particular generalised method is associated with actual significant rainfall events, the change in this quantity will vary with both location and time of year.

For each of GTSMR and GSAM, the combined *summer* and *autumn* events contribute to 90% and 75% of all events, respectively. Apart from SW WA, *winter* and *spring* significant rainfall events generally have not contributed to the PMP envelope for the relevant zone and time period. Therefore for the MSF, less emphasis should perhaps be given to changes during *winter* and *spring* throughout much of the continent.

Equations (1) and (2) describe the relationship between MSF, EPW and SPW. For the GTSMR, equation (1) can be applied to changes in *summer* and *autumn* events across most of the country (since for all but one event $MF < MF_{lim}$). Changes in MSF will be of opposite sign to changes in the SPW.

For GSAM, equation (2) will need to be considered, as well as equation (1); as a result, changes in the MSF will depend on both EPW and SPW[15]. However, since very few locations had significant change in the MF, and consequently the SPW, it is possible that there will be few changes to the MSF. Combined effects of moisture maximization and relative storm efficiency will be discussed in section 1.5.

Conclusions

Precipitable water estimated using two different methods [PW(ua), $PW(T_d)$] was assessed for changes over two time periods (1960-1980 and 1981-2003). PW(ua) was calculated directly from the upper-air specific humidity profile, whereas $PW(T_d)$ was determined from persisting 24h surface T_d data by assuming a saturated atmosphere with a pseudo-adiabatic lapse rate. The T_d data used are from a high-quality, homogenised dew-point data set. Although PW estimated using PW(ua) is theoretically more representative than $PW(T_d)$, changes in instrumentation and observation practices throughout the two periods mean that the changes in the statistics of $PW(T_d)$ are more reliable.

To assess how changes in the moisture availability will affect PMP estimates, the stage at which the PMP estimation process is carried out needs to be considered. For instance, if no new significant rainfall events are added to the generalised database, then the application of the PMP to a catchment need only consider changes in the EPW at the catchment, through the MAF (equation 3). This is the simplest adjustment. However, if allowance is made for future significant rainfall events to occur and be added to the generalised database, then changes in the MSF, as well as

[15] 26% of events have $MF > MF_{lim}$.

changes in the MAF are required to be assessed (equations 1 or 2, then equation 3). This significantly complicates the process, since a future significant rainfall event in one location could change the PMP estimates for all locations within the relevant zone, time of year and for a particular area.

Further work could assess the likelihood that a significant rainfall event will have a maximised-standardised convergence component rainfall that may exceed the current PMP envelope for a particular area and duration, and applicable for a zone and time of year. The likelihood can be used to develop an assessment of risk that may arise if an additional significant rainfall event occurs.

The changes in the seasonal EPW at different locations assist in determining how the MAF may have changed. The change in EPW was assessed by progressively comparing similarities between the changes in each of the 50^{th} and 90^{th} percentiles of PW as well as the extreme index T_dN90. For PW(ua), there is a lack of agreement between the percentiles for most seasons. The large-scale regions for which changes are of the same sign include:

- Central parts of coastal eastern Australian during *autumn* (increase)
- Southern eastern Australia, (Victoria) during *summer* and *spring* (decrease)
- Inland southern Australia (Woomera and Mildura) during *autumn* (decrease)
- Coastal subtropical region of Western Australia during *summer* (no change)

Individual localities with consistent change across seasons include:

- Darwin during *summer* and *autumn* (little or no change)
- Hobart during *summer*, *autumn*, and *spring* (little or no change)

Changes in the maximisation factor (MF) were used to infer changes in the moisture availability (or SPW) associated with significant rainfall events with both the GTSMR and GSAM. Overall, no significant change in the magnitude of the MF occurred for either GSAM or GTSMR events between two periods (1950-1975, 1965-2003). Perhaps of more importance is the change in the number of events, associated with a particular storm type, between two periods. The greatest change occurred for extra-tropical lows during May in the latter period. An analysis of additional non-generalised events using the homogenised T_d data was carried out. Of 38 locations, only two indicated a significant change in the MF, and there was no consistent change in the magnitude of MF, either by month or region. The lack of large-scale significant change in the MF for any generalised or non-generalised event, despite observed changes for the seasonal extremes of PW, may be attributed to relatively infrequent occurrence of the rainfall events. Small sample sizes will also make it difficult to establish future change in the MSF with some certainty.

A simple relationship between SST and coastal extreme $24T_d$, as proposed by WMO (1986), was not confirmed using the present data; however a more complex relationship may instead exist.

1.1.2 Projected changes in precipitable water content

Introduction

Changes in precipitable water based on observations are discussed in section 1.1.1. Upper air data at 19 locations was used to derive estimates of precipitable water for two periods: 1960 to 1980 and 1981 to 2003. Upper air observations were usually carried out once a day between 2000 UTC and 0000 UTC.

To investigate how precipitable water content may change over the next few decades climate model output is required. Projections from the CSIRO Mark 3 model were studied for three 20-year periods centred on 2020, 2050 and 2090.

CSIRO Mark 3 model (CSIRO-Mk3.0)

The CSIRO Mark 3 climate model is a coupled atmosphere-ocean model (Gordon et al. 2002). It consists of an AGCM (Atmospheric Global Climate Model) with land and ice model, and an ocean model. The model has 18 levels in the atmosphere and a further 31 levels in the ocean (including sea ice). Horizontal resolution for the atmosphere is 1.875°. The land model has 6 soil layers with 9 soil types and 13 vegetation types. Heat and water are conserved by the coupling scheme; no flux adjustments are applied. Only direct effects of aerosols are included (using monthly mean sulphate). The precipitable water was sub-sampled to a resolution of 3.75°, twice daily (00 and 12 UTC). To conform to the frequency of upper air data, model output was only used once a day. Comparisons showed that the choice of time had very little impact on the results.

Model output was used for three scenarios: A1B, A2 and B1 (see Figure 15). A2, B1 and A1B are marker scenarios for different 'storylines' (Nakićenović and Swart 2000). A2 describes a very heterogeneous world with an emphasis on family values and local traditions. B1 stands for a world of dematerialisation and introduction of clean technologies. The A1 family describes a world of rapid economic growth and rapid introduction of new and more efficient technologies. Three A1 groups are distinguished: fossil intensive, non-fossil energy sources and a balance across all sources (A1B). The three marker scenarios A2, B1 and A1B were selected to allow giving an indication of the probable range of emission scenarios.

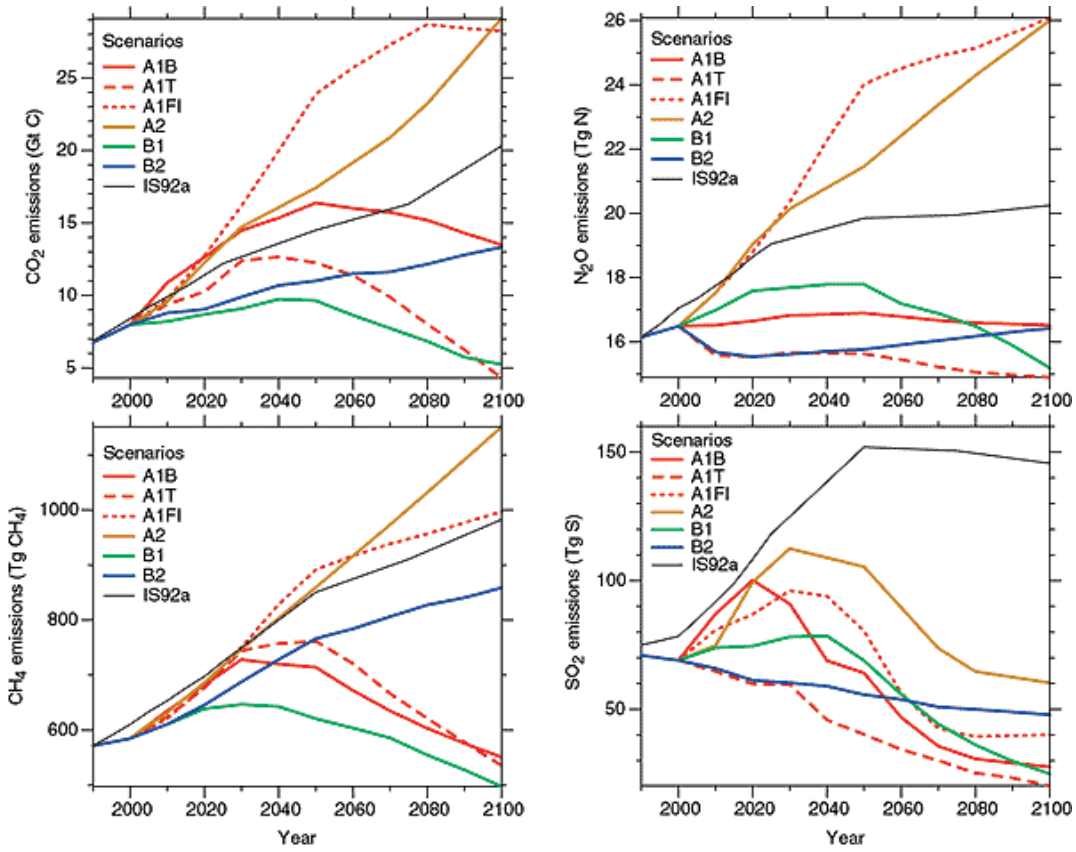

Figure 15 Anthropogenic emissions of CO_2, CH_4, N_2O and sulphur dioxide for the six illustrative SRES scenarios, A1B, A2, B1 and B2, A1FI and A1T. For comparison the IS92a scenario is also shown. [Based on IPCC Special Report on Emissions Scenarios.] source Climate Change 2001: The Scientific Basis.

Validation

Before interpreting projected changes in PW it is sensible to assess the performance of the model by comparing characteristics of observed PW to those from model output. Station data was gridded to the same resolution as the model output.
In the following, three characteristics will be compared: the median, the 90th percentile and the standard deviation.

The model generally suggests a strong meridional gradient in median PW[16] for all four seasons. Based on the observations it appears that average PW might also vary from the coast to the more central parts of the country. It should be kept in mind however that only a very limited number of stations (19) were used to derive these maps. In general, the spatial patterns derived from observations and model output respectively, match reasonably well and the seasonal variation in the observations is also found in the model output.

For the 90th percentile of PW the seasonal variation and the spatial patterns again show some good resemblance between modelled and observed data. However, there is a tendency for the model to underestimate the 90th percentile. This effect is particularly strong in *winter* but less pronounced in *summer*.

[16] PW was available twice daily, at 12 and 00 UTC. Model output was used for 00UTC. Comparisons showed that the choice of time had little impact on the results.

The standard deviation was calculated for model output and observations respectively. Typically the values from observations are considerably higher than for the model data. Such behaviour is not unusual for climate model output - even if the average conditions are reasonably well matched it can still prove a challenge to get the extremes right and it is not unusual for the variability in the model to be somewhat lower than in the observations. However, the spatial pattern is reasonably well replicated; with maxima in standard deviation occurring in similar locations for observed and modelled data respectively.

It is concluded that output from the CSIRO Mk3 model can be used to investigate trends in median and extremes of precipitable water, including their seasonality and spatial patterns. Caution however is advisable with regards to the magnitude of projected trends.

Changes in median and 90th percentile for the A2 scenario

It is sometimes assumed that changes in the mean (or median) of a climate variable will give an indication of how extremes are likely to change, with changes typically of the same sign but stronger for the extremes. In the following projected changes in both median and 90th percentile of precipitable water will be discussed. Changes here are expressed as percentage changes. These are calculated as

$$\frac{90\mathrm{PW}^{\,\mathrm{later}} - 90\mathrm{PW}^{\,\mathrm{early}}}{90\mathrm{PW}^{\,\mathrm{early}}} \times 100\% \qquad (6)$$

For the **2020s** there is a tendency to regions with an increase in median PW, both with respect to magnitude and spatial extent. No statistical testing has been undertaken but it is possible that these changes are not statistically significant. For the 90th percentile areas of decrease appear slightly more organised (particularly in *autumn*) and decrease in percentage terms is stronger. When comparing median and 90th percentile of precipitable water, there is some match between areas with increase and decrease respectively. For the **2050s**, although the median of precipitable water shows an area with decrease in the northwest of the country for *winter* there is little indication of a similar trend for the 90th percentile. For the **2090s** a decrease in the median of precipitable water in *winter* is matched by a decrease in the 90th percentile.

Changes in 90th percentile of precipitable water for scenarios A2, A1B and B1 and 2020s, 2050s and 2090s

Generally extreme precipitable water content is projected to increase from the 2020s to the 2050s and the 2090s. This increase is most pronounced for scenario A2.

For the **2020s** the 90th percentile of PW (90PW) shows regions of decrease as well as increase depending on scenario and season. All 3 scenarios show a decrease in *summer*; in western parts of Australia for A2; in the south and the west for A1B and over central and some southern parts for B1. *Autumn* similarly shows decrease over central parts of Australia for all three scenarios which is strongest for A2. For *winter*

90PW increases over most of the continent but all three scenarios indicate the possibility of decrease in 90PW over parts of Queensland and NSW. Projections for *spring* are less uniform - A1B projects an increase stronger than in any other season and over all of Australia while A2 shows some increase in northern parts of the country and even a slight decrease in south and east. B1 shows a pattern somewhere between projections from scenarios A1B and A2.

For the **2050s** the 90th percentile of precipitable water generally shows an increase. *Autumn* is a marked exception to this rule. Projections from A2 show decrease over central parts of Australia which is even more pronounced in B1. In A1B a similar area stands out because it does not show an increase. So while the exact magnitude of the decrease is not known, it does occur under all three scenarios and at similar locations and ties in with changes seen for the 2020s. For *winter* there is a possibility that 90PW could decrease in parts of NSW and Queensland. This effect is strongest in B1 (but still small in relative terms). There is some indication of such a decrease in A1B but not in A2. For *spring* a decrease in PW in the northwest and some parts of the southeast is projected in A1B. This decrease is stronger for B1 and extends over a larger region.

For the **2090s** A2 shows the strongest increase in 90PW. However, remarkably this scenario also shows drying over significant parts of the continent for *winter*. A1B like A2 shows some regions with decrease in 90PW with locations partially matching with regions that are projected to show a decrease in A2 and B1. B1 shows the strongest decrease over central parts of Australia but in *autumn* rather than *winter*. So in summary there is some possibility that for the 2090s - against the backdrop of typically increasing 90PW - there could be some regions showing a decline in 90PW. These are a) a region around Adelaide (in all three scenarios with slightly different magnitude but always for the same location and the same season: *summer*), b) for central parts of Australia (in *autumn* or *winter*) and c) for the northwest and the southeast in *spring* (from all three scenarios).

Figure 16 summarises the relative changes four all three scenarios. Changes are expressed as percentage difference to the modelled 90th percentile for 1990s.

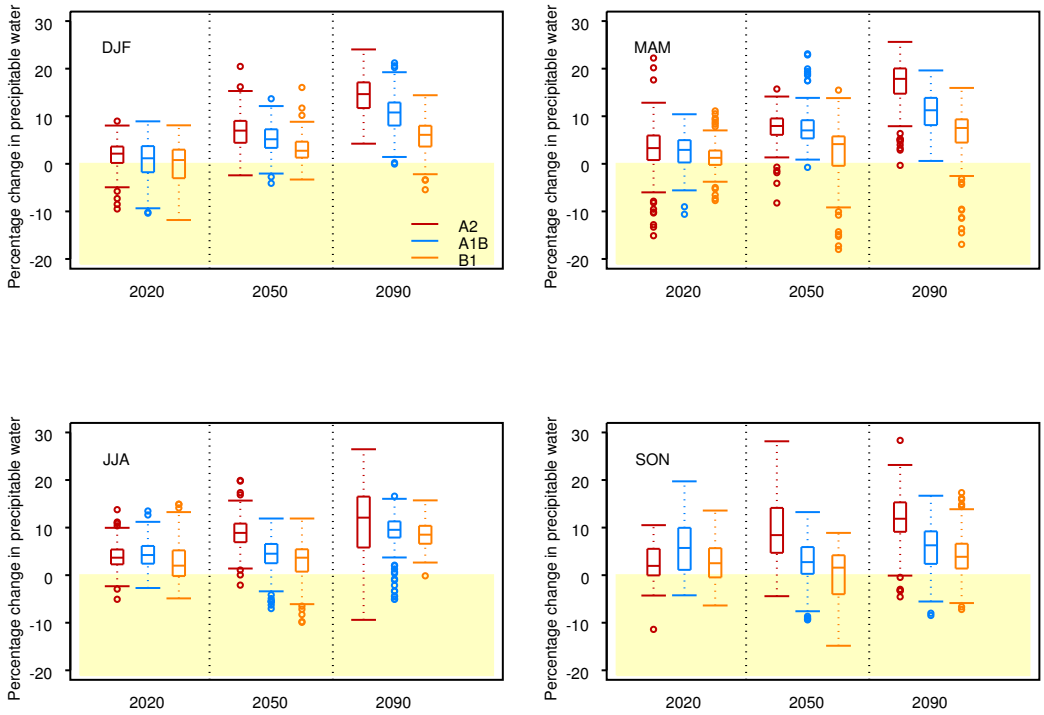

Figure 16 Percentage change in precipitable water by season for scenarios A2, A1B and B1. The box-whisker plots[17] indicate the range of projected changes (solid horizontal lines at the ends of the dashed vertical lines). The line dividing each of the boxes is the median (indicating the average change), the circles indicate outliers.

Summary

Model validation showed that the magnitude of the projected changes in the 90th percentile of precipitable water should only be considered a best guess. Three scenarios were investigated and the results (including seasonality of changes, spatial patterns and magnitude of changes) quite strongly depend on the scenario. Ideally output from a number of models would be used but precipitable water is typically only available monthly, not daily as required for these analyses.

Even given these caveats, it does not appear sensible to apply an across-the board adjustment to the extreme precipitable water. Such an adjustment should take into account location, season and time horizon. According to output from the CSIRO Mk3.0 model changes over Australia vary between -15 and +22% for 2020, between -8 and +28% for 2050 and -9 and +28% for 2090.

Changes in precipitable water need to be seen in conjunction with the seasonality of events producing significant rainfall at a given location. Since storms are standardised and maximised when deriving PMP estimates, increases in one location and decreases in another may affect the resulting PMP estimate.

[17] The box indicates the first and third quartile. The distance between these quartiles is also referred to as 'interquartile range' (IQR).The horizontal short lines at the end of the dashed vertical lines are plotted at 1.5 IQR. Values outside this range are considered outliers and are plotted as open circles.

1.2 Depth-duration-area curves

1.2.1 Changes in depth-duration-area curves

Introduction

For each of the storms in the databases, depth-duration-area curves had been constructed. Generalised and maximised depth-duration-area curves are enveloped to derive a PMP design storm with maximum moisture content and maximum efficiency. Depth-duration-area curves allow estimating rainfall depths for specified areas and durations.

Possible changes in depth-duration-area curves have been investigated using storms from two multidecadal non-overlapping periods. Based on the depth-duration-area curves, rainfall depths were derived for three durations and the 11 standard areas. Significance of changes in depth-duration-area curves will be judged based on changes in rainfall depths derived for these durations and areas. Possible effects of these changes on maximised depth-duration curves will be discussed.

Generalised Tropical Storm Method Revised (GTSMR) enveloping

The Generalised Tropical Storm Method has recently been revised (Walland et al. 2003) and is applicable over most of mainland Australia. The results presented in this section are based on events from the GTSMR database.

Deriving maximum storm depths requires enveloping generalised storms. The maximum storm depths for a given area will depend on the generalised rainfall derived from an observed event. Note that of the top 10 events in Figure 17 (according to their 72 h rainfall depths for the coastal zone during *summer* for 1000 km^2), only two occurred after 1950 (1974, rank 5 and 1979, rank 9) with the remainder occurring prior to 1920. It is concluded that estimates of generalised rainfall depth are not driven by storms that occurred over the last few decades. This is explored further in Section 1.5, where changes in the generalised rainfall depth for both GTSMR and GSAM events for each season are assessed.

Maximum storm depth for standard areas derived from the GTSMR storms database

Storm depth estimates were derived for 3 durations (24, 48 and 72 hours) and for three periods. One period is based on the full GTSMR storms database (January 1893 – June 2001), two others are shorter periods: 1950 to 1974 (Period A) and 1975 to 2000 (Period B). These are shown in Figure 18. To allow comparing estimates for the different periods, rainfall depths were in all instances derived from ‘raw’ events, that is no maximisation or generalisation was applied. This allows assessing changes in depth-duration-area curves separately from any effects from changes in moisture availability. Figure 18 shows that:

- The estimate using all storms in the GTSMR database estimate is never exceeded by the estimates for either of the shorter periods.

- For the two longer durations (48 and 72 hours) and for areas below 5000 km^2 estimates from the later period are higher than those from the earlier period. Conversely for the 24 hour duration, estimates from the earlier period are typically higher than those from the earlier period.
- Estimates for large areas (say above 10,000 km^2) show little and no systematic differences.

Differences in storm depth estimates depend on the area and duration considered, and no clear pattern emerges.

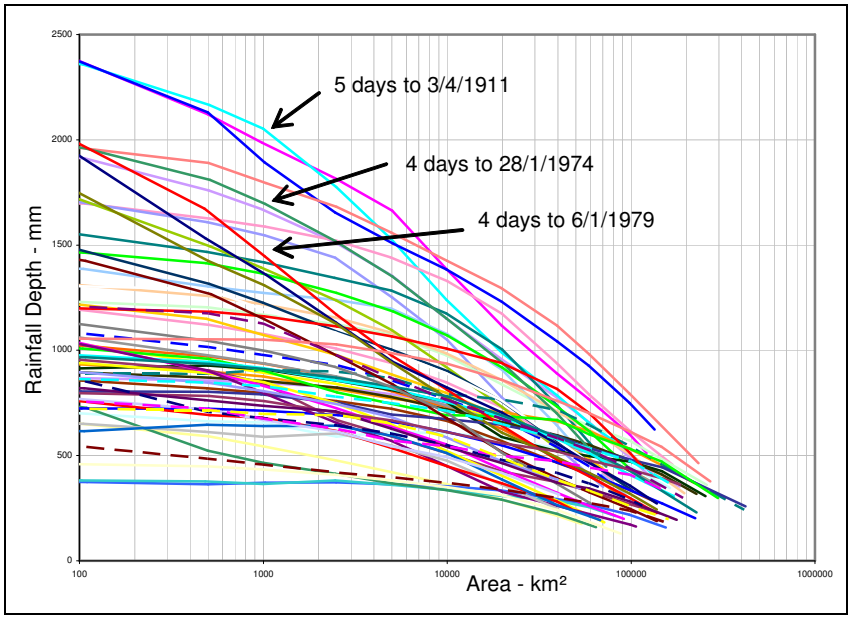

Figure 17 Generalised rainfall depths for the coastal application zone during *summer* for 72-h duration (shown for areas above 100 km^2).

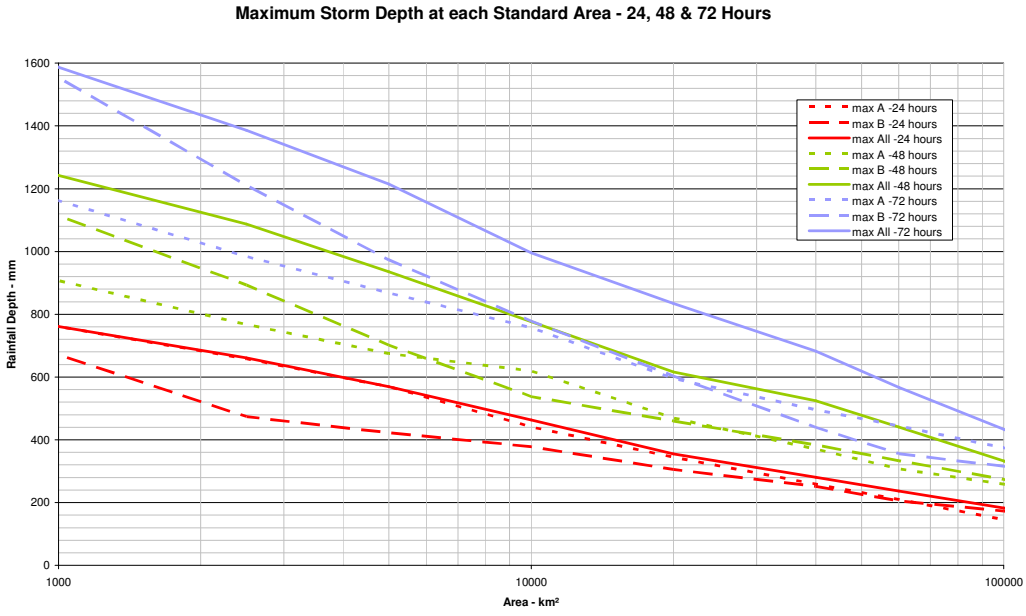

Figure 18 GTSMR maximum storm depth for standard areas. Period A is 1950-1974 and period B is 1975-2000.

Maximum rainfall depths for two periods

Looking at just the two shorter periods (1950 to 1974, Period A and 1975 to 2000, Period B) one can compare rainfall depth estimates across areas of different size.

Each curve in Figure 19 shows the estimated depths for an area of given size and for a range of durations (24 to 72 hours). The top curve with the steepest gradient represents 1000 km^2. The lowest and flattest of the curves stands for 100,000 km^2.

Estimates range from below 150 mm (for the earlier period, area 150,000 km^2 and 24 hours) to above 1500 mm (later period, area 1000 km^2, duration 72 hours).

- Rainfall depths increase with duration and the increase tends to be stronger for smaller areas.
- Gradients are steeper for the later period (for regions equal to or less than 10,000km^2). This leads to higher estimates at longer durations (for 10,000km^2 and above) even though estimates for the 24h duration are typically lower for the later period.

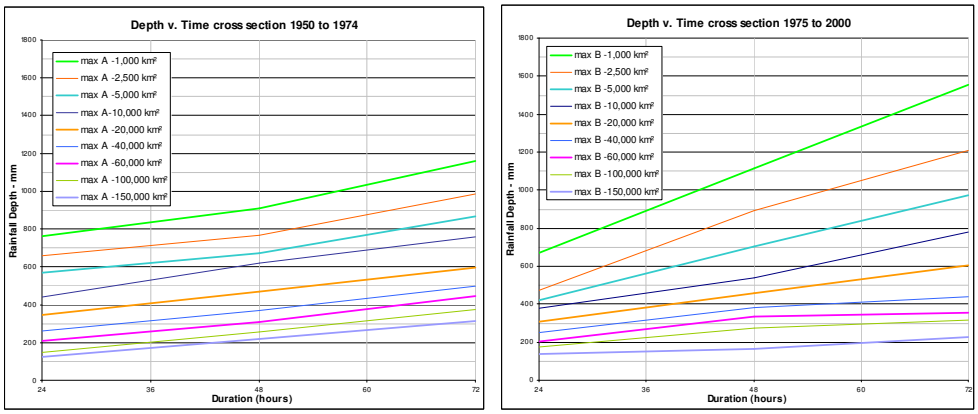

Figure 19 Depth v time cross sections. Left for period 1950 to 1974, right for 1975 to 2000.

Average rainfall depths for two periods

Average rainfall depths for the two periods can be compared. These comparisons are based on 'raw' rainfall depths; this means storms were neither adjusted for where they occurred nor for their moisture content. Such comparison could be flawed if certain geographical locations were preferred during a particular period. The geographical spread of significant events for the two periods is shown in Figure 20. (The location of a small number of significant rainfall events in southwest Western Australia is not shown. These events occurred during the *winter* months in the later period in connection with frontal systems. They do not form part of the GTSMR storms database.) The pattern is broadly similar for the two periods.

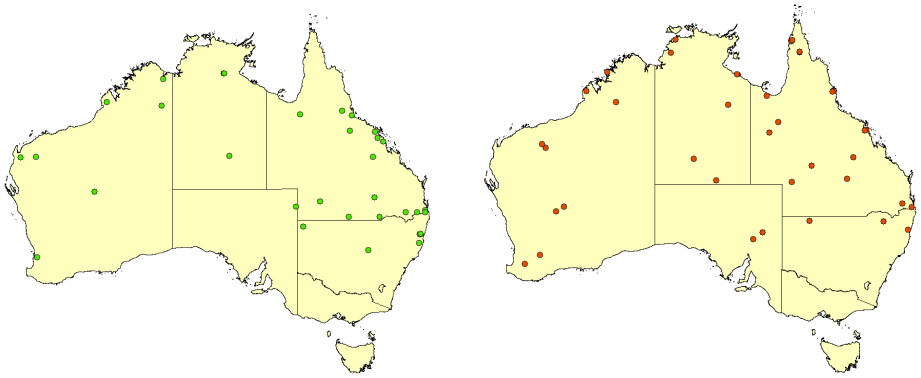

Figure 20 Significant events for the periods 1950 to 1974 (left) and 1975 to 2000 (right).

Based on Figure 21 one can compare average rainfall depths for the two periods for the three key durations. The yellow and green curves in Figure 21 show the median of the estimates of rainfall depths from significant events for two periods (1950 to 1974 and 1975 to 2000 respectively) for three durations (24, 48 and 72 hours) and for eight areas (1000, 2500, 5000, 10000, 20000, 40000, 60000 & 100000 km²).

The average rainfall depths are (with few exceptions) lower for the later period. So the average rainfall depths from significant events have not increased over the last few decades.

Most severe events

Estimation of PMP involves the process of enveloping which uses the maximum rainfall depth from the generalised depth-area curves for a given area and duration. However, when assessing changes over short periods (e.g. 25 years), including or excluding one particular event may have a significant impact on the enveloped rainfall depth, in contrast with changes for the median rainfall depth. As large events within the database occur relatively infrequently, it is necessary to assess for changes in the extremes over longer time scales. This is discussed in detail using the generalised depths of significant rainfall events in Section 1.5.

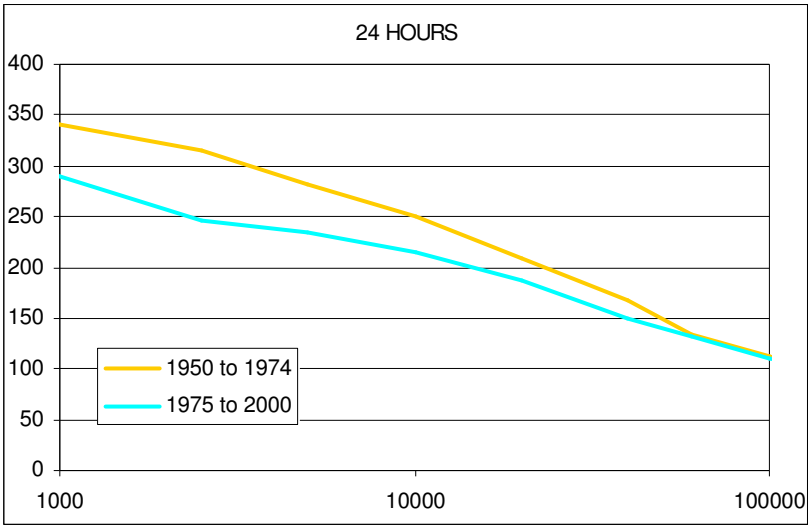

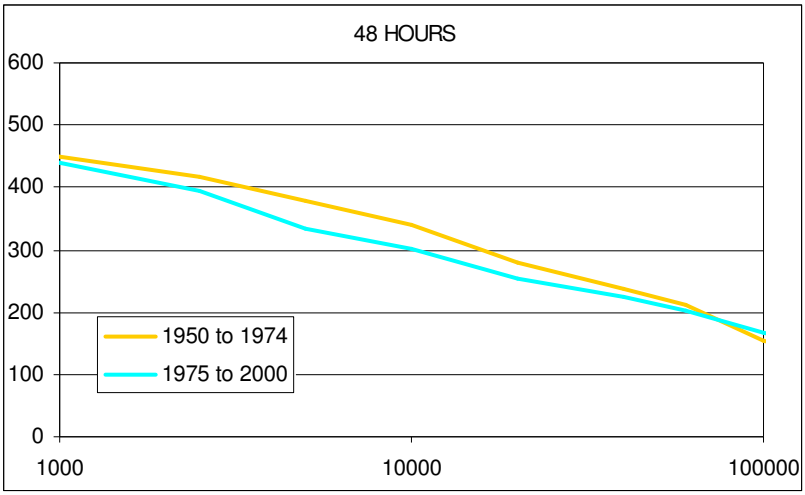

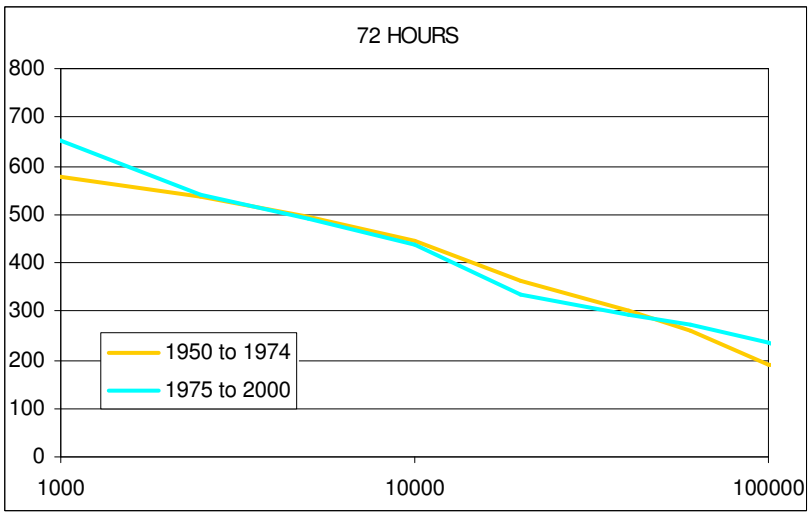

Figure 21 Median storm depths for 24, 48 and 72 hours (based on 'raw' storms).

Frequency of significant events

The frequency of significant events does not affect PMP estimation. However, it is still worth investigating whether the frequency of these events might have increased. This is against the background that observations (and to some degree model results) suggest that the frequency of the most intense tropical cyclones (category 4 and 5) might be increasing at least over some regions of the globe (Webster et al. 2005). A high-quality cyclone dataset for the Australian region is currently being prepared. However, the intensity is usually judged in terms of pressure or depths of the system rather than accompanying rainfall. While there are papers in the literature suggesting that in some areas precipitation from tropical cyclones could be decreasing (Ren et al. 2006) others suggest an increase in precipitation (Knutsen and Tuleya, 2004).

Average (median) and extreme storm depths were derived for 3 durations (24, 48 and 72 hours) and 3 area sizes (1000, 10,000 and 100,000 km^2) for two periods (1950-1974 and 1975-2000). For 1000 km^2 the average storm depth is always lower during the later period. However, variability and maximum storm depth are higher for the

later periods, both for 48 and 72 hours. Station data was gridded to the same resolution as the model output.

Depending on the event in question it may not be possible to derive estimates of storm depths for all durations and all areas (say for shorter events and those extending over small areas). For others, all 9 storm depths can be derived. The number of storm depth estimates is larger for the second part of the record (for all combinations of durations and areas). Altogether 200 estimates are available for the earlier period but 311 for the later period (ratio 0.64). These estimates are derived from 35 events in the earlier period and 42 events in the later period (ratio 0.83). It appears that the increase in the number of events can only partially explain the number of additional estimates available for the later period. Assuming that there are no issues with the methodology, this might imply that more events could exhibit a tendency to become longer and more widespread.

Summary

GTSMR estimates were derived for the full period (January 1893 to June 2001) and for two shorter 25-year periods for a number of durations and areas.

- Out of the top 10 events only 2 came from the last 50 years while six events occurred in less than a decade during a very active phase early in the 20th century.
- The number of significant events is higher in the later period (42 events compared to 35 in the earlier part of the record).
- The average storm depth (as defined by the median) is lower for the later period except for very large areas.
- Rainfall depth estimates are derived through enveloping which means only the maximum generalised rainfall depth at a given duration will directly feed into the PMP estimation.
- Based on the last 50 years or so and using data from the GTSMR storms database, there is no evidence that the rainfall depth from the most significant events has increased.
- Australia is a continent with a high degree of rainfall variability, both spatially and over time. Mechanisms such as El Nino Southern Oscillation (ENSO) and Interdecadal Pacific Oscillation (IPO) strongly modulate rainfall on different time scales. Observed changes in rainfall depth may be due to natural climate variability or climate change (or a combination of the two). On the other hand it is possible that natural climate variability impedes detecting changes due to a changing climate.

1.2.2 Changes in design rainfall estimates

Introduction

PMP estimates can be considered estimates of (very) extreme precipitation. Studying the effect of climate change on design rainfalls may therefore yield valuable insight into possible effects of climate change on PMP estimates.

Assessing changes in PMP Design Flood due to changes in the spatial distribution is outside the scope of this study. However, suggestions that climate change could lead to increase in extreme rainfall depth in mountainous areas but decrease elsewhere (Abbs, 2004) will be followed up by investigating changes in spatial patterns of design rainfalls.

A pilot study was recently undertaken at the Bureau of Meteorology to develop techniques for revising design rainfalls. These techniques can be used to explore whether any changes in the design rainfalls can be detected temporally or spatially.

Pilot study

Design rainfalls are used in the design of hydraulic structures such as bridges, stormwater drains and roof gutters. Such structures are designed to carry a specific volume of rainfall with an acceptable risk of failure that can be attributed to a particular structure. Design rainfalls are commonly provided in the form of intensity-frequency-duration (IFD) curves. These provide the annual exceedence probability that can be assigned to a particular rainfall intensity of a particular duration for a specific location. The current design rainfalls provided by the Bureau of Meteorology were published in Australian Rainfall and Runoff, 1987 (Institution of Engineers, 1987) (ARR87).

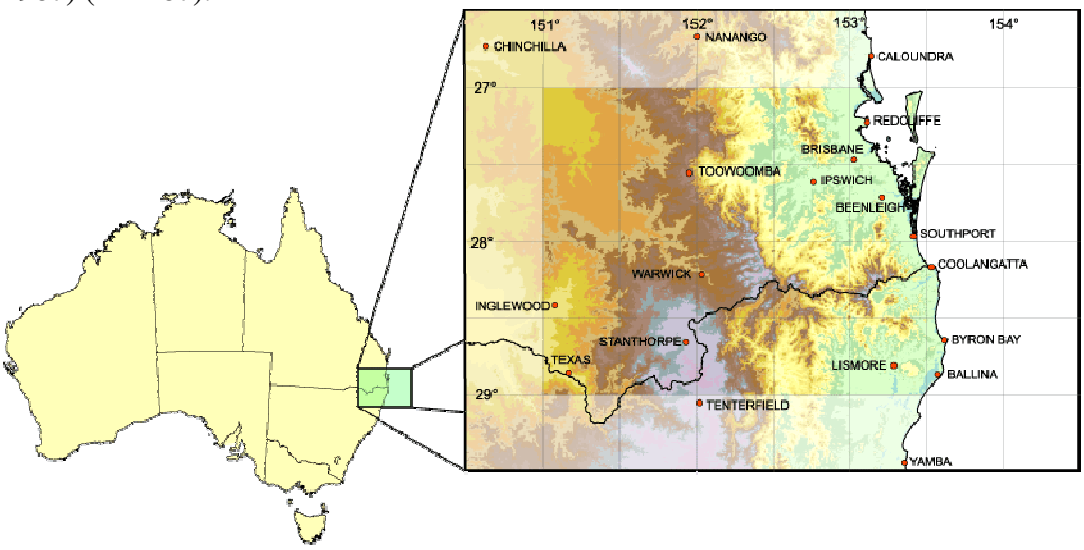

Figure 22 Location of the pilot study area.

The aim of this pilot study was to review methods for estimation of design rainfalls (Jakob et al. 2005). This included comparing design rainfalls derived using the method of L-moments and rainfall data up to end 2006 with estimates derived for ARR87. The pilot study area spans southeast Queensland and part of north eastern New South Wales. Its location is shown in Figure 22.

The analysis technique involves using the annual maximum rainfall series obtained from the complete quality controlled rainfall record of every rainfall station in the pilot study area. For the purposes of the study into climate change, the analysis can be carried out for two or more periods of record and the results compared for each record period. The design rainfalls for each record period can be mapped for selected

standard average recurrence intervals to investigate whether there is a trend in changes in design rainfalls over time or space.

Rainfall data from continuously recording rain gauges is sparse and typically has a relatively short record length of, on average, 25 years. Splitting up such a relatively short record would not be expected to result in reliable estimates. Therefore for the purposes of observing trends in design rainfalls, this study will focus on the 24-hour duration, which includes data from the daily rainfall network of rain gauges.

Selection of rainfall periods

For rainfall frequency analysis to be reliable, it is desirable to have as long a period of record as possible. By splitting the period of record, less reliable estimates would be expected particularly for higher average recurrence intervals of 50 or 100 years. Over the pilot study area the station with the longest period of record is Tenterfield (Station Number 56032) with 133 years of data. Out of a total of 747 daily rainfall stations, 87 have 100 years or more of data. In order to allow adequate comparisons of results between rainfall sites, it was considered necessary to select data over the same time interval for all the sites. In addition, several sites have missing data over part of the period of record. The period 1901 to 2000 was chosen because it gives an adequate number of sites with a complete 100 year rainfall record. This would give the two 50-year subperiods: 1901 to 1950 and 1951 to 2000. The rainfall frequency analysis can be carried out for the subperiods and comparison of the design rainfalls from data from the two sub periods can then be made to infer whether design rainfalls have changed over time. There are 26 sites with a complete 100-year daily rainfall record. Their locations are shown in Figure 23 (left panel). The period from 1951 to 2000 was also considered for analysis because there would be a larger number of sites available which would increase the spatial coverage of the data. This would give the two sub-periods: 1951 to 1975 and 1976 to 2000. For the period spanning 1951 to 2000, there are 121 sites with a complete 50-year daily rainfall record.

Frequency Analysis

Frequency analysis using the method of L-moments was carried out using daily rainfall data from 1901 – 1950 and 1951 – 2000; and also for data from 1951 – 1975 and 1976 – 2000 (locations of sites are shown in Figure 23, right panel).

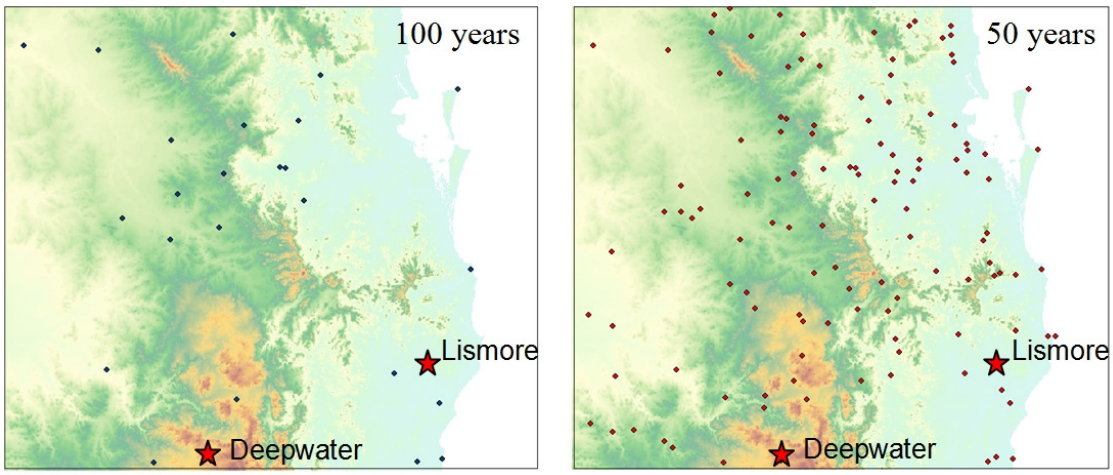

Figure 23 Locations of 26 sites with 100 complete years of rainfall data (left panel) and 121 sites with 50 complete years of rainfall data (right panel). The locations of two sites discussed later in the section - Deepwater and Lismore – are also shown.

The technique of frequency analysis was applied by using the annual maximum series from the site data to evaluate L-moments. From the L-moments, a frequency distribution was fitted to the data which gave the frequency curve. More details on the technique can be found in Jakob et al, (2005).

Significance of changes in design rainfall for two locations (Lismore and Deepwater)

An example of the rainfall frequency curves for Lismore (site 58037) is shown in Figure 24 along with 95% confidence intervals.[18] Following Buonomo et al. (2007), we will consider changes statistically significant at the 95% confidence level where an Average Recurrence Interval (ARI)[19] estimate for one period is located outside the confidence interval limits for the other period.

The frequency curve for 1901 - 1950 lies outside the range of the confidence intervals for 1951 - 2000 up to an ARI of about 10 years. The frequency curve for 1951 - 2000 also lies outside the range of the confidence intervals for 1901 - 1950 up to an ARI of about 10 years. Design rainfalls for 1951 - 2000 are therefore judged significantly higher than those for 1901 - 1950 up to an ARI of 10 years. Beyond 10 years there does not seem to be a significant difference between the design rainfalls for the two periods however the analysis is not deemed very reliable for ARI greater than 10 years because the record length is only 50 years.

The frequency curves for the two 25-year periods (Figure 24 (bottom)) show that the frequency curve for 1951 - 1975 lies above that for 1976 - 2000 and further the frequency curve for 1951 - 1975 lies outside the 95 percent confidence interval range for 1976 - 2000 for all ARI while the frequency curve for 1976 - 2000 lies just outside the 95% confidence interval range for 1951 - 1975 except for ARI of 100 years which is not very reliable from a 25 year dataset.

[18] Confidence intervals were constructed using a bootstrapping approach.
[19] The average, or expected, number of years between years in which there are one or more exceedences of a given rainfall total for a duration.

Figure 24 (top and bottom) suggest therefore that, for Lismore (site 58037), over the second half of the 100 year period between 1901 and 2000, design rainfalls tend to be higher than those in the first half of the century up to about 10 years ARI. Further, design rainfalls for the 1951 to 1975 year period tended to be higher than those between 1976 and 2000. Therefore when comparing the two 50 year periods, the later period gives higher design rainfalls than the earlier period, however when comparing the two 25-year periods, design rainfalls in the later period are lower than for the earlier period.

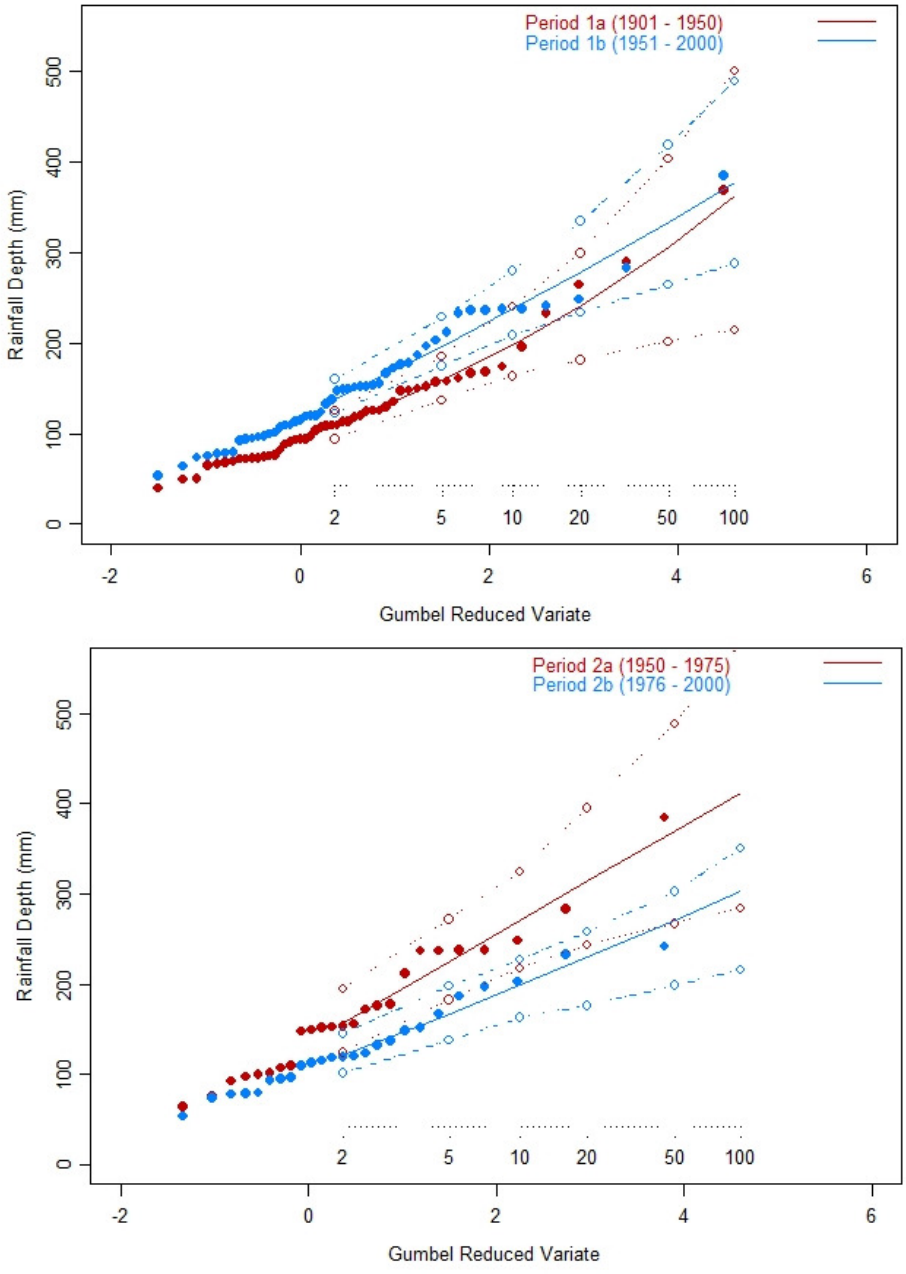

Figure 24 Frequency curves (solid lines), annual maxima (dots) and 95% confidence intervals (dashed lines) for Lismore for two 50-year periods (top) and two 25-year periods (bottom).

The annual maximum series, on which the frequency analyses shown in Figure 24 are based, is shown in Figure 25. The period between 1951 and 1975 does have a larger number of high annual maxima compared with the rest of the annual maximum series

record. The period between 1951 and 2000 also has more of the higher annual maxima compared with the period between 1901 and 1950.

The frequency curves for *Deepwater Post Office* (site number 56008, see Figure 23 for its location) were also investigated more closely. This site was chosen because the design rainfalls for this site for 1951 - 1975 and 1976 - 2000 do not appear to be as different as those for Lismore over the same period, and furthermore, design rainfalls from 1976 - 2000 do not appear significantly lower than design rainfalls from the period 1951 - 2000 as with the example for Lismore.

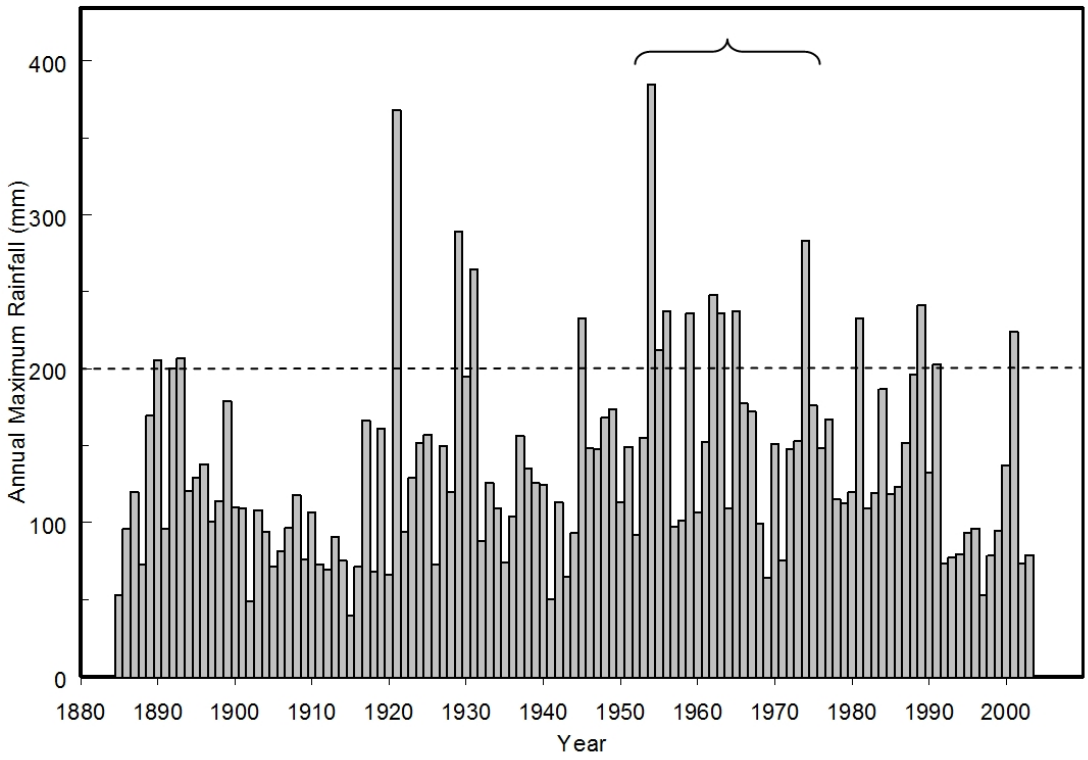

Figure 25 24-hour annual maximum time series for Lismore. The curly braces indicate the period 1951 - 1975. The dashed horizontal line marks a subjectively chosen threshold of 200 mm. This threshold is more frequently exceeded for the period 1951 - 1975 than for other periods (of similar lengths).

The frequency analyses for this site for the 25 and 50-year datasets are shown in Figure 26. The frequency curve for 1951 - 2000 lies within the limits of the 95% confidence intervals of the frequency curve of 1901 - 1950 up to an ARI of about 10 years. For ARI greater than 10 years up to 100 years, the design rainfalls for the period 1951 – 2000 are significantly higher than those for the period 1901 – 1950. Similarly the frequency curve for 1901 - 1950 lies within the limits of the 95% confidence intervals of the frequency curve for 1951 - 2000 up to an ARI of about 5 years. Beyond 5 years up to 100 years the differences in the design rainfalls between the two periods are significant.

The frequency curves for the two 25-year datasets do not appear to be significantly different from each other (Figure 26 bottom) (in contrast to Lismore (Figure 24

bottom). This is also evident in the time series of the annual maxima for Deepwater (Figure 27).

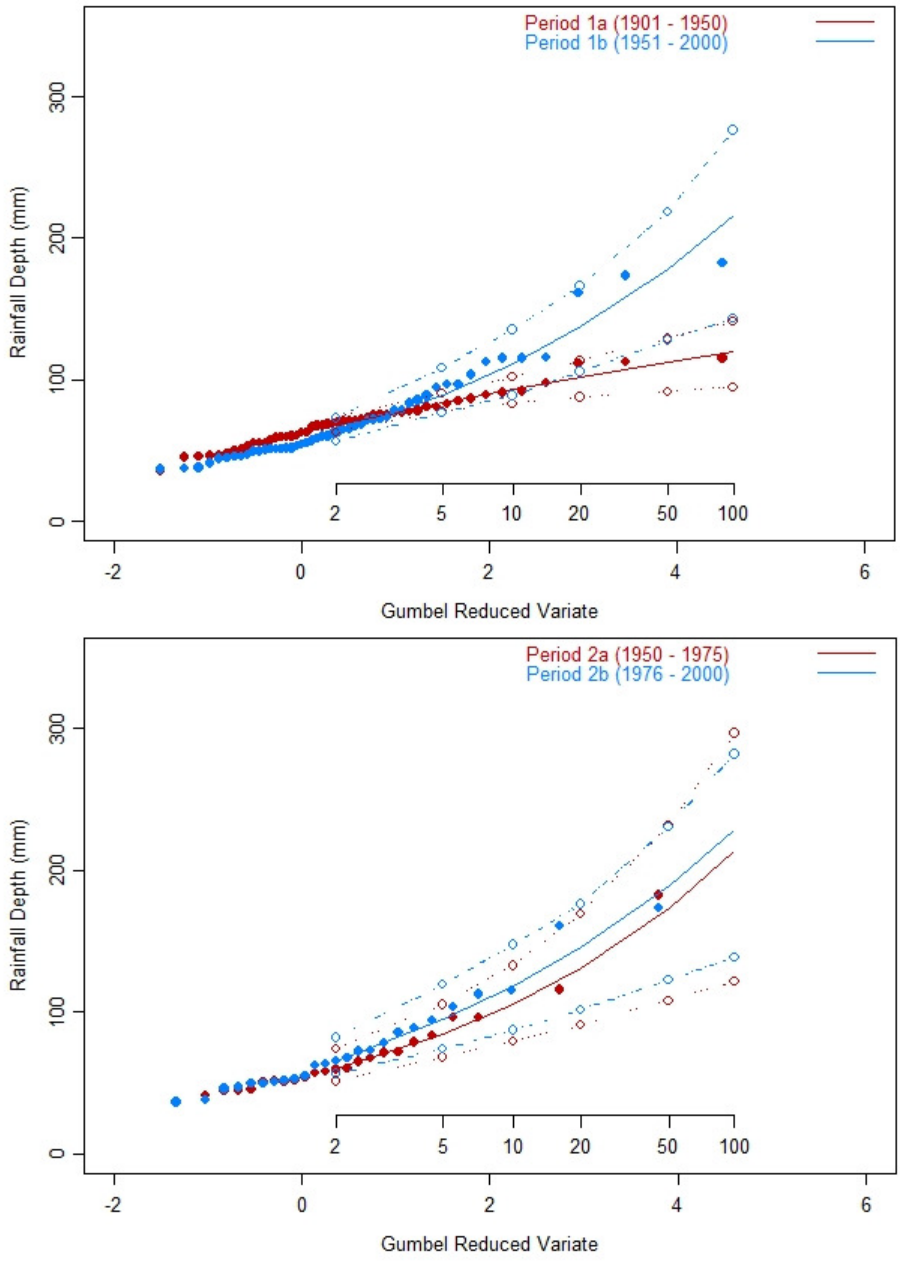

Figure 26 Frequency curves (solid lines), annual maxima (dots) and 95% confidence intervals (dashed lines) for Deepwater for two 50-year periods (top) and two 25-year periods (bottom).

Figure 27 shows that in 1951 - 2000 there were several unusually large annual maxima compared with 1901 - 1950. The unusually large annual maxima in 1951 - 2000 push the frequency curve up sharply for the higher ARIs for 1951 - 2000 compared with 1901 - 1950. For low ARI the frequency curves for the two periods are similar.

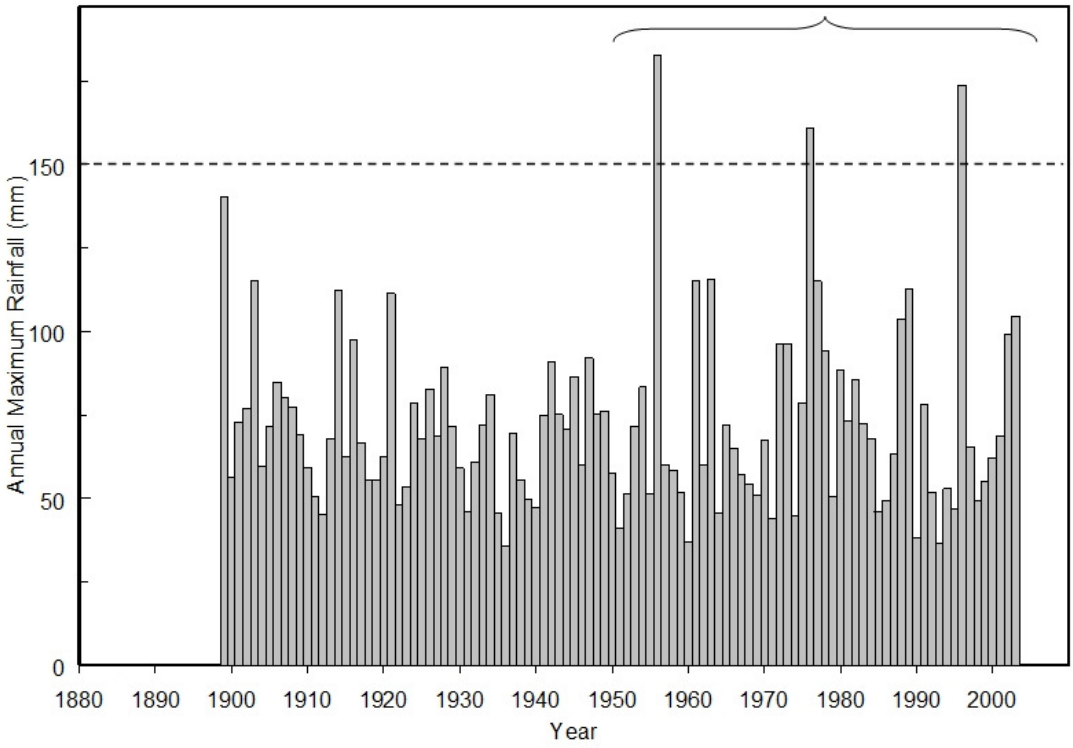

Figure 27 24-hour annual maximum time series for Deepwater (station 56008). The horizontal dashed line indicates a subjectively chosen threshold of 150 mm which for the period 1951 - 2000 (indicated by curly braces) is more frequently exceeded than for any other period.

The two 25-year periods from 1951 to 1975 and 1976 to 2000 do not appear to be markedly different. The number of high annual maxima is about the same in both periods which is consistent with Figure 26 (bottom).

So far, two detailed examples of the differences in design rainfalls have been examined. In the next section the differences will be assessed over the whole pilot study area.

Percentage differences in design rainfalls between the two 50 and 25 year datasets

Percentage differences in the design rainfalls between the two 50-year periods and the two 25-year periods were calculated for standard average recurrence intervals (ARI) of 2, 5, 10, 20, 50 and 100 years. The percentage differences were calculated as follows:

$$\mathrm{PD}_{\mathrm{ARI_i}}(\%) = \frac{\left(\mathrm{R}^{\mathrm{late}}_{\mathrm{ARI_i}} - \mathrm{R}^{\mathrm{early}}_{\mathrm{ARI_i}}\right)}{\mathrm{R}^{\mathrm{early}}_{\mathrm{ARI_i}}} \times 100 \qquad (7)$$

Where PD_{ARI_i} is the percentage difference in the rainfall for ARI *i* between the later and the earlier period. $\mathrm{R}^{\mathrm{early}}_{\mathrm{ARI_i}}$ is the 24-hour design rainfall for an ARI of *i*, for the early part of the period, $\mathrm{R}^{\mathrm{later}}_{\mathrm{ARI_i}}$ is the 24-hour design rainfall for an ARI of *i*, for the later part of the period. The percentage differences are shown mapped in for the two 50-year periods Figure 28 and Figure 29 for the two 25-year periods. An increase in ARI from

the earlier to the later period is denoted by blue circles, a decrease is denoted by red circles. Where percentage differences are judged statistically significant for a particular ARI (the point on the frequency curve for a particular ARI of one 50-year period lying outside the limits of the 95% confidence intervals of the other period, and similarly for the 25-year datasets) circles are denoted by a solid black outline.

Changes in design rainfall estimates for two 50-year periods

Figure 28 shows that 1951 - 2000 gives generally higher design rainfalls than 1901 - 1950 for most of the stations over a range of ARI. Since the frequency analyses are based on 50-year datasets, the results should not be considered reliable out to high ARI, say more than 50 years. For ARI greater than say 10 years comparison is still interesting, however, in a qualitative sense.

For an ARI of 10 years, considering percentage differences of more than 10% in magnitude, there is only one site where 1901 - 1950 gives significantly higher design rainfall. There are eight sites where 1951 - 2000 gives significantly higher design rainfalls (greater than 10%) compared with 1901 - 1950. The remaining sites show percentage differences of less than 10% in magnitude. For an ARI of 10 years up to 100 years, only two sites show design rainfalls in 1901 - 1950 exceeding those for 1951 - 2000 (Figure 28) by more than 10%. These sites are located in the western part of the pilot study area.

When only statistically significant changes are considered, design rainfalls tend to be higher for the later period than for the earlier period.

Changes in design rainfall estimates based on two 25-year periods

Figure 29 for the two 25-year datasets (based on data between 1951 and 2000) shows a different pattern. For an ARI of up to 5 years (where results would be considered to be reliable for a 25-year dataset) the later period shows lower design rainfalls than 1951 - 1975 predominantly over the eastern half of the pilot study area. Moreover, many of the differences between the two periods are considered significant. Only two sites have significantly higher design rainfalls at 5-year ARI for the later period of over 10% compared with the previous period. However, there are 32 sites where design rainfalls for the later period are less than those for the earlier period by more than 10%, and furthermore, for these 32 sites the differences are significant. At the higher ARIs the analysis results for 1976 - 2000 show significantly higher design rainfalls in the southwest quadrant. Over the rest of the area 1976 - 2000 has generally lower design rainfalls than 1951 – 1975 at all ARIs considered (Figure 29).

The percentage increases in design rainfall for the later 25-year period compared with the earlier 25-year period, can exceed 100% but the magnitude of percentage decreases rarely exceed 50% (Figure 30). It is likely that very large increases are caused by few very extreme events (e.g. tropical cyclones). These can lead to much higher estimates of design rainfall, in particular when estimating high ARI based on site data.

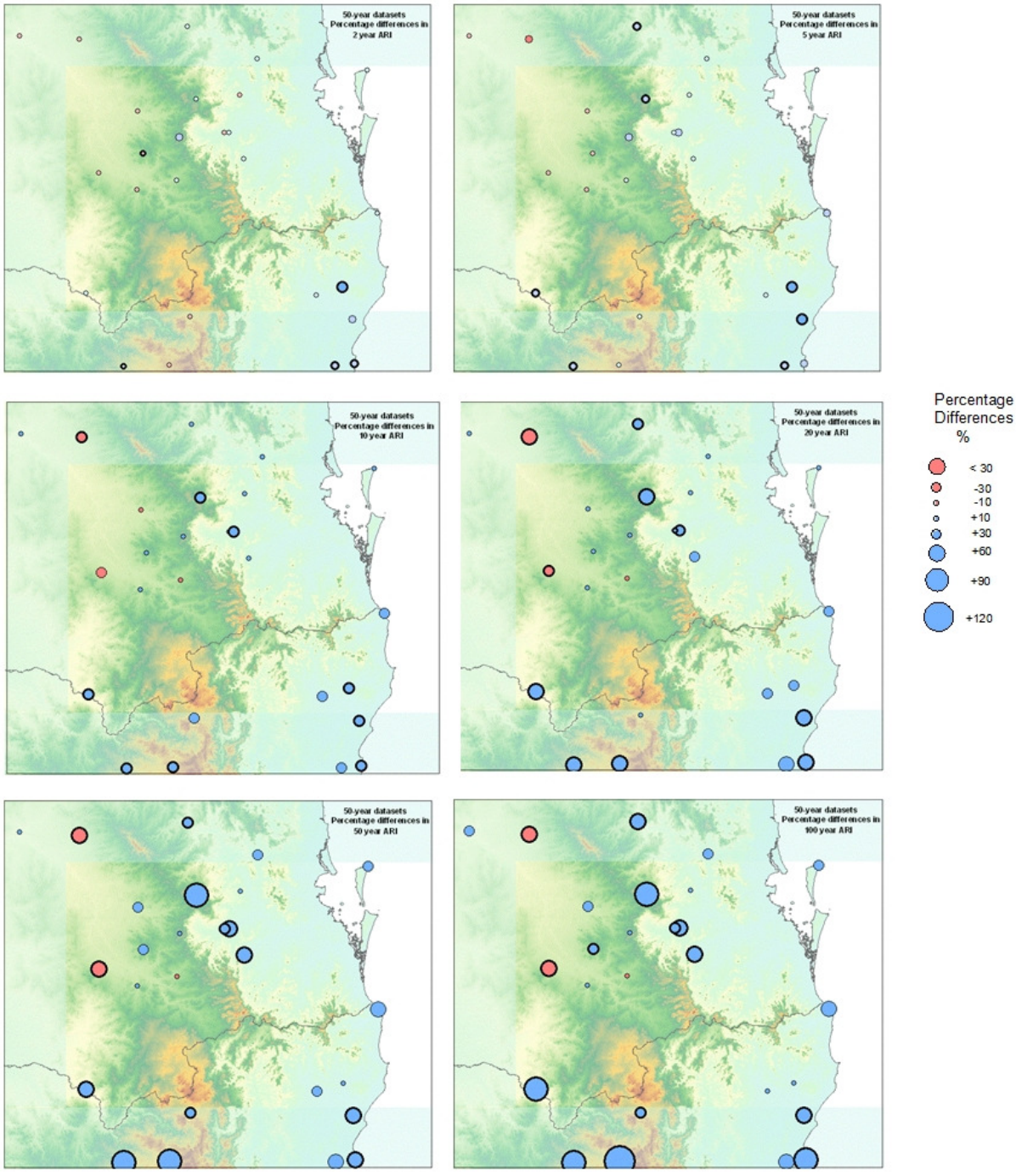

Figure 28 Percentage difference in design rainfall estimates for periods 1901 - 1950 and 1951 - 2000 for ARI 2, 5, 10, 20, 50 and 100 years. Solid black outline indicates differences are significant (for a definition of statistically significant refer text).

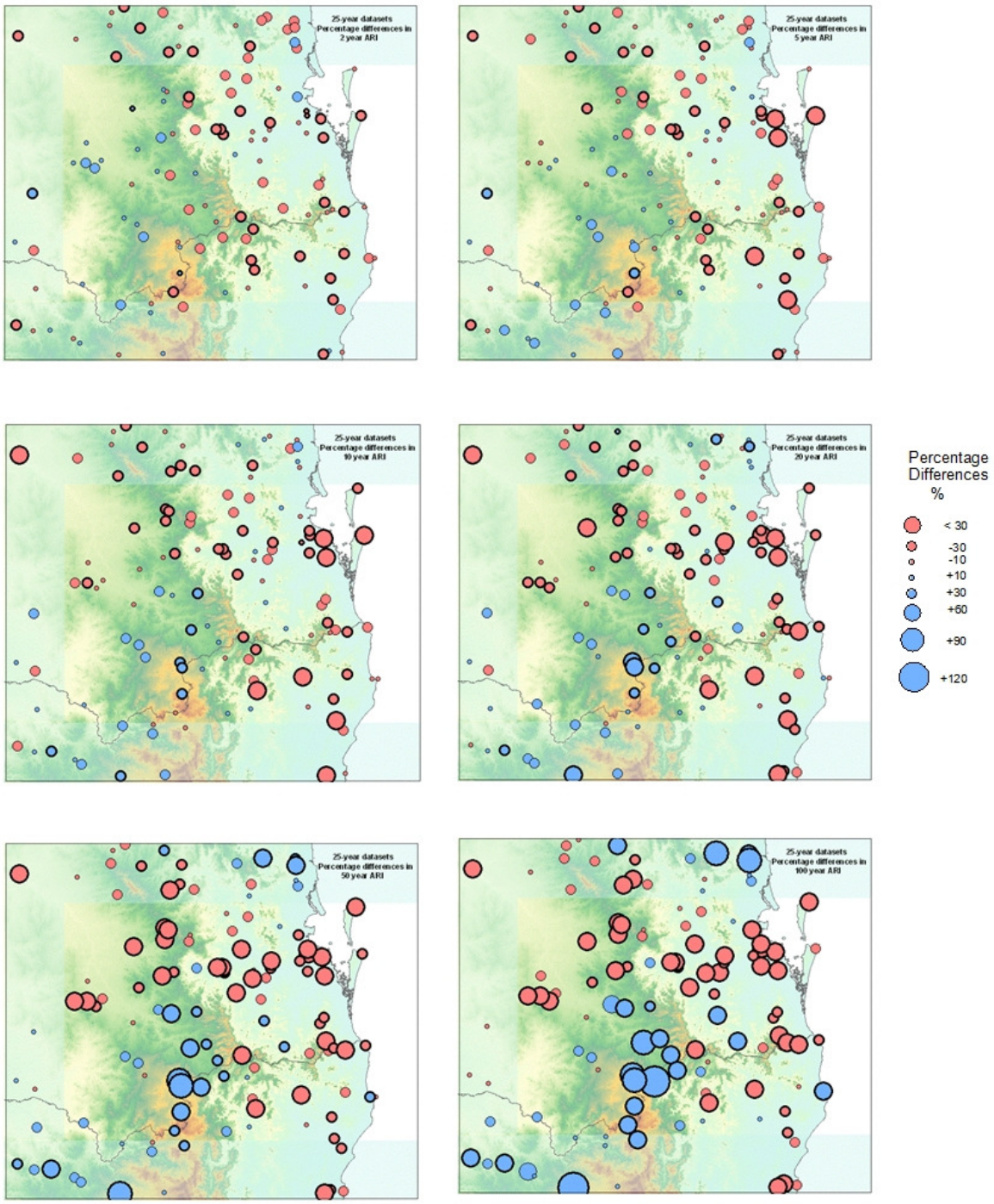

Figure 29 Percentage difference in design rainfall estimates for periods 1951-1975 and 1976 - 2000 for ARI 2, 5, 10, 20, 50 and 100 years. Solid black outline indicates differences are statistically significant (refer text).

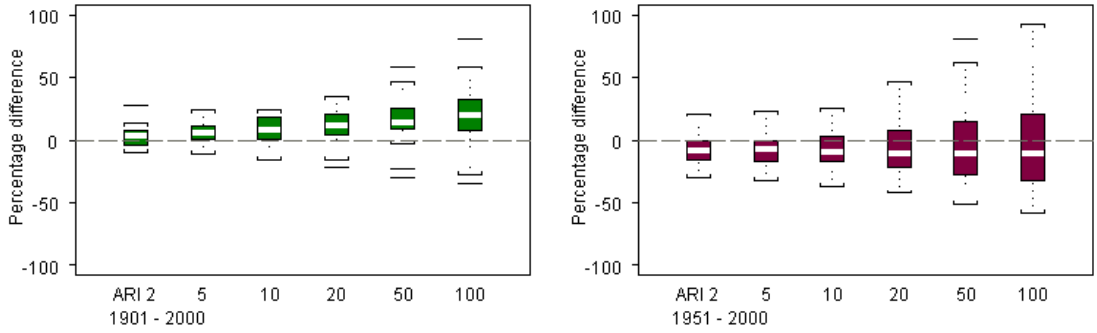

Figure 30 Boxplots showing percentage differences for locations in the pilot study area for ARI 2, 5, 10, 20, 50 and 100 years. Left panel: For two 50-year periods, right panel: for two 25-year periods.

Relationship between percentage increases/decreases and topography

Over the northwest, northeast and southeast quadrants of the pilot study area, the analysis based on the 25-year dataset suggests mostly a decrease in the design rainfalls in the later period compared with the earlier. The analysis for sites located in the southwest quadrant, however, gives higher design rainfalls at many more sites than lower design rainfalls for the later period compared with the earlier period.

The southwest quadrant has a distinctive topographic feature extending from south to north. There might be a relationship between the percentage differences and topography. Climate models suggest that large rainfall depths might be increasing in mountainous areas but could be decreasing elsewhere.

Figure 31 shows boxplots of percentage differences for sites in the pilot area grouped into three elevation ranges: 0 – 300 m, 301 – 600 m and 601 – 970 m. The boxplots for 1901 – 2000 suggest an increase in the mean for the 601 – 970 m elevation range. There is also an increase in positive percentage differences with few negative percentage differences. However there are only five sites contributing at this elevation range, therefore these results are not very reliable. From the 25-year datasets there are 16 sites contributing to the 601 – 970 m elevation range. The bottom right plot suggests positive mean percentage differences for ARIs of 20 years and above. The range of percentage increases above the mean are also much higher than the percentage decreases below the mean. For the lower elevation ranges these differences are not so large.

These results suggest that positive percentage differences are correlated with high elevation. So in mountainous regions design rainfalls have tended to become higher. This is consistent with results from climate models which suggest that increases in rainfall depths would be larger in mountainous regions under climate change. However, since the sites are not independent a few large rainfall events may have affected a number of sites which would push their frequency curves up particularly in the higher ARI range. The effect of these few events would then appear magnified in our results because a number of sites would be affected.

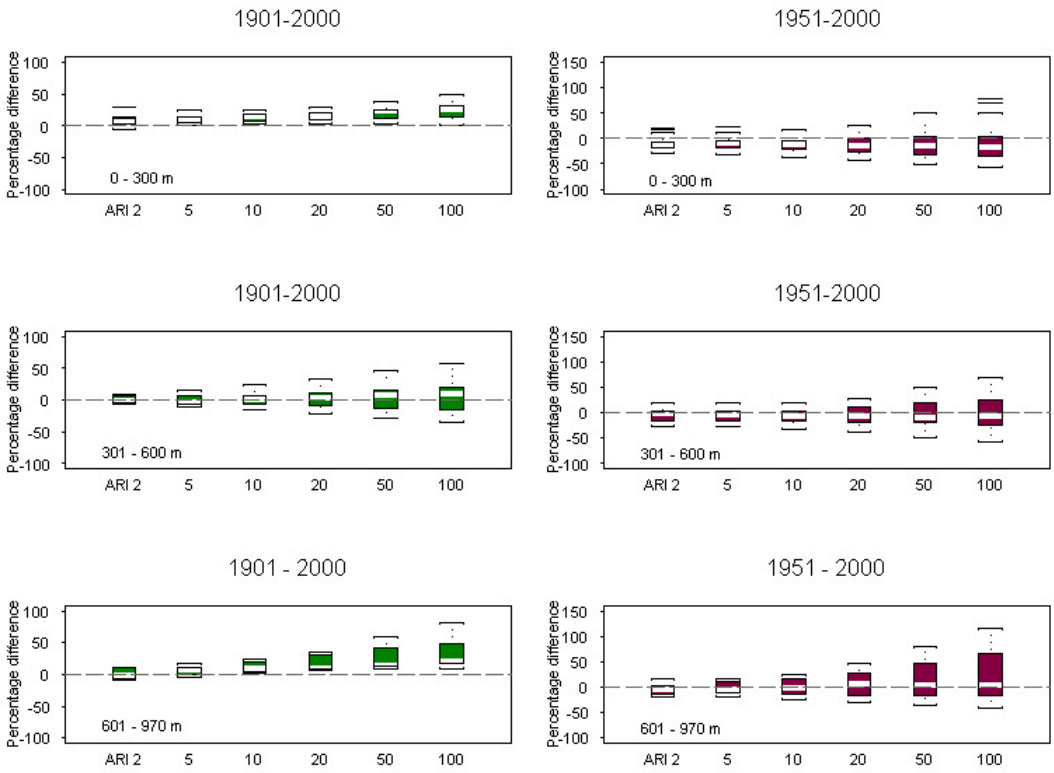

Figure 31 Boxplots showing percentage differences by range of elevation for ARI 2, 5, 10, 20, 50 and 100 years. Left panel: For two 50-year periods, right panel: for two 25-year periods.

Summary

Frequency analysis using the method of L-moments has been applied to 24-hour rainfall data in the pilot study area. The analysis has been carried out for two 50-year periods (1901 – 1950 and 1951 – 2000) and two 25-year periods (1951 – 1975 and 1976 – 2000). Confidence intervals have been constructed. Percentage differences in design rainfalls between the two 50-year analysis results and the two 25-year analysis results were calculated. The percentage differences when mapped show spatial consistency (Figure 28 and Figure 29). It is found that most of the differences are significant, i.e. the frequency curve at a particular ARI for one 50 or 25 year period lies outside the range of confidence intervals (at the same ARI) of the frequency curve for the other 50 or 25 year period.

Over most of the pilot study area, the analysis for the 50-year datasets suggests that design rainfalls for 1951 - 2000 are higher than those for 1901 – 1950 while the analysis for the 25-year datasets suggests that 1951 - 1975 gives generally higher design rainfalls than 1976 – 2000 (Figure 31). Since the 25 year periods are both subsets of 1951 - 2000, the tendency towards lower design rainfalls in the later period coupled with the higher design rainfalls for the later half of the century compared with the earlier half, suggests that 1951 - 1975 generally had more very large events in the annual maximum series than 1976 - 2000, and further that the magnitudes of these maxima were also higher than for the largest annual maxima in 1901 - 1950.

A possible relationship between the sign of the percentage differences and topography was explored (Figure 31). It is possible that very few extreme events in one period

could have led to marked changes at a number of sites. Annual maxima caused by the same event might have 'pushed up' frequency curves for those locations. However, it is possible that design rainfalls might be increasing in areas with significant topography. This would be consistent with results from climate models (Abbs, 2004). According to climate models, large rainfall depths might be increasing in mountainous areas but could be decreasing elsewhere.

1.3 Storm Types

Introduction

Storm types are used solely in defining zones (e.g. coastal and inland zone for GTSMR). Zone boundaries are drawn very conservatively. Significant events ('storms') from outside the zone were included in deriving the depth-area-duration curves. Maps will be prepared to address the question of whether we are already observing tropical cyclones penetrating further south.

Storms were classified using synoptic and upper air charts (Beesley et al. 2004). The following four categories were used:

- Extratropical Systems,
- Monsoon Low,
- Tropical Cyclone and
- Ex-Tropical Cyclone.

Events were selected based on the number of rain gauges where rainfall exceeded a 1 in 100 year event. This approach could be potentially problematic if there were significant positive or negative trends in rainfall extremes.

Rainfall, including significant rainfall events, underlies natural climate variability and year-to-year variability can be strongly modified by mechanisms such as the El Nino Southern Oscillation. Figure 32 shows the frequency of occurrence of storm types over time. There is a period between 1970 and 1980 over which a large number (27) of significant events of different types occurred. This was preceded by a much quieter decade (1960s) during which only five events occurred.

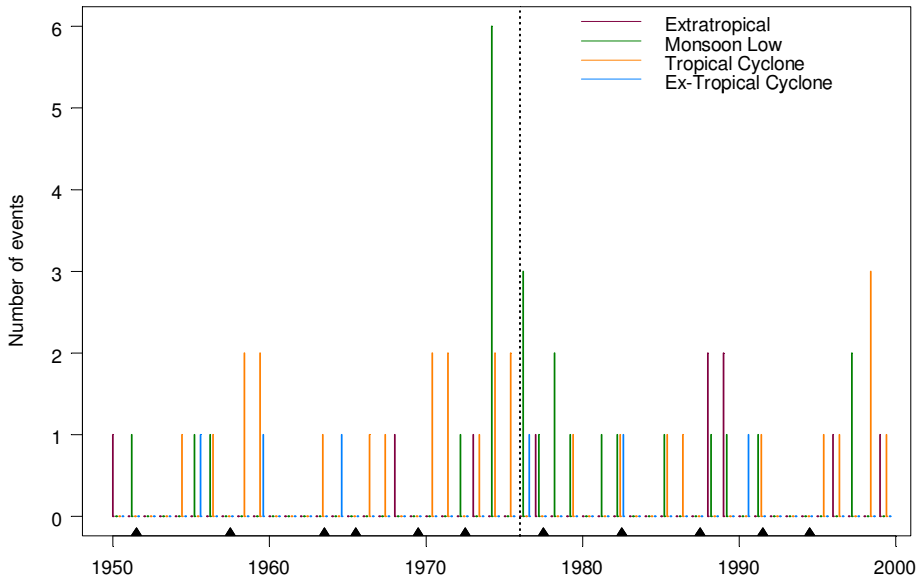

Figure 32 Occurrence of storm types over the period 1950 to 2001. Black triangles indicate El Niño events that had strong impact at least in some regions of Australia.

Frequency of storm types

The frequency of the four storm types was assessed for four periods:

- Period A 1893 -2001,
- Period B 1950 - 2001,
- Period C 1950 - 1975 and
- Period D 1976 - 2001.

The relative frequency of the four storm types is similar for period A and B (Figure 33). When period B is divided into two periods of same lengths (26 years), both periods show a similar number of events (34 and 36 respectively). The earlier period (C) shows a histogram similar in shape to that for the longer period. The later period (D) appears different because of an uncharacteristically low number of tropical cyclones.

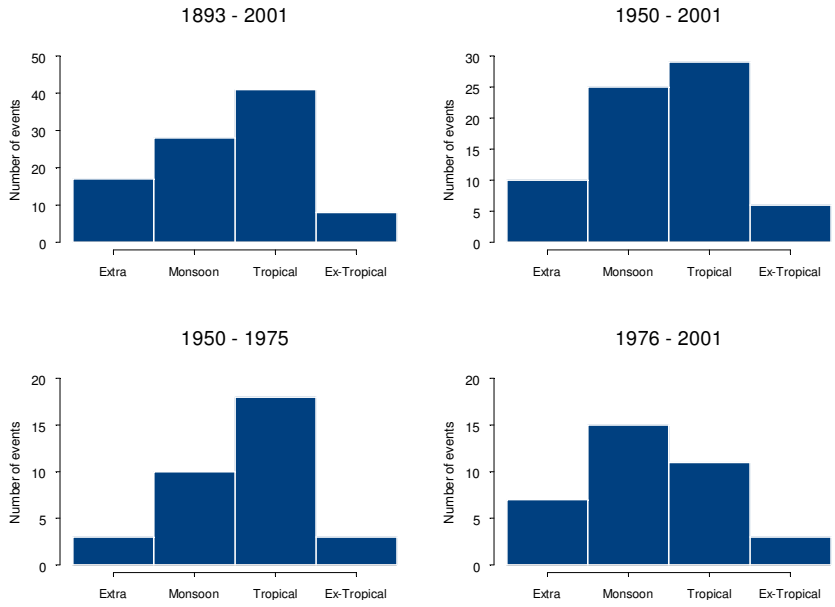

Figure 33 Frequency of storm types for four periods.

Frequency of storm type for a given duration

Most of the storms were identified for durations of one or two days but there is also a significant number of events for a duration of 7 days (Figure 34). For three of the four periods, the number of one and two day events is dominated by tropical cyclones. Relatively few one day events were selected for period C and most of those are monsoon activity rather than tropical cyclones.

It is unlikely that these apparent differences are caused by the procedure for selecting significant events. It is possible however that the classification into storm types could have been affected (for instance by increasing availability of satellite pictures and changes in pressure definition for tropical cyclones).

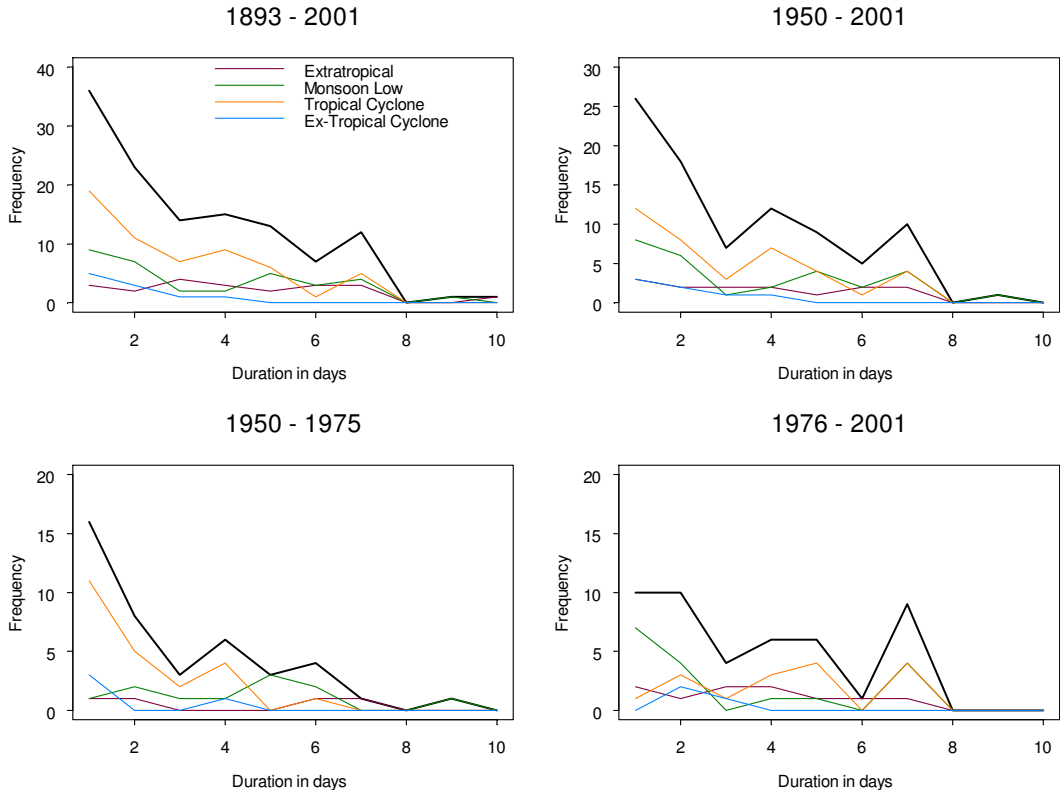

Figure 34 Frequency of storms types for given duration (black line - all storm types)

Location of storm centres

There are regions where annual rainfall totals have decreased over the last 50 years (such as in southwest western Australia and along parts of the east coast) and other areas where annual totals have increased (such as the northwest of Australia). If one were to assume that changes in rainfall extremes had the same sign as changes in annual rainfall totals, this would imply that there is the possibility that for the later period fewer events might be selected along the east coast and SWWA but relatively more events in the northwest of Australia.

The decline in SWWA is mainly a decline in *winter* rainfall. The increase in rainfall in northwest Australia is dominated by increases in wet season rainfall. Along the east coast, decrease in the north appears mainly due to a decrease in *summer* and *autumn* (extending inland) whereas decreases further south appear related to decrease in *winter* rainfalls.

Tropical cyclones would typically occur between early November and late April. Ex-tropical cyclones and monsoon activity is restricted to about the same season. Extratropical systems typically occur during the cooler months (say May to July). Tropical cyclones and monsoon lows are the two major rain producing storm events (for durations between 1 and 7 days.) Few events were classified as ex-tropical or extratropical cyclones.

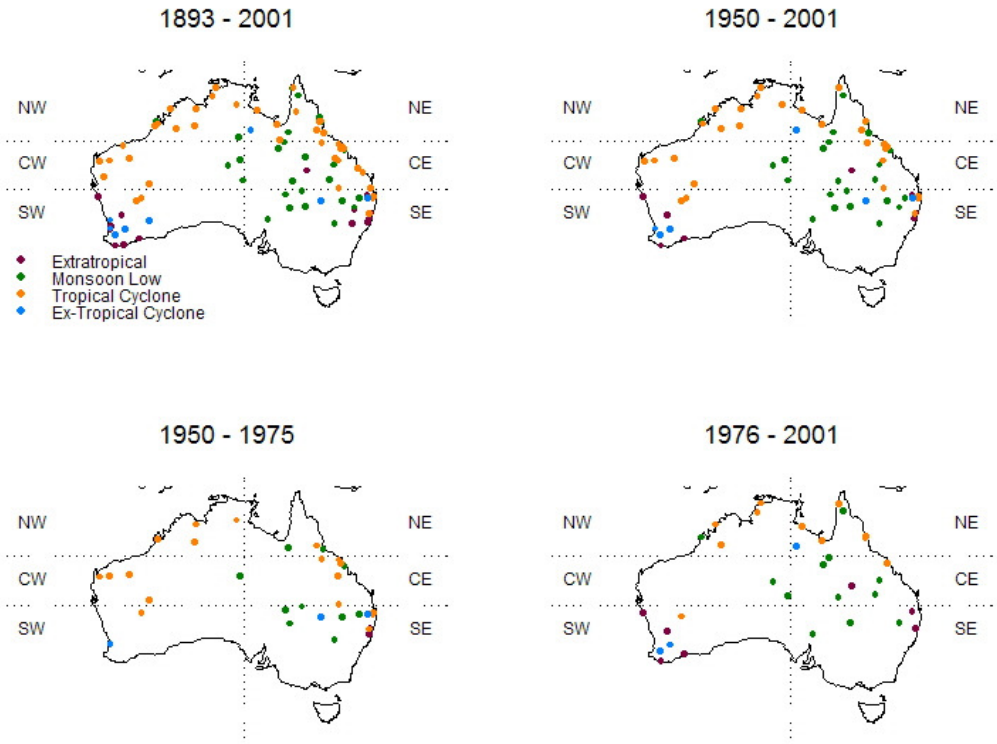

Figure 35 Location of storm centres for four periods, colour of points indicates storm type.

Australia was divided into six regions, along 135 E and 20 and 27 S. The region names are as follows NW (northwest), CW (central western parts), SW (southwest), NE (northeast), CE (central eastern parts) and SE (southeast) as shown in Figure 35. Comparing periods A and B (top row in Figure 35) it is found that the number of events is reduced for the shorter period but not in relationship to the length of the period. The last 50 years appear to contribute about 2/3 of the events. The pattern for the two periods appears almost unchanged. For the two shorter periods C and D (keeping in mind that there are few events) a surprisingly dissimilar pattern emerges. Even discounting storm types and just counting events in sub-regions.

Table 1 Frequency of storm types for four periods and six regions

Period	NW	CW	SW	NE	CE	SE	All
1893 - 2001 (A)	11	9	14	15	20	24	94
1950 - 2001 (B)	9	7	9	12	14	19	70
1950 - 1975 (C)	4	5	2	3	6	14	34
1976 - 2001 (D)	5	2	7	9	8	5	36

Considering the seasonal cycle in frequency of the four storm types and the main season of rainfall decrease/increase one might expect to see the following picture emerge:

- an increase in the number of tropical cyclones/ monsoon activity selected for NWA
- a decrease in the number of extra-tropical activity selected for SWWA
- a decrease in the number of tropical cyclones/ monsoon activity selected for northern parts of the east coast (and inland) and
- a decrease in the number of extra-tropical activity events selected for the southern parts of the east coast. (This part is not covered in the GTSMR.)

It was found that:

- The number of tropical and extra-tropical cyclones north of 20 S has doubled: from 7 significant events in the regions NW and NE for period C to 14 events in period D.
- The number of extra-tropical cyclones associated with significant rainfall events and reaching the southwest has actually increased from zero to 4.
- A decrease in the number of events classified as tropical cyclone and/or monsoon activity might have been expected. The number of tropical cyclone events for the central eastern parts (CE) dropped from 5 to 1, whereas the number of monsoon activity events increased from 1 to 6. This shift could well be related to a shift in rainfall patterns since extreme rainfall producing events occur now more frequently inland rather than near the coast or the mountain ranges.
- The total number of events producing extreme rainfalls in the southeast region (SE) has dropped drastically (from 14 to 5). This is due to a reduction in the number of monsoon lows and as well as the number of tropical cyclones/ex-tropical cyclones.

Summary

Based on the last 50 years, there is little evidence to support the notion that tropical cyclones (connected to major rainfall events) are penetrating further south or have become more frequent. The absolute (and relative) frequency of such events is lowest for the most recent period (1976 - 2001). At the same time, the number of monsoon lows exceeded the number of tropical cyclones for this period, while for all other periods tropical cyclones (associated with significant rainfall events) were more frequent than monsoon lows.

Changes in spatial patterns are discussed in section 1.2.2 ‘Changes in design rainfalls’). However, from these investigations it appears possible that there is chance that they could be changing. One should also consider the possibility that significant events might have a tendency to be more prolonged in the future.

Caution is advisable when interpreting these findings since only a relatively small number of significant rainfall events were used. No attempts have been made so far to attribute differences in frequency of storm types and their preferred location to natural climate variability or climate change.

1.4 Relative storm efficiency

1.4.1 Introduction

In a warmer climate, the global average of water vapour in the lower troposphere is expected to increase (Pall et al. 2007). This increase, according to the Clausius-Clapeyron relationship, is about 7% per K. This means for a projected temperature increase of 3 K one would expect a corresponding increase in water vapour of about 20%. Models do show these increases, both for current and future climate (20C3M and A1B). The associated increase in precipitation tends to be much lower at about 2.2% per 1 K.

It is possible that storms could be affected for instance by increase in intensity and decrease in duration or frequency or by changes in efficiency (Trenberth et al. 2005). The magnitude of extreme precipitation for an event of given duration could change due to two factors: a) more moisture being available and b) the same amount of moisture being converted more efficiently into precipitation (conversion rate changes).

Data

For storms in the GTSMR database, four related characteristics describing moisture availability are available: storm dew point, extreme dew point, storm precipitable water[20] and extreme precipitable water. In addition rainfall depths were available for 24, 48 and 72 hours (assuming the event extended over these durations) and for a number of areas between 100 and 150,000 km^2 (assuming the event extended over areas that size or larger).

Method

Pearse (1993) describes 3 different storm efficiency indices:

- A *proportional index of efficiency*, based on the assumption that 'the differences in the maximised-standardised convergence (MSC) depths data of storms of a particular area and duration are primarily the result of differences in efficiencies of storms'. It is equivalent to the ratio of the MSC depth to the PMP depth for a particular generalised method season and zone.
- A *surrogate index of storm efficiency*. This is similar to the proportional index of efficiency, in which 'the variation in MSC depths are themselves an indicator of the variation of the storm efficiency.'
- A *precipitation/moisture ratio index*, describing the 'capacity of a storm to extract a given amount of precipitation from a given amount of atmospheric moisture'.

[20] When converting storm dew point to PW a saturated atmosphere with a pseudo-adiabatic lapse rate is postulated. This assumption may warrant further investigation.

The latter definition will be used here for the efficiency η:

$$\eta = \frac{\text{rain rate}}{\text{storm PW}} \qquad (8)$$

Factors used in deriving PMP estimates are: rainfall over standard areas, storm type, orographic enhancement and local moisture availability. Extreme dew points (90th percentile) have increased in some seasons and for some locations (see Figure 8). Changes in storm precipitable water are typically smaller than changes in extreme precipitable water.

Assuming the storm PW (in mm, derived from surface dew points) is an appropriate measure for characterising the available moisture, one can calculate the ratio of rainfall depth (in mm) or rain rate (in mm/h) and PW. This ratio will give some indication of how much of the available moisture was converted into precipitation. This assumption is an oversimplification since the fact that air (and moisture) is constantly being replaced is neglected. The rate at which air will be replaced is likely to depend on the type of event and the season.

Largest storm efficiencies occur along central and northern parts of the east coast. Other regions with relatively high storm efficiency are along northern and central parts of the west coast as well as coastal southwest Western Australia. Storm efficiency typically decreases for events with storm centres further inland.

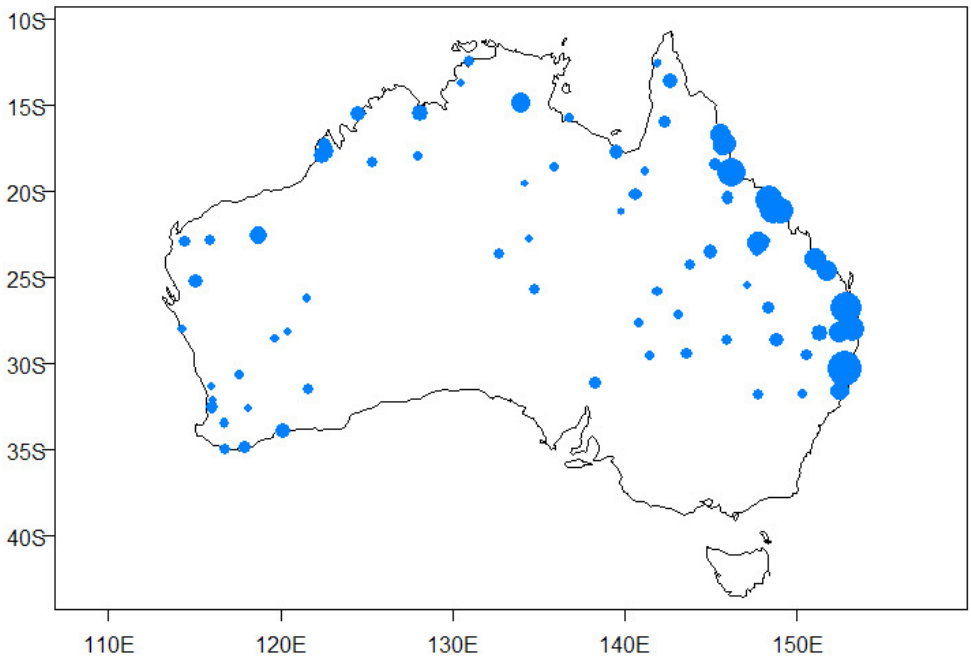

Figure 36 Relative storm efficiency for events from the GTSMR database. Relative storm efficiency is calculated as ratio of storm depth (at 24 h, 1000 km^2 converted to rain rate) and storm precipitable water. Symbols are plotted at the location of storm centres.

Rainfall can be orographically enhanced. In the method for PMP estimation a topographic adjustment factor is used to account for this fact (Minty et al. 1996).

Based on the 72 h, 50 year design rainfall estimates, this factor allows removing the part of the rainfall that is deemed to be caused by topography. The resulting rainfall depth is referred to as 'convergence depth'

A regression-based approach was used to establish how well the efficiency of a storm is defined purely by the location of its storm centre. It was found that only a small proportion of the variance could be explained. While location is an important factor for the relative efficiency of a storm event, other factors including season and type of event are likely of at least similar importance. These factors will be discussed in the following sections.

Rainfall depths and storm precipitable water are available for 38 locations for the top 30 one-day events for each of two periods (1960 to 1980 and 1981 to 2003) and changes in storm efficiency have been assessed (section 1.4.2.3). Since these changes are assessed 'in situ' (at a given location) there is no need to define the convergence rainfall since the effect of topography can be considered constant.[21]

1.4.2 Assessing relative storm efficiency

Relative storm efficiency will be assessed for events from the GTSMR database (section 1.4.2.1) and from the GSAM database (section 1.4.2.2). Compared to GSAM, the GTSMR is applicable for a larger region and the database contains more events. (There are 122 events in the GTSMR database compared to 110 events in the GSAM database. However, when independent events are considered, the number of events is the same in each database: 94).

1.4.2.1 Relative storm efficiency for GTSMR events

In the following, storm efficiency will be assessed based on an index that describes the ratio of precipitation to available moisture. Two refinements to this basic approach are considered: firstly, taking into account effects of topography on rainfall and secondly, the effect of moisture transport during an event.

Ratio of rainfall rate to storm precipitable water

The ratio of rain rate (rainfall depth in mm divided by 24 h) to storm precipitable water (SPW in mm) was assessed for a number of standard areas and for the durations: 24 h (black), 48 h (blue) and 72 h (red). Very few events will have a spatial extent greater than 40,000km^2. However, the relationship between rainfall depth and ratios appears largely unchanged. In the following only the 24 h duration will be considered and for an area of 1000 km^2.

[21] The method for PMP estimation assumes that the topographic adjustment factor (TAF) for a location does not change with the rarity or type of event.

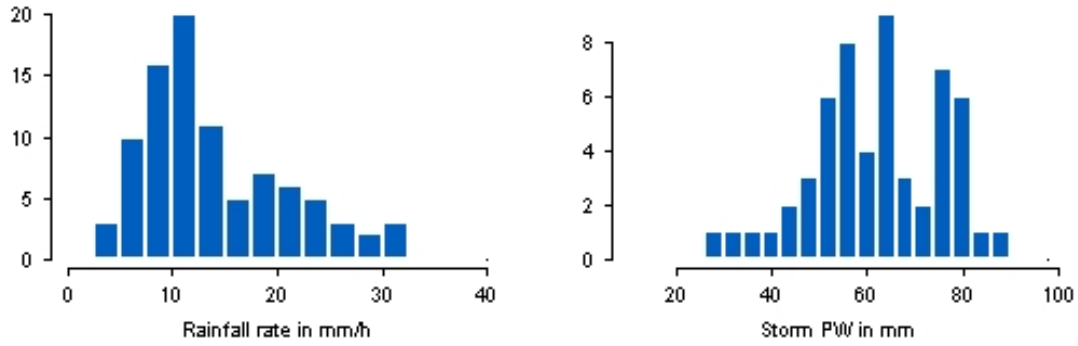

Figure 37 Histograms of rain rate (at 24 h, 1000 km^2) and corresponding storm PW.

The histograms in Figure 37 show that neither rain rate nor storm PW are normally distributed. Typical storm PW is about 60 mm. The histogram for rain rates shows that the frequency of rain rates peaks around 10 mm/h and a secondary peak exists around 20 mm/h. For these typical values the resulting ratios (rainfall rate to storm PW) are 0.17 and 0.33 respectively[22].

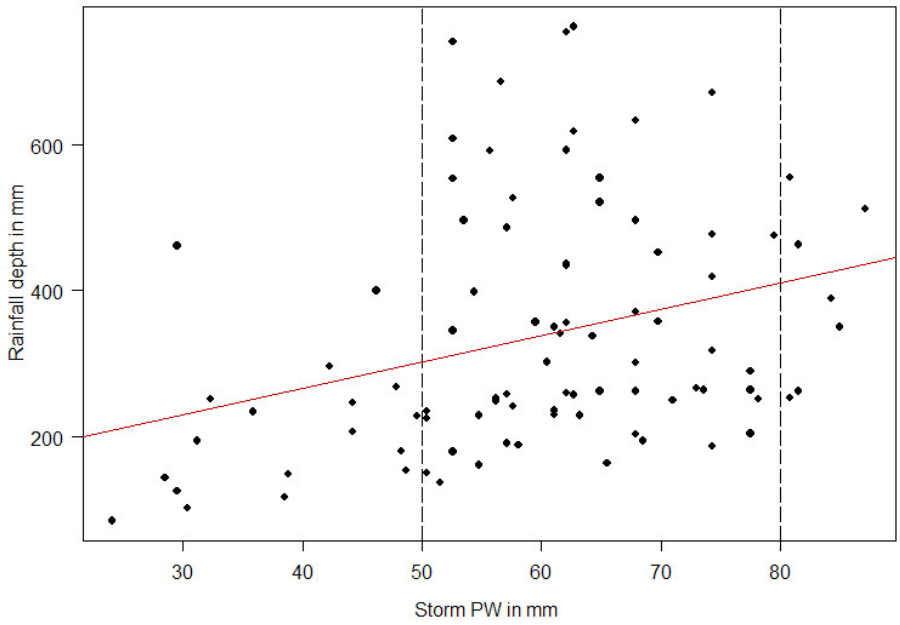

Figure 38 Storm PW and corresponding rainfall depth (24 h, 1000 km^2).

The scatterplot in Figure 38 shows that there is no strong relationship between the storm PW and the rainfall depth of an event. None of the events with storm PW below 50 mm totalled more than 600 mm in 24 h. On the other hand high storm PW (say above 80 mm) does not necessarily lead to higher rainfall depth.

[22] Efficiency is treated as dimensionless, regardless of the unit resulting from calculating the ratios. Definitions were chosen so that efficiency does not exceed 1.

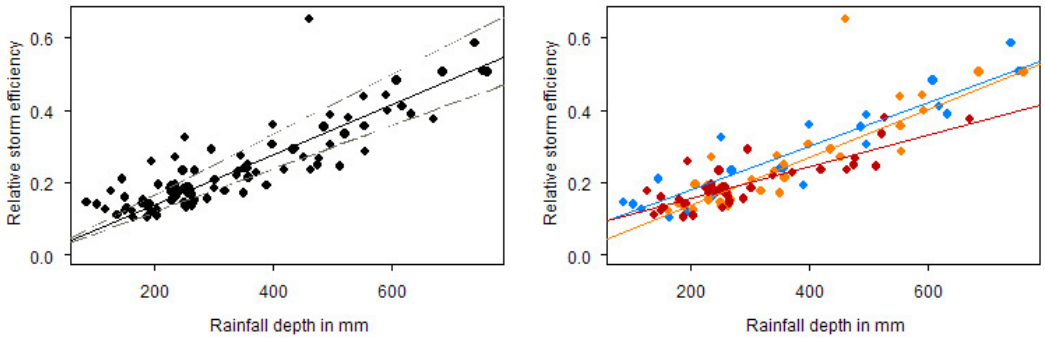

Figure 39 Relative storm efficiencies based on rain rates for 24 h, 1000 km^2. Left: for 1893 to 2000, right: split by period (pre1950 blue, 1950 - 1975 orange, post1975 red). Black lines (left panel only) indicate constant storm PW for 50, 60 and 70 mm. Coloured solid lines indicate best fit (right panel).

Per definition, relative storm efficiency for constant storm precipitable water will be higher for higher rainfall rates. Lines of constant storm PW for typical values (50, 60 and 70 mm) are indicated in Figure 39 (left panel). According to Figure 39 (right panel), the storm efficiency for a given rainfall depths has decreased from the period 1950 - 1975 to 1976 - 2000. This could be due to a lower conversion rate of moisture to precipitation or an increase in storm PW. The increase in storm PW could be due to either changes in the number of events at a location/for a season or changes in the PW for a location/season.

Based on analyses of ratios of rainfall rate to storm PW, there is no indication that in the most recent periods (according to the measure used here) available moisture is being converted more efficiently into precipitation. Most of the significant events occurred during the *summer* months (for GTSMR methods this is October to April)[23]. Far fewer events occur in *winter* (for GTSMR methods this is May to September). Ratios for *winter* events vary from about 0.1 to 0.6. It is possible, that on average storm efficiency could have decreased for events during the GTSMR *summer* period (October to April) although these changes are not statistically significant. Based on the conventional definition of seasons, only changes for *autumn* (March to May) show a significant decrease (at the 0.05 level).

The average storm efficiency for the period 1976 - 2000 is lower than for the period 1950 - 1975. The relative storm efficiency for the period prior to 1950 is on average higher than for the period 1976 - 2000. It is possible that these differences could be due to natural climate variability.

The event with the highest storm efficiency is a *winter* event (according to both GTSMR and conventional definition of seasons) and occurred in June 1950 (extratropical cyclone). The high ratio for the *winter* event is caused by the fact that despite a very low storm PW (and with MF = 1.87) the rainfall depth almost reaches that of the *summer* events.

As part of the generalisation procedure, storm rainfall depths are reduced to convergence depths. This is achieved by removing the part of the rainfall that is produced due to orographic effects. Estimates for the effect topography has on rainfall

[23] The seasons defined for GTSMR differ from the conventional seasons. Summer (the northern wet season) stretches over 7 months, from October to April. Winter (the northern dry season) lasts from May to September.

are based on design rainfall estimates (Minty et al. 1996). Changes in convergence depths can be used to investigate changes in storm efficiency. The adjusted storm efficiency is η_{topo} is defined as

$$\eta_{topo} = \frac{\text{rain rate (based on converg. depth)}}{\text{storm PW}} \qquad (9)$$

Adjusting the storm efficiency for orographic effects changes the picture somewhat but the average storm efficiency for the period 1976 to 2000 remains lower than for the period 1950 to 1975 (Figure 40).

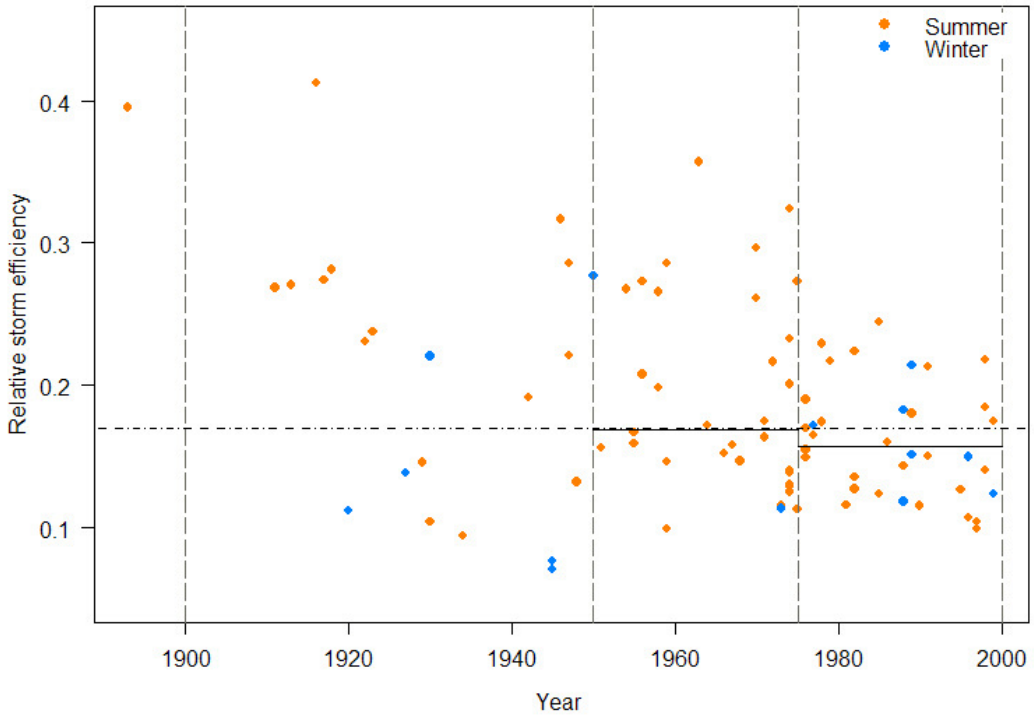

Figure 40 Adjusted storm efficiency. As above but based on convergence depth rather than storm depth.

Relative storm efficiency using upper-air wind speeds

Using data from upper-air stations, wind speeds were derived for GTSMR events. Due to data availability this was only possible for events that occurred from 1960 onwards. Based on the storm centre, the upper-air wind (at 850 hPa, which is nominally the top of the boundary layer, at 1.5 km) was derived from the nearest upper-air station. The results are shown in Figure 41. The coloured vertical lines indicate the range (10^{th} to 90^{th} percentile) of wind speeds observed over the duration of the event. The circles indicate the median wind speed for each event, colour denotes the event type. For comparison the climatology[24] is indicated in light blue in the background. Wind speeds during GTSMR events are (with very few exceptions) well above the climatological average. Highest average wind speeds occur in association with tropical cyclones but there are cases where average wind speeds

[24] This is based on upper-air wind speeds at the station nearest to the storm centre.

during ‘monsoon lows’ are higher than for some of the tropical cyclones or extratropical cyclones.

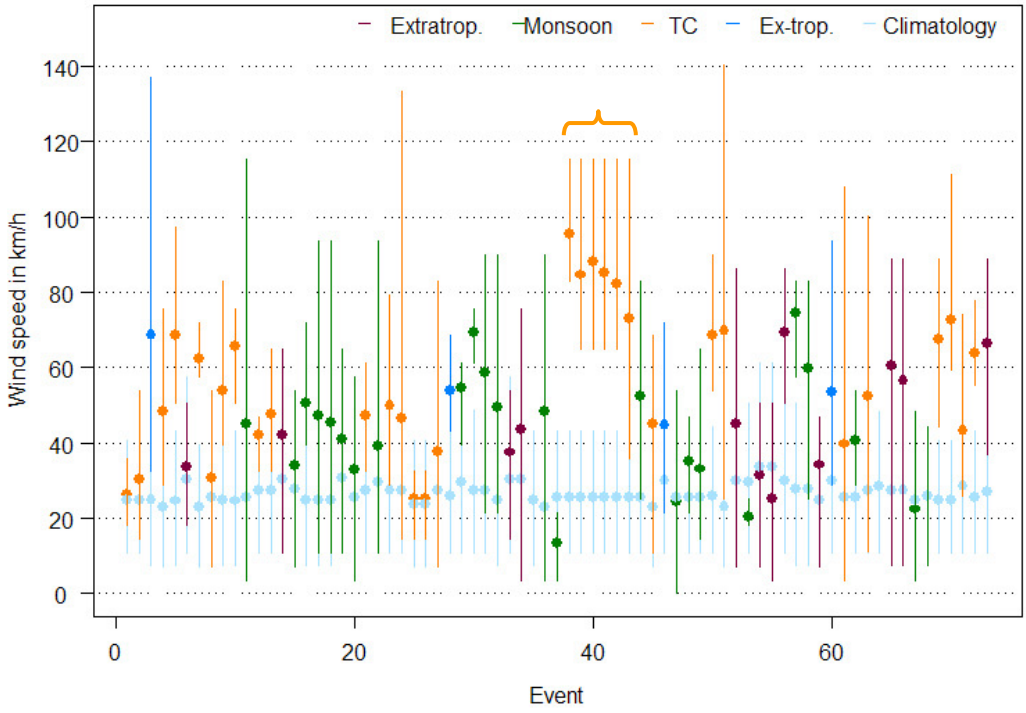

Figure 41 Wind speeds for events from the GTSMR database (period 1960 - 2003, level 850 hPa). Dots indicate average, lines indicate range over the duration of the event. Climatology is shown in cyan (10th and 90th percentile).

When a linear trend is fitted to average wind speeds for all events (regardless of event type, location of storm centre or season during which an event occurred), this trend is found not to be statistically significant. Average wind speeds for some event types may have increased (e.g. for extratropical cyclones) but may have decreased for other event types (e.g. monsoon).[25]
It was found that maximum rainfalls occur at high PW and high wind speeds but a secondary maximum exists at lower wind speeds and PW.

Event type is strongly related to geographical location of storm centre (see Figure 35 in section 1.3) and storm PW depends on location and season. The storm PW for a given event type is therefore to some extent predefined. It is found that while the storm PW for extratropical cyclones is typically below 50 mm, for tropical cyclones and monsoon lows it typically exceeds 50 mm.

[25] There is a tendency for average wind speed to decrease with increasing duration. An increase (over time) in average duration of events could therefore mask an increase in average wind speed. Analyses were therefore repeated but this time average wind speeds were calculated for the day with maximum rainfall (for a given event) only. No significant trend was found for average wind speeds derived for the day with maximum rainfall.

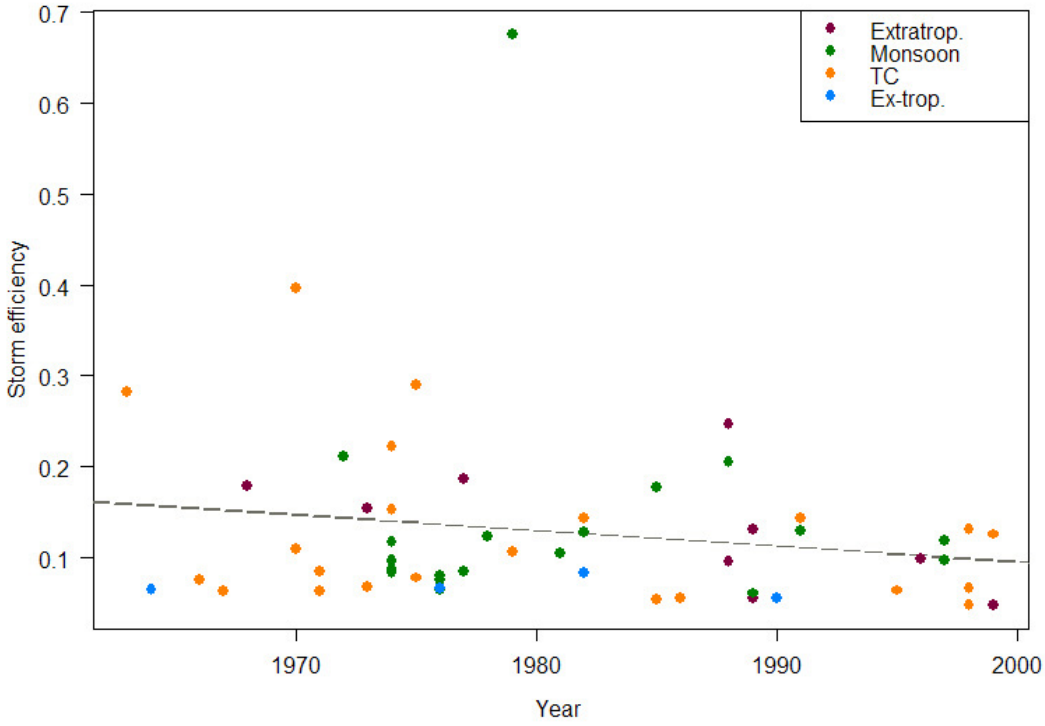

Figure 42 Relative storm efficiency calculated as the ratio of rainfall depth (mm) for 24h, 1000 km^2 to the product of storm precipitable water (mm) and average wind speed (km/h).

Estimates of relative storm efficiency were derived, taking into account that moisture is being imported over the lifetime of the event. For these estimates, the moisture available is characterised as the product of storm precipitable water (SPW) and average wind speed (Figure 42). The efficiency η_{wind} is defined as

$$\eta_{wind} = \frac{\text{rain rate}}{\text{storm PW} \cdot \text{wind speed}} \qquad (10)$$

According to this definition, relative storm efficiency will be high for: large rainfall depths, low values of SPW and low wind speeds[26]. The highest storm efficiency is found for a 'monsoon low' event that occurred in February 1979 (rainfall depths for 24h and 1000 km^2: 526 mm, SPW: 57.6 mm, median wind speed: 13.5 km/h).

For this definition of relative storm efficiency, there is a statistically significant downward trend in the storm efficiency. While it is unlikely that the changes in storm efficiency can be explained by the changes in wind speed, it is possible that these changes are a contributing factor.

Summary

Changes in relative storm efficiency were assessed for events from the GTSMR database on the basis of the ratio precipitation to moisture. Three slightly different definitions were used: η, η_{topo} and $\eta_{wind.}$ Regardless of the definition used, a decrease

[26] Efficiency is treated as dimensionless, regardless of the units involved when calculating the efficiency. An attempt was made to use definitions of storm efficiency that led to values between 0 and 1.

(over time) was found in relative storm efficiency. Changes are judged statistically significant only when wind speed is included in the definition of storm efficiency.

These changes would be consistent with:

- An *increase in storm PW* which is not accompanied by increase in rainfall rates. Changes in Maximisation Factor (MF = EPW/SPW where $\Delta MF/MF \approx -\Delta SPW/SPW$) were assessed in section 1.1.1. During *Autumn* there was a decrease in the MF, which corresponds to an increase in the storm PW. However, none of the events in the GTSMR database had significant changes in maximisation factors.
- *Changes in location* of storms. A small percentage of the variance in relative storm efficiency can be explained by the location of an event. Generally, events occurring along the northern and central parts of the east coast and northern parts of the west coast tend to have higher storm efficiency than events occurring further inland. If events were to occur more frequently further inland then the average storm efficiency would appear to decrease.
- *Increase in average wind speed* during an event. Wind speeds during storms are typically significantly higher than the climatological average. Average wind speeds for some event types may have increased (extratropical cyclones and tropical cyclones) while they could have decreased for other event types (monsoon lows). Depending on frequency of event types with an increase/decrease in average wind speed and the magnitudes of these changes, this might explain changes in η_{wind}.

1.4.2.2 Relative storm efficiency from GSAM database

For events from the GSAM database, the convergence depth has been derived. The ratio of convergence depth rate (in mm/h) to storm precipitable water (SPW) is used to characterise storm efficiency (Equation 9). This analysis is based on convergence depths derived for an area of 1000 km^2 and duration of 24 hours. The earliest event included in the GSAM database occurred in 1889, the last event in 1990. No additional events are included after this year even when the storm search is extended to the year 2003.

The classification for GSAM events differs from that for GTSMR events. For GSAM events the moisture source as well as the rainfall mechanism was taken into consideration. A simplified classification was used here:

- Tropical Depression
- Monsoonal Trough
- Cut off Low
- Easterly Trough

Largest rainfalls in the GTSMR database tend to result from tropical cyclones. In contrast to the GSAM database, very few of the events in the GTSMR database are *winter* events.

Relative storm efficiency by season and event type

The relative storm efficiency was plotted against the calendar year during which the event occurred. Linear trends were fitted for the full period (1889 - 2003) and for a shorter period (1950 - 2003) for both annual and seasonal values. The only statistically significant trend occurs for the period 1950 - 2003 for the *winter* months[27] (Figure 43). The horizontal dashed line indicates the 90th percentile in relative storm efficiency. This threshold is exceeded only during *autumn* and *winter* but for different event types.

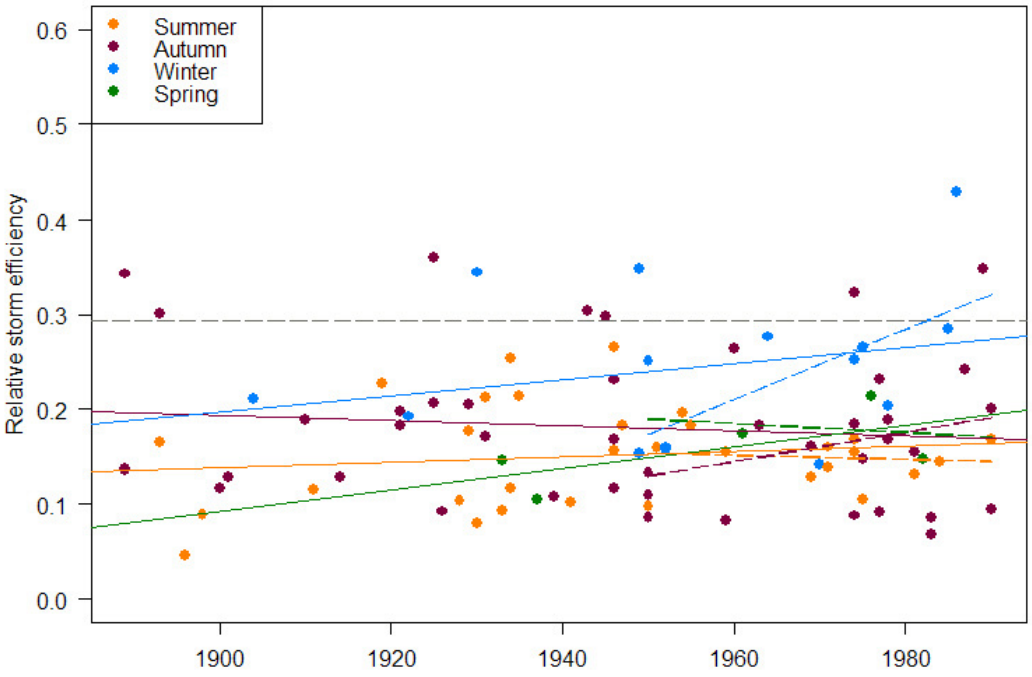

Figure 43 Relative storm efficiency (convergence depth/SPW) for events in the GSAM database. Colour denotes season. Solid lines indicate linear trends over the full period (1889 to 2003). Coloured dashed lines indicate trends from 1950. Horizontal dashed line indicates the 90th percentile (over all seasons).

For none of the seasons or event types is there an indication that over recent decades the 90th percentile has been more frequently exceeded than for the early part of the record.

Of particular interest are changes in storm efficiency over the most recent decades. The period 1950 to 2000 was divided into two shorter periods: 1950 to 1975 and 1976 to 2000. The largest variability in relative storm efficiency is found for *autumn* and *winter* (Figure 44). There are only very few events during *spring*. Significant changes are found for *winter* but this assessment is based on less than 10 events.

[27] The definition of seasons used for GSAM differs from the conventional definition of seasons and from the definition of seasons used in GTSMR. For GSAM, summer is defined as December to March (4 months), autumn is April to May (2 months), winter is June to September and spring is October to November. For simplicity and to ensure adequate sample sizes, conventional seasons were used here, that is summer is December to February etc.

Influence of storm precipitable water and convergence depth rainfall on relative storm efficiency

Relative storm efficiency η_{topo} (Equation 9) can be calculated as the ratio of convergence depth rate (mm/h) and storm precipitable water (mm). When studying changes in this ratio it is of interest to analyse these two components with regards to relative storm efficiency.

There is no strong relationship between SPW and relative storm efficiency. Judging from Figure 45 it appears that relative storm efficiency above the 90th percentile can occur for a wide range of SPW (between 20 and 65 mm). Typical SPW is higher in *summer* than in *autumn*, and will also depend on latitude (SPW is larger closer to the equator). SPW in *winter* is very low and for events from the GSAM database usually does not exceed 30 mm.

Changes in storm PW can be assessed through changes in maximisation factor (MF) and these are discussed in detail in section 1.1.1. No significant changes in MF (and therefore SPW) were identified for GSAM events.

Estimates of storm precipitable water are derived from estimates of storm dew points. The error margin for storm dew points is particularly large for *winter* events (up to +/- 2 °C). The associated error in storm precipitable water is about 8% per 1 °C and for an estimated relative storm efficiency (for *winter* events) of 0.3 the actual value could therefore range between about 0.25 and 0.35.

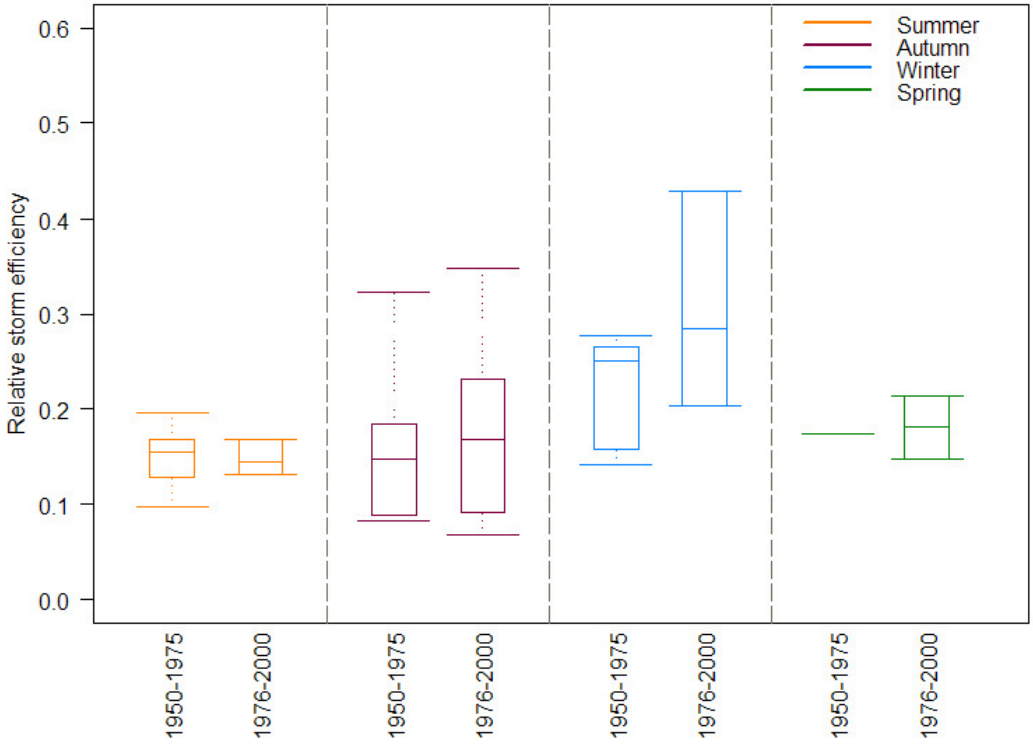

Figure 44 Boxplots indicating distribution of relative storm efficiency for two periods: 1950 to 1975 and 1976 to 2000 (by season). Note: there are only 5 events during *spring*.

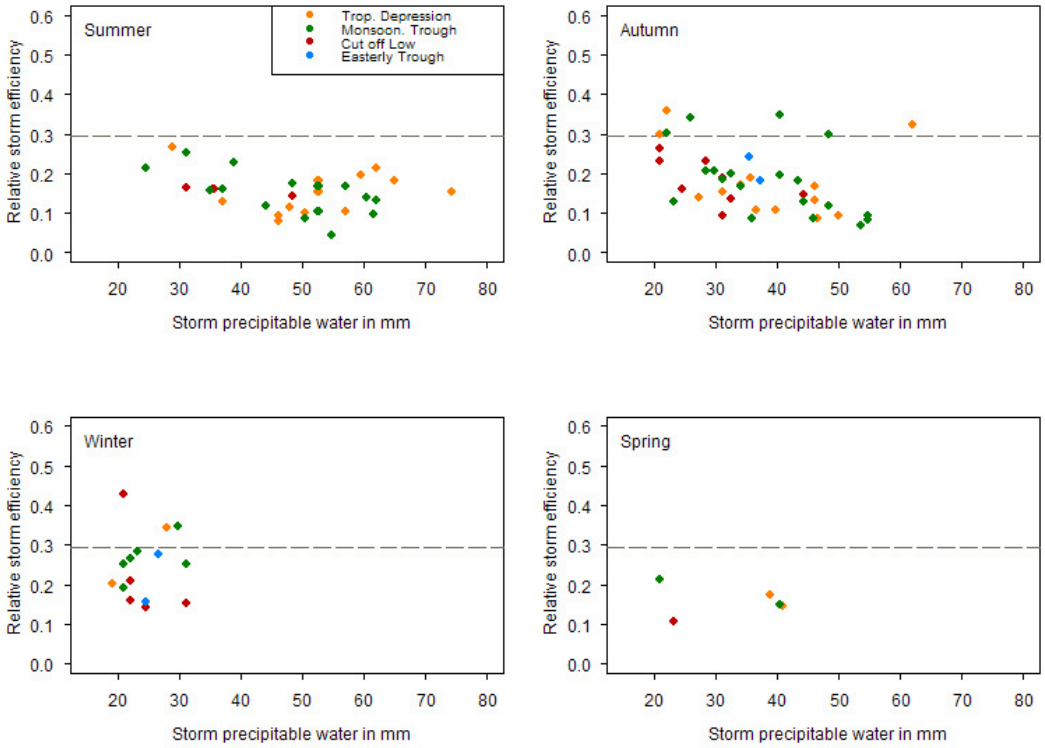

Figure 45 Scatterplot of relative storm efficiency against storm precipitable water, by season for GSAM events. Colour indicates event type. Horizontal line indicates the 90th percentile of relative storm efficiency.

Events with relative storm efficiency above the 90th percentile typically exceed 200 mm convergence depth. Generally, relative storm efficiency increases with increasing convergence depth and the relationship between convergence depth and relative storm efficiency appears to depend on the season. Typical SPW is higher in *summer* than in *autumn* and for the same rain rate *summer* efficiency would therefore be lower than for *autumn*.

Convergence depths for storms in the GSAM (Generalised Southeast Australia Method) database

The GSAM storms database contains 110 events for durations between 1 and 7 days. Only convergence depths for the 24 hour duration and an area of 1000 km^2 will be discussed. In cases where more than one convergence depths was available (derived for storms of different lengths) only the maximum of these depths was used (to avoid double-counting events).

Linear trends were fitted for two periods: 1900 to 2003 and 1950 to 2003. The only statistically significant trend (at 99%) is identified for *summer* for the period 1900 to 2003 (Figure 46). While the trend over the longer period for the *summer* season is positive (increasing convergence depths), the trend for the shorter period 1950 to 2003 is negative (although not statistically significant). The difference between the average convergence depth calculated for the earlier (1889-1949) and the later period (1950-2003) is statistically highly significant (at 98%). Events with the highest convergence depths tend to be caused by 'tropical depressions'.

An increase/decrease in convergence depth does not have to imply an increase/decrease in relative storm efficiency. A relative increase/decrease in storm types typically associated with high convergence depths would appear as an increased/decreased convergence depth (averaged over all storm types). To investigate whether the change in average convergence depths could be caused by changes in a particular event type, we repeated the significance test but each time one event type was excluded. It was found that the trend remained significant (although only at 90%) no matter which event type was excluded and changes are unlikely to be caused by changes associated with one particular event type.

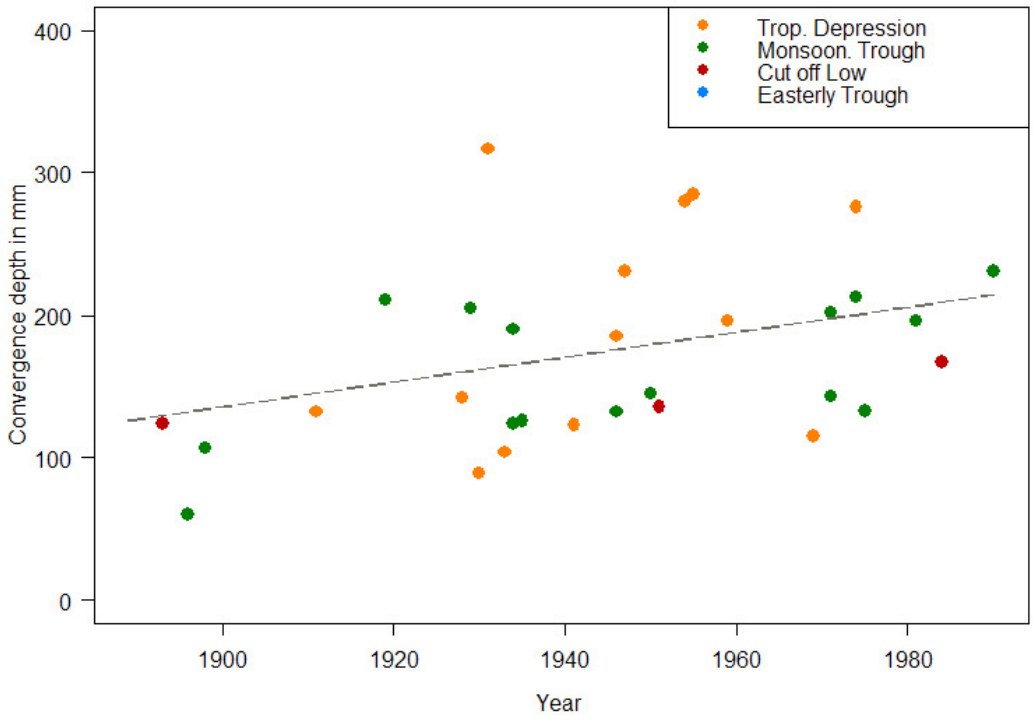

Figure 46 Convergence depths for GSAM *summer* events (December to February). Solid line indicates linear trend. Colour indicates event type.

Overall, 33 storms during the *summer* months are considered. 17 of these events occurred during the first, slightly longer part of the record (1889 to 1949) and 16 events occurred during the later period (1950 to 2003). An increase/decrease in convergence depth (over time) for a given storm type could be caused by a change in preferred location (possible to regions with higher moisture availability) or an increase in moisture availability (for a given location).

The location and type of GSAM events during *summer* were mapped for two periods (1889 to 1949 and 1950 to 2003, see Figure 47) to assess whether changes in preferred location for the three storm types had occurred. The maps in the bottom row show the event types for *summer* storms over the full period (left panel) and the location of all GSAM events (right panel) for completeness. There is little change in the frequency of the 3 event types (Figure 47). Tropical depressions have a tendency to occur further north during the later period. This fact could have led to an apparent increase in convergence depths but could be a sampling effect. Some of the Monsoonal troughs occurring during the later period are centred further inland.

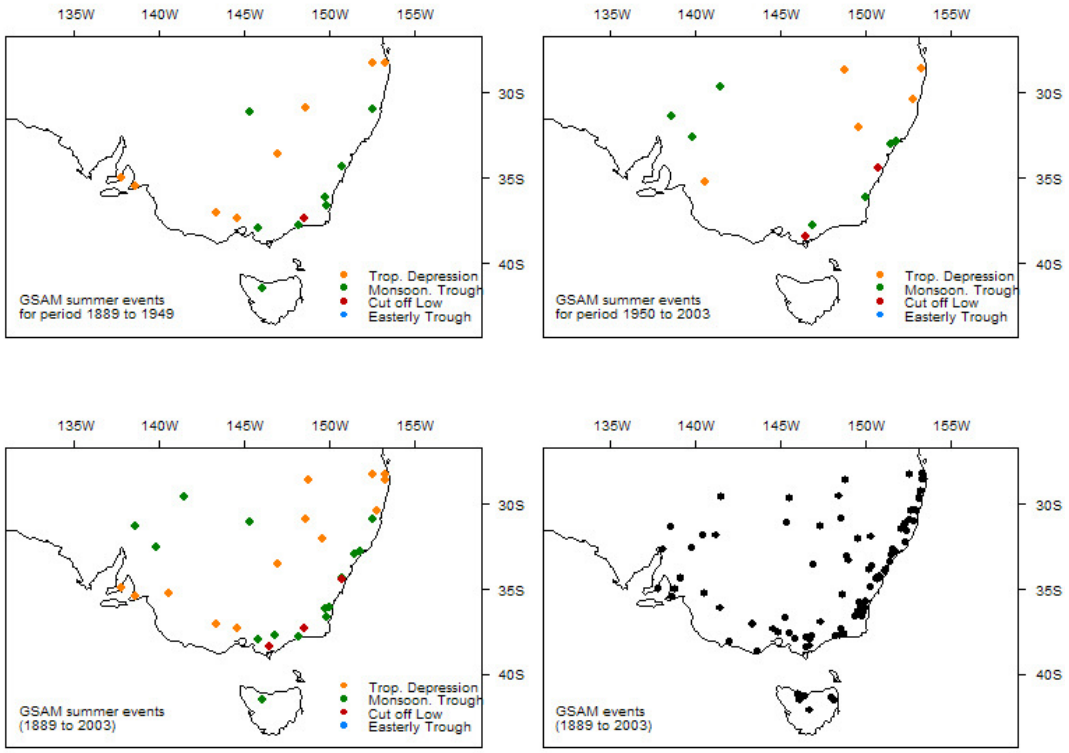

Figure 47 Location and type of events from the GSAM database.

Summary

Relative storm efficiency (defined as the ratio of convergence depth rate and storm precipitable water) for events in the GSAM database was analysed for one duration (24 hours) and one area (1000 km^2). Significant changes in relative storm efficiency were found only for *winter* events (an increase for the period 1950 to 2003, based on less than 10 events). The event with the highest storm efficiency is a cut-off low that occurred in August 1986 and had a convergence depth of 216 mm and an estimated storm precipitable water of 21 mm.

The convergence depths for storms from the GSAM database for the *summer* months (December to February) show a significant increase from the early to the late part of the 20th century. This increase might be related to the fact that during the later period tropical depressions tended to occur further north.

These results are based on events from the GSAM database and are not directly transferable to the larger GTSMR region because of factors such as seasonality and types of events. Storm efficiency based on GTSMR events (and three somewhat different definitions of storm efficiency) has on average decreased.

1.4.2.3 Relative storm efficiency based on station data at point locations

Section 1.4.2.1 and 1.4.2.2 assessed relative storm efficiency based on events from the GTSMR and GSAM databases. Climatology of precipitable water and rainfall depth will vary with location of events (represented by the storm centre), complicating the assessment of changes in relative storm efficiency. Alternatively, relative storm efficiency can be assessed for large events at a given location; this also has the advantage, that an adjustment for topography on rainfall is not required. However, results from event and point-based analysis may not be directly comparable. The following factors highlight differences between the two analyses:

- Rainfall depths at a point may not be representative of those for larger areas, whereas the assessment made for the generalised analyses focused on changes in the relatively storm efficiency for events of 1000 km^2.
- Climate change may affect events of higher and lower frequency in different ways (section 1.2.2, Figure 26). Changes in storm efficiency from the point-based analysis may be characteristic for more frequent events while changes derived from event based analyses are more characteristic for less frequent events (e.g. below an average recurrence interval of approximately 1 in 100 years).
- It is possible that changes in preferred location for a given storm type may affect the storm efficiency. Storm type was not considered for the point-based analyses.

These factors will be considered when drawing conclusions from the subsequent analysis.

At the high-quality dew-point temperature locations, the 30 largest independent rainfall depths for different rainfall accumulation durations (1, 2, 3 and 5 days)[28] ending at 0900 local standard time were obtained for each of the periods 1960-1980 and 1981-2003. Locations were selected only if the median annual rainfall was more than 350 mm. The relevant SPW prior to the event was estimated from the 24h persisting dewpoint ($24T_d$)[29] using the high-quality dew-point data. The relative storm efficiency based on the ratio of the hourly rainfall rate to SPW (equation 9) and the ratio of daily rainfall to the product of SPW and wind speed (equation 10) were calculated. In equation 10, the median wind speed at 850 hPa for the period associated with the rainfall was used. (Not all locations had upper-air data available).

Figure 48 shows the relative change between the medians of the 1981-2003 and 1960-1980 relative storm efficiency for each duration (1, 2, 3 and 5 days). Changes are only calculated for a season if at least 10 events occur within each period, and where the storm precipitable water is not unreasonably small (such that the corresponding maximisation factor is less than 3.5). Apart from Charleville, each location has only one season for which the change could be assessed. Overall, there are more locations

[28]Extensive investigation showed that rainfall accumulation of durations longer than 24 h provides the most robust assessment of changes in relative storm efficiency at point locations. This contrasts with analyses carried out for the significant rainfall events from each of the generalised databases. Although a duration of 24 h would have provided a closer comparison with the analysis of the generalised events, it was not possible to obtain consistent changes for this duration. In this section, results from rainfall accumulations over 24 h are presented for reference, but results are discussed in terms of the more robust changes from the longer durations (48 h, 72 h and 120 h).

[29]The 24h accumulated rainfall for the period over which $24T_d$ was calculated had to be less than 2.5 mm. Estimates with other thresholds were tested, although above 2.5 mm, results did not considerably change for durations longer than 24 h.

with a sufficient number of *summer* events (9-10 locations depending on duration) than for *autumn* (2-5) or *winter* (3-5). There are no events satisfying the selection criteria during *spring*. The *summer* events occur in locations across northern Australia, inland NSW and QLD, as well as parts of southern coastal Victoria. *Autumn* events occur primarily in coastal NSW, with *winter* events largely in SW Western Australia. The spatial distribution of locations selected for each season is representative of the coverage of higher density GTSMR and GSAM events (only locations within the inland regions are not well represented). The changes at inland locations would be susceptible to an insufficient number of large rainfall events occurring within each period. Although an arbitrary annual median of 350 mm was chosen as a threshold when selecting locations, the two locations with the lowest annual rainfall (Charleville and Cobar) have the greatest variability in the changes when different parameters (e.g. rainfall threshold) are used to calculate the SPW (not shown).

There are only two locations (Darwin during *summer* and Coffs Harbour during *autumn*) that have large, statistically significant changes in the relative storm efficiency at the 0.05 level; an increase and decrease respectively. These locations occur at durations of 2 and 3 days. Coffs Harbour also has a significant (but small) decrease at 5 days. For the remaining locations, and for durations of 2 and 3 days, there are general increases over NW Australia and a few inland NSW locations, with decreases for most of coastal eastern Queensland and NSW. *Winter* events at Perth suggest a consistent increase in the relative storm efficiency for all durations, which contrasts with *winter* time decreases observed nearby for Geraldton and Albany. Changes at locations for the longest duration (5 days) generally reflect those occurring at the shorter durations (2 and 3 days).

These changes in relative storm efficiency can be largely attributed to changes in the rainfall (Figure 49), rather than changes in the storm precipitable water (SPW[30], Figure 50). This is particularly the case for north Australian locations, and those on the west and east coasts of Australia. While a few locations do not indicate any change in the relative storm efficiency (e.g. Charleville for both *summer* and *autumn* for all durations) there is a relatively large increase in rainfall at this location (of the order of 20% for all durations) which is offset by a decrease in the storm precipitable water for 3 days and 5 days (represented by the increase in the maximisation factor).

The changes reported here for the longer durations generally agree with those from analyses carried out for GSAM and GTSMR events over approximately the same period (1950-2003), although those were only for the 24h duration. For the generalised events, there was an overall decrease in relative storm efficiency, although this was not significant.

Finally, relative storm efficiency was estimated using upper-level wind speed (equation 10). Due to a lack of upper-air data[31], this slightly reduces the number of

[30]SPW is represented in the denominator of the moisture maximisation factor, MF. This quantity allows for assessing the correspondence between changes of equal sign in both the relative storm efficiency and the inverse of the SPW. The maximisation factor is used, since it appropriately normalises the SPW to remove intra-seasonal variation in the PW.

[31]Changes were only computed where upper air data were missing for at most one event.

available locations. At locations where storm efficiency showed decrease in Figure 50, this decrease becomes more apparent (Figure 51) when wind speed is taken into account (particularly for longer durations, e.g. 5 days). However, this definition of storm efficiency might be less appropriate for inland location.

Summary

Although results from event and point based analyses may not be directly comparable (see discussion earlier within this subsection), it may still be possible to derive some qualitative conclusions that can be generally applied to both analyses. The most robust changes using the point-based method are for durations longer than 24 h. Only two locations report a change in relative storm efficiency that is statistically significant at the 0.05 level. For the remaining locations, the data indicate that coastal eastern Australia has the greatest reduction in relative storm efficiency between two periods (1960-1980; 1981-2003), and the coastal extent of this change increases with increasing duration. Changes for *winter* are associated with SW Western Australia, the sign of the change depends on the location. The changes in storm efficiency are least consistent for inland locations – perhaps associated with a lower annual rainfall compared with coastal locations. Based on station data at point locations, changes in rainfall totals have a more significant effect on relative storm efficiency than changes in the maximisation factor, particularly for coastal locations. Section 2.1 will assess more thoroughly the changes in observed extreme precipitation, particularly for 1 and 5 day durations.

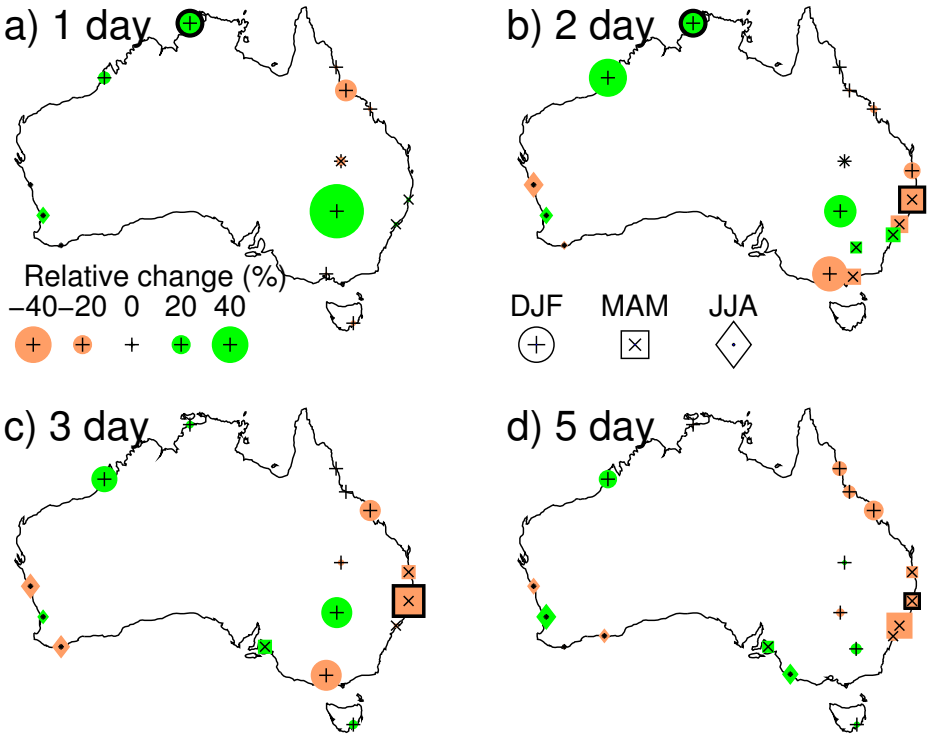

Figure 48 Seasonal variation of the relative change in relative storm efficiency (based on equation 9) for the 30 largest independent rainfall events for different durations. a) 1day, b) 2 day, c) 3 day and d) 5 day durations. The black circle outline indicates change is significant at the 0.05 level. Crosses, plus signs and point symbols denote locations that have sufficient data (10 events in each of 1960-1980 and 1981-2003) for *summer*, *autumn* and *winter* events respectively.

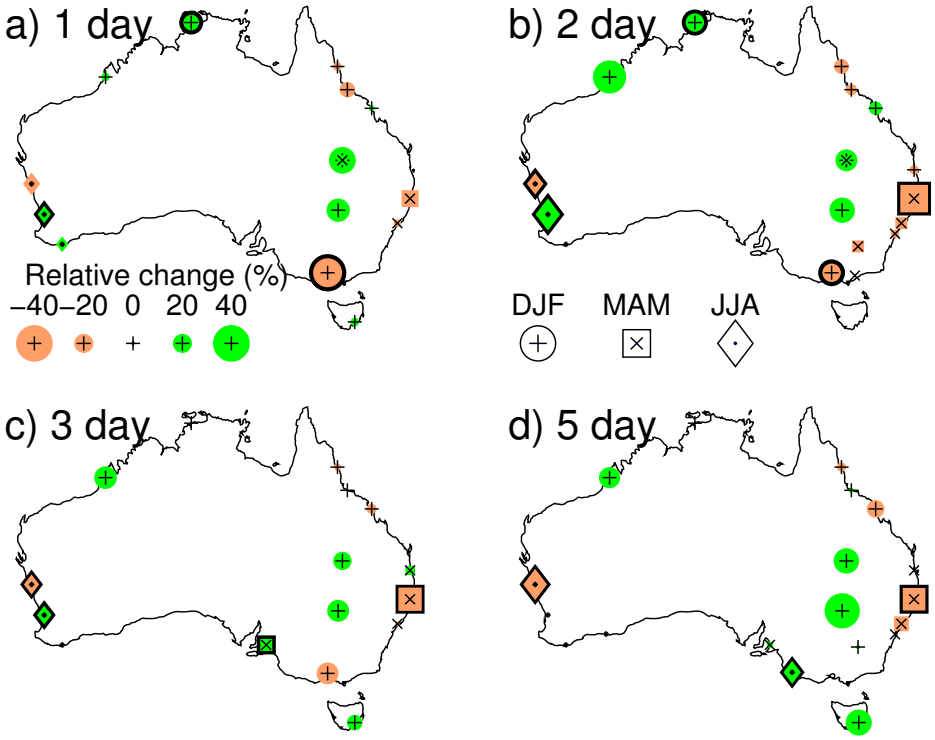

Figure 49 Seasonal variation of relative change in rainfall depth. Figure parts and symbols are as in Figure 48.

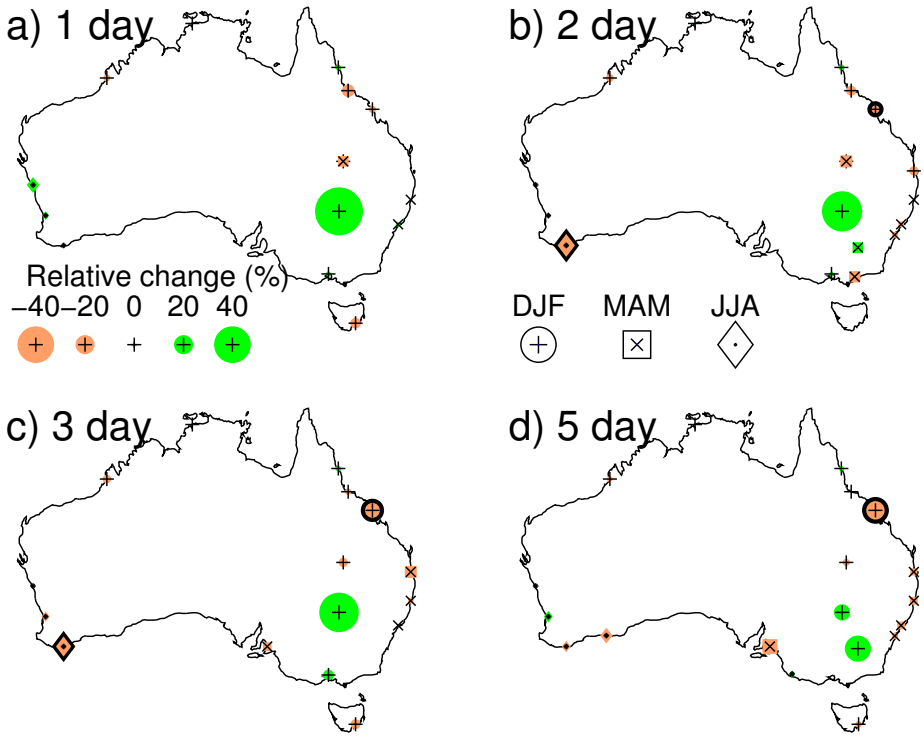

Figure 50 Seasonal variation of the relative change in the maximisation factor. Figure parts and symbols are as in Figure 48.

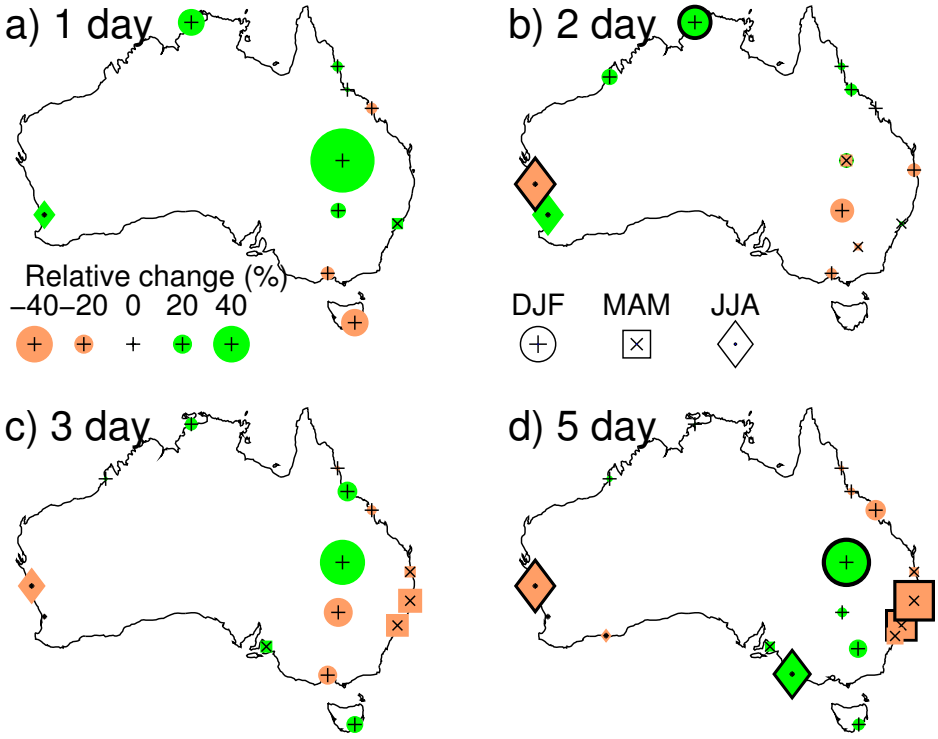

Figure 51 Seasonal variation of the relative change in the relative storm efficiency (including wind speed), based on equation 10. Figure parts and symbols are as in Figure 48.

1.4.3 A recent noteworthy event

A recent noteworthy event was analysed as a case study for this project. Significant rainstorms are routinely analysed as part of the on-going storm monitoring aspect of the GTSMR project. If depth-duration-area curves for such an event exceeded the depth-duration-area curves for the relevant season and region, the database would be updated to include the event and users would be notified.

Meteorology

The event occurred over three days, up to and including the 1st of July 2005. This event was characterised by intense rainfall and gale force winds, causing flooding along parts of the Gold Coast and northern NSW. Figure 52 shows an isohyetal analysis for 3-day rainfall depth up to 1 July 2005, with the related satellite image and mean sea level synoptic chart shown in Figure 53 and Figure 54 respectively.

Heavy rainfalls were caused by an upper trough in combination with an east coast low (Bureau of Meteorology 2005a). Such events tend to occur during *autumn* and early *winter* but can occur at any time of the year. The associated rainfall was the heaviest June daily rainfall in Queensland since 1967 (Bureau of Meteorology 2005b). At Carrara 585 mm were measured in the 24 h to 3 pm on the 30th June 2005 (Bureau of Meteorology 2005a). Heaviest rainfall occurred between 3 am and 12 am on the 30th June. At Carrara, for durations above 20 min rainfall intensity exceeded the 1 in 100 year event.

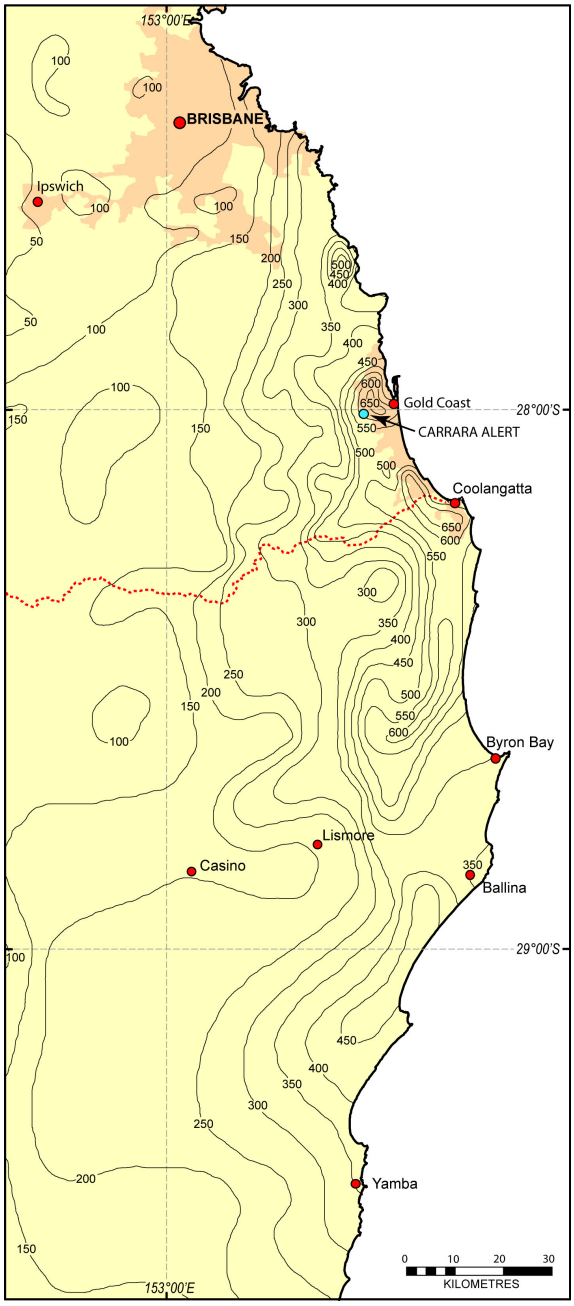

Figure 52 Isohyets for a 3-day storm ending 1 July 2005 (rainfall depth in mm, 9 am to 9 am)

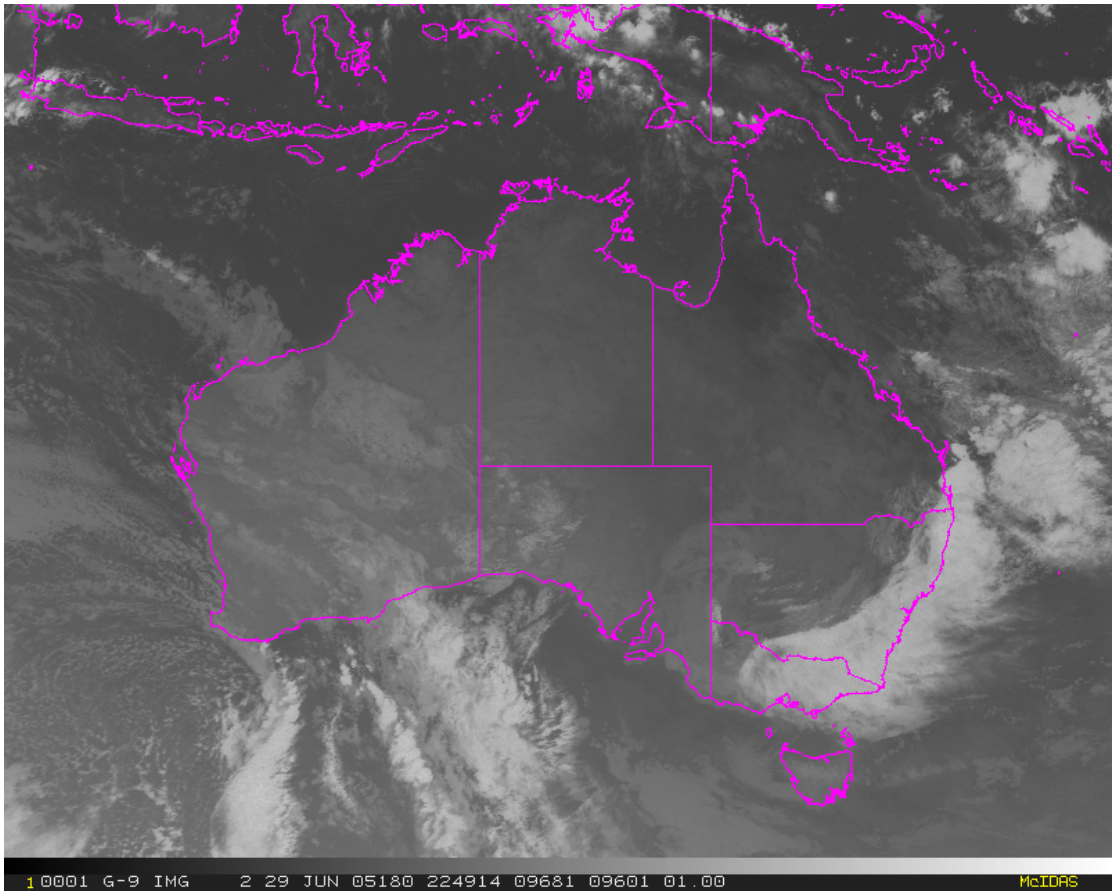

Figure 53 Satellite image (infrared) taken on 29th June 2005 at 23 UTC.

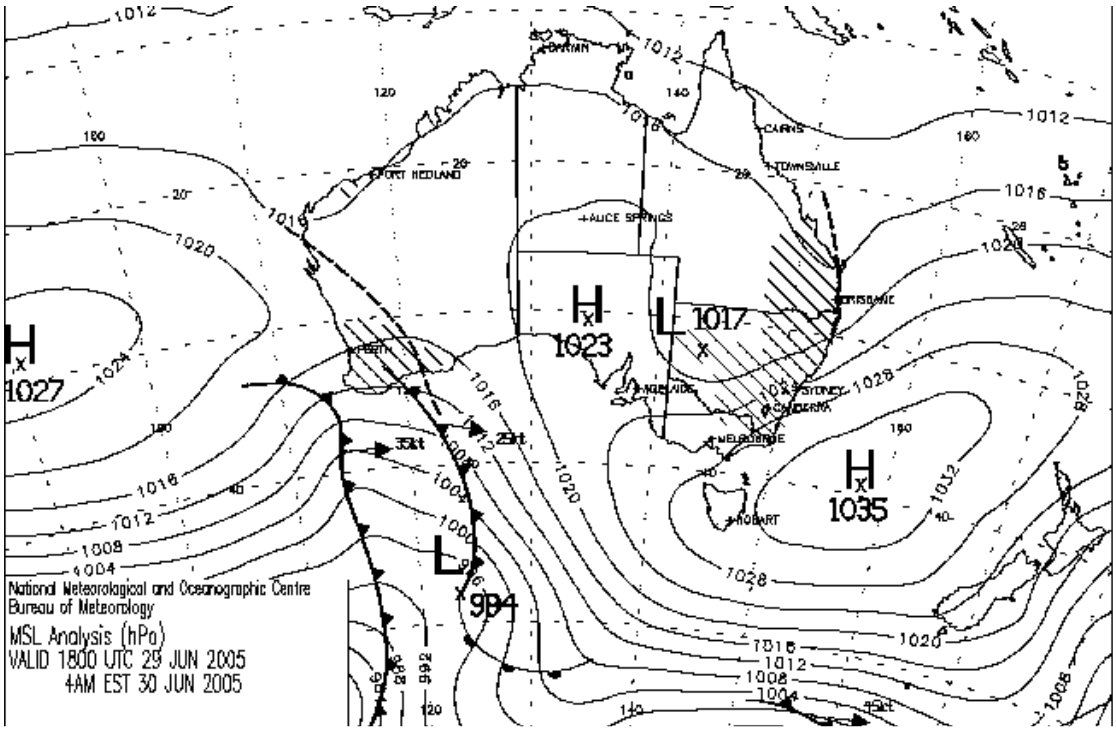

Figure 54 Synoptic chart for 29 June 2005, 18 UTC (30 June 2005, 4 am local time).

Moisture

The storm dew point[32] was estimated as 12.5 ºC. This was derived from dewpoint temperature observations at synoptic stations along the moisture inflow path. The vertical temperature and dewpoint temperature profiles (Figure 55) for Brisbane supports this estimate. Figure 55 shows a moist pseudoadiabatic layer between 900 and 700 hPa. The corresponding storm precipitable water (SPW) was estimated as 27.2 mm. The extreme dew point (derived from the 24 h persisting dew point for this location and time of the year) is 19.7ºC which corresponds to 51.4 mm extreme precipitable water (EPW). The maximisation factor (MF) is calculated as the ratio of EPW/SPW = 1.9.

The standardisation factor (SF) is based on Broome Airport's maximum persisting dew point for the months May to September. The standard EPW for this period is 82.3 mm. The standardisation factor is calculated as the ratio of $EPW_{standard}$ to EPW and is 82.3/51.4 = 1.6.

Deriving the generalised storm depth

Generalised storm depth is the storm rainfall that has been maximised for moisture availability and standardised to a location. By removing the effects of topography and removing the site specific features of the rainfall, the storm may then be compared with rainfall from other generalised storms.

Once isohyets have been constructed and digitised (Figure 52), storm depths for standard areas can be derived (dark blue line in Figure 56). The convergence depth[33] (magenta line in Figure 56) is derived by removing effects of topography on rainfall (by applying a topographic adjustment factor, TAF) and is therefore equal to or lower than the storm depth.

The convergence depth is multiplied by the maximisation factor, MF (here 1.89) to derive the maximised convergence depth (cyan line) and which is then standardised (multiplied by a standardisation factor, SF of 1.60) to derive the standardised, maximised convergence depth (orange line). Finally, the decay amplitude factor (DAF[34] , 0.975) is applied to derive the generalised depth (green line).

[32] Estimates of storm dew points for events occurring during the winter months are less accurate than for events that occur during summer. For winter events, the error could be of the order of 2 °C which would lead to an error of about 15% in the estimate of SPW. For the Gold Coast 2005 event the relative storm efficiency could therefore range between 0.57 and 0.77 (assuming an error in the estimate of storm dew point of +/- 2 °C).

[33] The total observed storm rainfall is considered to be partly due to topographic enhancement. Convergence precipitation is due to atmospheric processes unaffected by terrain. Orographic (or topographic) precipitation is caused entirely or mostly by the forced uplift of moist air over high ground.

[34] This factor is used to account for the decay in a storm mechanism as it propagates to remote locations. Note that the winter storms had the 'summer' decay amplitude factor (DAF) applied. Although there is still a residual signal present in winter, this DAF represents it less accurately.

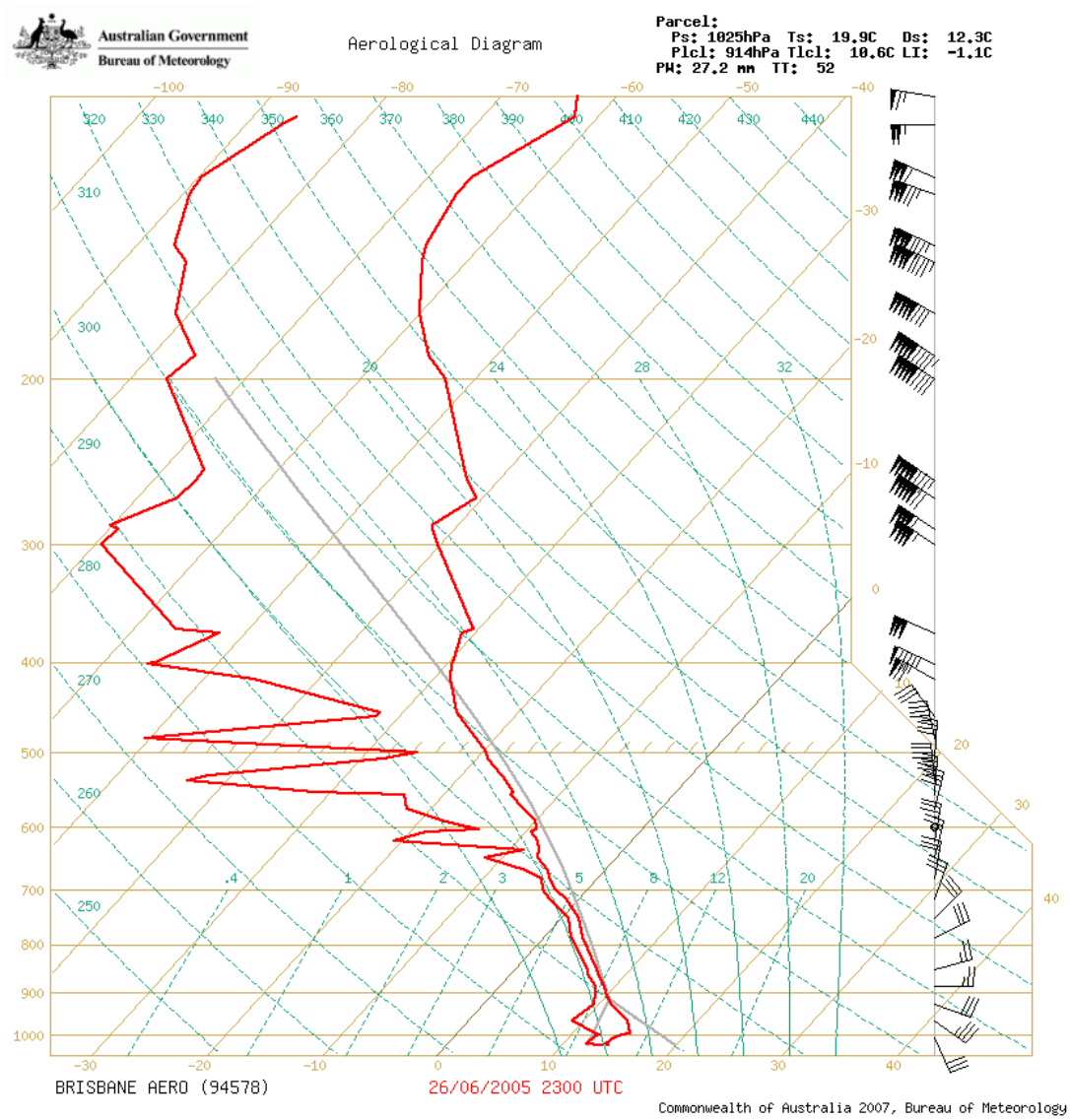

Figure 55 Thermodynamic diagram - vertical temperature and humidity profile and wind speed/direction for Brisbane Airport at 23 UTC, 26 June 2005.

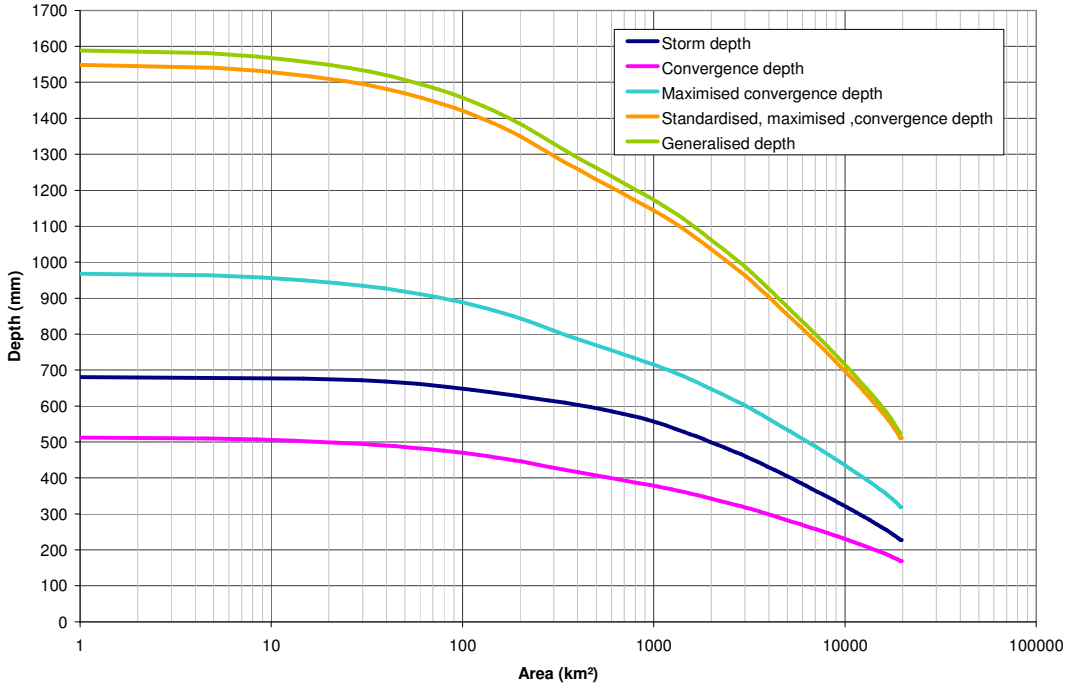

Figure 56 Deriving the generalised depth for the Gold Coast 2005 event.

Comparing storm depths with design depths

Generalised storm depths were derived for durations between 6 and 72 hours and for standard areas up to 20,000 km^2. The depth-area curves for the event are shown together with the design depth-area curves (Figure 57). The generalised depths are greater than the design depth for the Coastal Application Zone - *Winter* (CAZ-W)[35] for all durations above 6 hours and all areas below 1000 km^2.

The generalised depths for the complete 3-day event exceed the 72h design storm depths for areas below 3000 km^2 (Figure 58). Generalised rainfall depths from this event exceeded those from the *winter* storm database of the GTSMR which includes the most significant events over durations of 1 to 5 days across the GTSMR region from the entire rainfall record.

Relative storm efficiency

The relative storm efficiency of an event can be characterised by the ratio of storm depth to storm precipitable water (SPW, 27.2 mm). The storm depth for the Gold Coast 2005 event for a duration of 24 h over an area of 1000 km^2 is 426.1 mm, this equates to a rain rate of 17.75 mm/h. The resulting storm efficiency is 0.65.

Relative storm efficiencies have been derived for storms from the GTSMR database (for 24 h, 1000 km^2 and based on rain rates derived from storm depths). The event with the largest relative storm efficiency occurred during the *winter* months (June 1950), reaching an efficiency of 0.65.

[35] The Coastal Application Zone - Winter (CAZ-W) design depths are available for deriving PMP estimates. However, in practice these estimates are very rarely required. For this region, PMP estimates for the summer season are much higher and it is therefore sufficient to design for summer events.

The relative storm efficiency of the Gold Coast 2005 event is not exceeded by events in the GTSMR database. As for the *winter* event with extremely high efficiency (June 1950), the high relative storm efficiency results in part from the fact that the SPW estimate is very low compared to other events in the database.

Storm depths include effects of topography on rainfall. These effects are removed when the convergence depth for a storm is derived. Convergence depths for GTSMR are not generally available. However, an attempt was made to estimate convergence depths for GTSMR events (see section 1.4.1 for details). An 'adjusted storm efficiency' was calculated (taking into account topographic enhancement of rainfall) for events from the GTSMR database. The highest adjusted storm efficiency (0.41) is reached for a *summer* event (December 1916, topographic adjustment factor 1 at location of storm centre, rainfall depth for 24 h duration and 1000 km^2: 618 mm, storm precipitable water: 62.7 mm). The adjusted storm efficiency for the June 1950 event is considerably lower (0.33) than the relative storm efficiency based on the storm depth (0.65). If the same approach were used for the Gold Coast 2005 event, the adjusted storm efficiency would be the same as the relative storm efficiency (since the topographic adjustment factor for the location of the storm centre is 1.) The relative storm efficiency based on the convergence depth (289.3 mm for 24 h and 1000 km^2) is 0.44.

We conclude that although there is some degree of uncertainty in the estimates of convergence depth, and therefore the resulting adjusted storm efficiency, the storm efficiency for the Gold Coast 2005 event ranks among the highest efficiencies derived for GTSMR events and this is true for both the storm efficiency based on storm depth and convergence depth.

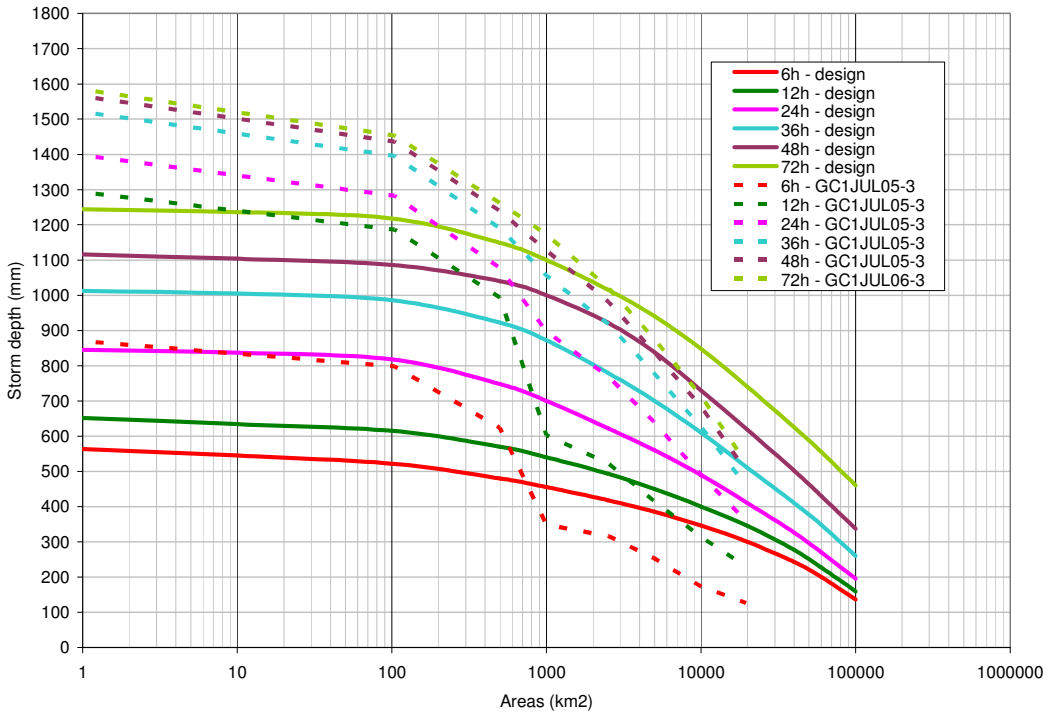

Figure 57 Depth-duration-area curves. Solid lines - depth-duration-area curves for the Coastal Application Zone *Winter* (CAZ-W), dashed lines - Gold Coast 2005 event. Colour denotes duration.

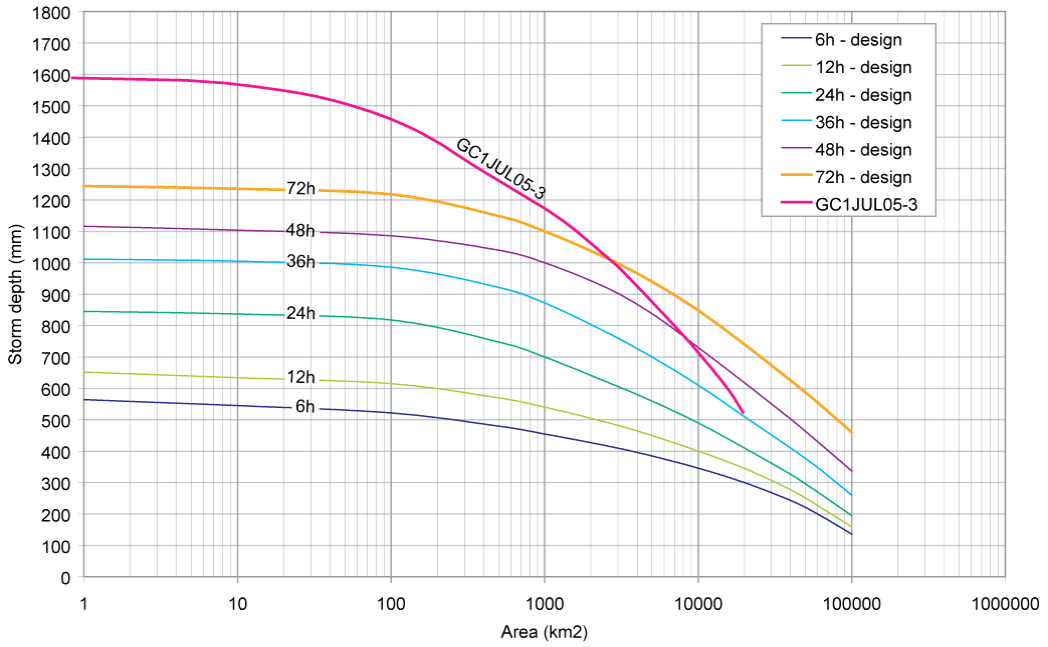

Figure 58 Depth-duration-area curves for the Coastal Application Zone *Winter* (CAZ-W) and 3-day Gold Coast 2005 event.

Summary

A recent noteworthy event was assessed. This event occurred during the *winter* months (June 2005). Record rainfalls led to extensive flooding along parts of the Gold Coast.

For a number of durations and areas, the depth-area estimates exceed the design estimates for the Coastal Application Zone - *Winter* (CAZ-W).

The relative storm efficiency for this event is similar to the highest efficiency for events in the GTSMR database (starting in 1893). Even after taking topographic enhancement of rainfall into account, the efficiency for this event ranks amongst the highest efficiencies derived for GTSMR events.

The recent event assessed here is a record-breaking event with very high relative storm efficiency. Typically, GTSMR events with very high efficiency tend to be *summer* or *autumn* events although very high efficiency was reached by a previous *winter* event (which occurred in June 1950).

Analyses based on GTSMR events lead to the conclusion that average storm efficiency may have declined over recent decades. This is consistent with model results (global averages) and theoretical considerations. However, based on the assessment of a recent event we need to consider the possibility that relative storm efficiency of events could increase for certain locations, event types and seasons.

1.5 Combined effects of changes in moisture maximisation and relative storm efficiency

To derive PMP estimates for catchments, a PMP envelope is required. This envelope is constructed for a given configuration of area, duration, season and zone through the generalisation of relevant significant rainfall events. The generalisation process incorporates the maximisation of moisture (within realistic limits) and the assumption that at least one of the significant rainfall events is operating at, or close to, maximum efficiency (Walland et al. 2003).

Changes in moisture maximisation and relative storm efficiency were discussed in sections 1.1 and 1.4. These two factors are combined when applying the generalised methods, although relative storm efficiency is not explicitly calculated. Maximised-standardised convergence (MSC) rainfall depth can be considered a surrogate index of storm efficiency (Pearse 1993, as discussed in section 1.4). For the GTSMR events, the MSC can also be defined as

$$\mathrm{MSC} = \frac{\mathrm{CR}}{\mathrm{SPW}} \mathrm{EPW}_{\mathrm{standard}}, \qquad (11)$$

where CR is the convergence rainfall depth and $\mathrm{EPW}_{\mathrm{standard}}$ is either 120.0 mm or 82.3 mm, depending on whether the event occurs in the GTSMR *summer* or *winter* season. However, the MSC may also be expressed as the product of the convergence rainfall depth and maximisation-standardisation factor (MSF, section 1.1),

$$\mathrm{MSC} = \mathrm{CR} \frac{\mathrm{EPW}_{\mathrm{standard}}}{\mathrm{SPW}}. \qquad (12)$$

There is considerable spatial variability in the relative storm efficiency (see section 1.4.2). Walland et al. (2003) partially accounted for this spatial variability by calculating a decay amplitude factor, DAF (Figure 59). Overall, the generalised-maximised-standardised convergence rainfall depth of GTSMR events is given by

$$\mathrm{GMSC} = \frac{\mathrm{MSC}}{\mathrm{DAF}} = \frac{\mathrm{CR}}{\mathrm{DAF}} \mathrm{MSF} \qquad (13)$$

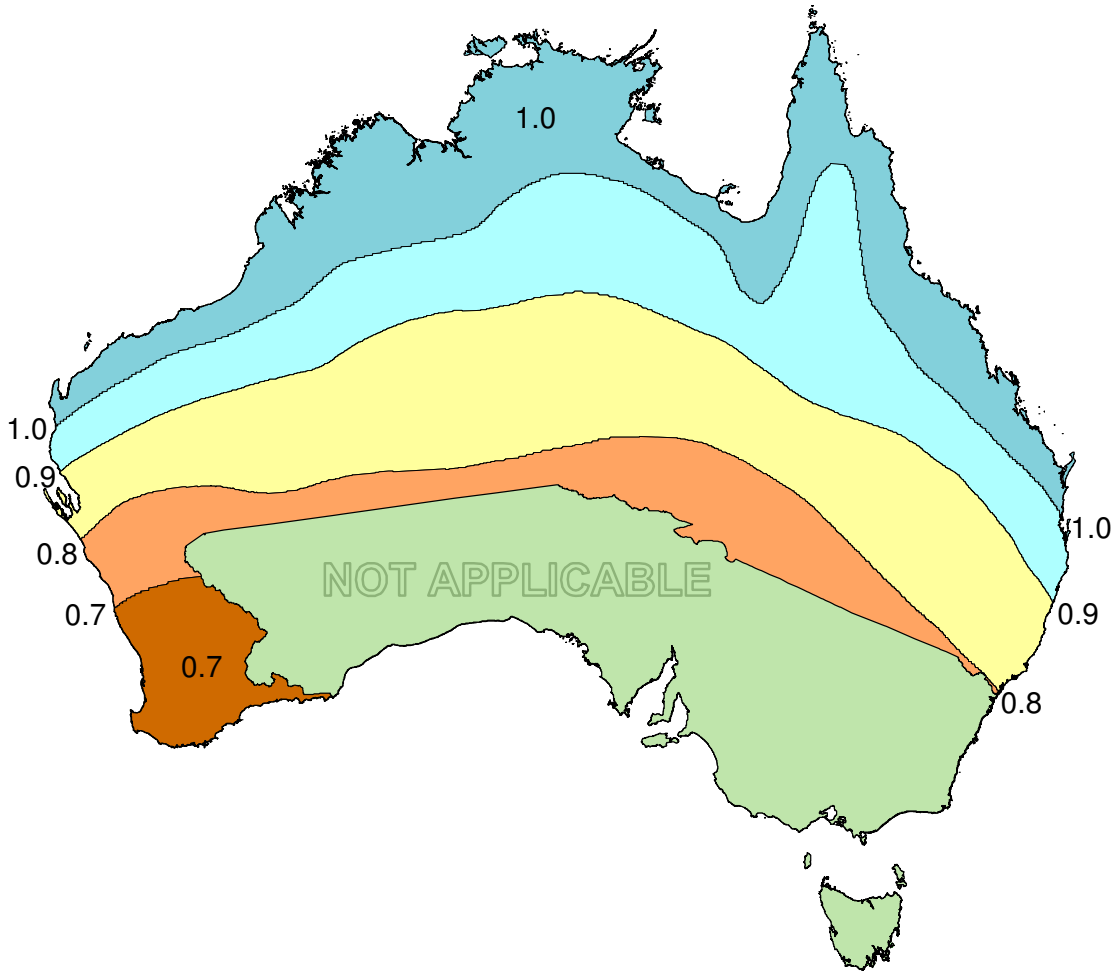

Figure 59 Decay amplitude factor for the GTSMR (from Walland et al. 2003).

For the GSAM, estimating the MSC is more complex even though the decay amplitude factor was not used. Since 26% of the events have a maximisation factor (MF) greater than MF_{lim} (equal to 1.8 for GSAM), the appropriate relation between MSC and storm efficiency is given by

$$MSC = \frac{MF_{lim}}{MF} CR \frac{EPW_{standard}}{SPW}, \qquad (14)$$

where the factor MF_{lim} / MF is always less than 1, since it is used to reduce the magnitude of the moisture maximisation. For GSAM events, the MSC for each season is proportional to the product of the relative storm efficiency and a moisture-maximisation reduction factor. The minimum reduction factor is 0.63 with genrally low values (i.e. greater reduction) for events on the NSW south coast during *autumn* (shown in Figure 60). The median reduction factor is 0.86.

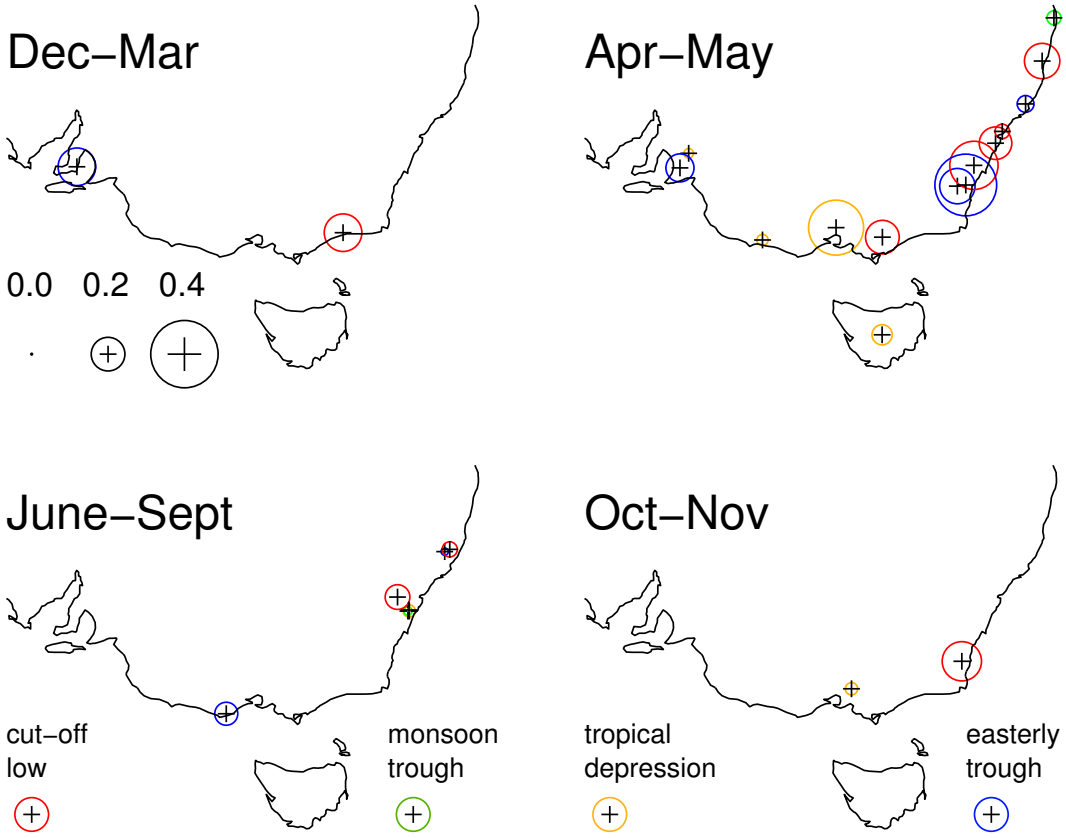

Figure 60 Magnitude of the GSAM reduction, equal to $1-MF_{\text{lim}}/MF$, so that the events with the greatest reduction have larger symbols.

The change in the GMSC for both the GTSMR and GSAM method can be calculated and discussed in terms of the changes already reported for both moisture maximisation and relative storm efficiency. The analysis of the combined changes to the events can be applied to their relevant application zone[36], season and for a set of standard duration and application areas.

For the coastal zone, the magnitude of the maximum GMSC (for each area and duration) has occurred primarily during the earlier period (1893-1949), and on average, 2/3 of events have occurred during the later period (1950-2003). It is likely that both the increased number of events in the second period and the lower median are artefacts of the method used to select events for the GTSMR database (Appendix A1). As a result, a significant decrease is reported for all but the largest areas.

The effect of the sample bias can be partially accounted for by applying a Mann-Whitney test to assess changes in significance of differences when removing the lowest ranking value in the second period one-by-one[37], testing at each step. The removal of the lowest ranking event continues until the difference between the two periods is no longer significant, or the number of data in the second period equals that in the first. Although this does not yield a quantitative measure of the significant

[36]Application zones (either inland or coastal) are relevant when estimating a PMP for a catchment. It is primarily related to the geographical distribution of significant rainfall events.
[37] This method can only be applied if the period with a lower median corresponds to the period with a greater number of events.

change (since the number of samples used is being reduced), it does provide an indication of the extent to which the lowest magnitude events bias the change.

Figure 61 shows all the data from the two periods for both *summer* and *winter* coastal events, and the resulting significant change at the 0.05 level, before the minimum number of data from the second period has been removed. This is only applied to *summer* data (orange and black circles), since *winter* events (blue circles) did not indicate a significant change for any area or duration. Black circles correspond to the lowest ranking events that have been removed in the second period, prior to the change being reported as insignificant. Horizontal lines in Figure 61 (indicating the median in each period) indicate that a significant change at the 0.05 level does occur.

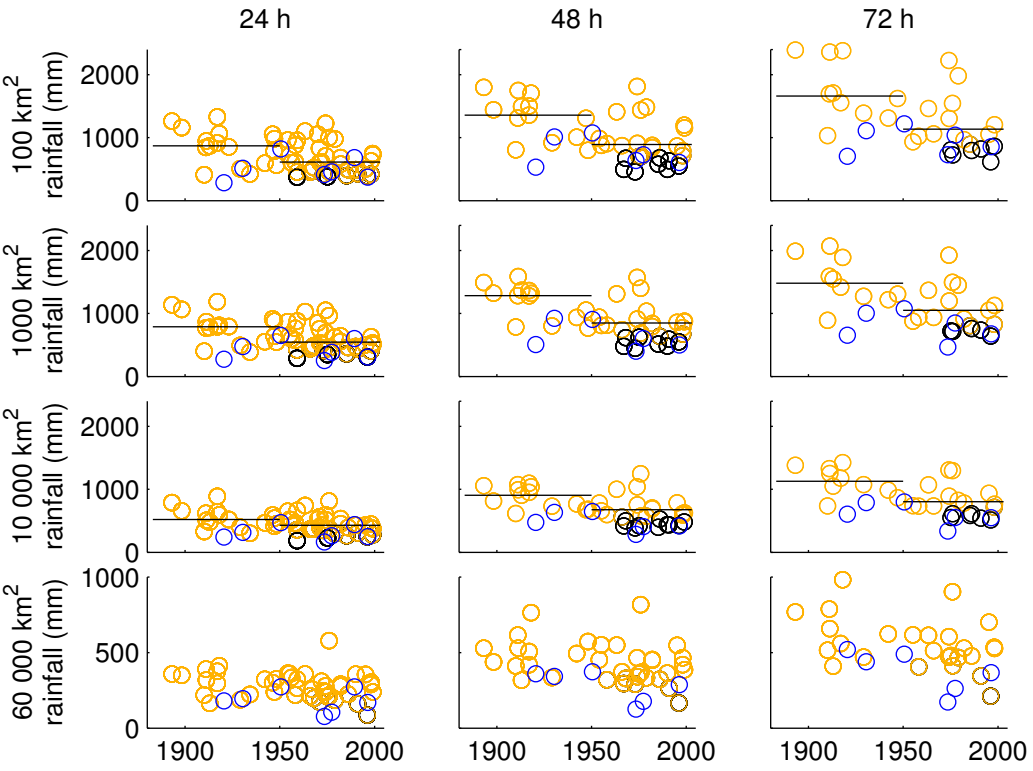

Figure 61 GTSMR coastal GMSC for independent *summer* (orange and black) and *winter* (blue) events. A black circle corresponds to events excluded when the number of samples is progressively reduced when testing for statistical significance between the two longer periods (1893-1949 and 1950-2003). Horizontal lines denote the median for each period, but only when there is a significant difference at the 0.05 level.

A low percentage of events removed, indicates that the change between two periods is most likely not significant (which is the case for all areas over the 24h period). A larger percentage removal (of the order of 15%, which reduces the proportion in each period closer to 50%) may imply that the original significant difference is not due to artefacts in selecting events. For 48 h and 72 h events, the number of events removed is approximately 8% for all but the largest area. As a result, it is uncertain whether these changes should be considered significant.

No significant decrease was found for either inland zone (*winter*) or SWWA zone (*winter*) events and there were no significant changes in either zone or season

between the two shorter periods (1950-1975, 1976-2003). However, there are too few *winter* events to reliably assess for changes between two periods. As expected, the GMSC for *winter* events are lower than for *summer*, which is largely attributed to the large ratio (46%) between the *winter* and *summer* values for EPW_{standard}.

For the GSAM, the change in GMSC was assessed for two sets of periods (1889-1950 and 1951-2003; 1950-1975 and 1976-2003). A significant change in the median GMSC is found for one category only (inland, *summer*, 24h 100 km^2). For the coastal and inland zones the highest MSC are typically related to *summer* and *autumn* events, respectively.

Overall, for both generalised methods, and for all but the largest area (60 000km^2) zone-season-area-duration categories, the maximum generalised rainfall depth is not considerably greater than for other highly ranked events (i.e. events ranked 1 are in general not too much larger than those ranked 2-3). This indicates the robustness of the generalised methods, particularly the moisture maximisation and standardisation process.

2. Probable Maximum Precipitation as extreme rainfall

The definition of Probable Maximum Precipitation (PMP) states that the PMP is *'The greatest depth of precipitation for a given duration meteorologically possible over a given size storm area at a particular location at a particular time of the year, with no allowance made for [future] long term climatic trends.'* (WMO 1986). While PMP estimates should not be equalled or exceeded, events close to the PMP could occur and would be regarded as significant rainfall events. These events (significant over large areas, as applicable for a PMP) would more than likely involve extreme point rainfall depths at one or a number of locations. Based on changes found for extreme point rainfalls, conclusions can be drawn how such changes might affect PMP estimates.

This section will assess for changes in extreme rainfall across Australia, using both observations from the 20th century and projections into the 21st century using climate model output, as used in the Coupled Model Intercomparison Project 3 (CMIP3). The climate model output from nine models will be validated against gridded observation data.

2.1 Trends in observed rainfall extremes

2.1.1 Introduction

Rainfall in Australia is highly variable, both spatially and temporally (e.g. over interannual and interdecadal timescales). One method to assess for trends in a highly variable quantity, such as rainfall, is to calculate suitable indices from high-quality daily rainfall data. Trends in Australian rainfall extremes have been investigated extensively using a variety of indices (e.g. Alexander et al. 2006, Alexander et al. 2007, Haylock and Nicholls 2000, Hennessy et al. 1999, Manton et al. 2001). However, changes in extremes are more difficult to quantify than changes in the annual or seasonal totals, since they require a high temporal resolution of observations (at least daily), which also extend over a reasonable time period (i.e. at least 50 years). These conditions, as well as the requirement that instruments at stations be free from malfunction, unsuitable exposure and observer errors, significantly reduce the number of locations used for analysis.

2.1.2 Data and Methods

The number of stations used for analysis of extreme rainfall is highly dependent upon the method used to select the stations. Selection criteria include overall quality of the station and quality of the data as well as appropriateness of observation methods. Appendix A2 provides details on selecting stations used for the current analysis. A major focus was to ensure that a sufficient number of stations across northern Australia (particularly in Queensland) were selected, although there are still large areas that have insufficient coverage. For the period 1910 to 2005, a total of 308

stations are available with useful data for trend analysis of extreme rainfall. Although fewer stations are available during the earlier period (e.g. 1910 – 1950), there is large year-to-year variability in the data quality at many stations. For each trend analysis period (e.g. 1910-2005 or 1951-2005), a station was selected if the proportion of quality checked data was at least 85% complete, and the station data started and ended within 6 years of the trend analysis period[38].

Rainfall indices used are selected from those recommended

- by the Expert Team on Climate Change Detection and Indices (ETCCDI)[39],
- for use in global studies of observations (Alexander et al. 2006) and
- for comparison of output from different climate models (Tebaldi et al. 2006).

The indices were computed on both monthly and annual scales, as described by Alexander et al. (2006) and (2007). Those used here are defined in Table 2[40].

The monthly indices, (1-day and 5-day maximum rainfall – *RX1day* and *RX5day* respectively), are reported on seasonal and annual timescales. The annual indices include the count of heavy rain days (*R10mm* where daily rainfall threshold is at least 10mm), and the relative contribution of rainfall from very wet days to total annual rainfall (*R95pT*). Although the method used to compute the indices exactly follows that of Alexander et al. (2007), trends and the significance of the trends are computed differently[41]. Our analyses identified more locations with significant trends than Alexander et al. (2007).

There are two indices (*R20mm* and *R99pT*) which, although appropriate for extreme precipitation, are not adequate for assessing trends for all of Australia. For more than half of the country, the index *R20mm* (number of days with more than 20 mm of rainfall) has a mean of less than 5 days. Of the remaining area, the trends are of similar sign and magnitude to *R10mm*. The index *R99pT* is highly variable and trends were not spatially consistent. Since neither index is available for the climate model data used in Section 2.2, they are not shown here.

[38] e.g. For the period 1910-2005, there has to be at least 85% data coverage at each station, with station start and end years no later and earlier than 1915 and 2000 respectively. This is more restrictive than the 80% requirement used by Alexander et al. (2007).

[39] A full list of all recommended indices with definitions is at http://cccma.seos.uvic.ca/ETCCDMI/

[40] Some of these indices correspond with those used in other studies, but are named differently. For instance, Hennessy et al. (1999) defined their seasonal *very heavy rainfall* being equivalent to the seasonal *1-day maximum rainfall* (*RX1day*).

[41] Both the linear trends and significance of the trends are computed using a modified version of the non-parametric Kendall rank correlation and Kendall tau test respectively. These are fully described in Wang and Swail (2001). Both tests are robust to the effect of outliers in the series, correctly account for ties in the ranked series and for positive autocorrelation in the timeseries, which nominally rejects the null hypothesis more often than specified by the significance level.

Table 2 The extreme rainfall indices used in this study, as recommended by the ETCCDI

Index	Name	Definition
RX1day	Max 1-day rainfall total	Seasonal maximum 1-day rainfall
RX5day	Max 5-day rainfall total	Seasonal maximum 5-day rainfall
R10mm	heavy rainfall days	Annual count of days where rainfall > 10 mm
R95pT	Proportion of annual rainfall from very wet days	Total annual rainfall from wet days (≥ 1 mm) with rainfall above the 95th percentile for wet days in the 1961-1990 period, divided by the annual rainfall

Trends are reported over two periods; 1910 - 2005 (the full period, corresponding to 96 years) and 1951 – 2005 (55 years) respectively. The trends are reported at station locations and are not gridded (see section 2.2.1). Trends obtained over the 96-year period will be more robust to interdecadal variability compared with 1951-2005. The shorter period indicates how climate has been changing in the more recent past, and will be useful for climate model output comparison. The shorter period is similar to that used in section 1 of this report and that used by Alexander et al. (2006). It also relates closely to a shift in rainfall characteristics occurring between 1945 and 1950 within SW and SE Australia (Vivès and Jones 2005). The later part of the shorter period has been associated with increased occurrence of ENSO events[42] associated with El Niños, which generally cause dryer conditions for eastern Australia (Suppiah 2004). Trends will also be reported over two non-overlapping periods (1910-1950; 1951-2005). This will allow assessing whether the signs of trends are consistent over time.

Seasonal trends have been computed for *RX1day* and *RX5day*. However, results from the analyses of significant rainfall events within the generalised methods and results from the analysis of storm efficiency (Section 1.4.2) indicated that significant rainfall events during *spring* are less frequent (and as a result, generally not as large) than for other seasons. To aid comparison with results from the analyses presented in section 2.1, absolute trends have been calculated for each location (as in Alexander et al. 2006) in contrast with trends relative to the mean for the index as carried out by Alexander et al. (2007). Trends in seasonal and annual rainfall totals had been derived by the Bureau's National Climate Centre based on gridded rainfall data[43] for the period 1910-2006.

2.1.3 Results

Trends in gridded seasonal rainfall totals

Figure 62 and Figure 63 show the trends in the gridded seasonal rainfall totals (derived from monthly rainfall data) for two overlapping periods, 1910-2006 and 1950-2006 respectively. The trends for all seasons indicate a greater magnitude of change in the later, shorter period compared with the longer period. The magnitude of

[42] ENSO: El-Niño Southern Oscillation. The result of a coupled global ocean-atmosphere interaction. The oscillation contributes to the natural variability within the climate system that affects eastern Australia. Strong negative values of an ENSO index (SOI), which occur during an El-Niño, have been associated with reduced rainfall over eastern Australia.

[43] http://www.bom.gov.au/cgi-bin/silo/reg/cli_chg/trendmaps.cgi

trends assessed in the more recent period (1950-2006) can be compared with those from the longer period.

Trends that are of the same sign indicate that either the more recent, larger magnitude trends are dominating the longer-term interdecadal variability, or that there is an overall consistent trend over the longer period. For both periods, the regions with large-area increasing trends are across NW Australia and Cape York Peninsula during *summer*. However, it is unfortunate that these regions lack sufficient high-quality daily data to adequately assess trends in extreme rainfall. Other areas with consistent same-sign trends across the two periods are associated with decreases. These are outlined by a red line in Figure 62.

There are notable decreases for both periods across coastal eastern Queensland during *summer* and coastal SW WA during *winter* (thick red lines). Other large areas with smaller levels of decrease in both periods include SE Australia and coastal SW WA during *autumn* and parts of southern Queensland, northern NSW during *winter* (thin red lines).

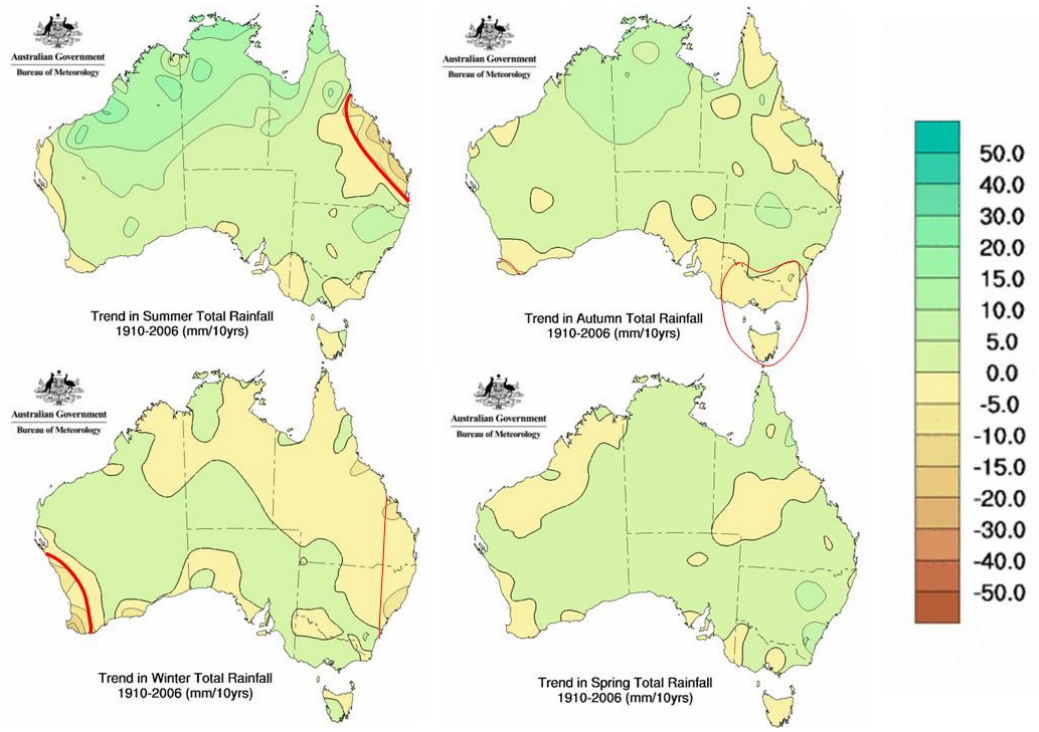

Figure 62 Trends in seasonal rainfall totals for 1910-2006 (maps prepared by the Bureau's National Climate Centre). Large areas with relatively strong (smaller) negative trends for both the period 1910-2006 and the 1950-2006 (Figure 63) periods are indicated by a thick (thin) red line. Trends are reported as mm/decade.

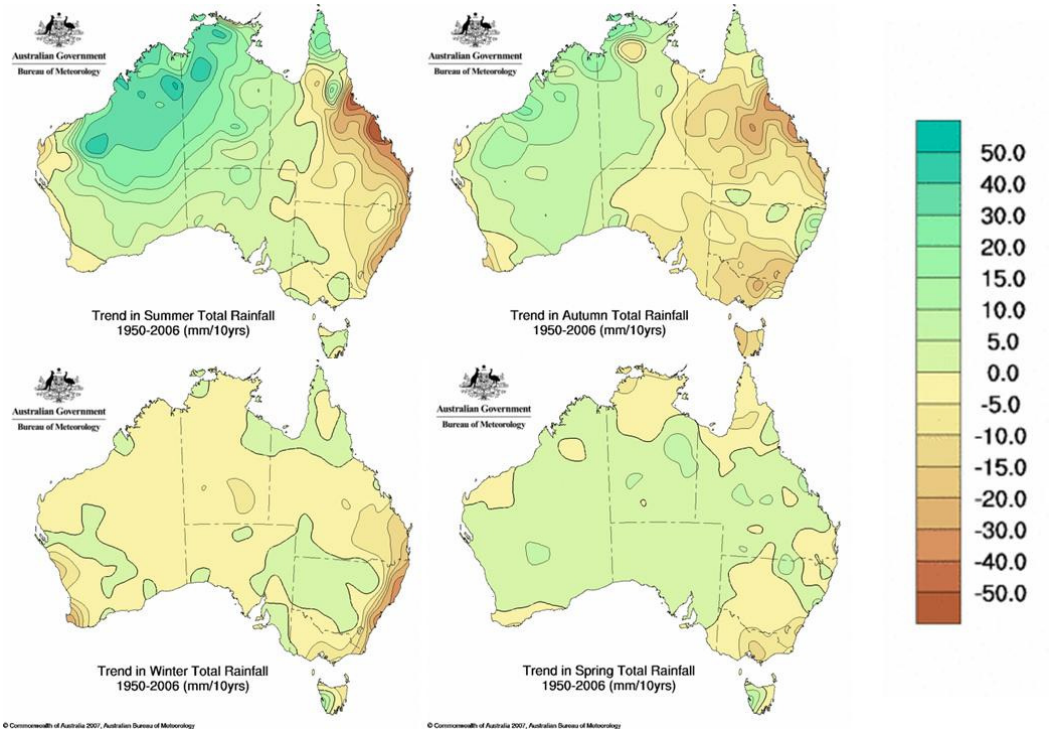

Figure 63 Trends in seasonal total rainfall for 1950-2006 (maps prepared by the Bureau's National Climate Centre). Trends are reported as mm/decade.

Seasonal and annual trends in rainfall indices across periods

Seasonal trends were only calculated where the magnitude of the seasonal medians of *RX1day* and *RX5day* were greater than an arbitrary threshold[44] to ensure seasonal trends were considered only where seasonal *RX1day* and *RX5day* constitute significant rainfall. Trends in seasonal *RX5day* exhibit some geographical coherence, although magnitudes are small (Figure 64). The sign of many of the trends over large areas changes with season.

- There are a few significant increases for parts of northern Australia during *summer*, as well as the northern tablelands of northern NSW. Otherwise most of the increases, although widespread, are not significant.

- There are significant decreases for SW WA, particularly during *winter*, and to a lesser extent in *autumn*.

- A decrease occurs for many southern coastal locations and parts of Queensland during *autumn* (but few are significant) whereas an increase occurs for many of the inland NSW locations, and extending through to the north west of Australia during *autumn*.
- There are many locations reporting little overall change (less than 1 mm/decade) for much of southern Australia, particularly for inland SW WA, SA and parts of western Victoria.

[44] This is determined by comparing the median seasonal rainfall between 1910 and 2005 at each location with an arbitrary fraction of the 1-year 24h ARI (corresponding to an AEP of 0.63). A reasonable overall seasonal distribution of the rainfall stations is obtained with the fraction set at 0.42. For convenience, the same locations within each season are used for both the *RX1day* and *RX5day* indices. This method does not need to be applied to the annual indices.

Across most of the country the magnitudes of decadal trends in *RX1day* are much smaller than trends in *RX5day*. However, regions across northern Australia which did have some large magnitude trends for *RX5day* do also have similar sign (but smaller magnitude) trends for *RX1day*. Since these two indices have similar trends and *RX1day* is not directly calculated using model output (see Section 2.2), it is not reported further.

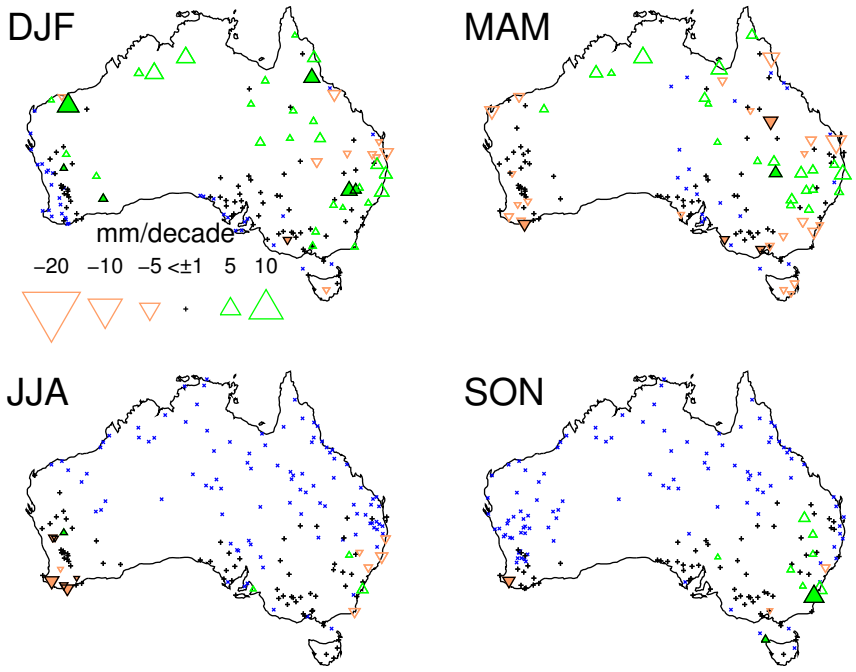

Figure 64 Seasonal trends for *RX5day*, for the period 1910-2005. Trends significant at the 0.05 level are solid with a black outline. Trends with a magnitude of less than 1mm/decade are shown as a black +, and locations with insufficient rainfall for each season are represented by a blue x.

The annual indices *R10mm, RX5day* and *R95pT* generally show a decrease in SW WA and parts of inland Queensland but an increase through parts of northern NSW (Figure 65). This is in approximate agreement with trends in annual total rainfall (bottom right panel in Figure 65). The *R10mm* index (number of heavy rainfall days) shows increase for much of SE Australia, and only for coastal SW WA are there significant decreases. For the annual maximum 5-day rainfall (*RX5day*), the signs of the trends reflect the predominant seasonal contribution (Figure 64). Annual trends across northern Australia are dominated by *summer* and *autumn* trends. For southern Australia *winter* trends dominate. Of note is the absence of change across much of inland SW WA, SA and western Victoria.

The index *R95pT* shows few regions with significant change. These are constrained to coastal SW WA (decrease), and increases for the northern tablelands of NSW, in agreement with the general changes for *R10mm* and annual rainfall. There are a number of locations across South Australia and central western Victoria with decreases, although only one of these significant.

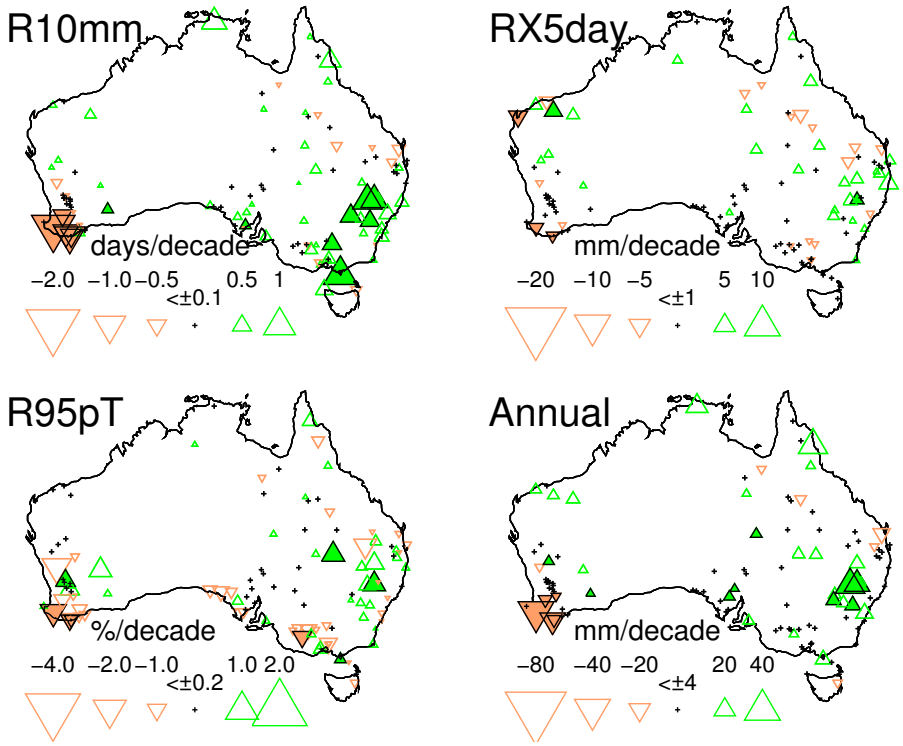

Figure 65 Annual trends in three rainfall indices (R10mm, RX5day and R95pT), and annual total rainfall, for the period 1910-2005. Symbols are as in Figure 64.

Compared with the longer period, the more recent of the shorter periods (1951-2005) has many locations with larger magnitude trends, accompanied at many locations by a change in sign. This reflects the interdecadal variability of 20th century Australian rainfall. For *RX5day* (Figure 66), there are many more locations that indicate widespread significant negative trends on a seasonal basis. As with the longer period, trends for 1951-2005 reproduce the decreases for SW WA and coastal eastern Australia during *winter*. However, additional large areas with significant decrease include most of the eastern Australian states; particularly South Australia, western Victoria and Tasmania during *autumn*.

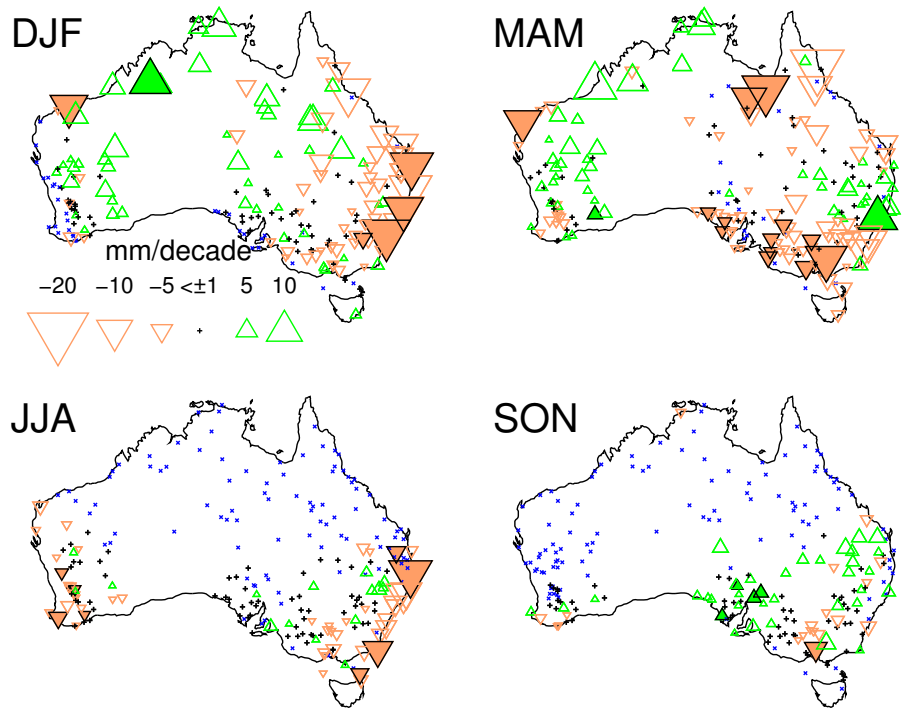

Figure 66 Seasonal trends for *RX5day*, for the period 1951-2005. Symbols are as in Figure 64.

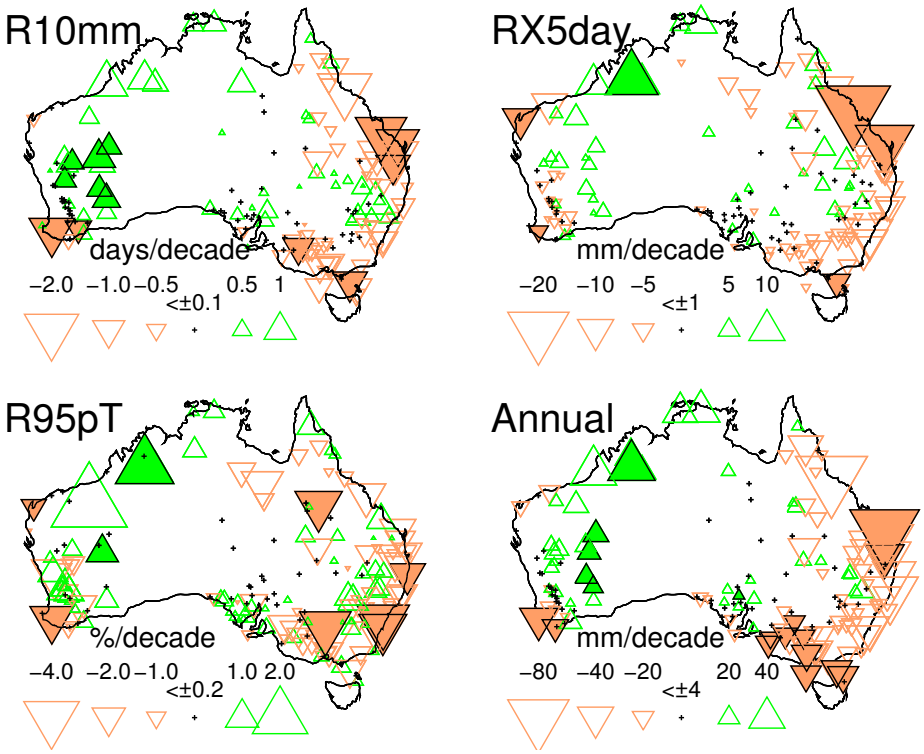

Figure 67 Annual trends in three rainfall indices (*R10mm*, *RX5day* and *R95pT*), and annual total rainfall, for the period 1951-2005. Symbols are as in Figure 64.

For the annual indices, there are considerably more locations with significant trends over the shorter period (Figure 67), particularly for SW WA, SE Australia as well as coastal eastern Australia. Increases also occur for inland and NW WA, which is in general agreement with trends in annual rainfall.

Comparison of trends for two consecutive periods

To investigate whether trends are indicative of long-term climate change, a 'combined trend' is calculated. This measure is based on trends derived for two consecutive periods (1910-1950 and 1951- 2005) and the full period (1910-2005).

The magnitude and significance of combined trends are calculated only where trends for all three periods have the same sign. The combined trend is calculated as the cube root of the product of the trends, i.e.

$$\text{combined trend} = \sqrt[3]{\text{trend}_{1910}^{1950} \times \text{trend}_{1951}^{2005} \times \text{trend}_{1910}^{2005}} \qquad (15)$$

Although the magnitude of the combined trend has no physical significance, it does clearly indicate the locations that have a similar sign trend across all periods, and would possibly be indicative of regions associated with a long-term climatic change. Locations with a lack of agreement in sign are likely indicative of long-term interdecadal variability in the rainfall.

Based on the *RX5day* index, there are no locations with *significant* combined trends (Figure 68). However, there are still a large number of locations with same-sign trends. *Autumn* has the greatest proportion, indicating decreases throughout both of the shorter periods, although increases do occur in northern NSW and southern Queensland. There are small decreases for southern coastal eastern Australia in all periods during *winter*. There are also a number of locations reporting little change, particularly across southern inland Australia and inland WA during *winter* and *spring*.

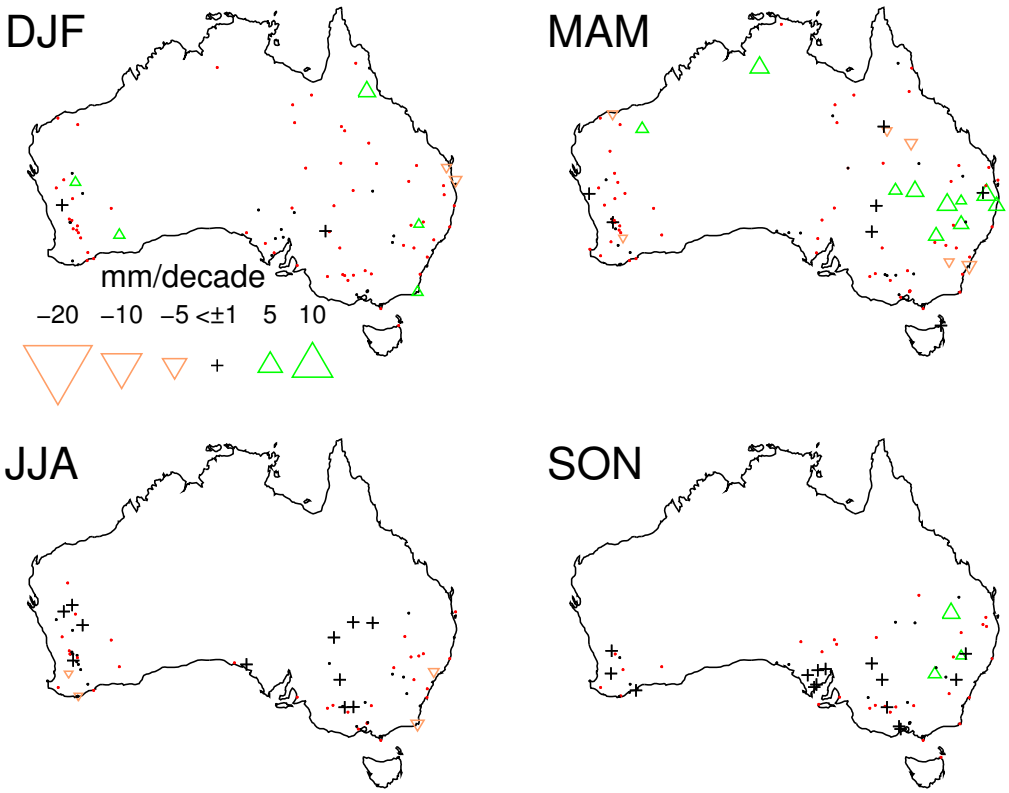

Figure 68 Combined trends (*RX5day)* from two consecutive periods (1910-1950; 1951-2005) and the full period. Trends within each period that are of similar sign are denoted by a triangle (or + for all less than 1 mm/decade). Where trends have the same sign, and are significant in each period, symbols are solid and outlined. The remaining symbols (black and red dots) represent combined trends that differ considerably (either in magnitude or sign; represented by a black dot or red dot, respectively).

No significant trends were found for any of the annual extreme indices (Figure 69). Of note are three locations in SW WA with decreases for *R10mm* over all three periods. There are also decreases for parts of Victoria (*R10mm* and *R95pT*). For *RX5day,* the results reflect those from the contributing seasons in Figure 68. The index *R95pT* exhibits a combination of both increases and decreases, indicating much greater spatial variability than the other indices.

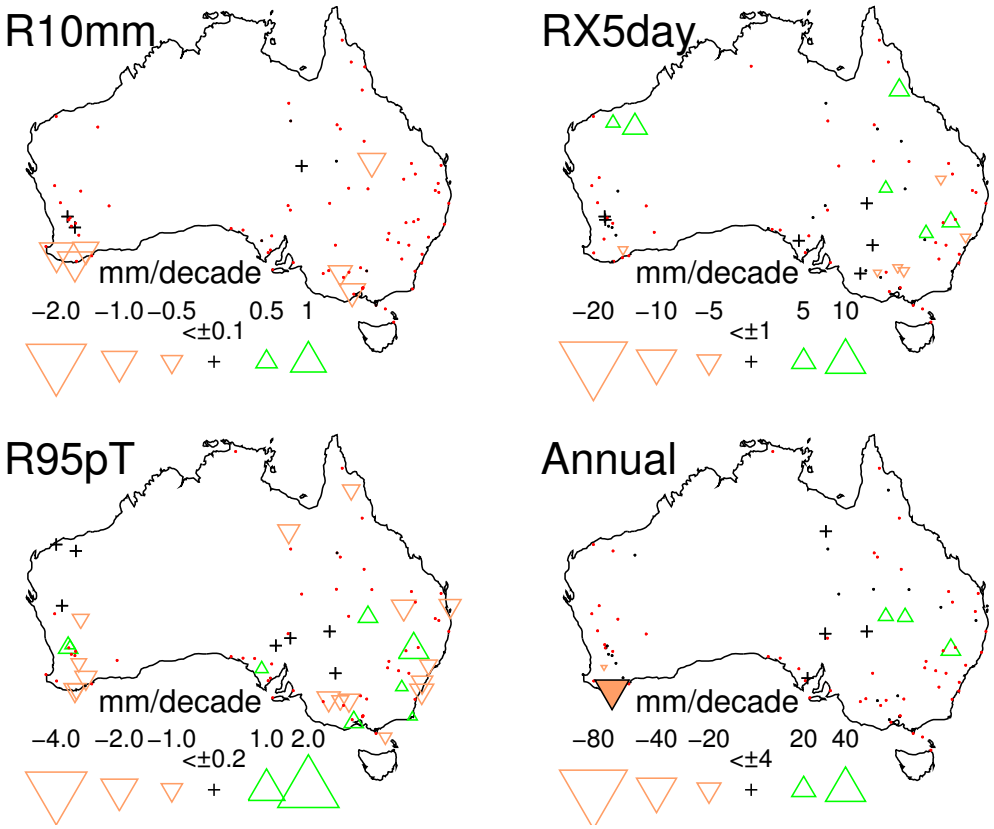

Figure 69 Combined annual trends from two non-overlapping periods (1910-1950; 1951-2005) and the full period. Symbols as in Figure 68.

2.1.4 Discussion

Australian rainfall is highly variable, with influences from various long timescale and large-scale systems. The strongest regional influence of natural variability in rainfall over eastern and northern Australia is due to the El-Niño Southern Oscillation (ENSO), although other influences associated with the Indian Ocean also affect most of the continent. Much of the climate variability occurs over interdecadal timescales. Techniques for trend analysis have to account for this variability. Trends were analysed over two non-overlapping periods, as well as for the full period.

For the seasonal index *RX5day*, there are no statistically significant changes at the 0.05 level since 1910. There are, however, certainly long-term increases (since 1910) in seasonal *RX5day* for parts of northern NSW/SW Queensland during *autumn* and to a lesser extent during *spring*. For trends in annual indices *R10mm* and *RX5day*, changes occur particularly for SW WA and in northern NSW/SW Queensland.

There is agreement between the sign of annual total rainfall trends and each index; in particular for *R10mm,* and to a lesser extent with *RX5day* and *R95pT*. Alexander et al. (2007) noted that for Australia, the percentage trends of the extreme indices (*R10mm*, *RX5day*, *R95pT*) were larger than the percentage trends in the total annual rainfall.

Although most trends are likely to be related to climate variability, the decrease of SW WA *winter* rainfall since about the mid-1970s has been analysed in detail and partly attributed to a range of influences, including anthropogenic causes. These

include a change in synoptic-scale atmospheric circulation system (which have been identified as having shifted further southwards, Hope et al. 2006) and possibly changes in land cover (Timbal and Arblaster 2006). Decreases in extremes since 1951 in other regions (particularly the decrease across much of SE Australia and central coastal Australia) have yet to be directly attributed to either natural variability or anthropogenic causes (Hennessy et al. 2007).

There is speculation that an increase in monsoon rainfall over the NW of the country may be attributed to increased aerosols resulting from Asia (Nicholls 2006, Rotstayn et al. 2007), although influences from natural climate variability or land-use changes cannot be dismissed. It is important to note that based on annual rainfall, Trenberth et al. (2007) identified NW Australia as the largest land-area region of the globe with the greatest percentage trends of annual precipitation in two periods (1901-2005 and 1979-2005), with much of eastern Australia having smaller magnitude trends.

2.2 Assess ability of global climate models to reproduce trends and variability in rainfall indices

2.2.1 Introduction

Over recent decades, global climate models (GCMs) have been developed by meteorological agencies and research institutions to provide simulations and projections of the global climate. The numerical experiments carried out using the climate models are based on the governing physical laws of the atmosphere and ocean processes. Some processes, including precipitation, cloud formation and dissipation require small-scale (i.e. sub-grid scale) parameterisation. There are numerous model parameterisation schemes available, and when applied to a range of models can result in differences in extreme rainfall between models (Emori et al. 2005). As well as differing parameterisation schemes, the numerical calculations used to advect model variables in space and time (or spectrally) also vary between models.

Due to the complexity of the ocean-atmosphere system, there are a wide range of possible outcomes, given a set of initial conditions and forcings[45]. For the preparation of the IPCC assessment reports, a number of institutions and meteorological agencies have been providing systematic model experiments to the Coupled Model Intercomparison Project 3 (CMIP3) database. Although monthly output is available for 23 different models, only nine models have suitable model output for assessing global rainfall extremes.

In contrast with changes in temperature, increasing greenhouse gas concentrations do not directly influence rainfall. Generally, it is the atmospheric circulation which largely controls mean precipitation patterns, although feedbacks involving land surface (soil and vegetation) changes and ocean circulation will also affect precipitation. An increase in global mean temperature, will result in the atmosphere being able to hold more water vapour (see Section 1.1.2). This could potentially lead to heavier rainfall events occurring more frequently. The influence from the atmospheric water vapour change is noted as the *thermodynamic component* of precipitation change (Emori and Brown 2005). More importantly, however, it is necessary to explore the influence that a changing climate has on atmospheric circulation systems (defined as the *dynamic component*).

Despite the widespread use of GCM output, there is still uncertainty as to the best method for assessing the performance of climate models, particularly for extremes. Overall, it is how the GCM data are to be used which usually dictates how the model outputs are to be assessed against observations. Many studies assess model performance by comparing area-averaged timeseries (global, continental or zonal) of model data for each index. Watterson (1996) used a non-dimensional measure of similarity based on pattern correlation and errors. Whetton et al. (2007) assessed regional climate change using the pattern of response per degree of global warming, which removed variations in the global average warming response of the models (for

[45] Initial conditions involve the starting point for the simulation of each model's atmospheric and oceanic processes, whereas forcings include for instance radiative forcings.

the A2 emission scenario). Glecker et al. (2008) used an assessment of the relative error to rank monthly model data for each atmospheric variable (e.g. precipitation, precipitable water or surface temperature). They found that the relative ranking of models depends on the variable considered, and that overall, the multi-model mean consistently outperforms all models for nearly every variable. Despite the model mean performing well, they noted that to judge models solely on how well they simulate the annual mean climate would likely be misleading. Instead, a number of metrics should be considered when assessing model performance. One of these is constructed using the Taylor diagram, which will be used in this section.

2.2.2 Model simulations, indices and method of analysis

Extreme rainfall indices for the 20th century and three emission scenarios were available for 9 GCMs (Table 3). All of the models have at least one model run for the 20th century climate, which allows comparison with observed data. Only three of the rainfall indices (*R10mm, RX5day* and *R95pT*) associated with extreme rainfall, are available as direct output from the climate models. Apart from the *cnrm* model, all models have indices available for both the land and ocean areas, and each model has its own specified grid. To compare each model with data and to calculate a multi-model ensemble, the models (and the observed indices) are regridded to a pre-defined grid. For convenience, and to allow comparison with other studies with focus on the Australian region, we chose a latitude-longitude grid resolution of 2.5° x 3.75°. This is defined as the HADEX grid (see Alexander et al. 2006)[46]. The indices are gridded using a modified version of Shepard's angular distance weighting (New et al. 2000), which was also carried out by Alexander et al. (2006). Details on the gridding method and parameters used are provided in Appendix A3.

The ability of the models to reproduce Australian rainfall for the 20th century is initially assessed by comparing the mean and the spatial pattern of the gridded indices with observations (using a Taylor diagram). Subsequently, linear trends in indices are assessed.

[46] It has been suggested (Chen and Knutson 2008) that model data should not be regridded, and comparison with data should be carried out on each model's native grid. However, this prevents creation of a multi-model ensemble.

Table 3 Global Climate Models (GCMs) used in the study. The number of available model runs is given for the 20th century (20C3m) and three emission scenarios (A1B, A2 andB1).

Model's originating organisation	Model name	Approx. grid resolution†	Number of model runs			
			20C3m	A1B	A2	B1
Meteo-France (France)	*cnrm*	5.63° x 2.72°	1	1	1	1
Geophysical Fluid Dynamics Lab (USA)	*gfdl 2.0*	4.0° x 2.5°	3	1	1	1
Geophysical Fluid Dynamics Lab (USA)	*gfdl 2.1*	4.0° x 2.5°	3	1	1	1
Institute of Numerical Mathematics (Russia)	*inmcm*	8.0° x 5.0°	1	1	1	1
Centre for Climate Research (Japan)	*miroc3.2-hi*	2.3° x 1.1°	1	1	0	1
Centre for Climate Research (Japan)	*miroc3.2-med*	5.6° x 2.8°	3	3	3	3
National Center for Atmospheric Research (USA)	*icm1*	5.6° x 2.8°	4	4	4	4
National Center for Atmospheric Research (USA)	*ccsm3.0*	2.8° x 1.4°	1	1	0	1
Meteorological Research Institute (Japan)	*mri-cgcm2.3.2*	5.6° x 2.8°	5	5	1	0

† grid resolution is approximate since the grids are not always linear in space.

2.2.3 Comparison of 20th century modelled and observed means of rainfall indices for Australia

Means from model output of 20th century rainfall indices have been compared with observations for a range of time periods. To be consistent with standard climate normals, a 30-year period (e.g. 1961-1990) should normally be considered as the period over which trends are to be assessed. However, to allow for comparison with other studies (e.g. Alexander and Arblaster 2008 and Tebaldi et al. 2006) and for assessing projected changes, the period 1980-1999 is used instead. To properly assess the means for the 20th century, two longer periods are also considered: 1951-1999 and 1910-1999.

Heavy rainfall days (R10mm)

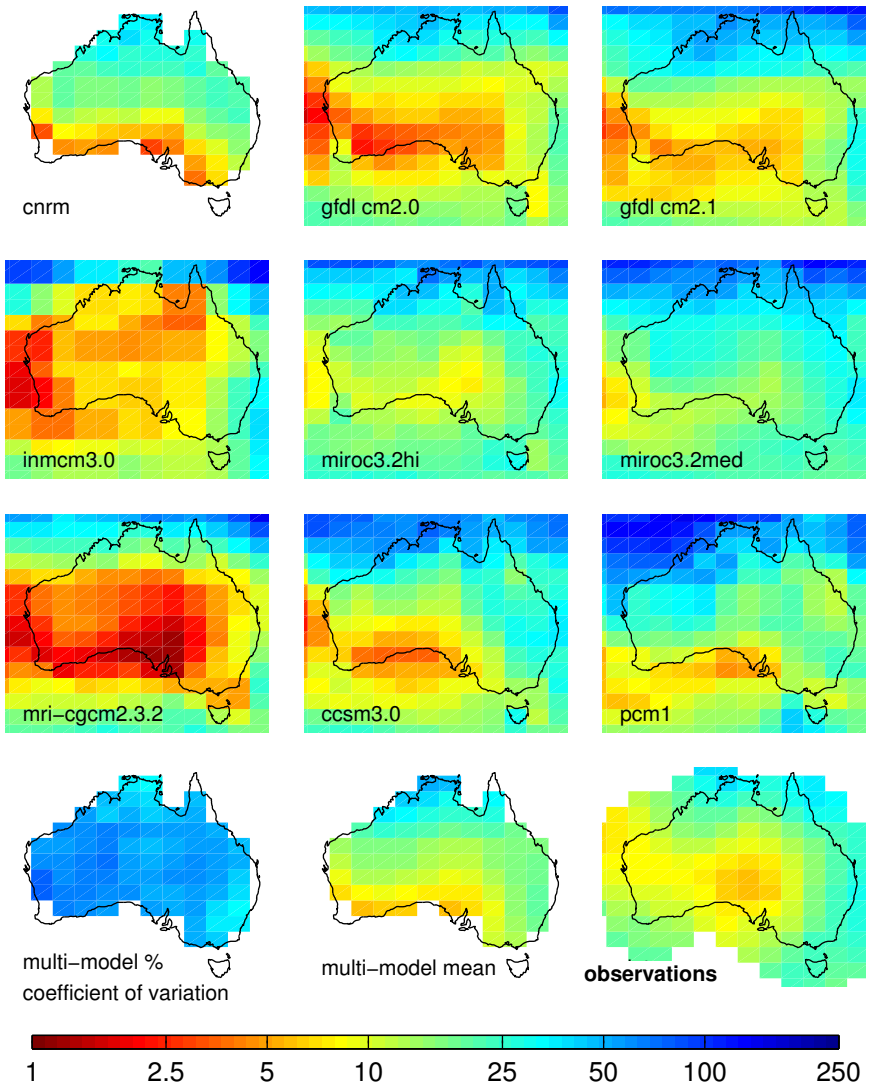

Figure 70 Statistics for index *R10mm* over the period 1980-1999. First 3 rows: means from multiple runs Last row: Coefficient of variation, multi-model mean and observations respectively. (Units for all except coefficient of variation is days; coefficient of variation is percent). A log scale is used.

Figure 70 shows each model's multi-run mean for the index *R10mm*[47], as well as the gridded observed *R10mm* data. Also shown (last row) is the multi-model mean from the ensemble of nine models, as well as the multi-model coefficient of variation (ratio of the multi-model standard deviation to the multi-model mean). The full spatial domain across the Australian region is shown for the models (except *cnrm*), to assist in assessing how well the models perform over both the land and the sea area. Due to the large range in *R10mm* across a number of models, the data have been plotted on a log-scale.

None of the models show good agreement in either the spatial distribution or magnitude when compared with the data. In contrast, the multi-model mean exhibits the best overall agreement in magnitude and spatial distribution when compared with the observations. Although the model data have been regridded to the same grid, the model with originally the finest grid resolution (*miroc3.2hi*) has a better spatial distribution and possibly closer agreement in magnitude with the observed data than its medium resolution counterpart (*miroc3.2-med*), and is certainly closer than the model with the poorest spatial resolution (*inmcm3.0*). Particular models also have a distinct bias in the number of days with at least 10 mm of rainfall. Both *inmcm3.0* and *mri-cgcm2.3.2* have a small bias throughout the continent (not enough days with at least 10 mm of rainfall), whereas the two *miroc3.2* models have a distinct overall large bias. The *pcm1* model does not adequately represent the spatial variation of *R10mm* across the continent, with magnitudes too large in central Australia and too small for coastal Queensland.

There is large inter-model variability in modelled magnitudes of the *R10mm* index, with the coefficient of variation of the order of 55%-80%. This lack of agreement between models is most apparent for Western Australia.

The Taylor diagram (Taylor 2001) is used to compare model and observed data using the relationship[48] between the centred RMS error (*E*'), the pattern correlation (*R*) and standard deviation (σ). Figure 71 shows an example of the Taylor diagram with all quantities normalised by the standard deviation of the observations (σ_{obs}), such that the observed data must be at (1,1), and the normalised centred RMS error (E'/σ_{obs}) is proportional to the distance between the two markers. The normalised standard deviation of the model data is $\sigma_{model}/\sigma_{obs}$, with the pattern correlation being proportional to the cosine of the angle.

[47] Within each model, there is little difference in the means for each of the individual model runs for models with more than one run. The Taylor diagram (Figure 71) shows a summary of the differences from individual model runs.

[48] For a set of *N* grid point observations (r_n) and *N* model data (f_n) (with means and standard deviations of $\langle r \rangle, \langle f \rangle$ and $\sigma_{obs}, \sigma_{model}$ respectively), the centred mean-square difference is $E'^2 = \frac{1}{N}\sum_{n=1}^{N}\left[(f_n - \langle f \rangle)^2 - (r_n - \langle r \rangle)^2\right]$. The relationship between these quantities, as well as the pattern correlation (R) is based on the law of cosines, (i.e. $E'^2 = \sigma_{obs}^2 + \sigma_{model}^2 - 2\sigma_{model}\sigma_{obs}R$). Throughout, the normalised standard deviation is denoted as σ_n.

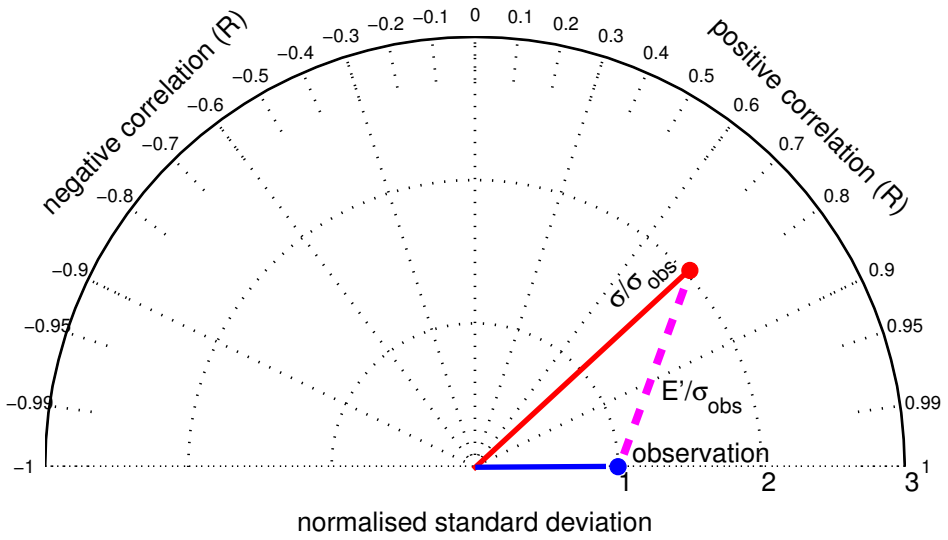

Figure 71 Geometry and relationship between statistical quantities used in the Taylor diagram. Observation is shown as a blue circle at (1,1), the model is represented by a red circle (in this example at (2,0.7). See text for a full description.

For the index *R10mm* (Figure 72), the correlations from the individual model runs for each model are generally in close agreement, with a small variation in the normalised standard deviation. The figure shows that there is little difference in the statistics between the periods 1980-1999 (left) and 1951-1999 (right). Probably the best performing model is *mri-cgcm2.3.2* (red), with a correlation and normalised standard deviation (R,σ_n) pair of (0.89, 0.8). The worst performing model is the *pcm1* (black; 0.48, 2.1). This model has both poor spatial correlation and amplitude variance. Although *miroc3.2-hi* (pink) has good pattern correlation, (R = 0.91), it overestimates the standard deviation (σ_n = 2.0). On the Taylor diagram the multi-run ensemble for each model is always within the distribution of the individual run members (for clarity these are not shown). The multi-model ensemble (average of 9 models) has a (R,σ_n) pair of (0.87, 1.3).

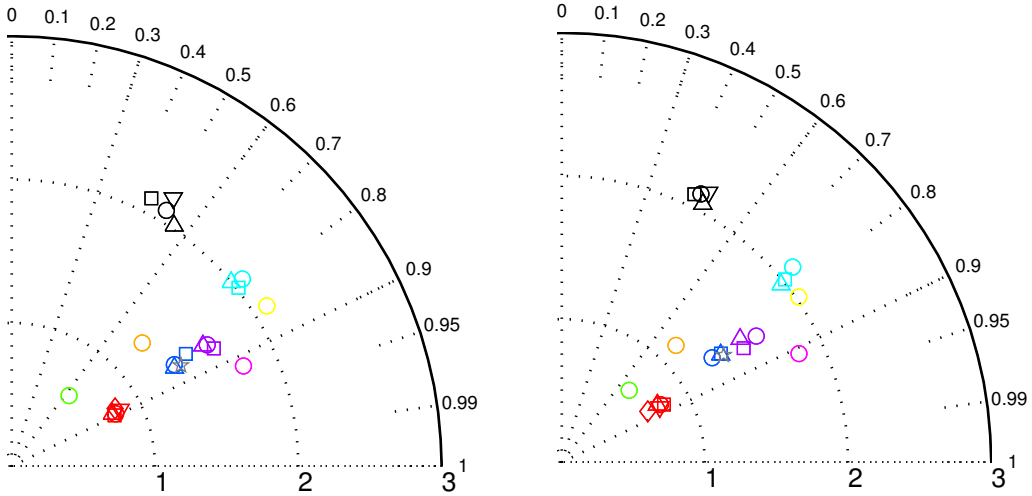

Figure 72 Taylor diagram for *R10mm* for the periods 1981-1999 (left) and 1951-1999 (right). Shown are the means of the individual model runs compared with observations across the land area of Australia. The first model run for each model is a circle. **O**: cnrm, **O**: gfdl cm2.0, **O**: inmcm3.0, **O**: gfdl cm2.1, **O**: miroc3.2hi, **O**: miroc3.2med, **O**: pcm1, **O**: mri-cgcm2.3.2, **O**: ccsm 3.0. grey star is the multi-model ensemble mean. Different model run numbers associated with each model are identified by a different symbol.

The change in the reference period (from 1981-1999 to 1951-199) only slightly increases σ_n with little change in the correlation. This indicates that with the introduction of more data, the models have a tendency to increase the year-to-year variability relative to the observed data.

Maximum 5-day rainfall total (RX5day)

The performance of models to reproduce the observed index *RX5day* over the period 1980-1999 can only be assessed over a limited area of Australia, due to the much smaller coverage when gridding, as a result of a shorter decorrelation length scale for this index (see Appendix A3). Nevertheless, there appears to be good agreement for some models over southern Australia and away from the immediate eastern coastline. In terms of the mean field, the worst performing models are *mri-cgcm2.3.2* and *inmcm3.0*. Three of the models (*gfdl cm2.0, incm3.0* and *mri-cgcm2.3.2*) have a dry bias across much of southern Australia. *Miroc3.2hi* reproduces well the large magnitudes for coastal eastern Australia and SW WA. As with *R10mm*, the coefficient of variation is smallest for the top end of Northern Territory and SE Australia.

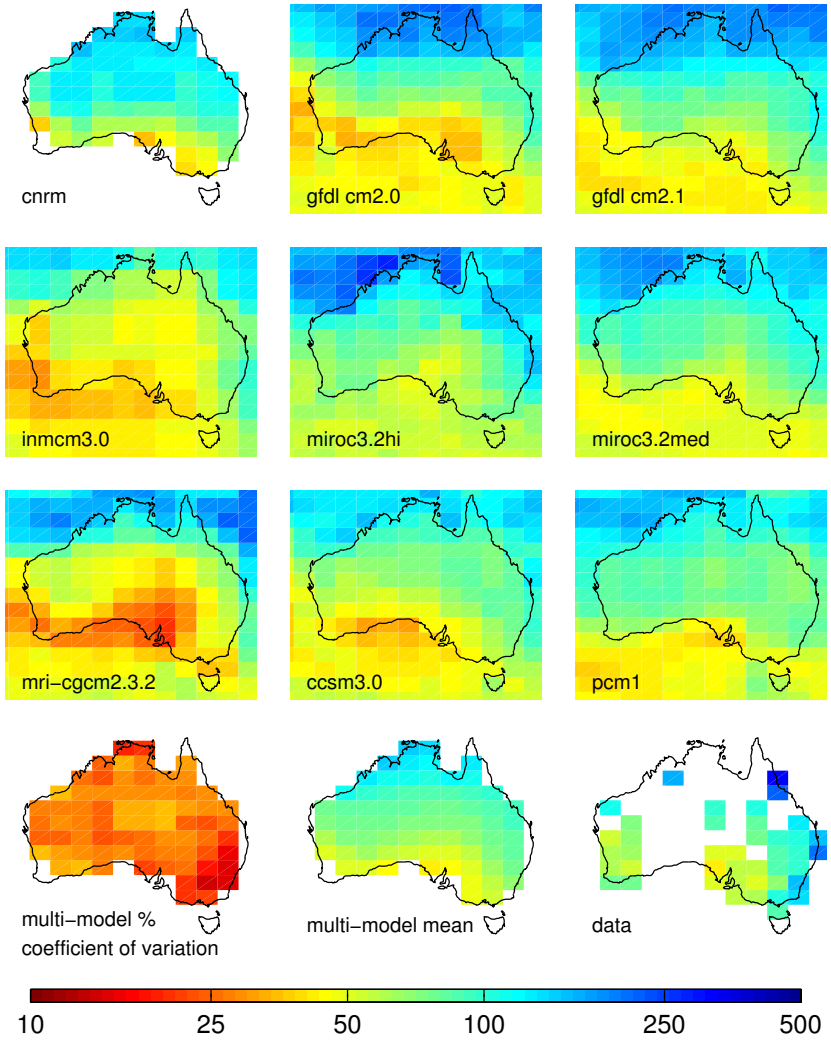

Figure 73 Statistics for index *RX5day* over the period 1981-1999. First 3 rows: model run means. Last row: Coefficient of variation, multi-model mean and data respectively. (Units for all except coefficient of variation is mm; coefficient of variation is percent). A log scale is used.

The Taylor diagram (Figure 73) for the period 1980-1999 indicates that the best performing model is the *miroc3.2hi* (R,σ = 0.87,0.65) with the poorest being *pcm1* (0.5,0.4). Apart from *cnrm* and *ccsm3.0*, all other models show approximately the same relative performance as for the *R10mm* index. The normalised standard deviation is always less than one, indicating that the models do not adequately represent the observed spatial variability. When the time period is extended to 1951-1999 the normalised standard deviation decreases by approximately 0.1 for each model run, although the correlation is approximately the same. This indicates that the models have perhaps not adequately captured the interdecadal variability of the more infrequent maximum 5-day rainfall events over the longer period.

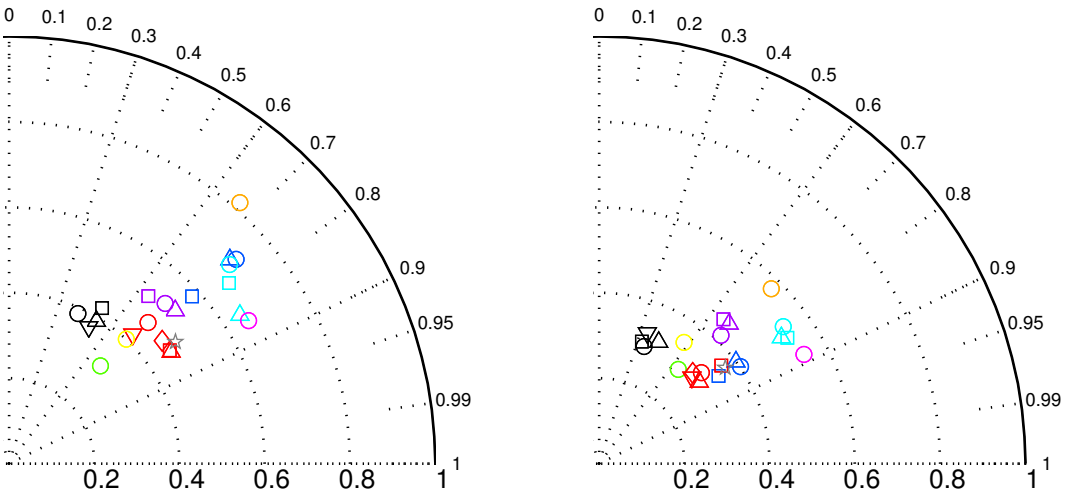

Figure 74 Taylor diagrams for *RX5day* for the periods 1981-1999 (left) and 1951-1999 (right). Shown are the means of the individual model runs compared with observations across the land area of Australia. The first model run for each model is a circle. **O**: cnrm, **O**: gfdl cm2.0, **O**: inmcm3.0, **O**: gfdl cm2.1, **O**: miroc3.2hi, **O**: miroc3.2med, **O**: pcm1, **O**: mri-cgcm2.3.2, **O**: ccsm 3.0. grey star is the multi-model ensemble mean. Different model run numbers associated with each model are identified by a different symbol.

Proportion of annual rainfall from very wet days (R95pT)

The modelled percentage contribution of annual rainfall above the 95th percentile (*R95pT*) has a relatively poor agreement with the observed data (Figure 75). Apart from *mri-cgcm2.3.2* (which has a large bias (~ 80%) towards excessive contributions from the 95th percentile), most models underestimate the relative contribution from the 95th percentile. The best performing model is again *miroc3.2hi* (Figure 76). The worst model is *mri-cgcm2.3.2*, which has both low correlation and a normalised standard deviation of approximately 6 (not shown, off the scale). All other models have very poor correlations ($-0.7 < R < 0.5$) with large run-to-run variability for models with more than one run. These results indicate that these models cannot successfully reproduce infrequently occurring large rainfall events.

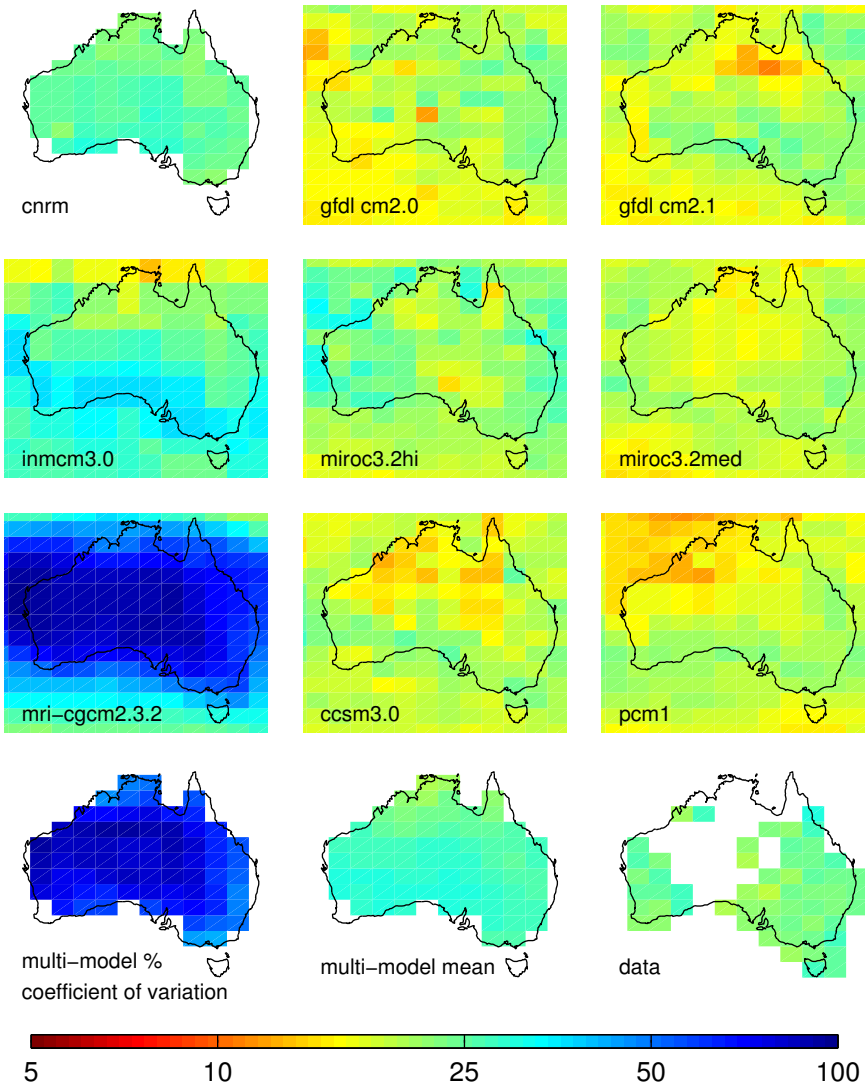

Figure 75 Statistics for index *R95pT* over the period 1981-1999. First 3 rows: ensemble from model run means. Last row: Coefficient of variation, multi-model mean and data respectively. (Units are %). A log scale is used.

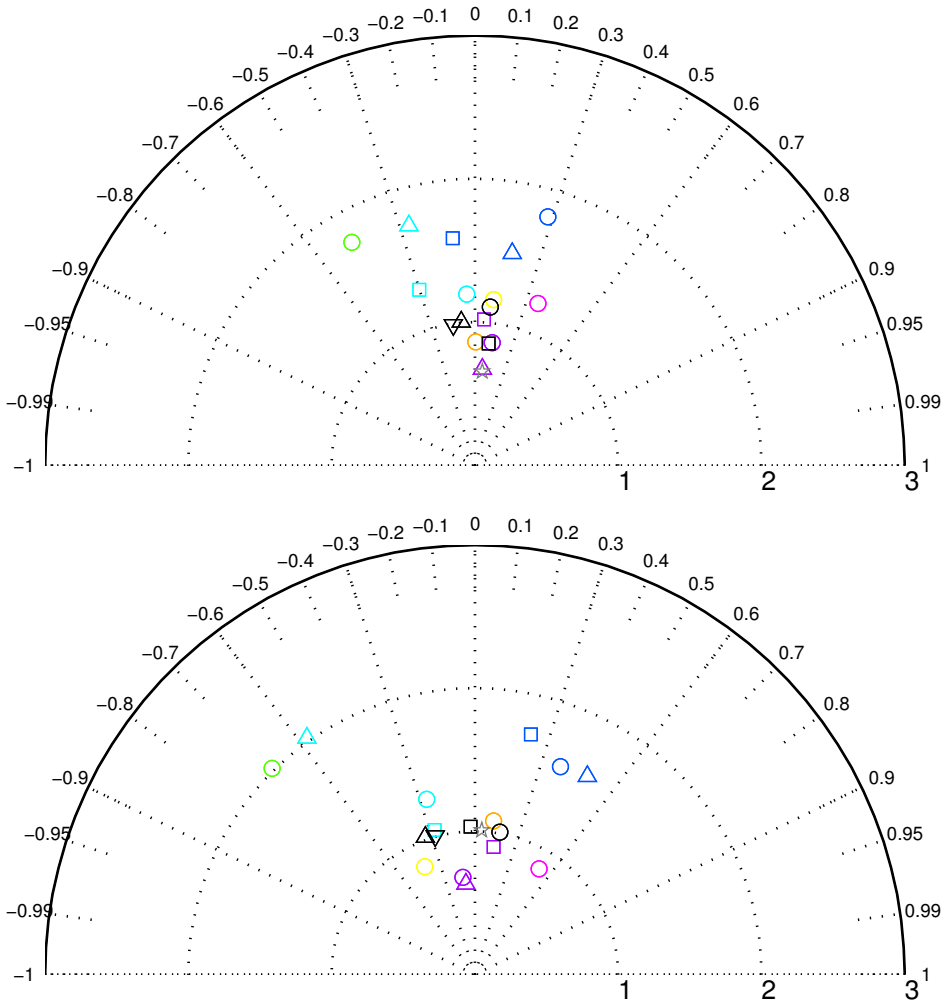

Figure 76 Taylor diagrams for *R95pT* for the periods 1981-1999 (top) and 1951-1999 (bottom). Shown are the trends of the individual model runs compared with observations across the land area of Australia. The first model run for each model is a circle. **O**: cnrm, **O**: gfdl cm2.0, **O**: inmcm3.0, **O**: gfdl cm2.1, **O**: miroc3.2hi, **O**: miroc3.2med, **O**: pcm1, **O**: ccsm 3.0. grey star is the multi-model ensemble mean. Different model run numbers associated with each model are identified by a different symbol. (mri-cgcm2.3.2 not shown)

2.2.4 Comparison of 20th Century model and data trends of rainfall indices for Australia.

For the period 1957-1999, Alexander and Arblaster (2008) showed that the multi-model trends for the rainfall indices *R10mm*, *RX5day* and *R95pT* were always of smaller magnitude than observations. They indicated that very few model runs had good spatial and temporal similarity. In the present work, trends are compared for two periods: 1951-1999 and 1910-1999. No assessment is made of the trend significance, since very few grid points reported significant change at the 0.05 level for both the data and models.

Heavy rainfall days (R10mm)

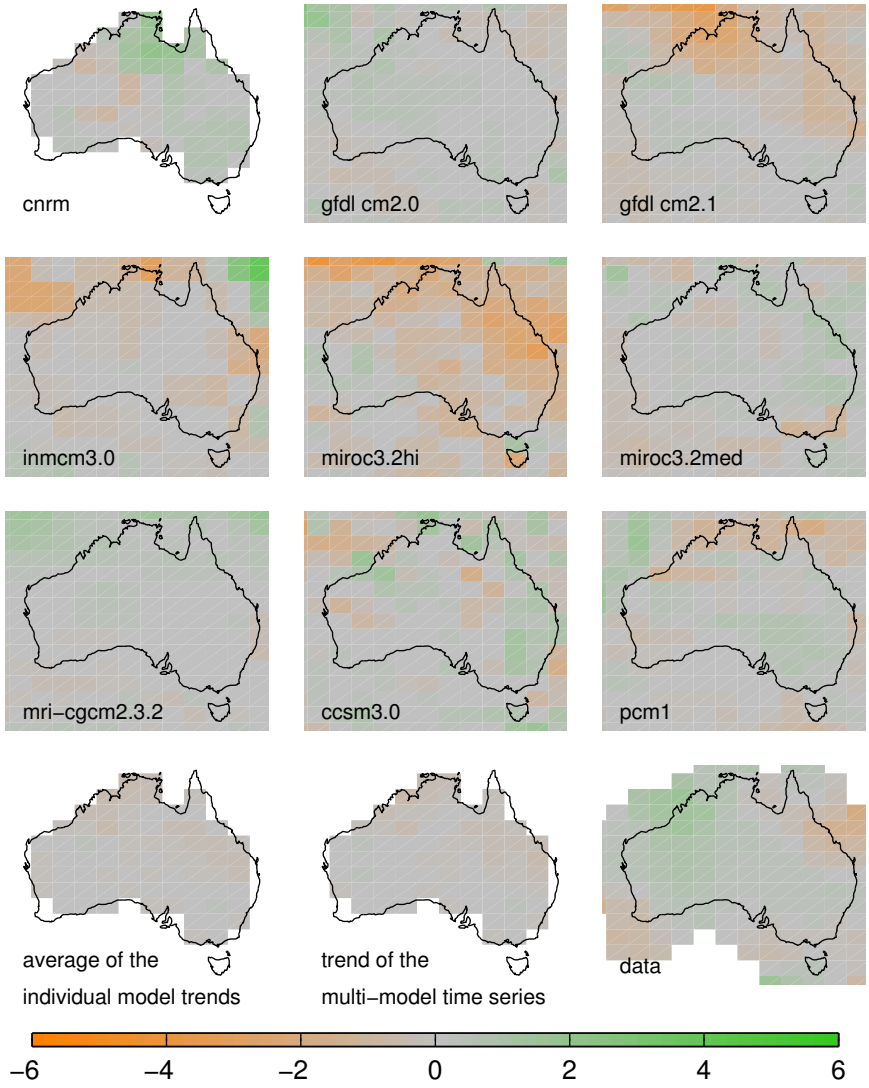

Figure 77 Trends for index *R10mm* over the period 1951-1999. First 3 rows: trends from the ensemble time series of model runs. Last row: Average of the individual model trends, trend of the multi-model time series and data respectively.

Figure 77 shows each model's multi-run ensemble trend for the period 1951-1999. The multi-run ensemble trend was calculated from the multi-run time series for each model. There is a tendency for models to have smaller magnitude trends when the number of ensemble members is large. In particular, *miroc3.2hi*, which consists of one member, has the largest magnitude trends (increases over most of northern and eastern Australia). *mri-cgcm2.3.2, pcm1* and *miroc3.2med* each have smaller magnitude trends, and consist of 5, 4 and 3 ensemble members respectively. The largest magnitude trends are generally found for the tropics, consistent with observed trends.

The multi-model trends have been computed using two methods. For the first method, the average of each of the model's trends is calculated (bottom left in Figure 77). The more precise method creates a multi-model time series of each model's multi-run ensemble. The results from both methods give spatially consistent trends of similar magnitude with small increases for much of Queensland. This is in broad agreement with the observed trends along parts of the eastern Queensland coastline. There is a small tendency towards an increase for parts of NSW, but the observed increase for NW Australia is not apparent in the multi-model ensemble trend.

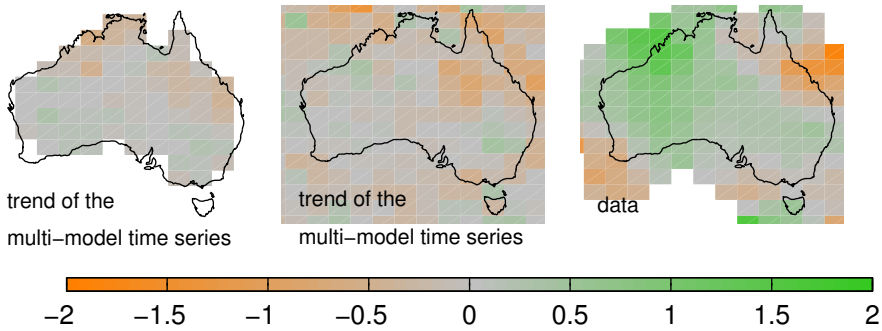

Figure 78 Trends for index *R10mm* over the period 1951-1999, but rescaled (finer trend resolution). (Units days/decade). Left, rescaled version of the last row middle column in Figure 77 (trends with all models). Middle: trends calculated with only 4 models, (gfdl cm2.0, *miroc3.2hi*, miroc3.2med, ccsm3.0). Right: observations.

The influence of excluding the poorest performing models was also tested. Five models (*pcm1*, *incm3.0, cnrm*, *gfdlcm2.1* and *mri-cgcm2.3.2*) identified in section 2.2.2 were excluded when calculating the multi-model trends. There is a tendency (see Figure 78) that the multi-model trends are in closer agreement with the data, particularly for coastal eastern Queensland, northern NSW and even parts of SW WA. Of the four models included (middle plot in Figure 78), none have good agreement with the trends in data for every part of Australia. Overall, the better agreement that between multi-model ensemble trends and observations may by chance.

For the longer period (1910-1999) the trends should only be calculated for models that were considered reasonable for the shorter period, although for simplicity the results using all models will also be used. Figure 79 indicates that the trends are overall inconsistent with the data for most areas of Australia when using either all models, or just the selected four models (*gfdlcm2.0*, *miroc3.2hi*, *miroc3.2med*, *ccsm3.0*). The large-area increase for much of Queensland is due to projections from the *miroc3.2hi* model (not shown), which again have excessively large positive trends for most of eastern Australia.

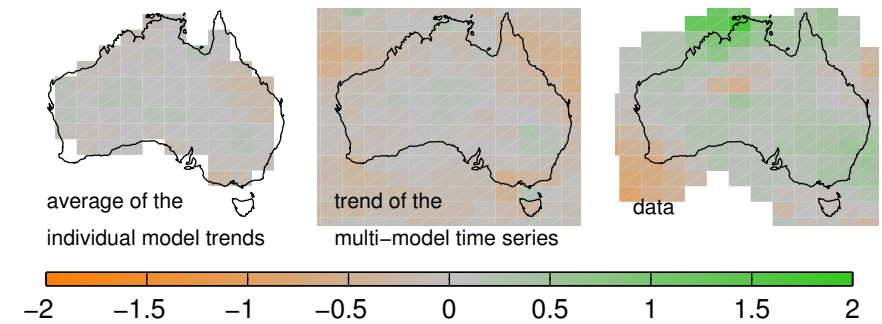

Figure 79 Trends for index *R10mm* over the period 1910-1999. (Units days/decade). Left, trends calculated using all models. Middle: trends calculated only with 4 models, (*gfdl cm2.0*, *miroc3.2hi*, *miroc3.2med, ccsm3.0*) and right: observed data.

The comparison of spatial correlation and variability of trends using the Taylor diagram (Figure 80) for the periods 1951-1999 and 1910-1999 indicates large variability in the models' ability at simulating the spatial trends.

In contrast to the close agreement between *means* derived from individual model runs (Figure 72), the *trends* from individual model runs differ markedly. The multi-run trend is generally of smaller magnitude compared with the contributing runs. The best performing individual model is the fourth of the five *mri-cgcm2.3.2* runs with a correlation of 0.3. In contrast with the Taylor diagram for the model means, *miroc3.2hi* has very poor correlation ($R = 0$). Generally the longer period reduces the spatial variability of the individual model trends and reduces the magnitude of the correlation. This suggests that the models may not correctly represent features of inter-decadal variability.

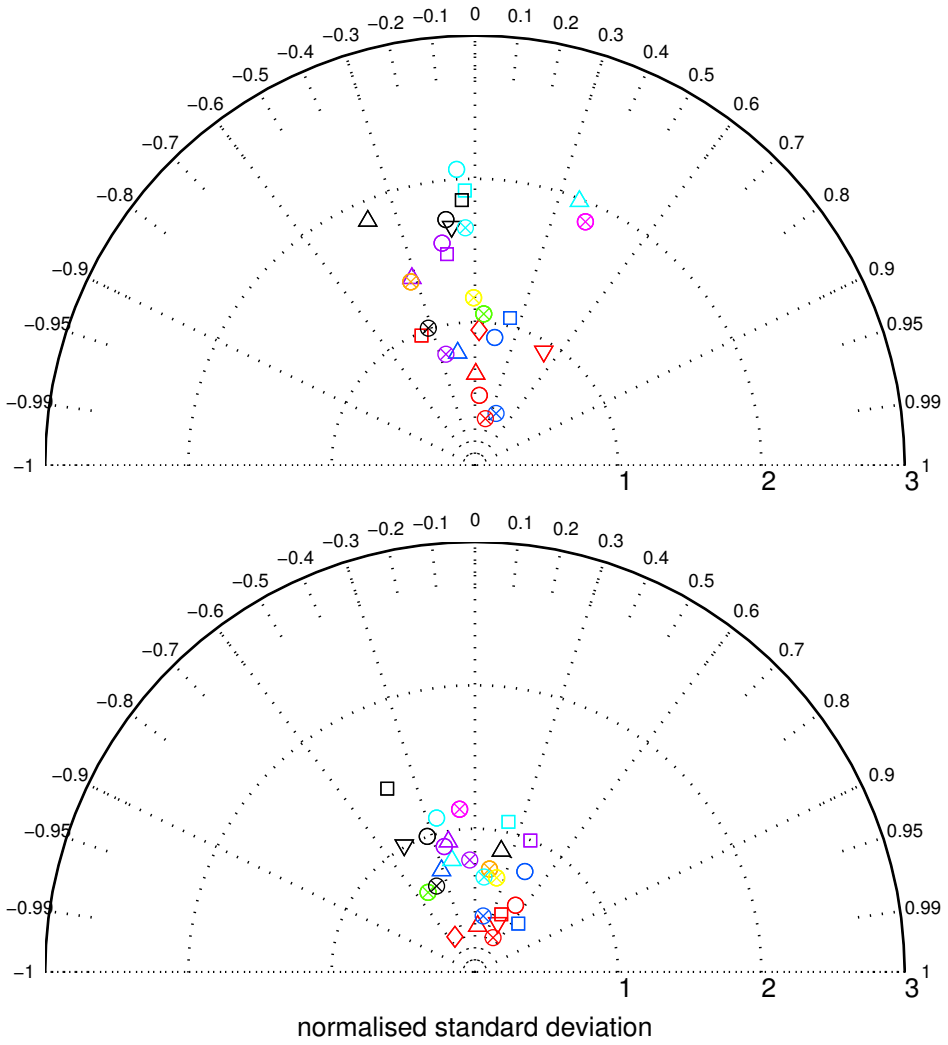

Figure 80 Taylor diagrams for trends in *R10mm* for the periods 1951-1999 (top) and 1910-1999 (bottom). Shown are the trends of the individual model runs compared with observations across the land area of Australia. The first model run for each model is a circle. **O**: cnrm, **O**: gfdl cm2.0, **O**: inmcm3.0, **O**: gfdl cm2.1, **O**: miroc3.2hi, **O**: miroc3.2med, **O**: pcm1, **O**: mri-cgcm2.3.2, **O**: ccsm 3.0. Different model run numbers associated with each model are identified by a different symbol. Also indicated are the multi-run ensemble model trends (crossed circles).

Maximum 5-day rainfall total (RX5day)

For the *RX5day* index (Figure 81) there is little consistency in the trends between many of the models and when comparing models with observations. Compared with the modelled *R10mm* trends, there is a higher level of spatial variability when modelling *RX5day* trends. However, the trends calculated from the multi-model ensemble have less overall spatial variability and better agreement with observations. Results for the longer period (which are based on a smaller number of models) are similar.

As with trends for *R10mm*, the Taylor diagram (Figure 82) indicates lack of consistency between model runs, with the multi-model trends generally indicating less spatial variability and correlation than the contributing model runs. As the time period increases to 1910-1999, the correlation and normalised standard deviation both decrease.

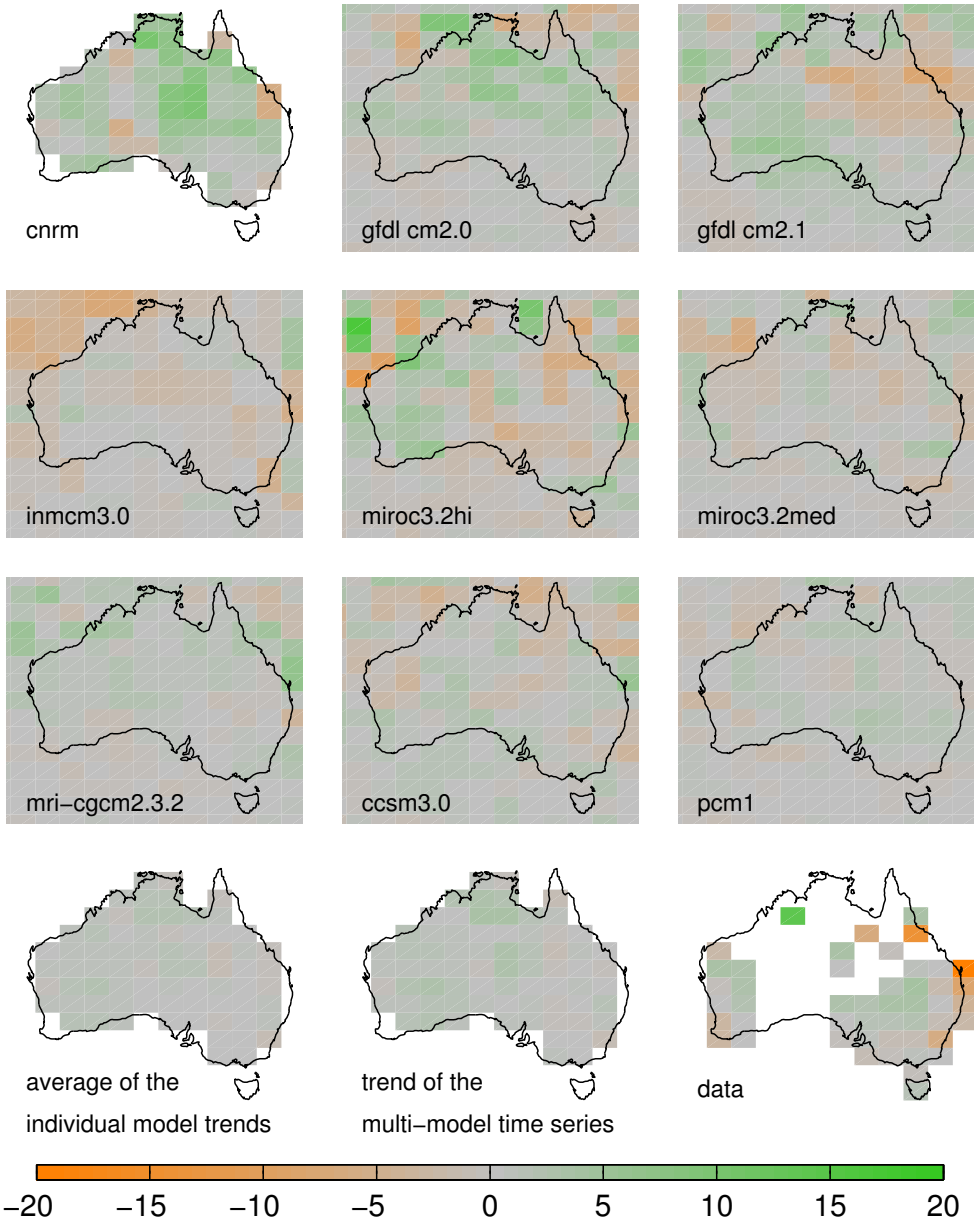

Figure 81 Trends for index *RX5day* over the period 1951-1999. First 3 rows: trends from the ensemble time series of model runs. For each of the last row: Average of the individual model trends, trend of the multi-model time series and data respectively. (Units mm/decade).

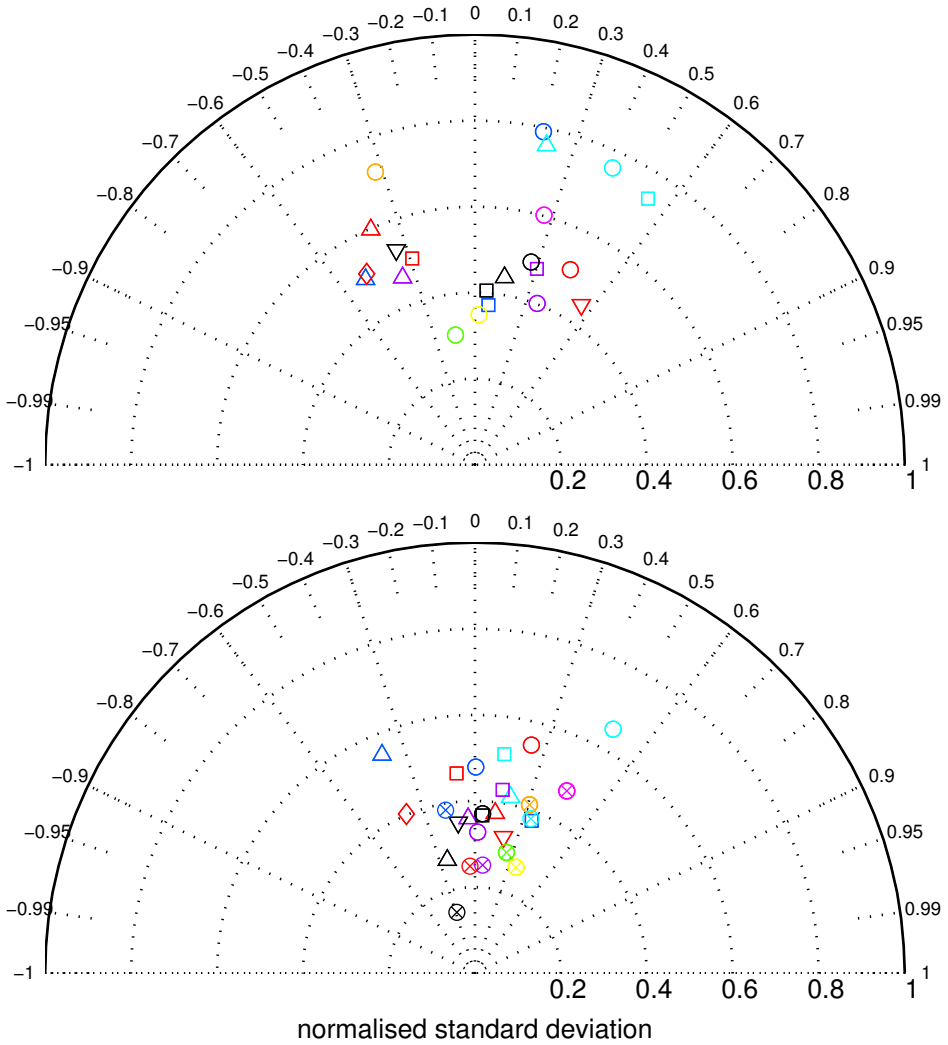

Figure 82 Taylor diagram for trends in *RX5day* over the period 1951-1999 (top) and 1910-1999 (bottom). Shown are the trends of the individual model runs compared with observations across the land area of Australia. The first model run for each model is a circle. **O**: cnrm, **O**: gfdl cm2.0, **O**: inmcm3.0, **O**: gfdl cm2.1, **O**: miroc3.2hi, **O**: miroc3.2med, **O**: pcm1, **O**: mri-cgcm2.3.2, **O**: ccsm 3.0. Different model run numbers associated with each model are identified by a different symbol. Also indicated are the multi-run ensemble model trends (crossed circles).

Proportion of annual rainfall from very wet days (R95pT)

For the means, the index *R95pT* had the poorest overall agreement between different runs of the same model and also between the model means with the observed data (Figure 75). Models have little skill in reproducing observed trends, at least for the period analysed (1951-2005). Trends are shown in Figure 83 for the period 1951-2005. There is little spatial consistency in modelled trends. The multi-model mean therefore has very small trends, which are generally smaller in magnitude than observed trends.

The Taylor diagram for the trends associated with *R95pT* (Figure 84) shows that none of the models reproduce the spatial pattern of observed trends throughout Australia.

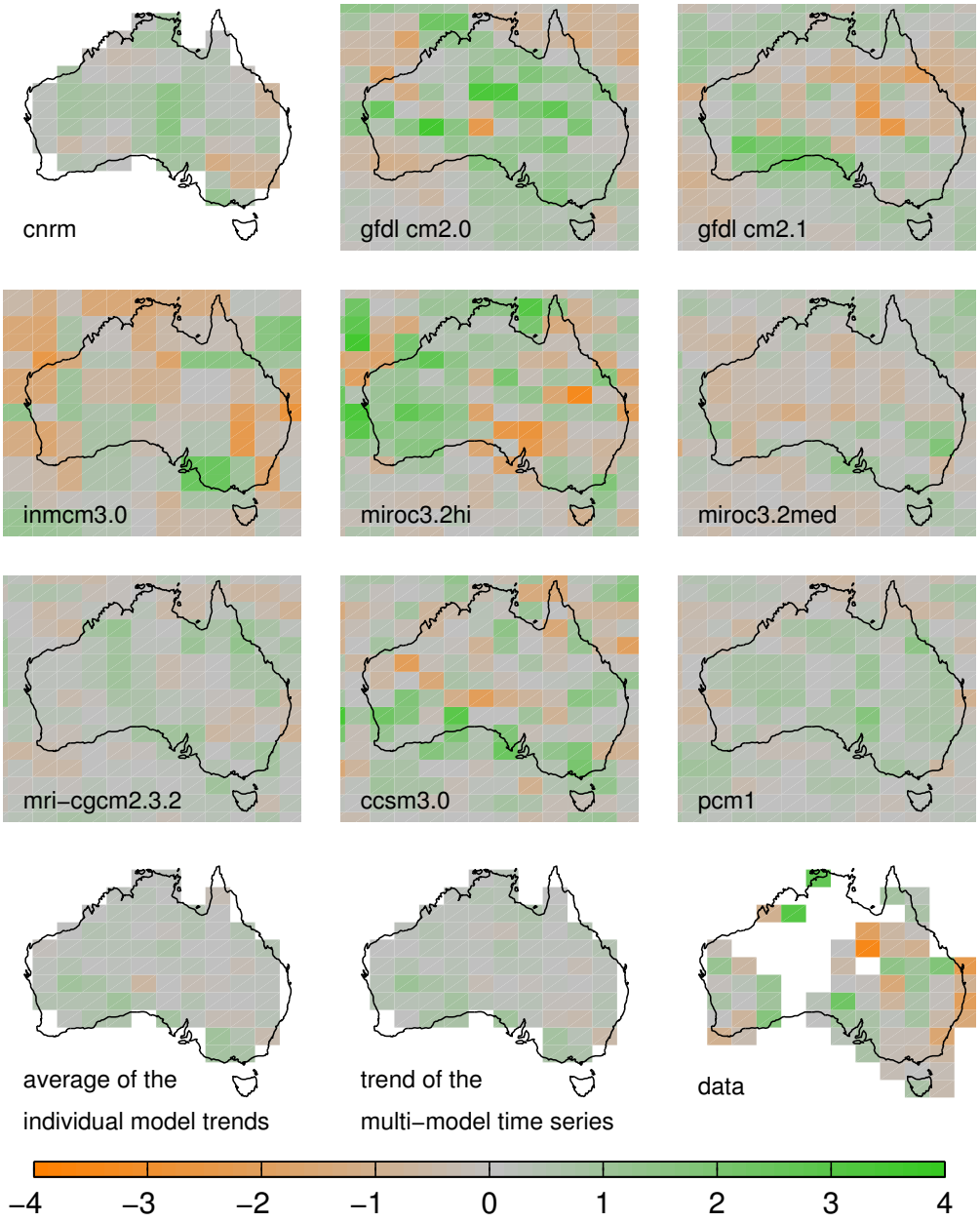

Figure 83 Trends for index *R95pT* over the period 1951-1999. First 3 rows: trends from the ensemble time series of model runs. For each of the last row: Average of the individual model trends, trend of the multi-model time series and data respectively. (Units %/decade).

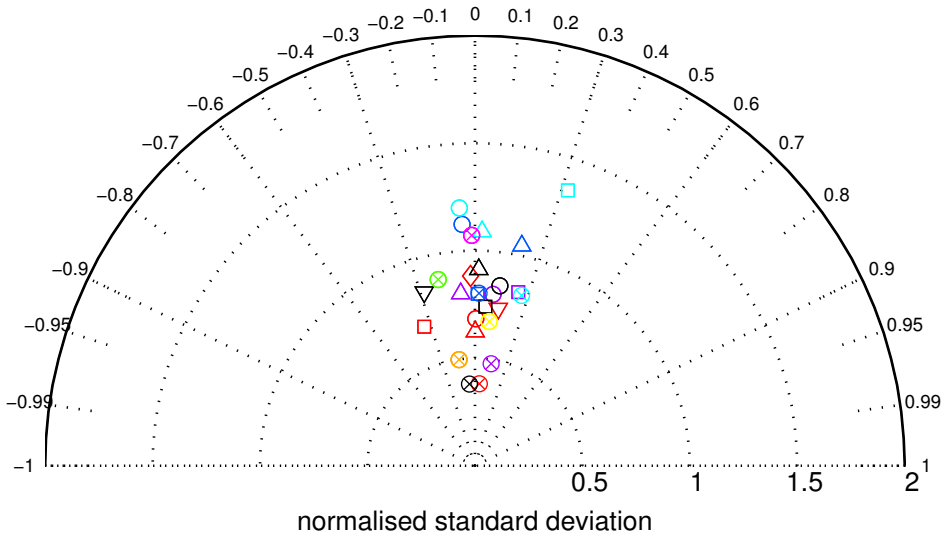

Figure 84 Taylor diagram for trends in *R95pT* for the period 1951-1999. Shown are the trends of the individual model runs compared with observations across the land area of Australia. The first model run for each model is a circle. **O**: cnrm, **O**: gfdl cm2.0, **O**: inmcm3.0, **O**: gfdl cm2.1, **O**: miroc3.2hi, **O**: miroc3.2med, **O**: pcm1, **O**: mri-cgcm2.3.2, **O**: ccsm 3.0. Different model run numbers associated with each model are identified by a different symbol. Also indicated are the multi-run ensemble model trends (crossed circles).

Discussion

This section summarises the comparison of modelled and observed means and trends in rainfall indices for the 20th century (sections 2.2.3 and 2.2.4). Extreme rainfall can be reported using a number of indices, the choice of which depends on the location and application. *R10mm*, *RX5day* and *R95pT* were chosen since they cover a range of measures for extreme rainfall and are provided as model output. A quantitative assessment of each GCM's ability to model 20th century rainfall mean patterns and trends was carried out using a Taylor diagram for each index and time period. A summary of all the Taylor diagrams is shown in Figure 85 using coupled box-and-whisker plots for both the pattern correlation (R) and a measure of spatial variability (E') for both the mean and trends over the period 1951-1999[49]. Indicated in each figure panel is the median, inter-quartile range and outliers corresponding to each model run. As with the Taylor diagram, the better performing models should be closer towards (1,1). This figure clearly highlights the index *R10mm* has most models with relatively high pattern correlation for the mean, although, as with all indices, it has generally poor correlation for 20th century trends. The index *R95pT* was not modelled well by any model or by the multi-model mean.

[49]The summary box and whisker plot can be used since the majority of model pattern correlations extend across the approximate linear region of the Taylor diagram (i.e. $|R| < 0.8$).

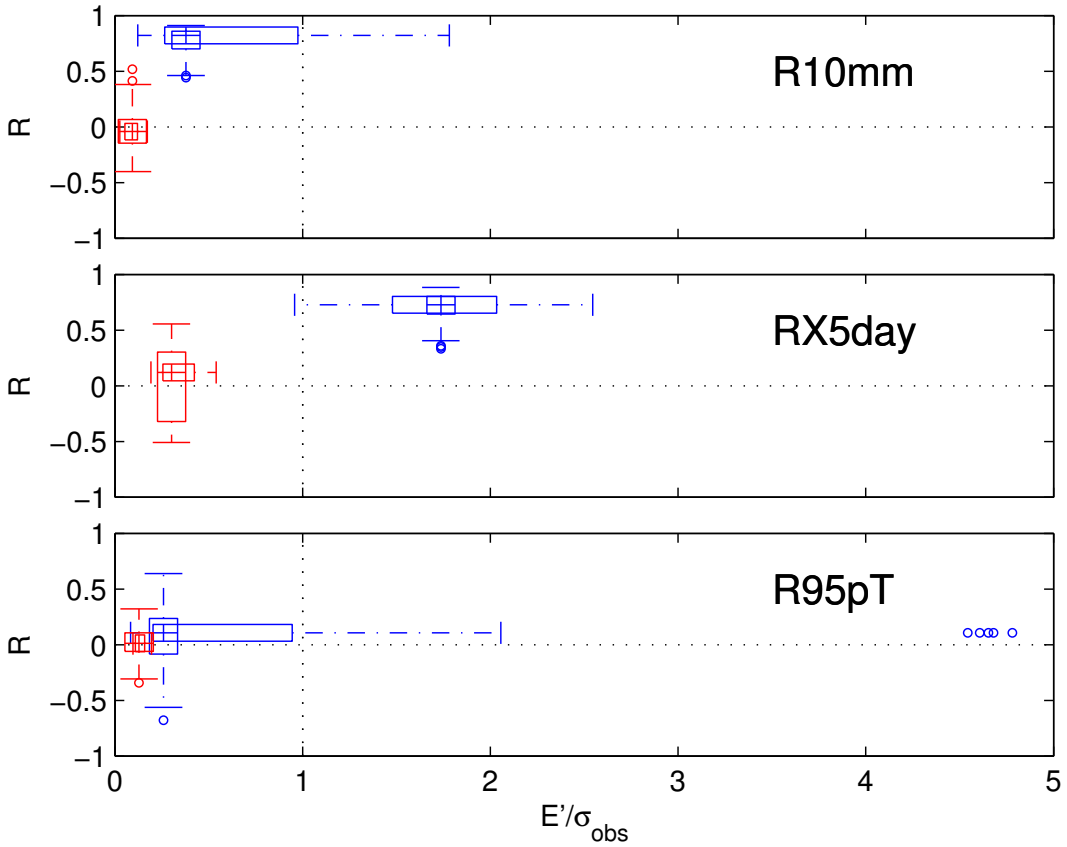

Figure 85 Pattern correlation (R: vertical box and whiskers) and normalised RMS standard error (E'/σ_{obs}: horizontal box and whiskers) relative to the observations for the mean (red) and trends (blue) for the period 1951-2005. The axis for each box and whisker for (R, E'/σ_{obs}) is centred on the median of its counterpart (E'/σ_{obs}, R).

2.3 Projected changes in extreme precipitation

Climate models provide projections of the atmosphere-ocean system using a number of emission scenarios. Of the six Special Report on Emission Scenarios (SRES) scenarios (B1, A1T, B2, A1B, A2 and A1FI), the CMIP3 dataset provides projections for at most three (B1, A1B and A2) scenarios, although not for all models. A summary of available model runs is given in Table 3.

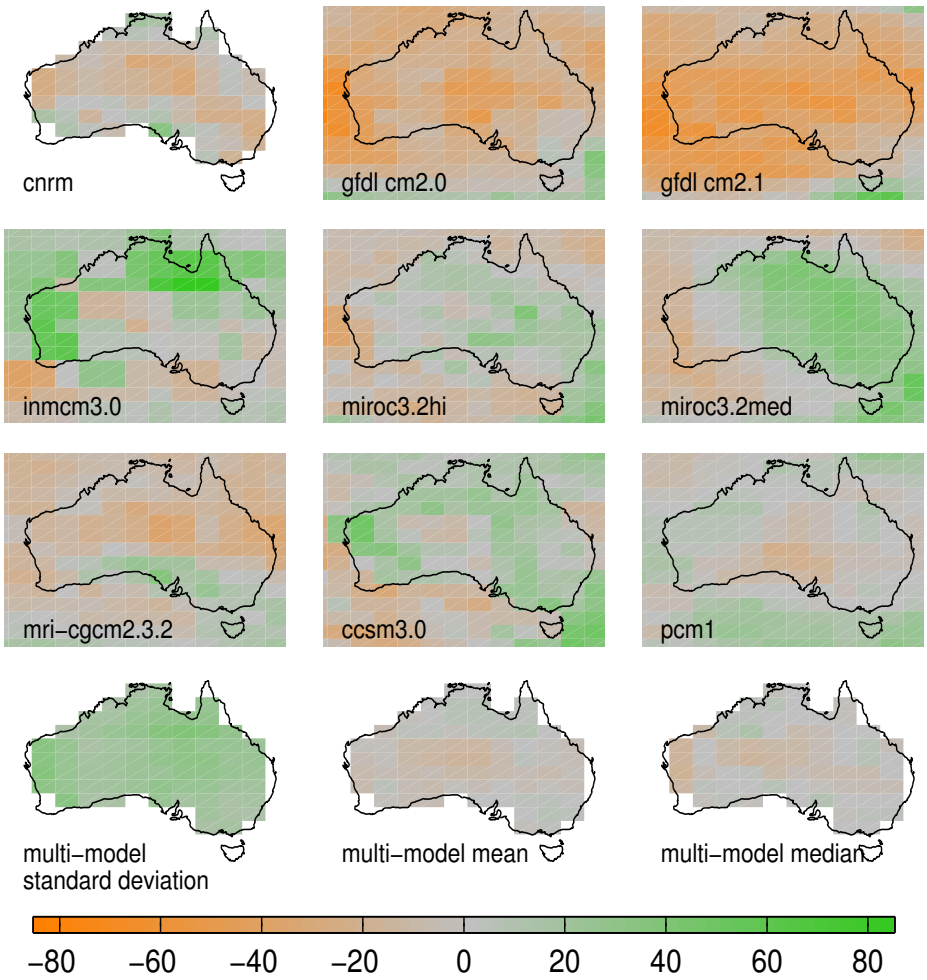

Figure 86 Relative change (%) for scenario A1B and the index *R10mm* over the period 2080-2099 compared with 1980-1999. First three rows, individual model trends. Last row: multi-model standard deviation, mean and median.

The relative change in the multi-run ensembles for the projections for three periods over the 21st century were compared with a 20 year period (1980-1999) for each of the three SRES emission scenarios and three indices. The time horizons over the 21st century are 2010-2029, 2040-2059 and 2080-2099 with indices *R10mm*, *RX5day* and *R95pT*. In contrast with Section 2.1, the inclusion of three scenarios and three time horizons greatly increases the model output that needs to be assessed[50]. For the sake of clarity, the assessment process is carried out in a systematic fashion. Projected

[50] From each of the models, also including the multi-model ensemble, there are 243 possible projections to be assessed.

changes against the period 1980-1999 are assessed for one index (*R10mm*), one time horizon (2080-2099), and one scenario (A1B) (Figure 86). The changes range from -50% to 85%, with a few models indicating continental-scale decrease (*gfdl cm2.0* and *gfdl cm2.1*), with others (e.g. *miroc3.2hi* and *pcm1*) having smaller changes of both signs. Overall, there is a large degree of inter-model variability (the standard deviation is of the order of 40%). This results in the multi-model mean having a much smaller magnitude than any of the individual models.

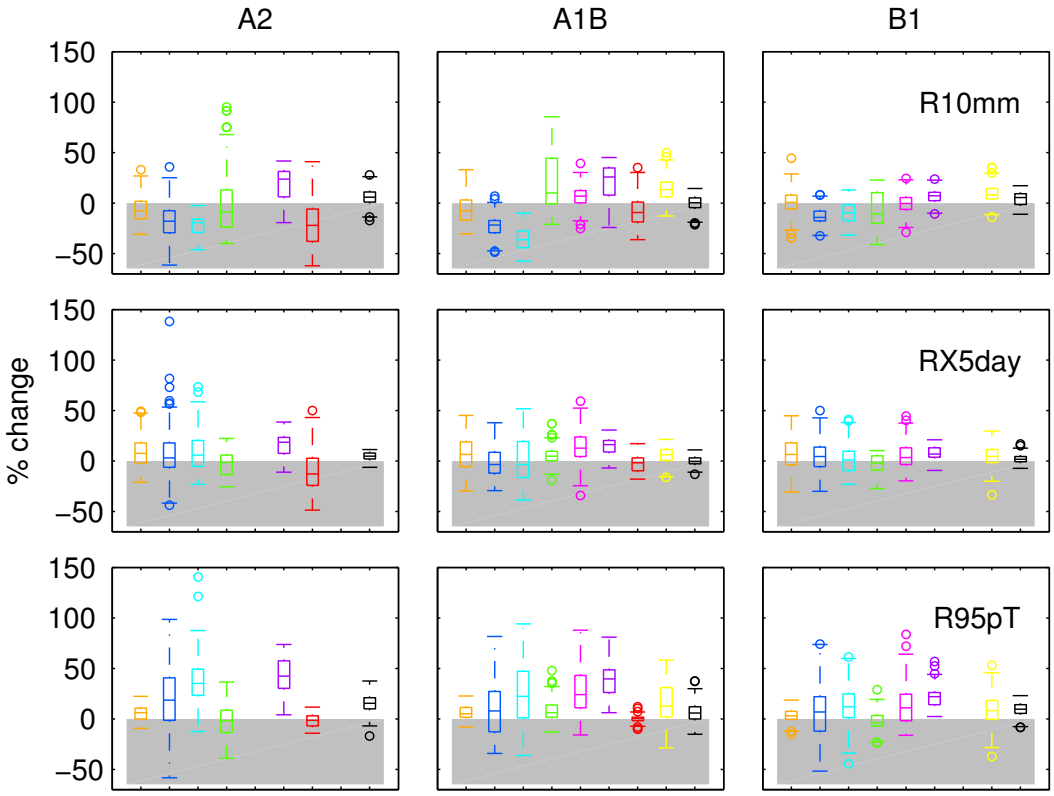

Figure 87 Box and whisker plot summarising the relative change (%) for the period 2080-2099 relative to 1980-1999 using all models with available data for mainland Australia. Indices *R10mm*, *RX5day* and *R95pT* for SRES A2, A1B and B1 have been used. The top centre panel is a summary of the individual models from Figure 86. Colours indicated by **O**: cnrm, **O**: gfdl cm2.0, **O**: inmcm3.0, **O**: gfdl cm2.1, **O**: miroc3.2hi, **O**: miroc3.2med, **O**: pcm1, **O**: mri-cgcm2.3.2, **O**: ccsm 3.0

Subsequent analyses for the period 2080-2099 were based on projections from all three scenarios. A box and whisker plot[51] was used to summarise the spatial variability of the relative change over mainland Australia (Figure 87). The top centre panel contains the spatial summary of the relative change reported in Figure 86. *R10mm* generally decreases. *RX5day* typically shows the smallest changes. *R95pT* indicates an overall increase in the mean and a high level of spatial variability within each model.

The remaining assessment is carried out on the multi-model means. The relative change of the multi-model means for the period 2080-2099 is shown in Figure 88. Overall, the results indicate consistency for the set of scenarios. There is a general decrease in *R10mm*, particularly over Western Australia, with a small increase for

[51] The box part of the plot shows median and inter-quartile range, with the whiskers indicating the range equivalent to the lesser of 1.5 times the interquartile range or the limits of the data. Values outside beyond these limits are indicated by open circles.

eastern Australia. For *RX5day*, there are a range of changes, with an increase throughout much of northern Australia. *R95pT* shows a large increase, in agreement with findings by Alexander and Arblaster (2008).

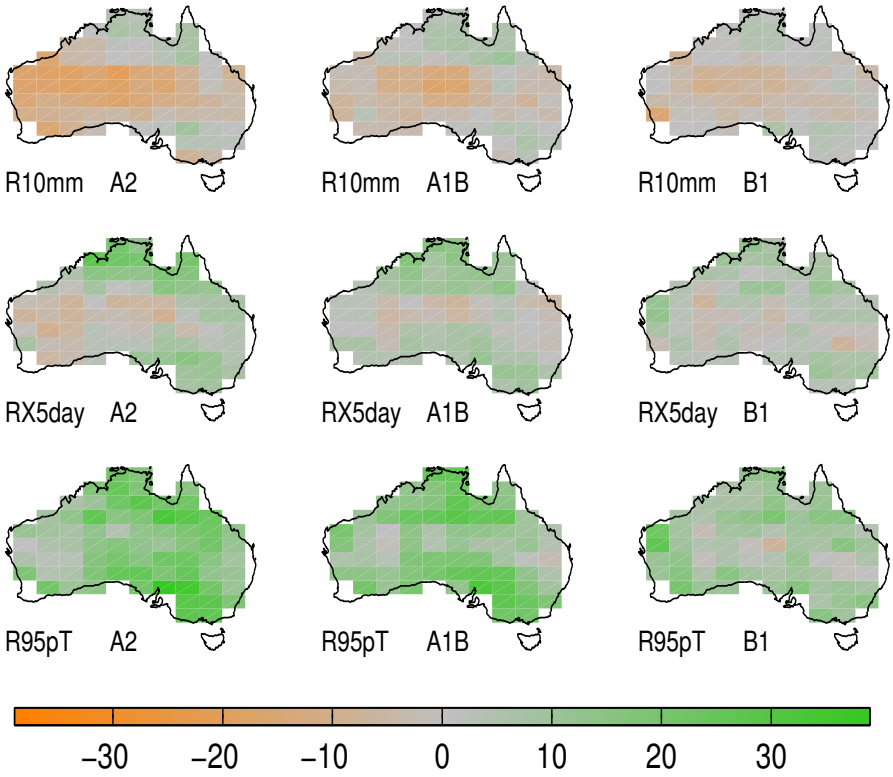

Figure 88 Relative change (%) of the multi-model mean for the period 2080-2099 relative to 1980-1999 for three scenarios and indices.

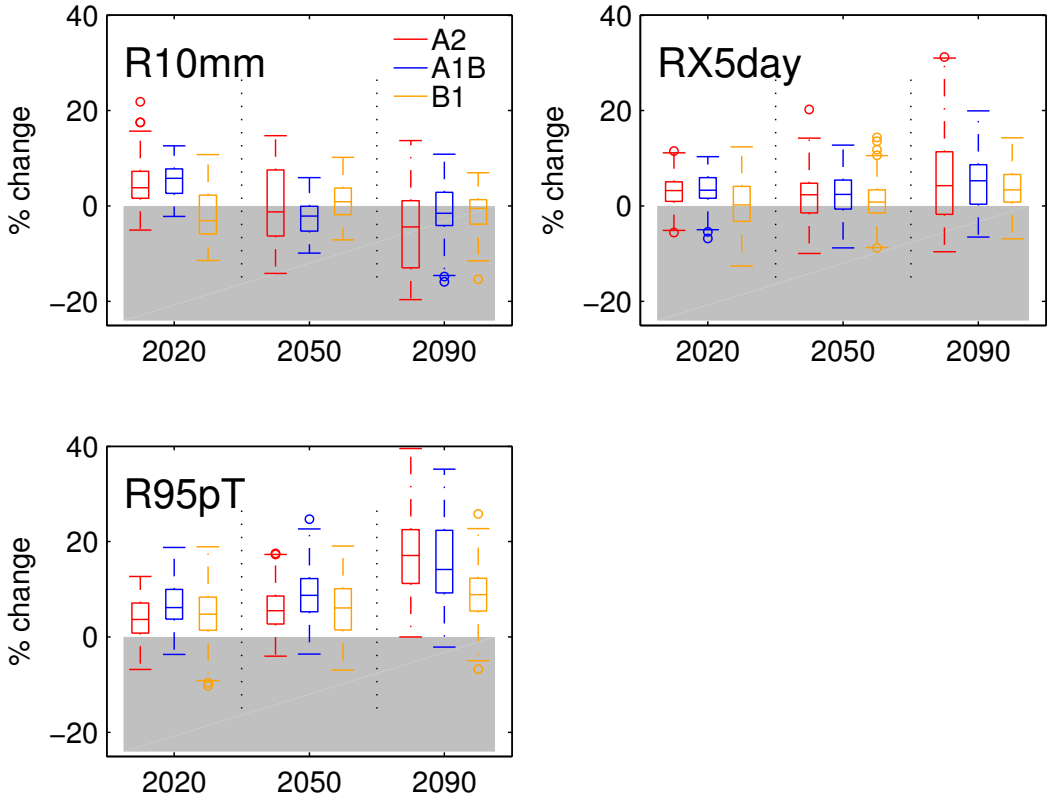

Figure 89 Relative change in the multi-model mean indices for three periods relative to the period 1980-1999. All models with available data for mainland Australia and indices *R10mm*, *RX5day* and *R95pT* for A2, A1B and B1 have been used. The markers 2020, 2050 and 2090 correspond to periods 2010-2029, 2040-2059 and 2080-2099.

The final analysis (Figure 89) summarises the relative change of all quantities for all time horizons. The largest magnitude changes occur for *R95pT* and *RX5day* for the period 2080-2099, however *R95pT* indicates an overall increase throughout all periods with only few decreases. Of the three scenarios, B1 indicates the smallest overall change and projected changes are smallest for *R10mm*.

2.4 Concluding discussion

An analysis was carried out on changes in extreme rainfall with the assumption that these changes can be used as a surrogate for changes in extreme rainfall associated with probable maximum precipitation. Three extreme rainfall indices (*R10mm*, *RX5day* and *R95pT*) were calculated from observed 20th century rainfall, climate model simulations of 20th century rainfall and projected rainfall for three periods and three emission scenarios into the 21st century (using 9 models and a multi-model ensemble).

Trends in 20th century annual rainfall closely match those for *R10mm*, with less agreement and more spatial variability for the more extreme index *R95pT*. The most consistent long-term trends indicate that decreases in the *R10mm* and *RX5day* indices occur across SW WA and increases occur for a small part of inland northern NSW. Climate models have a very limited ability at simulating the mean for the most extreme rainfall index (*R95pT*). However, they do have reasonable skill in simulating the spatial pattern of the means for *R10mm* and *RX5day* when compared with the respective mean of the gridded observed indices.

Projections into the 21st century for the extreme indices show large inter-model variability; with *R10mm* having much smaller overall change compared with the more extreme indices *RX5day* and *R95pT*. The large increase reported for *R95pT* has important consequences when assessing model projections of extreme rainfall. Despite poor agreement between observations and models for both the mean and trends for the latter part of the 20th century, there is an indication that *R95pT* for most grid points over Australia increases (Figure 87). This increase is monotonic for the three time horizons considered and for the emission scenarios A1B and A2. This would suggest that changes in this index may be more closely related to increasing global mean temperatures than for the less extreme rainfall indices (*R10mm* and *RX5day*).

These results should be interpreted in context with Chapters 10 and 11 of IPCC AR4 (Meehl et al. 2007 and Christensen et al. 2007), discussing global and regional climate projections respectively. Christensen et al. 2007 noted that for the Australian region, extremes of daily precipitation intensity[52] are very likely to increase, except possibly in areas of significant decrease in mean rainfall (SW WA, Timbal 2004). Despite the poor performance when modelling extreme precipitation (Randall et al. 2007), both theoretical and climate models suggest that a warming climate may influence extreme precipitation more than the mean (Hegerl et al. 2007). In future, an anthropogenic influence may be easier to detect using extreme precipitation (Bates et al. 2008), since extreme precipitation is more likely to be constrained by the availability of water vapour, which increases globally at approximately 7% per °C of global mean temperature (Held and Soden 2006). Emori and Brown (2005) separated the dynamical[53] and thermodynamical components of mean and extreme precipitation and showed that changes to the dynamic component generally play a more important role for mean precipitation changes than for the extremes, particularly over subtropical areas.

While there is some certainty about changes in projected rainfall extremes over Australia, a high degree of uncertainty remains for certain parts of the country. Christensen et al. (2007) showed that apart from SW WA during *winter*, there is considerable inter-model variability in the projections of seasonal rainfall, with the coefficient of variation always greater than 1. The lack of agreement is generally

[52]The extreme rainfall index used for IPCC projections (Meehl et al. 2007 and Christensen et al. 2007) was based on the rainfall intensity (total annual or seasonal wet day (>1 mm) rainfall divided by the number of rain days), which does not represent the extremes as well as the indices *R10mm*, *RX5day* or *R95pT*. In contrast, the IPCC chapter 3 on changes in observations (Trenberth et al. 2007) reported indicies that were more consistent with *R10mm* and *R95pT*.

[53] Dynamical component is that associated with the strength and frequency of the vertical wind speed at 500 hPa. The thermodynamical component is associated with atmospheric moisture content.

associated with factors that influence rainfall in both northern and central Australia. The ENSO dynamics and monsoon rainfall often vary between models, and in general projections during *summer* have the greatest inter-model variability. The present resolution of climate models prevents an accurate representation of tropical cyclones and heavy rainfall (Randall et al. 2007). Despite studies which have indicated that the large rainfall events will occur more frequently (e.g. Abbs 2004 using a dynamical downscaling showed that current 1 in 40 year events would correspond to a 1 in 15 year event in 2040), Barnett et al. (2006) suggest that model parameterisation uncertainty associated with rainfall (as discussed in Section 2.2.1) prevents a definite estimate in the change to the frequency of extreme rainfall.

Similar work reported in CSIRO and the Bureau of Meteorology (2007) assessed changes in both mean and extreme rainfall (99^{th} percentile) by using a local response per degree of global warming. This was then used to calculate a net projected change based on a global mean warming value by assuming an exponential relationship between percentage decrease in rainfall and change in global temperature. This process is more fully described in Watterson (2008).

In conclusion, although there is considerable uncertainty related to how rainfall may change in a warmer climate, there is an indication from both theoretical and climate models that changes in rainfall resulting from thermodynamic processes will lead to more frequent and perhaps more intense extreme events. In particular this will occur in regions with increase in mean precipitation. However, currently a quantitative assessment of changes to rainfall extremes cannot be made with the same level of confidence as for changes to atmospheric surface temperature. Improvements to the model dynamics of atmospheric process and parameterisation schemes, as well as increased model resolution will assist in providing better assessments of projected changes to extreme rainfall. Incorporation of more relevant downscaling approaches (statistical, dynamical and stochastic) will be useful for future assessments.

References

Abbs, D J (2004). The effect of climate change on the intensity of extreme rainfall events presented at International Conference on Storms, AMOS 11th National Conference, Brisbane, Australia, 5-9 July 2004.

Alexander, L V and Arblaster J (2008). Assessing trends in observed and modelled climate extremes over Austraila in relation to future projections. Submitted to International Journal of Climatology.

Alexander, L V, Hope, P, Collins, D, Trewin, B, Lynch, A and Nicholls N (2007). Trends in Australia's climate means and extremes: a global context, Australian Meteorological Magazine, 56, 1–18

Alexander, L V et al. (2006). Global observed changes in daily climate extremes of temperature and precipitation, Journal of Geophysical Research, 111, D05109, DOI:10.1029/2005JD006290

Barnett, D N et al. (2006). Quantifying uncertainty in changes in extreme event frequency in response to doubled CO2 using a large ensemble of GCM simulations. Climate Dynamics, 26, 489–511.

Bates, B C et al. (2008). IPCC Technical Paper on Climate Change and Water. Available online http://www.ipcc.ch/meetings/session28/doc13.pdf (accessed 30 April 2008).

Beesley, C A, Meighen, J and Xuereb, K C (2004). Catalogue of Significant Rainfall Occurrences of Tropical Origin over Australia, HRS Report No. 9, Hydrology Report Series, Bureau of Meteorology, Melbourne, Australia, February 2004, 147 pp.

Buonomo, E, Jones, R, Huntingford, C and Hannaford J (2007). On the robustness of changes in extreme precipitation over Europe from two high-resolution climate change simulations. Quarterly Journal of the Royal Meteorological Society, 133: 65–81

Bureau of Meteorology (2005a). *Heavy Rainfall Gold Coast – 30th June 2005*, Internal report.

Bureau of Meteorology (2005b). The Meteorology of the Gold Coast floods – 29th–30th June 2005, Internal report available online at http://www.bom.gov.au/inside/services_policy/public/sigwxsum/sigwmenu.shtml.

Chen, C-T and Knutson, T (2008). On the verification and comparison of extreme rainfall indices from climate models. Journal of Climate, 21, 1605–1621. DOI: 10.1175/2007/JCLI1494.1

Christensen, J H et al. (2007). Regional Climate Projections. In: Climate Change 2007: The Physical Science Basis. Contribution of Working Group I to the Fourth Assessment Report of the Intergovernmental Panel on Climate Change [Solomon, S., D. Qin, M. Manning, Z. Chen, M. Marquis, K.B. Averyt, M. Tignor and H.L. Miller (eds.)]. Cambridge University Press, Cambridge, United Kingdom and New York, NY, USA.

CSIRO and the Bureau of Meteorology (2007). Climate Change in Australia: Technical report 2007. 148 pp. www.climatechangeinaustralia.gov.au

Emori, S and Brown, S J (2005). Dynamic and thermodynamic changes in mean and extreme precipitation under changed climate. Geophysical Research Letters. L17706. 10.1029/2005GL023272.

Gaffen, D J (1993). Historical changes in radiosonde instruments and practices, WMO/TD–No. 541, Instruments and observing methods Rep. 50. World Meteorological Organization, 123 pp.

Gaffen, D J, and Ross, R J (1999). Climatology and trends of US surface humidity and temperature, Journal of Climate, 12, 811– 828.

Glecker, P J, Taylor, K E and Doutriaux, C (2008). Performance metrics for climte models. Journal of Geophysical Research 113, D60104. DOI:10.1029/2007JD008972

Gordon, H B, Rotstayn, L D, McGregor, J L, Dix, M R, Kowalczyk, E A, O'Farrell, S P, Waterman, L J, Hirst, A C, Wilson, S G, Collier, M A, Watterson, I G, and Elliott, T I (2002). The CSIRO Mk3 Climate System Model [Electronic publication]. Aspendale: CSIRO Atmospheric Research. (CSIRO Atmospheric Research technical paper; no. 60). 130 pp. http://www.cmar.csiro.au/e–print/open/gordon_2002a.pdf (accessed 13 May 2008)

Haylock, M and Nicholls, N (2000). Trends in extreme rainfall indices for an updated high quality data set for Australia (1910–1998). International Journal of Climatology 20, 1533–1541.

Held, I M, Soden, B J (2006). Robust responses of the Hydrological Cycle to Global Warming, Journal of Climate, 19 (21), 5686–5699.

Hegerl, G C et al. (2007). Understanding and Attributing Climate Change. In: Climate Change 2007: The Physical Science Basis. Contribution of Working Group I to the Fourth Assessment Report of the Intergovernmental Panel on Climate Change [Solomon, S., D. Qin, M. Manning, Z. Chen, M. Marquis, K.B. Averyt, M. Tignor and H.L. Miller (eds.)]. Cambridge University Press, Cambridge, United Kingdom and New York, NY, USA.

Hennessy, K J, Suppiah, R and Page, C M (1999). Australian rainfall changes, 1910–1995. Australian Meteorological Magazine 48, 1–13.

Hope, P K, Drosdowsky, W and Nicholls, N (2006). Shifts in the synoptic systems influencing southwest Western Australia. Climate Dynamics. 26, 751–764.

Intergovernmental Panel on Climate Change (IPCC) (2001). Climate Change 2001: The Scientific Basis: Contribution of the Working Group I to the Third Assessment Report of the Intergovernmental Panel on Climate Change, edited by J. T. Houghton et al., 881 pp., Cambridge Univ. Press, New York.

Institution of Engineers, Australia (1987). Australian Rainfall and Runoff – A Guide to Flood Estimation, Vol. 2, R P Canterford (ed.), Institution of Engineers, Australia, Barton, ACT, 1987.

Jakob, D, Taylor, B F and Xuereb, K C (2005). A Pilot Study to Explore Methods for Deriving Design Rainfalls for Australia – Part 1, HRS Report No. 10, Hydrology Report Series, Bureau of Meteorology, Melbourne, Australia, June 2005, 59 pp.

Jones, D A and Minty, L J (1996). The generation of extreme persisting dew–point temperature analyses for Australia. Internal Report, Hydrometeorological Advisory Service. Bureau of Meteorology, Melbourne, Australia. December 1996.

Knutson, T R and Tuleya, R E (2004). Impact of CO2–Induced Warming on Simulated Hurricane Intensity and Precipitation: Sensitivity to the Choice of Climate Model and Convective Parameterization. Journal of Climate 17, 3477–3495.

Lavery, B, Kariko, A P and Nicholls, N (1997). An extended high–quality historical rainfall dataset for Australia. Australian Meteorological Magazine. 46, 27–38.

Lavery, B, Joung, G, and Nicholls, N (1992). A high–quality historical rainfall data set for Australia. Australian Meteorological Magazine. 40, 33–39.

Lucas, C (2006). An examination of dew–point biases introduced by different instrumentation, BMRC Research Letters No. 4, Bureau of Meteorology Research Centre. Bureau of Meteorology, Melbourne.

Manton, M J, et al. (2001). Trends in extreme daily rainfall and temperature in southeast Asia and the South Pacific: 1916–1998. International Journal of Climateology 21, 269–284.

McIntosh, P C, Pook, M J, Risbey, J S and Lisson S. (2006). Towards better seasonal climate forecasts for farmers [invited paper]. In: "Groundbreaking stuff: Proceedings of the 13th Australian Agronomy Conference 2006", Australian Society of Agronomy: Perth, WA.

Meehl, G A et al. (2007). Global Climate Projections. In: Climate Change 2007: The Physical Science Basis. Contribution of Working Group I to the Fourth Assessment Report of the Intergovernmental Panel on Climate Change [Solomon, S., D. Qin, M. Manning, Z. Chen, M. Marquis, K.B. Averyt, M. Tignor and H.L. Miller (eds.)]. Cambridge University Press, Cambridge, United Kingdom and New York, NY, USA.

Minty, L J, Meighen, J and Kennedy, M R (1996). Development of the generalised southeast Australia method for estimating Probable Maximum Precipitation, HRS Report No. 4, Hydrology Report Series, Bureau of Meteorology, Melbourne, Australia, August 1996, 42 pp.

Nakićenović, N and Swart, R (eds.) (2000). Special Report on Emissions Scenarios. A Special Report of Working Group III of the Intergovernmental Panel on Climate Change. Cambridge University Press, Cambridge, United Kingdom and New York, NY, USA, 599 pp.

New, M G, Hulme, M and Jones, P D (2000). Representing twentieth–century space–time climate variability. Part II: Development of 1901–1996 monthly grids of terrestrial surface climate, Journal of Climate, 13, 2217–2238.

Nicholls, N (2006). Detecting and attributing Australian climate change: a review. Australian Meteorological Magazine **55**, 199–211.

Pall, P, Allen, M R, Stone, D A (2007). Testing the Clausius–Clapeyron constraint on changes in extreme precipitation under CO2 warming. Climate Dynamics 28, 351–363. DOI: 10.1007/s00382–006–0180–2

Pearse, M A (1993). A joint probability approach for estimating annual exceedence probabilities of extreme rainfall and flood events, Civil Engineering Research Report 1/1993.

Peterson, T C and Easterling, D R (1994). Creation of homogeneous composite climatological reference series. International Journal of Climatology 14, 671–679.

Randall, D A et al. (2007). Climate Models and Their Evaluation. In: Climate Change 2007: The Physical Science Basis. Contribution of Working Group I to the Fourth Assessment Report of the Intergovernmental Panel on Climate Change [Solomon, S., D. Qin, M. Manning, Z. Chen, M. Marquis, K.B. Averyt, M.Tignor and H.L. Miller (eds.)]. Cambridge University Press, Cambridge, United Kingdom and New York, NY, USA

Rayner, N A, Brohan, P, Parker, D E, Folland, C K, Kennedy, J J, Vanicek, M, Ansell, T and Tett, S F B (2006). Improved analyses of changes and uncertainties in sea surface temperature measured *in situ* since the mid–nineteenth century: the new HadSST2 data set, Journal of Climate 19, 446–469.

Ren, F, Wu, G, Dong, W, Wang, X, Wang, Y, Ai, W and Li, W (2006). Changes in tropical cyclone precipitation over China. Geophysical Research Letters Vol. 33.

Rakich, C S, Holbrook, N J H and Timbal, B (2008). A pressure gradient metric capturing planetary–scale influences on eastern Australian rainfall, Geophysical Research Letters, 35, L9813, DOI:10.1029/2007GL032970

Suppiah, R (2004). Trends in the southern oscillation phenomenon and Australian rainfall and changes in their relationship. International Journal of Climatology 24, 269–290.

Taylor, K E (2001). Summarizing multiple aspects of model performance in a single diagram. Journal of Geophysical Research. 106, 7183–7192.

Tebaldi, C, Hayhoe, K, Arblaster, J and Meehl, G (2006). Going to the extremes. An intercomparison of model–simulated historical and future changes in extreme events. Climatic Change. DOI:10.1007/s10584–006–9051–4

Timbal, B (2004). Southwest Australia past and future rainfall trends. Climate Research, 26, 233–249.

Timbal, B and Arblaster, J M (2006). Land cover change as an additional forcing to explain the rainfall decline in the south west of Australia. Geophysical Research Letters, 33, L07717

Trenberth, K E, Fasullo, J, Smith, L (2006). Trends and variability in column–integrated water vapour, Climate Dynamics 24, 741 – 758.

Trenberth, K E, et al. (2007). Observations: Surface and Atmospheric Climate Change. In: Climate Change 2007: The Physical Science Basis. Contribution of Working Group I to the Fourth Assessment Report of the Intergovernmental Panel on Climate Change [Solomon, S., D. Qin, M. Manning, Z. Chen, M. Marquis, K.B. Averyt, M. Tignor and H.L. Miller (eds.)]. Cambridge University Press, Cambridge, United Kingdom and New York, NY, USA.

Viney, N R and Bates, B C (2004). It never rains on Sunday: The prevalence and implications of untagged multi-day rainfall accumulations in the Australian high quality data set. International Journal of Climatology 24, 1171–1192.

Vivès, B and Jones, R N. (2005). Detection of abrupt changes in Australian decadal rainfall (1890 – 1989). Technical Paper No. 73, CSIRO Atmospheric Research, 54 pp.

Walland, D J, Meighen, J, Xuereb, K C, Beesley, C A and Hoang, T M T (2003). Revision of the Generalised Tropical Storm Method for Estimating Probable Maximum Precipitation, HRS Report No. 8, Hydrology Report Series, Bureau of Meteorology Melbourne, Australia, August 2003, 78 pp.

Wang, J X L and Gaffen, D J (2001). Late-twentieth century climatology and trends of surface humidity and temperature in China, Journal of Climate, 14, 2833 – 2845.

Watterson, I G (1996). Nondimensional measures of climate model performance, International Journal of Climatology. 16, 379 – 391.

Watterson, I G (2008). Calculation of probability density functions for temperature and precipitation change under global warming, Journal of Geophysical Research DOI:10.1029/2007JD009254, in press.

Webster, P J, Holland, G J, Curry, J A, and Chang, H-R (2005). Changes in tropical cyclone number, duration, and intensity in a warming environment, Science, 309(5742), 1844 – 1846.

Whetton, P, Macadam, I, Bathols, J and O'Grady, J (2007). Assessment of the use of current climate patterns to evaluate regional enhanced greenhouse response of climate models, Geophysical Research Letters. 34, 114701, DOI: 10.1029/2007GL030025

World Meteorological Organisation (1986). Manual for Estimation of Probable Maximum Precipitation. Second Edition. Operational Hydrology Report No. 1, WMO – No. 332, Geneva.

Zhang, X, Hegerl, G, Zwiers, F W and Kenyon, J (2005). Avoiding inhomogeneity in percentile–based indices of temperature extremes, Journal of Climate. 18, 1641–1651.

Publications

Papers and presentations

Jakob, D, Smalley, R J, Meighen, J, Taylor, B and Xuereb, K (2007). Climate Change and Probable Maximum Precipitation, NZSOLD/ANCOLD 2007 Conference 'Dams - Securing Water for our future', 19-20 November 2007, Queenstown, New Zealand.

Jakob, D, Smalley, R J, Meighen, J, Taylor, B and Xuereb, K (2007). Climate Change and Probable Maximum Precipitation, Water Down Under 2008, 31st Hydrology and Water Resources Symposium, 14-17 April 2008, Adelaide, Australia.

Smalley, R J, Jakob, D, Meighen, J, and Xuereb, K (2008). Changes in extreme moisture availability and precipitation efficiency associated with significant rainfall events. 15th National AMOS Conference, 29 January-1 February 2008, Geelong, Australia.

Smalley, R J, Jakob, D, Jones, D A, Meighen, J, Taylor, B F and Xuereb, K C (2006). The effect of changes in dew-point temperatures on estimates of Probable Maximum Precipitation. 30th Hydrology and Water Resources Symposium, 4 – 7 December 2006, Launceston, Australia.

Posters

Jakob, D, Smalley, R, Xuereb, K and Meighen, J (2007). Climate Change and Probable Maximum Precipitation, Third International Conference on Climate and Water, 3-6 September 2007, Helsinki, Finland.

Jakob, D, Smalley, R, Xuereb, K and Meighen, J (2007). Could factors used in estimating Probable Maximum Precipitation (PMP) change under a changing climate? 14th National AMOS Conference, 5 - 8 February 2007, Adelaide, South Australia.

Jakob, D, Smalley, R, Xuereb, K and Meighen, J (2006). Probable Maximum Precipitation and Climate Change. Living with Climate Variability and Change, 17 - 21 July 2006 Espoo, Finland.

Jakob, D, Smalley, R J, Meighen, J, Taylor, B, Xuereb, K (2007). Impact of climate change on factors relevant to probable maximum precipitation estimates. Presented at Greenhouse 2007, 2-5 October 2007, Sydney, Australia.

Smalley, R J, Jakob, D, Meighen, J, Xuereb, K (2007). Impact of climate change on factors relevant to probable maximum precipitation estimates. Presented at Hydrological Consequences of Climate Change Symposium. 15-16 November, 2007, Canberra, Australia.

Smalley, R J, Jakob, D, Jones, D, Meighen, J, Taylor, B F, Xuereb, K C (2006). Effects of climate trends on precipitable water and probable maximum precipitation estimates. 17th Australia New Zealand Climate Forum, Australian National University, Canberra, ACT, Australia, 5-7 September 2006 p.76.

Glossary

$24T_d$ - persisting 24h dew-point temperature.

50PW; 90PW – median and 90th percentile, precipitable water quantities.

average recurrence interval, ARI - average value of periods between exceedences of a given rainfall total for a given duration. When applied to the annual maximum series: the average number of years between years in which there are one or more exceedences of a given rainfall total for a given duration.

convergence depth; **convergence component rainfall** - rainfall due to any atmospheric process unaffected by terrain

decay amplitude factor, DAF - Factor to account for the decay in a storm mechanism as it propagates to remote locations. The DAF was determined as the product of smoothed design rainfall estimates (for the 72-hour duration and a 50-year average recurrence interval) and the standardisation factor.

dew-point temperature, T_d – the temperature at which saturation is attained when air is cooled at constant pressure without the addition or subtraction of water vapour.

emission scenarios – defined in the Special Report on Emission Scenarios (SRES). Emission scenarios are based on four narrative storylines that describe the relationships between the forces driving greenhouse gas and aerosol emissions and their evolution during the 21st century.

EPW – Extreme **precipitable water**, generally derived from the *Extreme 24-hour persisting dew-point temperature,* which is the analysed maximum value of persisting 24-hour dew-point temperature at a given location and time of year.

generalised methods of PMP estimation **–** methods which utilise the rainfalls recorded over a large region by separating the portion of rainfall arising from 'site-specific' influences from that portion arising from regional influences. Such methods provide regional consistency of PMP estimation.

GSAM - Generalised Southeast Australia Method of PMP estimation. A generalised method for estimating longer-duration PMP in southeast Australia.

GTSMR - Revision of the Generalised Tropical Storm Method of PMP estimation. A generalised method for estimating longer-duration PMP in those parts of Australia affected by tropical storms.

HAS - Hydrometeorological Advisory Service

HRS - Hydrometeorological Report Series

location – a locality which may comprise of a number of observation stations in the vicinity. (This allows for station changes with a uniquely defined locality)

maximisation Factor (MF) – The factor by which storm convergence component rainfalls are multiplied to simulate maximised storm moisture content, defined as:

$$\frac{\text{Extreme Precipitable Water (at storm location and time of year)}}{\text{Storm Precipitable Water}}$$

Maximisation-standardisation factor (MSF) - The product of maximisation and standardisation factor which is used to simulate the maximised storm moisture content when standardised, such that events from all locations can be compared.

Moisture adjustment factor (MAF) – The factor by which the standard convergence PMP is multiplied to simulate the transposition of this component from a standard location of standard moisture potential to the location of the catchment and its specific moisture potential. It is defined as

$$\frac{\text{Extreme Precipitable Water (at catchment location)}}{\text{Extreme Precipitable Water (at standard location)}}$$

moisture maximisation – *'the process of adjusting observed precipitation amounts upwards based upon the hypothesis of increased moisture inflow to the storm'* (WMO, 1986). The increase is generally to theoretical values that could be reached if the moisture content of the air had been at the maximum recorded for that location and season, but the other meteorological conditions affecting the storm had remained unchanged.

persisting n-h dew-point temperature – the dew-point temperature at a station that has been equalled or exceeded throughout a period of n consecutive hours. Commonly durations of 12 or 24 h are used, though other durations may be used at times.

PMF – Probable Maximum Flood. The flood produced when runoff from the PMP is routed through the catchment.

PMP – Probable Maximum Precipitation is *'the greatest depth of precipitation for a given duration meteorologically possible over a given size storm area at a particular location at a particular time of the year, with no allowance made for long-term climatic trends.'* (WMO, 1986).

precipitable water (PW) – total water vapour contained in an atmospheric column of unit cross-section, expressed in terms of the depth of an equivalent mass of liquid water of the same cross-section.

pseudo-adiabat – line on thermodynamic diagram showing the pressure and temperature changes undergone by saturated air rising in the atmosphere, without ice-crystal formation and without exchange of heat with its environment other than that involved in assuming that the liquid water, formed by condensation, drops out. It is the heat exchange associated with condensation that forces the term *pseudo*.

R10mm – The number of heavy rainfall days; calculated from the annual count of days when rainfall > 10 mm.

R95pT – Proportion of annual rainfall from very wet days; calculated as the total annual rainfall from wet days ($\geq$ 1 mm) with rainfall above the 95th percentile for wet days (based on the period 1961-1990), divided by the annual rainfall

RX1day – The seasonal or annual maximum 1-day rainfall total.

RX5day – The seasonal or annual maximum 5-day rainfall total.

relative storm efficiency (or short 'storm efficiency') - A precipitation/moisture ratio index, describing the 'capacity of a storm to extract a given amount of precipitation from a given amount of atmospheric moisture'. Efficiency is treated as dimensionless, regardless of the unit resulting from calculating the ratios. Definitions were chosen so that efficiency does not exceed 1.

saturation – upper limit of water-vapour content of an airmass, which is solely a function of temperature.

season - Conventionally seasons are defined as 3 month-periods (e.g. *summer* for the months December, January and February). For GTSMR, two seasons are defined: a 7-month *summer* period from October to April (coinciding with the northern wet season) and a 5-month *winter* period from May to September (coinciding with the northern dry season). For GSAM, four seasons are defined as follows: *summer* from December to March, *autumn* for April and May, *winter* for June to September and *spring* for October and November.

specific humidity, q – mass of water vapour per unit mass of moist air.

SPW – storm precipitable water associated with **persisting 24h storm dew-point temperature**.

SST - sea surface temperature

station – observation site defined by a unique station number.

standardisation factor (SF) – The factor by which the storm *convergence component rainfalls* are multiplied to simulate transposition to a standard location, defined as:

$$\frac{\text{Extreme Precipitable Water (at standard location)}}{\text{Extreme Precipitable Water(at storm location and time of year)}}$$

storm dew-point temperature – the 1000hPa dew-point temperature that is representative of the rain-producing airmass of the storm.

(T_d) –quantity derived from the **persisting 24 h dew-point temperature**.

T_dN90p – percentage of days where the daily minimum T_d is greater than the 90th percentile of an appropriate climatological base period.

Topographic adjustment factor (TAF) - The average enhancement of storm rainfall due to the presence of topography, defined as:

$$\frac{\textit{Total 72-h, 50-y rainfall intensity}}{\textit{Convergence Component of the 72-h, 50-y rainfall intensity}}$$

(ua) –quantity derived from upper-air **precipitable water** data

WMO – World Meteorological Organisation.

Appendix

A1 Method used for selecting significant rainfall events

For both the GTSMR and GSAM, the significant rainfall event databases were constructed using multi-stage methods. The methods differ slightly, due to the different computational facilities available at the time of the development of each method. The methods are described in detail within Walland et al. (2003) and Minty et al. (1996) respectively, and are summarised here:

For the GTSMR

1. For each station, the top ten rainfall totals for each duration spanning 1 – 7 days were ranked, and those occurring on the same date for nearby stations were grouped and associated as the same event.
2. The events were ranked, separately for each duration, as to how many 1:100 ARI daily rainfall observations occurred at the stations associated with each event.
3. The selected events were divided geographically, such that the representation was from all areas, rather than those which appeared to be the largest across the whole GTSMR area. Events were sorted within 17 regions (or sub-zones). This resulted in at least 5 times the number of events used in the final selection.
4. The final list was determined from the largest ranked events, with a representation across each region. In addition, events in SWWA during *winter* are also included (since *winter* events are particularly important for flooding in this region), which might have been excluded based on an automated ranked-analysis process.

For the GSAM,

1. As in 1 for GTSMR
2. Station rainfall totals were compared to the 72h 50 y rainfall intensity at the station locations, with the largest rainfall depth being selected for each event area.
3. Although events were not divided into regions, or sub-zones, those occurring in coastal SA or Tasmania were given greater chance of being included – at the possible expense of additional, but relatively larger magnitude events for coastal NSW.

Stage 3 of these selection methods, particularly for the GTSMR, attempts to equally weight all regions, such they contribute at least 1 event.

Selection of independent events

The generalised databases are based on events that are significant for different areas and durations. However, there are occasions where events have been selected that are common when applied to multiple durations. Events are initially categorised as independent if they occur outside of a 7 day window[54]. For those within a 7 day

[54] There are only two GTSMR events with durations longer than 7 days.

window, event pairs are segregated according to type and distance. Event centres with a separation distance greater than 3° or are different types of events are classified as independent.

For GTSMR event pairs with similar type, within 3° and a 7 day window of each other, only two events are considered independent. All other events that fall within this categorisation are considered to be related. This results in 94 GTSMR independent events, in agreement with separate analysis undertaken prior to the current project.

For GSAM event pairs with similar type, within 3° and a 7 day window of each other, three events are considered independent. All other events that fall within this categorisation are considered to be related. By chance, this also results in 94 independent GSAM events.

A2 Selection of rainfall stations used in section 2.1

From a network of approximately 6400 stations observing rainfall across Australia, only 379 'high-quality stations' were suitable for analysis of monthly rainfall changes, for at least part of the period between 1910 to 1995 (Lavery et al. 1997). These are used by the Bureau of Meteorology's National Climate Centre when gridding seasonal and annual rainfall totals across Australia. When daily data are considered (which are required for this study), the number of stations of sufficient quality reduces to 191 (Lavery et al. 1992). Subsequent stringent reanalysis by Haylock and Nicholls (2000) reduced the number of available stations with daily data to 91. This substantially reduced the availability of data for coastal and northern Queensland; removed all stations in Northern Territory and most of those from Western Australia, apart from the south west.

To improve coverage in these areas, the network of monthly high-quality data stations was used to select daily data that only have 1-day rainfall accumulations[55]. This resulted in a maximum of 308 stations that may be considered. An additional quality check involves removing individual station-years that have suspect untagged accumulations occurring on Sundays. This was carried out using the method of Viney and Bates (2004)[56] and applied to all stations within Lavery et al. (1997).
Figure A1 and
Figure A2 show the yearly occurrence for each station of the possible instances of untagged accumulations for the original daily high-quality rainfall stations and those where the daily data are extracted from the monthly high quality rainfall stations. The greatest number of untagged accumulations occurs in SA, parts of SW WA and northern NSW for the period between 1910 and 1974.
Despite the increase in the number of stations with data available when incorporating those in
Figure A2, there are still insufficient data to adequately cover most of the northern region of Australia for the longer period (1910-2005).

[55]In Lavery et al. (1997) some of the stations in the monthly dataset were comprised of two nearby stations of shorter lengths, and were joined after comparing overlapping years and appropriately scaling the monthly rainfall totals. For daily analysis, creating a composite station is not possible, and so only the last station out of any pair has been used.
[56]The method calculates the probability that the number of rainy Sundays in any given year for a particular station could actually be as few as observed. This is calculated by comparing the Sunday rainday probability with that for the period Tuesday to Friday (assumed to be tagged correctly). When the Sunday rainday probability is less than a critical threshold, it is assumed that a 1-day rainfall recorded on a Monday may incorporate an untagged accumulation from the Sunday.

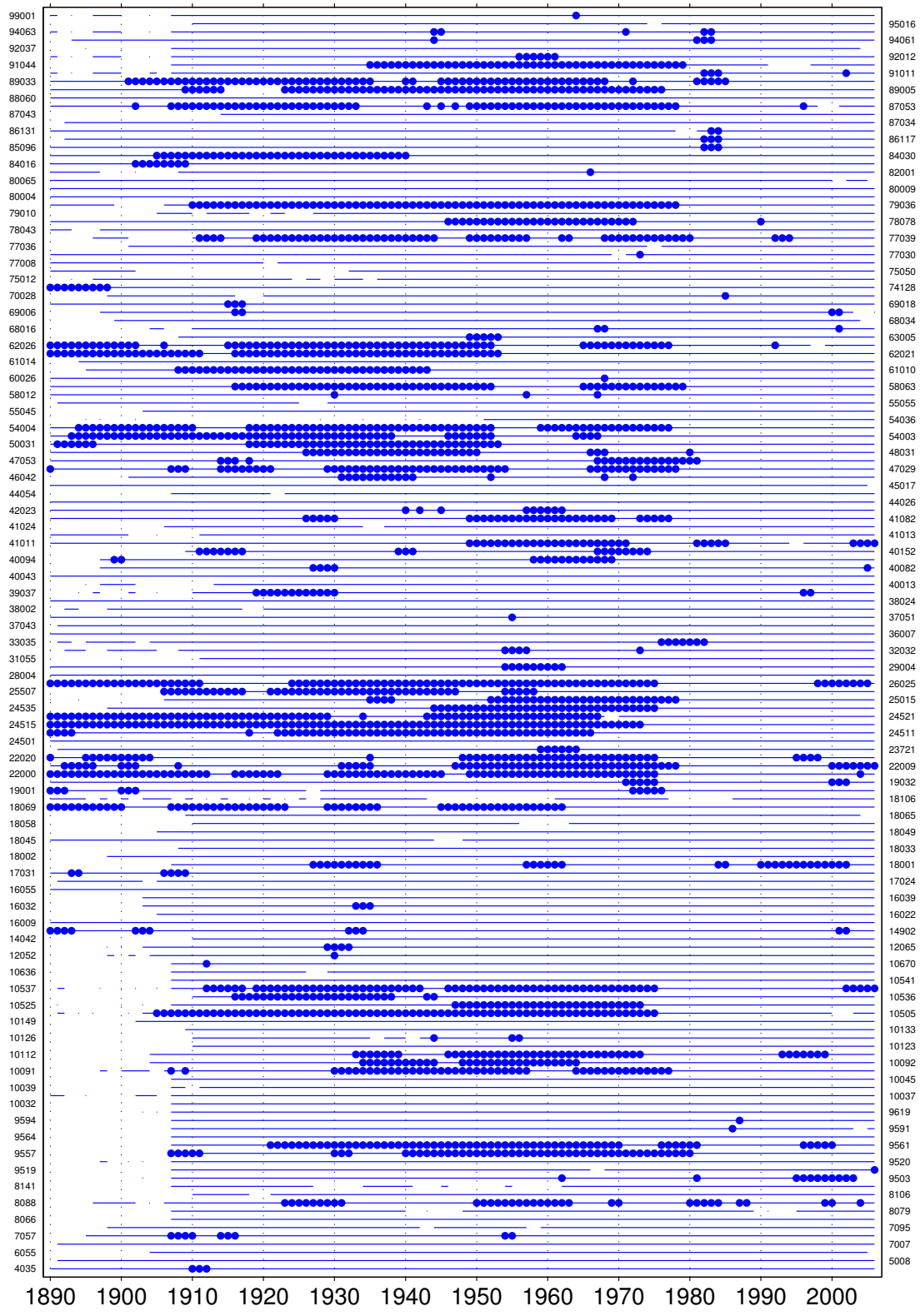

Figure A1 Abacus plot indicating stations from Lavery et al. (1992) that have possible occurrences of untagged accumulations on Sundays (indicated for each year with a circle) for the period 1890-2005. Station numbers are sorted by state (bottom to top). WA: 0000-13999; NT: 14000-15999; SA: 16000-26999; QLD: 27000-45999; NSW: 47000-75999; VIC: 76000-90999; TAS: 91000-99999.

Figure A2 Abacus plot indicating additional stations from Lavery et al. (1997) that have possible occurrences of untagged accumulations on Sundays (indicated for each year with a circle) for the period 1890-2005. Station numbers are sorted by state (bottom to top). WA: 0000-13999; NT: 14000-15999; SA: 16000-26999; QLD: 27000-45999; NSW: 47000-75999; VIC: 76000-90999; TAS: 91000-99999. The stations in Lavery et al. (1997) which are already represented in Figure A1 are not shown.

A3 Gridding of observed rainfall indices

Station data is represented on a grid based on a modified version of the angular distance weighting (ADW) method as described in Alexander et al. (2006). This method has been assessed by New et al. (2000) as being suitable for gridding irregularly spaced data. The rainfall indices are gridded onto a latitude-longitude grid (2.5° x 3.75°) by weighting each station index value by its distance and angle from the centre of a search radius. The angular part of the weighting (represented by the *cos* term below) ensures that stations in close proximity of each other are given lower weight than a station which is relatively isolated. For every grid square, the weighting function w_i, for station i relative to the location of other stations in the search radius is

$$w_i = f_i^m \left\{ 1 + \frac{\sum_k f_k^m \left[1 - cos(\theta_k - \theta_i) \right]}{\sum_k f_k^m} \right\}, \quad i \neq k ,$$

where the f_i is a decorrelation function $\left(f_i = e^{-r_i / L} \right)$ for station i, θ is the angle between a station and each grid point and m is a parameter which defines the steepness of the decay for the decorrelation function (equal to 4 in this case). The search radius is equal to L, which is defined by the decorrelation length scale for the relevant index when applied to a spatial correlation of the data. At least 3 stations need to exist within the search radius for a weighting function to be calculated. In analysis of global indices, Alexander et al. (2006) defined the decorrelation length scale in zonal bands (e.g. 0-30°S, 30°S-90°S) which was equal to the distance where the mean correlation is less than 1/*e*. The same method will be applied here, but to Australian data only. For rainfall indices, there is high variability in the spatial correlation, and so the calculated decorrelation length scales are somewhat subjective.

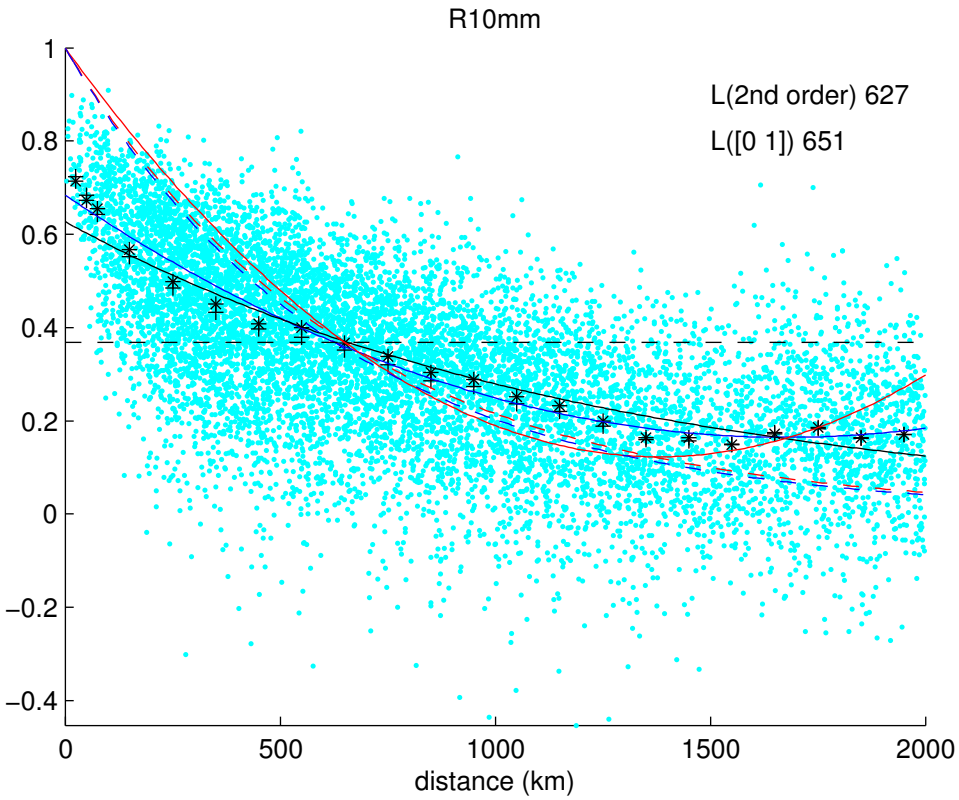

Figure A3 Station correlations for index R10mm in the Australian zonal band 0°-30°S. The individual station correlations (cyan dots) are averaged over each 50 km interval (black +). A second order polynomial and exponential function are fitted to the data for distances less than 2000 km. The distance at which the correlation equals 1/e is defined as the decorrelation length scale, L (indicated in the top right in km).

HYDROLOGY REPORT SERIES

HRS1	Temporal Distributions Within Rainfall Bursts	September 1991
HRS2	Analysis of Australian Rainfall and Rainday Data with Respect to Climatic Variability and Change	February 1992
HRS3	Catalogue of Significant Rainfall Occurrences Over Southeast Australia	October 1995
HRS4	Development of the Generalised Southeast Australia Method for Estimating Probable Maximum Precipitation	August 1996
HRS5	Temporal Distributions of Large and Extreme Design Rainfall Bursts over Southeast Australia	December 1998
HRS6	Rainfall Antecedent to Large and Extreme Rainfall Bursts over Southeast Australia	December 1999
HRS7	Development of the Method of Storm Transposition and Maximisation for the West Coast of Tasmania	January 2001
HRS8	Revision of the Generalised Tropical Storm Method for Estimating Probable Maximum Precipitation	August 2003
HRS9	Catalogue of Significant Rainfall Occurrences of Tropical Origin Over Australia	February 2004
HRS10	A Pilot Study to Explore Methods for Deriving Design Rainfalls for Australia - Part 1	June 2005
HRS11	A Pilot Study to Explore Methods for Deriving Design Rainfalls for Australia - Part 2	January 2009
HRS12	Climate Change and Probable Maximum Precipitation	March 2009